

The Effects of Hypercapnia on CFTR- Dependent HCO₃⁻ Secretion in Human Airway Epithelia

Mark John Turner
(BSc., MSc., MRes.)

Thesis submitted for the degree of Doctor of Philosophy

Institute for Cell and Molecular Biosciences
Newcastle University Medical School



Date of Submission: September, 2014

Abstract

Hypercapnia is clinically defined as an arterial blood partial pressure of CO₂ of above 40mm Hg and is a symptom of chronic lung disease. In renal epithelia, hypercapnia can reduce agonist-stimulated cAMP levels and impair regulation of cAMP-dependent ion transporters. In the airways, elevations in intracellular cAMP in serous cells of the submucosal glands, activates CFTR-mediated HCO₃⁻ and fluid secretion, which contributes to airway surface liquid homeostasis. The aim of the current work was to investigate the effects of both acute and chronic hypercapnia on cAMP-regulated ion and fluid transport in Calu-3 cells, a model of human serous cells.

Acute hypercapnia significantly reduced both forskolin-stimulated elevations in intracellular cAMP and forskolin-stimulated increase in short-circuit current, suggesting CO₂ reduced cAMP-regulated, CFTR-dependent anion secretion. Stimulation of Calu-3 cells with cAMP agonists induced a reversible intracellular acidification that was a result of CFTR-dependent HCO₃⁻ secretion. In acute hypercapnia, this intracellular acidification was significantly augmented yet neither CFTR-dependent HCO₃⁻ efflux, nor NBC-dependent HCO₃⁻ influx, were found to be CO₂-sensitive. However, ouabain blocked the augmentation induced by hypercapnia implicating the Na⁺/K⁺-ATPase in mediating the effects of raised CO₂ on cAMP-mediated cytosolic acidification. In addition, both BAPTA-AM and the phospholipase C inhibitor, U77312, also blocked the effect of hypercapnia, implying a role for PLC-regulated Ca²⁺ mobilization in the pH response to hypercapnia. Although addition of exogenous ATP in normocapnia mimicked the effect of hypercapnia, there was little evidence that CO₂-induced ATP release from Calu-3 cells, which therefore suggests the effect of hypercapnia is not due to ATP/Ca²⁺ signalling via purinergic receptors.

Exposure of Calu-3 cells to 24 hours hypercapnia caused a significant reduction in the volume of fluid secreted but did not affect the HCO₃⁻ or mucus content of this secreted fluid. These data suggest that transporters involved in regulating the volume of secreted fluid have differential CO₂ sensitivity compared to transporters involved in regulating its composition. These findings reveal that both acute and chronic hypercapnia affected ion and fluid transport in human airway epithelial cells, and suggests hypercapnia could have pronounced effects on the properties of the airway surface liquid which would be predicted to have important consequences for the innate defence mechanisms of the lungs.

Acknowledgements

First and foremost, I would like to thank my supervisory team, Dr. Mike Gray and Dr. Martin Cann, for their constant support, guidance and for showing me what it requires to be a good scientist. I would like to thank Martin who, even though he has supervised me from afar, has had very valuable inputs and into my work which I very much appreciate. I would like to sincerely thank Mike for everything he has done for me in order for me to have completed my PhD. Not only has he provided fantastic guidance and demonstrated large amounts of patience with me but also was only too happy to assist with any personal issues that arose throughout my PhD and for all of this, I am very grateful.

I am also very grateful to my fellow laboratory members, Salam Ibrahim, Waseema Patel and Dr. Bernard Verdon who have all helped me to be able to complete all the experiments I set out to do.

I would also like to thank my fellow members of the ERG at Newcastle University for their friendship, support and technical expertise. In particular, I would like to thank Maxine Geggie, for her valuable assistance in tissue culture and Dr. Alison Howard for her help and patience when teaching me certain molecular biology techniques. I should also thank members of Prof. Jeff Pearson's lab for the regular borrowing of chemicals and other equipment!

I would like to thank my family and friends who all, in some way, have helped me reach this point. The friendliest running club in the North East, Jesmond Joggers, provided me with a great way to unwind and relax, although I might not have felt that on a Saturday morning running cross country! My friends from Bury were always supportive and were only too eager to grab a beer with me when I was at home and for that, I thank them too.

Finally, I would like to thank my Mum and Dad who have been a constant source of both emotional and financial support and whom, without, I could not have completed my PhD. I am so very grateful for everything you have done and continue to do for me.

Table of Contents

Abstract	i
Acknowledgements	ii
Table of Contents	iii
List of Figures	ix
List of Tables	xvii
List of Abbreviations	xviii
Chapter 1: Introduction	1
1.1. Carbon dioxide acts as a cell signalling molecule in a variety of species	1
1.1.1. Drosophila	1
1.1.2. Caenorhabditis elegans	2
1.1.3. Mammals	2
1.2. The effect of CO ₂ on cell signalling second messengers	4
1.2.1. The adenylyl cyclase/cAMP signalling pathway	4
1.2.2. CO ₂ can modulate adenylyl cyclase activity	5
1.2.3. CO ₂ can modulate intracellular Ca ²⁺ levels	6
1.3. CO ₂ signalling in mammalian airways	6
1.4. CO ₂ and airway disease	7
1.5. The role of bicarbonate in human physiology	9
1.6. HCO ₃ ⁻ Secretion in Human Airways	11
1.6.1. Role of CFTR and Anion Exchangers in HCO ₃ ⁻ Secretion	15
1.6.1.2. CFTR is contained within a macromolecular complex	18
1.6.2. Sodium Bicarbonate Cotransporters	20
1.6.3. Model of anion secretion in Calu-3 cells	21

1.7. Aims	22
Chapter 2: Methods.....	24
2.1. Cell Culture	24
2.2. Transepithelial Resistance Measurements	24
2.3. Short circuit current measurements using an Ussing Chamber.....	25
2.4. Intracellular pH Measurements	26
2.4.1. Intracellular pH Calibration	28
2.4.2. Determining Intracellular Buffering Capacity	29
2.5. Intracellular Ca^{2+} Measurements.....	30
2.6. Fluid Secretion Assays	31
2.7. Radiolabelled cAMP Assay	31
2.8. Measurements of extracellular ATP.....	32
2.9. PAS Assay.....	33
2.10. Wound Healing Assay	34
2.11. Confocal Microscopy	35
2.12. End Point PCR.....	36
2.13. Western Blot	38
2.14. Solutions and Reagents.....	40
2.15. Statistical Analysis	41
Chapter 3: Effect of acute hypercapnia on cAMP-dependent HCO_3^- transport in Calu-3 cells	42
3.1. Introduction	42
3.2. Acute hypercapnia attenuates forskolin-stimulated cAMP levels in Calu-3 cells	42
3.3. Acute hypercapnia reduces forskolin-stimulated increases in short-circuit current .	44
3.4. cAMP agonists produce an intracellular acidification in Calu-3 cells	49
3.5. Profile of cAMP-induced intracellular acidification	49

3.5.1.	HCO ₃ ⁻ Dependence	49
3.5.2.	Effect of membrane potential.....	51
3.5.3.	SQ 22,536 Sensitivity	52
3.5.4.	H-89 Sensitivity	53
3.5.5.	GlyH-101 Sensitivity	54
3.6.	Hypercapnia increases the magnitude and rate of cAMP-induced intracellular acidification.....	55
3.7.	CO ₂ <i>per se</i> mediates the effects of hypercapnia.....	58
3.7.1.	The effect of CO ₂ -induced intracellular acidosis.....	58
3.7.2.	The effect of CO ₂ -induced extracellular acidosis	60
3.7.3.	The effect of carbonic anhydrase-dependent hydration of CO ₂	62
3.7.4.	CO ₂ does not mediate its effects on cAMP-regulated HCO ₃ ⁻ transport <i>via</i> sAC...	63
3.7.5.	CO ₂ does not mediate its effects on adenosine-stimulated HCO ₃ ⁻ transport <i>via</i> regulation of PLA ₂	64
3.8.	Hypocapnia does not modulate cAMP-regulated HCO ₃ ⁻ transport.....	65
3.9.	Permeability of Calu-3 Cells to CO ₂	66
3.10.	CO ₂ elicits membrane specific effects.....	68
3.11.	Recovery of pH _i from CO ₂ -induced acidosis	69
3.12.	Effects of hypercapnia on other cAMP signalling agents	70
3.12.1.	IBMX	71
3.12.2.	Dibutryl-cAMP	72
3.12.3.	Multidrug Resistance Proteins	74
3.13.	Disruption of compartmentalization of cAMP signalling does not prevent the effect of hypercapnia	78
3.14.	Effects of acute hypercapnia on specific H ⁺ /HCO ₃ ⁻ transporters	82
3.14.1.	Apical HCO ₃ ⁻ efflux	82

3.14.2.	Basolateral HCO_3^- Influx	86
3.14.3.	Src kinase	97
3.14.4.	PI3 Kinase	99
3.14.5.	Basolateral AE2 activity.....	100
3.14.6.	Na^+/H^+ Exchangers.....	102
3.14.7.	$\text{Na}^+-\text{K}^+-\text{Cl}^-$ cotransporter.....	103
3.14.8.	$\text{Na}^+/\text{K}^+-\text{ATPase}$	104
3.14.9.	AMP Kinase	106
3.15.	Discussion.....	108
3.15.1.	The effects of hypercapnia on Calu-3 cells.....	108
3.15.2.	Acute hypercapnia modulated $[\text{cAMP}]_i$ and cAMP-regulated anion secretion	109
3.15.2.	How does a CO_2 -induced reduction in $[\text{cAMP}]_i$ lead to an apparent increase in cAMP-regulated HCO_3^- transport?	110
3.15.2.	CO_2 exhibits differential effects on cAMP-elevating agonists	113
Chapter 4:	The role of $\text{Ca}^{2+}/\text{ATP}$ signalling in underlying the effects of hypercapnia	117
4.1.	Introduction	117
4.2.	The role of Ca^{2+} signalling in response to hypercapnia	118
4.2.1.	Inhibition of intracellular Ca^{2+} signalling	118
4.2.2.	Effect of CO_2 on intracellular Ca^{2+}	129
4.2.3.	Activation of intracellular Ca^{2+} signalling.....	131
4.3.	The effect of exogenous ATP.....	135
4.4.	Possible mechanisms for CO_2 -Induced ATP release	151
4.4.1.	Connexins	151
4.4.2.	Pannexins.....	157
4.4.3.	Exocytosis of ATP-containing vesicles	162

5.4.4.	P-glycoproteins	164
4.5.	Other potential targets for CO ₂ signalling	167
4.5.4.	NADPH Oxidase.....	167
4.6.	Discussion	169
4.6.1.	Indications that acute hypercapnia induced an IP ₃ -dependent Ca ²⁺ release to modulate cAMP signalling in Calu-3 cells	169
4.6.2.	How do potential modulations of Ca ²⁺ affect cAMP signalling?	172
4.6.3.	Indications that acute hypercapnia does not induce an IP ₃ -dependent Ca ²⁺ release to modulate cAMP signalling in Calu-3 cells.....	173
Chapter 5:	The effects of chronic hypercapnia on Calu-3 cells.....	179
5.1.	Introduction	179
5.2.	Calu-3 transepithelial electrical resistance is unaffected by chronic hypercapnia..	180
5.3.	Chronic hypercapnia reduces the volume of forskolin-stimulated fluid secretion but has no effect on the composition on secreted fluid	180
5.4.	Chronic hypercapnia has no effect on I _{sc} in Calu-3 cells	186
5.5.	Chronic hypercapnia reduces the expression of CFTR in Calu-3 cells	190
5.6.	CFTR-dependent anion exchange activity is unaffected by chronic hypercapnia..	190
5.7.	Chronic hypercapnia elicits highly variable effects on wound healing of Calu-3 cells	192
5.6.	Discussion	198
5.6.1.	The effect of chronic hypercapnia on cAMP-regulated ion and fluid transport – similar mechanisms to acute hypercapnia?.....	198
5.6.2.	The effect of chronic hypercapnia on cAMP-regulated ion and fluid transport – differences to acute hypercapnia?	200
5.6.3.	Applying the effects of hypercapnia to a more clinical setting by investigating Calu-3 cell wound repair.....	201
Chapter 6:	Discussion	204

6.1.	Summary of main findings	204
6.2.	Clinical relevance of findings to hypercapnic lung disease patients	206
6.3.	Future experiments	207
6.4.	Final conclusions	211
	References	212

List of Figures

Figure 1.01: The structure of transmembrane adenylyl cyclase.	4
Figure 1.02: Chest X Rays to show the effects of ARDS on the lungs.	9
Figure 1.03. Hypothesis for the role of HCO_3^- secretion in mucus release and expansion from mucin granules.	11
Figure 1.04: The conducting airways are covered with a thin layer of airway surface liquid (ASL).	12
Figure 1.05: Schematic diagram of how the periciliary layer may exist as a mesh due to the presence of mucins tethered to the cilia of surface epithelia.	13
Figure 1.06: The submucosal gland is responsible for the majority of the airway surface liquid and mucus secretion.....	14
Figure 1.07: Structure and gating of CFTR.	15
Figure 1.08: The physical and functional interaction between CFTR and SLC26 transporters.	18
Figure 1.09. CFTR is contained within a macromolecular complex at the apical membrane of airway cells to allow compartmentalization of the cAMP signalling machinery.	20
Figure 1.10: A model of anion secretion in the Calu-3.....	22
Figure 2.01: Change in the transepithelial electrical resistance (TEER) of Calu-3 cells grown as a polarised monolayer on permeable transwell supports.	25
Figure 2.02: Diagram to show how short-circuit current was measured using an Ussing chamber.....	26
Figure 2.03. Analysis of pH_i experiments.....	27
Figure 2.04: Intracellular pH_i calibration of Calu-3 cells.	28
Figure 2.05: Buffering capacity of Calu-3 cells when exposed to different concentrations of CO_2	30

Figure 2.06: Standard curve generated for the Periodic acid Schiffs assay.....	34
Figure 2.07: Example analysis of wound healing assay.	35
Figure 2.08. Standard curve for protein quantification generated using the Peirce Assay.	39
Figure 3.01: Acute hypercapnia attenuates forskolin-stimulated cAMP levels in Calu-3 cells.	43
Figure 3.02: Acute hypercapnia reduces forskolin-stimulated I_{sc} in Calu-3 cells.	45
Figure 3.03: Forskolin-stimulated increases in I_{sc} are cAMP and PKA-dependent.	46
Figure 3.04: Acute hypercapnia increases total CFTR expression in Calu-3 cells.....	48
Figure 3.05: cAMP agonists induced a reversible intracellular acidification in Calu-3 cells..	49
Figure 3.06: Forskolin-stimulated intracellular acidification is HCO_3^- dependent.....	50
Figure 3.07: Depolarization of Calu-3 cells prevents forskolin-stimulated intracellular acidification.....	51
Figure 3.08: Preincubation of Calu-3 cells with SQ 22,536 causes a reversible decrease in the rate of the forskolin-stimulated intracellular acidification.....	52
Figure 3.09: Preincubation of Calu-3 cells with H-89 causes a reversible decrease in the rate of the adenosine-stimulated intracellular acidification.	54
Figure 3.10: GlyH-101 inhibits forskolin-stimulated intracellular acidification.	55
Figure 3.11: Acute hypercapnia increases the magnitude and rate of forskolin and adenosine- stimulated intracellular acidification.....	57
Figure 3.12: The effect of hypercapnia on the dose response of forskolin-stimulated acidification in Calu-3 cells	58
Figure 3.13: CO_2 -induced intracellular acidosis does not contribute to the effect of hypercapnia on cAMP-regulated HCO_3^- transport.	59

Figure 3.14: The effects of hypercapnia on the forskolin-stimulated intracellular acidification are not due to differences in extracellular pH.	61
Figure 3.15: Acetazolamide does not block the effect of hypercapnia on the forskolin-stimulated acidification.	63
Figure 3.16: KH7 does not block the effect of hypercapnia on the forskolin-stimulated intracellular acidification.	64
Figure 3.17: AACOCF ₃ does not block the effect of hypercapnia on adenosine-stimulated intracellular acidification.	65
Figure 3.18: Hypocapnia does not modulate forskolin-stimulated HCO ₃ ⁻ transport in Calu-3 cells.	66
Figure 3.19: Only the apical membrane of Calu-3 cells is permeable to CO ₂	68
Figure 3.20: Only apical CO ₂ induced modulations to forskolin-stimulated intracellular acidification.	69
Figure 3.21: pH _i recovery after CO ₂ -induced acidosis is Na ⁺ -dependent and inhibited by forskolin.	70
Figure 3.22: Hypercapnia does not alter the IBMX-stimulated intracellular acidification.	72
Figure 3.23: Hypercapnia is able to modulate dibutyryl-cAMP-stimulated intracellular acidification in Calu-3 cells.	73
Figure 3.24: MK-571 blocks the effect of hypercapnia on the forskolin-stimulated intracellular acidification.	75
Figure 3.25: Apical but not basolateral MK-571 blocks the effect of hypercapnia on the forskolin-stimulated intracellular acidification.	76
Figure 3.26: Acute hypercapnia has no effect on the rate of MRP-mediated GSMF efflux from Calu-3 cells.	78
Figure 3.27: The effect of cytochalasin D and latrunculin B on actin cytoskeleton integrity and transepithelial electrical resistance in Calu-3 cells.	80

Figure 3.28: Cytochalasin D does not block the effects of hypercapnia on the forskolin-stimulated intracellular acidification.....	81
Figure 3.29: Latrunculin B does not block the effects of hypercapnia on the forskolin-stimulated intracellular acidification.....	82
Figure 3.30: Apical HCO_3^- efflux is unaffected by acute hypercapnia.....	84
Figure 3.31: CFTR-dependent anion exchange activity is unaffected by acute hypercapnia..	85
Figure 3.32: Members of the NBC family, SLC4A4 and SLC4A7, are expressed in Calu-3 cells.	86
Figure 3.33: cAMP agonists stimulate Na^+ -dependent HCO_3^- import in Calu-3 cells.	87
Figure 3.34: Acute hypercapnia does not affect forskolin-stimulated NBC activity.....	88
Figure 3.35: Acute hypercapnia does not affect adenosine-stimulated NBC activity.	89
Figure 3.36: Acute hypercapnia does not affect the activity of $\text{Na}^+/\text{HCO}_3^-$ Cotransporters when measured in the presence of GlyH-101.	90
Figure 3.37: Acute hypercapnia does not alter the activity of a putative Na^+ -dependent $\text{Cl}^-/\text{HCO}_3^-$ exchanger.	92
Figure 3.38: Hypercapnia augments forskolin-stimulated intracellular acidification even in absence of basolateral Na^+	93
Figure 3.39: Hypercapnia increases $\text{Na}^+/\text{HCO}_3^-$ Cotransporter activity in basal conditions. ...	95
Figure 3.40. Acute hypercapnia reduces WNK4 expression under basal conditions in Calu-3 cells.	97
Figure 3.41: Src kinase inhibition does not block the effects of hypercapnia on the forskolin-stimulated intracellular acidification.....	99
Figure 3.42: PI3 Kinase inhibition does not block the effects of hypercapnia on the forskolin-stimulated intracellular acidification.....	100

Figure 3.43: Acute hypercapnia is unable to relieve the cAMP-induced inhibition of basolateral AE2 but does reduce AE2 activity in basal conditions.	101
Figure 3.44: CO ₂ -induced modulation of forskolin-stimulated intracellular acidification is not due to changes in Na ⁺ /H ⁺ Exchanger activity.....	103
Figure 3.45: CO ₂ -induced modulation of forskolin-stimulated intracellular acidification is not due to changes in Na ⁺ -K ⁺ -Cl ⁻ Cotransporter activity.....	104
Figure 3.46: Ouabain treatment blocks the effect of acute hypercapnia on the forskolin-stimulated intracellular acidification.....	106
Figure 3.47. AMP Kinase inhibition does not block the effects of hypercapnia on the forskolin-stimulated intracellular acidification.....	107
Figure 3.48. Major effects of acute hypercapnia on cAMP-dependent HCO ₃ ⁻ transport in Calu-3 cells.	116
Figure 4.01. Preincubation of cells with BAPTA-AM blocks the effect of hypercapnia on the forskolin-stimulated intracellular acidification.....	119
Figure 4.02: Inhibition of phospholipase C blocks the effect of hypercapnia on the forskolin-stimulated intracellular acidification.....	120
Figure 4.03: 2-APB blocks the effect of acute hypercapnia on the forskolin-stimulated intracellular acidification.	122
Figure 4.04: Acute hypercapnia reduces p-IRBIT expression in Calu-3 cells.	124
Figure 4.05: Inhibition of CaM Kinase Kinase does not block the effect of hypercapnia. ...	125
Figure 4.06: Depletion of intracellular Ca ²⁺ does not alter the effect of hypercapnia.....	126
Figure 4.07: Removal of extracellular Ca ²⁺ does not alter the effect of hypercapnia on the forskolin-stimulated intracellular acidification.....	128
Figure 4.08: Ca ²⁺ plays a role in mediating the intracellular pH recovery in response to CO ₂ -induced acidosis.	128

Figure 4.09: Acute hypercapnia does not cause an increase in intracellular Ca^{2+} in Calu-3 cells.	131
Figure 4.10: Thapsigargin treatment does not mimic the effect of hypercapnia on the forskolin-stimulated intracellular acidification.	133
Figure 4.11: Basolateral carbachol mimics the effect of hypercapnia on the forskolin-stimulated intracellular acidification.	134
Figure 4.12: Exogenous ATP induces a Ca^{2+} -dependent, transient intracellular acidification which is modulated by acute hypercapnia.	136
Figure 4.13: Exogenous ATP mimics the effect of hypercapnia on the forskolin-stimulated intracellular acidification.	137
Figure 4.14: Exogenous apical ATP has a small effect on the forskolin-stimulated intracellular acidification.	139
Figure 4.15: Exogenous basolateral ATP mimics the effect of hypercapnia on the forskolin-stimulated intracellular acidification.	140
Figure 4.16: The effect of exogenous ATP on the forskolin-stimulated intracellular acidification is predominantly basolateral.	140
Figure 4.17: The effect of ATP on the forskolin-stimulated intracellular acidification is Ca^{2+} -dependent.	142
Figure 4.18: Suramin prevents ATP-mediated augmentation of forskolin-stimulated intracellular acidification.	143
Figure 4.19: Exogenous UTP partially mimics the effect of hypercapnia on the forskolin-stimulated intracellular acidification.	145
Figure 4.20: Suramin does not block the effect of hypercapnia on the forskolin-stimulated intracellular acidification.	147
Figure 4.21: Apyrase does not block the effect of hypercapnia on the forskolin-stimulated intracellular acidification.	148

Figure 4.22: CGS-15943 does not block the effect of hypercapnia on the forskolin-stimulated intracellular acidification.	150
Figure 4.23: Carbenoxolone treatment blocks the effect of hypercapnia on the forskolin-stimulated intracellular acidification.....	152
Figure 4.24: Cobalt chloride does not block the effect of hypercapnia on the forskolin-stimulated intracellular acidification.....	154
Figure 4.25: Proadifen does not block the effect of hypercapnia on the forskolin-stimulated intracellular acidification.	156
Figure 4.26: The effect of connexin inhibitors on the intracellular pH recovery in response to CO ₂ -induced acidosis.....	157
Figure 4.27: Panx-1, but not Panx-2, is expressed in Calu-3 cells.	158
Figure 4.28: Probenecid reduces the effect of hypercapnia on the forskolin-stimulated intracellular acidification.	159
Figure 4.29: A low concentration of carbenoxolone reduces the extent by which hypercapnia enhances the forskolin-stimulated intracellular acidification.	161
Figure 4.30: Hypercapnia does not mediate its effects on <i>via</i> activation of TRPV4 channels and Rho Kinase signalling.	162
Figure 4.31: Brefeldin A does not block the effects of hypercapnia on the forskolin-stimulated intracellular acidification.....	164
Figure 4.32: Inhibition of P-glycoproteins does not block the effects of hypercapnia on the forskolin-stimulated intracellular acidification.....	165
Figure 4.33: Acute hypercapnia does not increase the extracellular concentration of ATP..	166
Figure 4.34: Dual oxidase inhibition reduces the effects of hypercapnia on the forskolin-stimulated intracellular acidification.....	168
Figure 4.35: Proposed mechanism for CO ₂ -induced mobilization of Ca ²⁺ and the potential effects this has on cAMP-regulated HCO ₃ ⁻ transport.	178

Figure 5.01: Chronic hypercapnia reduces forskolin-stimulated fluid secretion in Calu-3 cells.	182
Figure 5.02: Chronic hypercapnia has no effect on IBMX-stimulated fluid secretion in Calu-3 cells.	183
Figure 5.03: Chronic hypercapnia reduces forskolin + IBMX-stimulated fluid secretion in Calu-3 cells.	184
Figure 5.04: BAPTA-AM reduces basal fluid secretion in Calu-3 cells but does not prevent the increase in fluid secretion stimulated by forskolin.	185
Figure 5.05: BAPTA-AM prevents the effect of hypercapnia on forskolin-stimulated fluid secretion in Calu-3 cells.	186
Figure 5.06. Chronic hypercapnia has no effect on forskolin-stimulated changes in I_{sc} in Calu-3 cells.	188
Figure 5.07: Chronic hypercapnia reduces forskolin-stimulated fluid secretion in Calu-3 cells in the presence of a basolateral to apical Cl^- gradient.	189
Figure 5.08: Chronic hypercapnia reduces CFTR expression in Calu-3 cells.	190
Figure 5.09: Chronic hypercapnia does not alter CFTR-dependent HCO_3^- transport in Calu-3 cells.	192
Figure 5.10: Representative images showing the wound administered to Calu-3 cells at 0, 12, 24 and 36 hours post-scratch.	194
Figure 5.11: Hypercapnia increases the rate of wound healing in Calu-3 cells incubated in high Cl^- Krebs solution.	195
Figure 5.12: Growth medium reduces the rate of wound healing in Calu-3 cells in both normocapnia and hypercapnia.	196
Figure 5.13: Hypercapnia has no effect on the rate of wound healing in Calu-3 cells.	197
Figure 5.14: Grouping the data from three separate experiments shows that hypercapnia increases the rate of wound healing in Calu-3 cells.	198

List of Tables

Table 2.01. Conditions for reverse transcription of mRNA into cDNA	37
Table 2.02. Conditions for End Point PCR.....	37
Table 2.03. Primer sequences, annealing temperatures and expected product size for End Point PCR experiments.....	38
Table 3.01: Modifications to high Cl^- Krebs solution in order to assess the effects of hypercapnia when extracellular pH is equal in both normocapnic and hypercapnic conditions.	60

List of Abbreviations

AC	Adenylyl cyclase
ACTZ	Acetazolamide
Ado	Adenosine
AE	Anion exchanger
ALI	Acute Lung Injury
ARDS	Acute Respiratory Distress Syndrome
ASL	Airway Surface Liquid
ATP	Adenosine-5'-triphosphate
BAPTA-AM	1,2-Bis(2-aminophenoxy)ethane-N,N,N',N'-tetraacetic acid tetrakis(acetoxymethyl ester)
BCECF-AM	2'-7'-bis(carboxyethyl)-5(6)-carboxyfluorescein acetoxymethyl ester
cAMP	3'-5'-cyclic adenosine monophosphate
CBX	Carbenoxolone
Cch	Carbachol
CFTR	Cystic fibrosis transmembrane conductance regulator
CREB	cAMP-response element binding
DAG	Diacylglycerol
DAPI	4',6-diamidino-2-phenylindole
db-cAMP	dibutyl-3'-5'-cyclic adenosine monophosphate
DIDS	4,4'-Diisothiocyano-2,2'-stilbenedisulfonic acid
EGTA	Ethylene Glycol Tetraacetic Acid
EIPA	5-(N-Ethyl-N-isopropyl)amiloride

EMEM	Eagle's Minimum Essential Medium
ENaC	Epithelial Na ⁺ channel
Fsk	Forskolin
Fura-2-AM	2-[6-[Bis[2-[(acetyloxy)methoxy]-2-oxoethyl]amino]-5-[2-[2-[bis[2-[(acetyloxy)methoxy]-2-oxoethyl]amino]-5-methylphenoxy]ethoxy]-2-benzofuranyl]-5-oxazolecarboxylic acid (acetyloxy)methyl ester
IBMX	3-Isobutyl-1-methylxanthine
IP ₃	Inositol triphosphate
I _{sc}	Short circuit current
-J(B)	Transmembrane HCO ₃ ⁻ efflux
MSD	Membrane spanning domain
NBC	Na ⁺ /HCO ₃ ⁻ cotransporter
NBD	Nucleotide binding domain
NDCBE	Na ⁺ -dependent Cl ⁻ /HCO ₃ ⁻ Exchanger
NHE	Na ⁺ /H ⁺ exchanger
NHERF	Na ⁺ /H ⁺ Exchange Regulatory Factor 1
PBS	Phosphate Buffered Saline solution
pCO ₂	Partial pressure of CO ₂
PDE	Phosphodiesterase
PFA	Paraformaldehyde
pH _i	Intracellular pH
pH _e	Extracellular pH
PIP ₂	Phosphatidylinositol 4,5-biphosphate

PKA	Protein kinase A
PKC	Protein kinase C
R	Regulatory domain of CFTR
sAC	Soluble adenylyl cyclase
TEER	Transepithelial Electrical Resistance
tmAC	Transmembrane adenylyl cyclase
UTP	Uridine 5'-triphosphate
VIP	Vasoactive intestinal peptide
$\beta_{\text{HCO}_3^-}$	$\text{CO}_2\text{-HCO}_3^-$ buffer system-dependent buffering capacity
β_i	Intrinsic buffering capacity
β_{tot}	Total buffering capacity
$[\text{cAMP}]_i$	Intracellular concentration of cAMP
$[\text{Ca}^{2+}]_i$	Intracellular concentration of Ca^{2+}
$[\text{Ca}^{2+}]_e$	Extracellular concentration of Ca^{2+}

Chapter 1: **Introduction**

1.1. Carbon dioxide acts as a cell signalling molecule in a variety of species

Carbon dioxide is formed in all cells of the body as a waste product of respiration and is removed from the blood during ventilation. Normal arterial blood CO_2 (P_aCO_2) is approximately 40mmHg (5% (v/v) CO_2) in healthy individuals but in certain lung diseases, such as chronic obstructive pulmonary disease (COPD), in which gas exchange at the alveoli is impaired, the removal of CO_2 can be inadequate causing P_aCO_2 levels to increase (Lourenco and Miranda, 1968). A P_aCO_2 of above 40mmHg is defined as hypercapnia and can lead to serious health problems. For instance, CO_2 can displace oxygen binding to haemoglobin and therefore reduce the oxygen carrying capacity of red blood cells (Dahms *et al.*, 1972; Kilmartin, 1976) whilst elevated P_aCO_2 also causes respiratory acidosis – a decrease in blood pH due to the reaction of CO_2 with H_2O to form carbonic acid. Respiratory acidosis has been reported to reduce ventricular myocyte contractility in both rats and dogs (Walley *et al.*, 1990; Harrison *et al.*, 1992) as well as decreasing diaphragm function in dogs (Yanos *et al.*, 1993) with Harrison *et al.* (1992) suggesting that acidosis affected muscle contractile proteins as well as intracellular Ca^{2+} ($[\text{Ca}^{2+}]_i$) homeostasis in myocytes. Thus hypercapnia can have major implications for cardiovascular health in mammals. Perhaps unsurprisingly, given the toxic nature of this naturally occurring gas, the effect of elevated CO_2 has been studied in a variety of species. Not only has it been shown that organisms are able to sense changes in environmental CO_2 but CO_2 can act as a cell signalling molecule to affect organism physiology.

1.1.1. Drosophila

The eukaryotic organism *Drosophila melanogaster* has been studied for its gas sensing behaviour, notably in hypoxia where its homolog of the mammalian transcription factor HIF-1 acts to upregulate the expression of certain genes (Lavista-Llanos *et al.*, 2002). *Drosophila* are also affected by changes in environmental CO_2 . Helenius *et al.* (2009) demonstrated that in hypercapnic conditions (13% CO_2), both fertility and embryo development were both impaired. Hypercapnia also altered the gene expression profile of the organism with

substantial downregulation of antimicrobial peptide genes which compromised the organisms' innate defences. Thus, for *Drosophila*, hypercapnia is detrimental to the organism and, as a result, being able to sense changes in environmental CO₂ is of evolutionary importance. *Drosophila* are able to sense changes in CO₂ due to the activation of CO₂-sensitive olfactory receptors Gr63a and Gr21a (Jones *et al.*, 2007) which indicates that, in lower organisms at least, changes in CO₂ trigger olfactory receptor-mediated responses, implicating CO₂ as a signalling molecule in this instance.

1.1.2 *Caenorhabditis elegans*

Similar to *Drosophila*, *Caenorhabditis elegans* can also serve as a powerful model to investigate the effects of environmental factors on the organism's physiology and genetics. Sharabi *et al.* (2009) demonstrated that *C. elegans* grown in a hypercapnic environment showed reduced production of eggs, reduced motility and deterioration in muscle morphology and an extension to lifespan. Animals grown in 19% CO₂ demonstrated an 89% reduction in the amount of eggs laid compared to animals grown in normal air but also lived, on average, 5.5 days longer than control animals. These effects of chronic hypercapnia were accompanied by major changes in gene expression which likely contributed to the altered phenotypes observed. As well as CO₂ being able to cause long term changes in *C. elegans* physiology by inducing changes in gene expression, it has recently been shown that BAG neurones of *C. elegans*, located towards the head of the organism, respond to CO₂ *per se* in a dose dependent fashion (Smith *et al.*, 2013). Elevated CO₂ led to the activation of BAG neurones, as measured by increases in [Ca²⁺]_i, which show that *C. elegans* possess specific sensors for CO₂. This work highlights the importance of being able to detect changes in environmental CO₂ for these organisms, although whether changes in gene expression are due to a CO₂-transduced signal, or serve as an adaptive response to the environmental hypercapnia still remains to be determined.

1.1.3. Mammals

In mammalian cells, a wide range of effects of hypercapnia have been reported in a variety of different tissues. Work published from the group of Nicholas Dale particularly supports the notion that CO₂ is a key signalling molecule in mammals. In 2010, Huckstepp *et al.* (2010b)

investigated the mechanism behind the increased respiratory drive displayed by animals in response to hypercapnia. They demonstrated that increasing CO₂ from 35mmHg (4.6% CO₂) to 55mmHg (7.2% CO₂) and 70mmHg (9.2% CO₂) triggered a dose-dependent release of ATP from cells located in the medulla oblongata of rats with 70mmHg increasing the amount of ATP released by ~0.9μM compared to control conditions. As the medulla oblongata is the site of the central chemoreceptors involved in controlling ventilation rates in response to changes in blood O₂, CO₂ and H⁺, it suggested a possible mechanism in which the medulla oblongata can sense changes in arterial blood CO₂. The released ATP may act directly on purinergic receptors of local respiratory neurones, or be broken down into adenosine, to regulate ventilation rate in response to hypercapnia. Further experiments identified that pharmacological blockade of connexin hemichannels prevented the ATP release from the medulla oblongata and blocked the increased respiratory drive in response to hypercapnia. Connexin 26 (Cx26) was found to be expressed on the ventral surface of the medulla oblongata and was suggested as being the CO₂-sensitive connexin mediating ATP release from these cells. Expression of Cx26 in HeLa cells induced a dose-dependent increase in whole cell conductance in response to CO₂ which was also observed in Cx32 but not Cx30 or Cx43-expressing cells, implicating only certain members of the connexin family are sensitive to CO₂ (Huckstepp *et al.*, 2010a). Huckstepp and Dale (2011) have also reported that CO₂ dose-dependently increased the open probability of a member of the inwardly rectifying family of K⁺ channels and highlights the ability of CO₂ to influence ion transport in mammalian and human tissue .

Human retinal pigment epithelia (RPE) play a major role in removing waste products from the subretinal space that surround nearby photoreceptors. Due to the high metabolic rate of photoreceptors, the apical membrane of RPE are exposed to high levels of CO₂ and Adjianto *et al.* (2009) have demonstrated membrane transporter activity to be sensitive to this hypercapnic microenvironment. Exposure of RPE to 13% CO₂ stimulated the activity of a basolateral Na⁺/HCO₃⁻ cotransporter (NBC) which increased Na⁺ and HCO₃⁻ uptake into the cell and contributed to ~80% observed increase in fluid reabsorption. Conversely, RPE cells exposed to 1% CO₂ had reduced NBC activity and a ~64% decrease in fluid reabsorption. However, the data was limited by the fact that altering CO₂ levels caused a change in the intracellular pH (pH_i) of the RPEs and therefore determining whether the changes in basolateral NBC activity was due to CO₂ *per se* or changes in pH_i was difficult. These studies provide valuable indications that hypercapnia is able to modulate plasma membrane

transporter activity to bring about a change in ion and fluid transport in animals and indeed humans. Therefore, gaining further insights into the molecular mechanisms underlying this is of major interest in the field of epithelial membrane transport physiology.

1.2. The effect of CO₂ on cell signalling second messengers

1.2.1. The adenylyl cyclase/cAMP signalling pathway

Cyclic adenosine 3',5'-monophosphate (cAMP) is a key cellular second messenger first discovered by Berthet *et al.* (1957). ATP is converted into cAMP by a reaction catalyzed by the enzyme adenylyl cyclase (AC). This enzyme was first purified from bovine brain in 1985 (Pfeuffer *et al.*, 1985) and the entire coding sequence for bovine brain AC was published four years later (Krupinski *et al.*, 1989). There exists two forms of adenylyl cyclase: transmembrane adenylyl cyclase (tmAC) (of which nine isoforms exist) and soluble adenylyl cyclase (sAC). Amino acid sequencing has revealed that each tmAC isoform contains two transmembrane spanning domains (Tm1 and Tm2), as well as two catalytic domains, namely C1 and C2 (fig. 1.01). Each catalytic domain contains an ATP binding site which, upon tmAC activation, is converted into cAMP (Cooper *et al.*, 1995). cAMP has a host of downstream targets ranging from the activation of cAMP-dependent protein kinase A (PKA), to the activation of transcription factors such as cAMP response element binding protein (CREB), allowing it to regulate gene expression in cells.

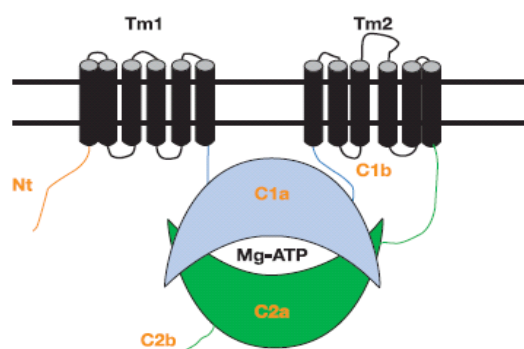


Figure 1.01: The structure of transmembrane adenylyl cyclase. TmAC contains two transmembrane spanning domains (Tm1 and Tm2) joined by an intracellular catalytic domain which can be further divided into the highly conserved catalytic domains 1a (C1a) and 2a (C2a) with C1b and C2b being less conserved domains. This is the site for ATP binding for conversion into cAMP. Figure adapted from Cooper (2003).

1.2.2. CO₂ can modulate adenylyl cyclase activity

As previously discussed, there exists a great deal of evidence that implicates CO₂ as a signalling molecule in a host of different organisms. One reason why cells are able to sense, and thus respond to, CO₂ is due to a CO₂ induced effect on key intracellular second messengers, notably cAMP and Ca²⁺. It was initially shown that adenylyl cyclase activity was modulated by inorganic carbon (C_i) and thus responsive to both CO₂ and HCO₃⁻. However, Hammer *et al.* (2006) showed that the activity of the prokaryotic class III adenylyl cyclase, Slr1991, isolated from *Synechocystis* PCC 6803, was increased by CO₂ but not HCO₃⁻, which gave an early indication that adenylyl cyclase was sensitive to CO₂ rather than carbon *per se*. This work was followed by a publication from our laboratory in which the role of CO₂ on adenylyl cyclase activity across different species was investigated (Townsend *et al.*, 2009). In this study, a recombinant, catalytically active, mammalian, transmembrane adenylyl cyclase protein, named 7C₁•2C₂, was expressed in HEK 293T cells and it was found that isoproterenol-induced ATP to cAMP conversion was significantly higher in cells exposed to 5% CO₂ compared to those exposed to 0.03% CO₂. Interestingly, further increase of CO₂ to 10% CO₂ caused 7C₁•2C₂ activity to plateau, thus highlighting that CO₂ has dose-dependent effects on adenylyl cyclase activity. This was the first work to show that mammalian transmembrane adenylyl cyclases are sensitive to CO₂. Parfenova and Leffler (1996) demonstrated that cultured microvascular smooth muscle cells release higher amounts of cAMP into the extracellular space in response to a 15 minute exposure to hypercapnia suggesting either a greater production of cAMP or perhaps an increased activity of cAMP transporters such as the multidrug resistance proteins (Jedlitschky *et al.*, 2000; Chen *et al.*, 2001; Osycka-Salut *et al.*, 2014). Finally, our laboratory has shown that incubating OK cells (a renal cell line that is a model for proximal tubule cells) in 10% CO₂ caused a ~20% and ~30% reduction in parathyroid hormone and forskolin-stimulated intracellular cAMP levels ([cAMP]_i) respectively, compared to cells incubated in 5% CO₂ (Cook *et al.*, 2012). This phenomenon was not observed in the presence of BAPTA-AM, the inositol 1,4,5-trisphosphate (IP₃) receptor blocker 2-aminoethoxydiphenyl borate (2-APB) or in DT40KO cells which do not express any of the three IP₃ receptor subtypes, suggesting that CO₂ stimulated IP₃-induced Ca²⁺ signalling which reduced tmAC activity and subsequent cAMP production. Furthermore, hypercapnia enhanced the activity of the Na⁺/H⁺ exchanger 3 (NHE3) in OK cells, a transporter negatively regulated by cAMP/PKA. Thus, our laboratory

has shown hypercapnia can affect cAMP-regulated transporters although precisely how this occurs is not fully understood.

1.2.3. CO₂ can modulate intracellular Ca²⁺ levels

As described in 1.2.2., Cook *et al.*, (2012) demonstrated a role for a change in [Ca²⁺]_i in the response of renal cell lines to hypercapnia, and Ca²⁺ is indeed another very important second messenger that can be affected by environmental CO₂. When measuring [Ca²⁺]_i levels in rabbit proximal tubule, Bouyer *et al.* (2003) found applying 5% CO₂ to the basolateral membrane, but not the apical membrane, induced an increase in [Ca²⁺]_i. This increase in [Ca²⁺]_i was even further augmented in the presence of 20% basolateral CO₂. The source of Ca²⁺ was found to be from intracellular stores but Ca²⁺ release was insensitive to thapsigargin, caffeine and retonone, suggesting the stores were not the endoplasmic reticulum or mitochondria but potentially could be lysosomal. Similar observations have been made by Briva *et al.*, (2011) who demonstrated that [Ca²⁺]_i levels increase in the presence of 10% CO₂ in alveolar type II cells. However, in this instance the increase in [Ca²⁺]_i was due to Ca²⁺ entry from the extracellular medium. Interestingly, in human endothelial cells, although hypercapnia induced a small increase in [Ca²⁺]_i, the largest increase in [Ca²⁺]_i was in response to hypocapnia (2% CO₂) (Nishio *et al.*, 2001). This change in [Ca²⁺]_i was thapsigargin-insensitive and shows that distinctly different mechanisms for CO₂ sensing exist in mammalian endothelial cells compared to epithelial cells.

1.3. CO₂ signalling in mammalian airways

In mammalian airways, fluid reabsorption is governed by the rate of Na⁺ transport across airway cells, which generates an osmotic gradient for water absorption. The epithelial Na⁺ channel (ENaC), expressed on the apical membrane of absorptive lung epithelia, transports Na⁺ into the cell which is effluxed across the basolateral membrane and into the bloodstream via the Na⁺/K⁺-ATPase (Fang *et al.*, 2002). Briva *et al.* (2007) demonstrated that exposing isolated rat lung tissue to hypercapnia (60mmHg CO₂) decreased Na⁺/K⁺-ATPase activity and consequently reduced alveolar fluid reabsorption. This occurred due to a CO₂-dependent translocation of PKC-α and PKC-ζ to the basolateral membrane of alveolar type II cells, which triggered the endocytosis of the α subunit of Na⁺/K⁺-ATPase and consequently reduced pump activity in these cells. Follow up studies showed that the CO₂-induced

translocation of PKC to the basolateral membrane of rat ATII cells was dependent on a CO₂-induced rise in [Ca²⁺]_i as well as CO₂-dependent activation of extracellular signal regulated kinase (ERK) 1/2 and adenosine monophosphate kinase (AMPK) (Vadasz *et al.*, 2008). These findings provide fascinating insights into the effect of CO₂ on key components of intracellular signalling pathways.

1.4. CO₂ and airway disease

Although it is often used as a marker for lung disease, hypercapnia is also associated with the treatment of the lung diseases Acute Respiratory Distress Syndrome (ARDS) and Acute Lung Injury (ALI). These are diseases of the lung caused by the release of proinflammatory cytokines at the alveoli which recruits neutrophils, and inflammation of the lungs occurs (Martin, 1999; Pierrakos *et al.*, 2012). An X-Ray of ARDS lungs showing clearly visible lung inflammation is shown in figure 1.02 (right panel). Therapeutic strategies employed to treat ARDS and ALI involve reduction of ventilation by mechanical measures to produce a tidal volume of approximately 6ml/kg body mass. This was based on findings in mice that revealed a high tidal volume increases the release of inflammatory mediators such as TNF- α and IL-6 (von Bethmann *et al.*, 1998). A trial into the effects of ventilation in ARDS patients revealed that patients with a tidal volume of 6.2ml/kg body mass had a significant reduction in mortality and organ failure compared to the control group with a tidal volume of 11.8ml/kg body mass (Network, 2000). These results supported earlier work by Amato *et al.* (1998) who also found that a reduction in tidal volume improved survival in ARDS patients. How this form of treatment is beneficial to ARDS patient is still not well understood but one explanation could be linked to the result of the hypercapnia that arises due to the nature of the therapy. Prin *et al.* (2002) reported a mean P_aCO₂ of 67 \pm 9 mmHg for ARDS patients undergoing treatment. This “permissive hypercapnia” - so called in that it must be tolerated in order for the treatment to have any benefits to the patient - may contribute to the effects on survival seen when tidal volume is reduced. Laffey *et al.* (2000) demonstrated in an *in vivo* rabbit model of ALI, that hypercapnia caused a reduction in pulmonary microvascular permeability as well as a decrease in the level of the proinflammatory cytokine TNF- α , compared to the normocapnic control group, implicating hypercapnia to have anti-inflammatory effects in response to lung injury. Similar findings were also reported by Sinclair *et al.* (2002) and De Smet *et al.* (2007).

These findings suggest hypercapnia can help reduce the inflammation associated with ARDS and ALI and so prevent progression of the disease. Although the current mechanism for how this occurs remains to be determined, it appears that hypercapnia can regulate the activity of NF- κ B, a master regulator of genes involved in inflammation and repair. Hypercapnia has been shown to reduce NF- κ B activation following stretch-induced injury of A459 cells, which was accompanied by a fall in the level of the proinflammatory cytokine IL-8 and an increase in cell viability (Contreras *et al.*, 2012). Similarly, Oliver *et al.* (2012) demonstrated that hypercapnia induced RelB (a member of the NF- κ B family) cleavage and nuclear translocation, in both A459 cells and in an *in vivo* rat model of lung injury, which corresponded with a reduction in the levels of TNF- α . These results suggest that CO₂ modulates NF- κ B signalling and consequentially expression of proinflammatory genes. In the lungs of newborn mice, Li *et al.* (2006) showed that hypercapnia induced downregulation of many genes involved in immune responses and supports the idea that hypercapnia can act as an anti-inflammatory agent to reduce progression of ARDS/ALI. These results were interesting in that mild hypercapnia (8% CO₂) had much more pronounced effects than severe hypercapnia (12% CO₂) suggesting cells are highly sensitive to the degree of CO₂ in which they are exposed.

Although there exists several studies which support the idea of hypercapnia as an anti-inflammatory agent, it is worth noting that other studies have reported that increasing CO₂ levels can actually trigger pulmonary inflammation. Murine lung tissue exposed to hypercapnia for one hour demonstrated an upregulation and increased secretion of the proinflammatory cytokines IL-6, IL-8 and MIP-2 (Abolhassani *et al.*, 2009). Interestingly, this was thought to be due to a CO₂-induced nuclear translocation of p65 (a member of the NF- κ B family) and not RelB as shown by Oliver *et al.*, (2012). MUC5AC protein levels, another marker of pulmonary inflammation, were also increased in hypercapnia. These findings provide fascinating insights and promote interesting debates into whether permissive hypercapnia does slow disease progression in ARDS/ALI. Given the contradictory nature of the findings, it reinforces the importance of fully understanding the effects of CO₂, particularly as a potential beneficial signalling molecule.

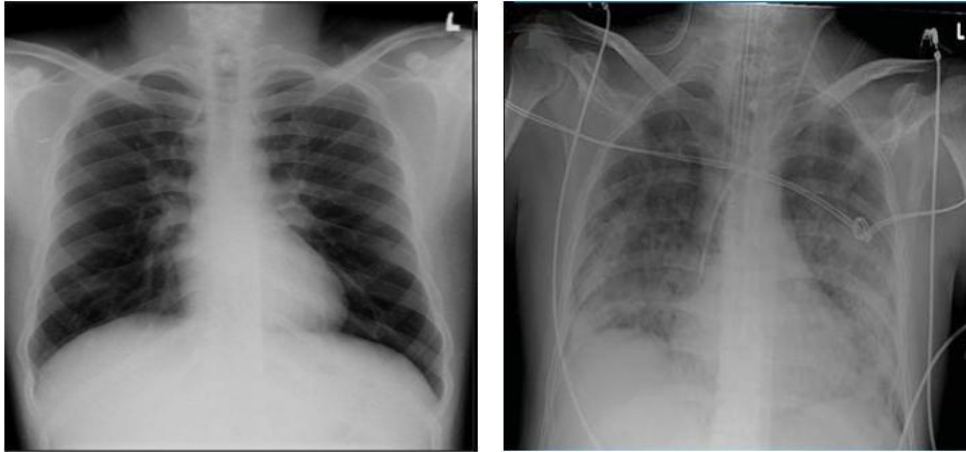


Figure 1.02: Chest X Rays to show the effects of ARDS on the lungs. Left image is of a healthy individual and was obtained from Karippacheril and Joseph (2010) whilst the right image is of an ARDS patient and was obtained from Mackay and Al Haddad (2009).

1.5. The role of bicarbonate in human physiology

The anion bicarbonate (HCO_3^-) plays an important role in mammalian physiology, particularly in the regulation of intracellular and extracellular pH. Its ability to be reversibly converted into CO_2 , *via* an reaction with H^+ , not only provides a way for HCO_3^- to diffuse across cell membranes in a gaseous form but it also forms the CO_2 - HCO_3^- buffer system to maintain the pH of body fluids (Marques *et al.*, 2003). The effect of CO_2 and HCO_3^- on pH is summarized by the Henderson-Hasselbalch equation which states that:

$$\text{pH} = \text{pK}_a + \log_{10} \left(\frac{[\text{HCO}_3^-]}{0.03 \times \text{pCO}_2} \right)$$

in which $\text{pK}_a = 6.1$ (the negative log of the carbonic acid dissociation constant).

Another critically important role for HCO_3^- is in mucosal protection of the GI Tract. A high HCO_3^- concentration in the stomach, combined with gastric mucins, provides the stomach mucosa with a protective barrier against stomach acid and pepsin (Flemstrom and Isenberg, 2001; Allen and Flemstrom, 2005). Mammalian pancreatic duct cells have been shown to secrete HCO_3^- in response to cAMP agonists, primarily forskolin and secretin (Banwell *et al.*, 1967; Ishiguro *et al.*, 1996) whereupon it helps solubilize digestive enzymes as well as neutralizing the acidic chyme entering the small intestine to provide the optimum conditions for pH-sensitive digestive enzymes to function (Scratcherd and Case, 1973). Further down the GI tract, Flemstrom *et al.* (1982) and (1984) showed HCO_3^- secretion to occur in the

mammalian duodenum whilst Seidler *et al.* (1997) have also demonstrated cAMP-regulated HCO_3^- secretion to occur in the duodenum, jejunum and ileum of mice. Here, HCO_3^- secretion again acts to neutralize gastric acid and thus protect the surface epithelium of the intestine. Another important role of HCO_3^- secretion in the GI tract, which has only recently come to light, is that it is important in mucus release. As shown in figure 1.03, it is known that mucins, the large glycoproteins that constitute mucus, are stored in mucin granules due to the presence of the cations Ca^{2+} and H^+ which allows negatively charged mucins to be tightly packed together. Chelation of these cations causes the negatively charged mucins to repel one another and thus expand to form the macromolecular structure of mucus. Indeed, in cervical tissue, mucus secretion is impaired when extracellular Ca^{2+} or extracellular H^+ are increased (Espinosa *et al.*, 2002) and there exists several studies that implicate HCO_3^- in having a major role in chelation of H^+ and Ca^{2+} . Garcia *et al.* (2009) demonstrated that prostaglandin and serotonin-stimulated mucus secretion in mouse intestine was impaired in the absence of serosal HCO_3^- or when mucosal HCO_3^- secretion was inhibited. Similar findings have also been reported by Gustafsson *et al.* (2012) who found reducing basolateral HCO_3^- in mouse ilea significantly increased the thickness of secreted mucus that was rescued by addition of apical HCO_3^- . Furthermore, HCO_3^- mimicked the effect of EGTA on mucus diffusivity in airway epithelia supporting the hypothesis that HCO_3^- acts to chelate Ca^{2+} and thus allow for efficient mucus expansion and release (Chen *et al.*, 2010). More recently, Ridley *et al.* (2014) studied the biophysical properties of MUC5B, a mucin found in the airways. They found that MUC5B bound Ca^{2+} at its N-terminal D3-domain which caused the formation of cross-links between the MUC5B polymers allowing them to be tightly condensed into vesicles. The conformational state of the polymers to allow for Ca^{2+} -mediated cross-links was dependent on a low pH in the vesicle. Therefore, this study proposed HCO_3^- secretion would induce a conformational change within the MUC5B polymers, abolish the Ca^{2+} -mediated cross-links, and allow for efficient mucus expansion and secretion. Together, these studies indicate that impaired epithelial HCO_3^- secretion, as observed in Cystic Fibrosis, a hereditary disease in which mutations in the gene for the Cl^- channel, Cystic Fibrosis Transmembrane Conductance Regulator (CFTR) leads to loss of functional expression at the apical membrane of secretory epithelia (see section 1.6.1), contributes to the thick, sticky mucus observed in mucus secreting organs that characterizes this disease. HCO_3^- transport can also act as a stimulus for important physiological processes to occur. For instance, fertilisation relies heavily on the presence of HCO_3^- . Both spermatogenesis in Leydig cells and capacitation of sperm inside the female reproductive tract require the transportation of HCO_3^- into sperm

cells to trigger cell signalling cascades that initiate these processes key to reproduction (Zeng *et al.*, 1995; Hess *et al.*, 2005). Thus it is clear that HCO_3^- has important roles in a variety of tissue in the body. However, currently it is its role in the lungs which is gaining major interest within the field of airway physiology and pathophysiology.

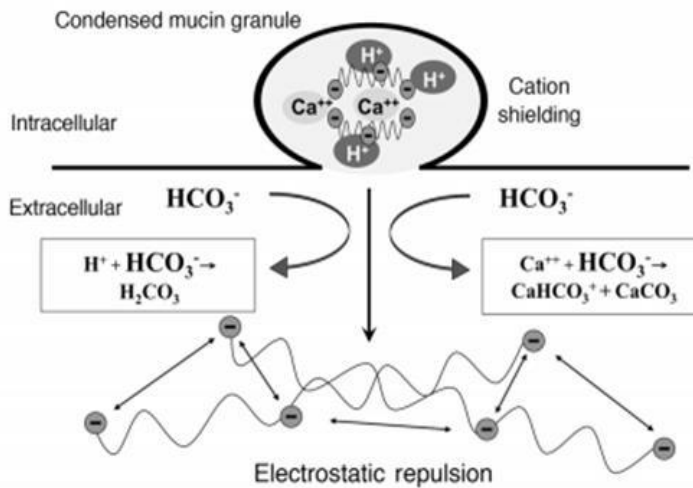


Figure 1.03. Hypothesis for the role of HCO_3^- secretion in mucus release and expansion from mucin granules. Chelation of the cations Ca^{2+} and H^+ by secreted HCO_3^- causes negatively charged mucins to repel one another and therefore rapidly expand when released from goblet or mucus cells. Figure taken from Garcia *et al.* (2009).

1.6. HCO_3^- Secretion in Human Airways

The human airways can be separated into two components: the conducting airways, which include the larynx, trachea, bronchi and bronchioles and are responsible for the transportation of gas inside the lungs; and the respiratory airways, which include the alveoli and which is the site of gas exchange (Fowler, 1948). Lining the conducting airways is a thin layer of fluid (6-10 μm) known as the airway surface liquid (ASL) which is shown in figure 1.04.

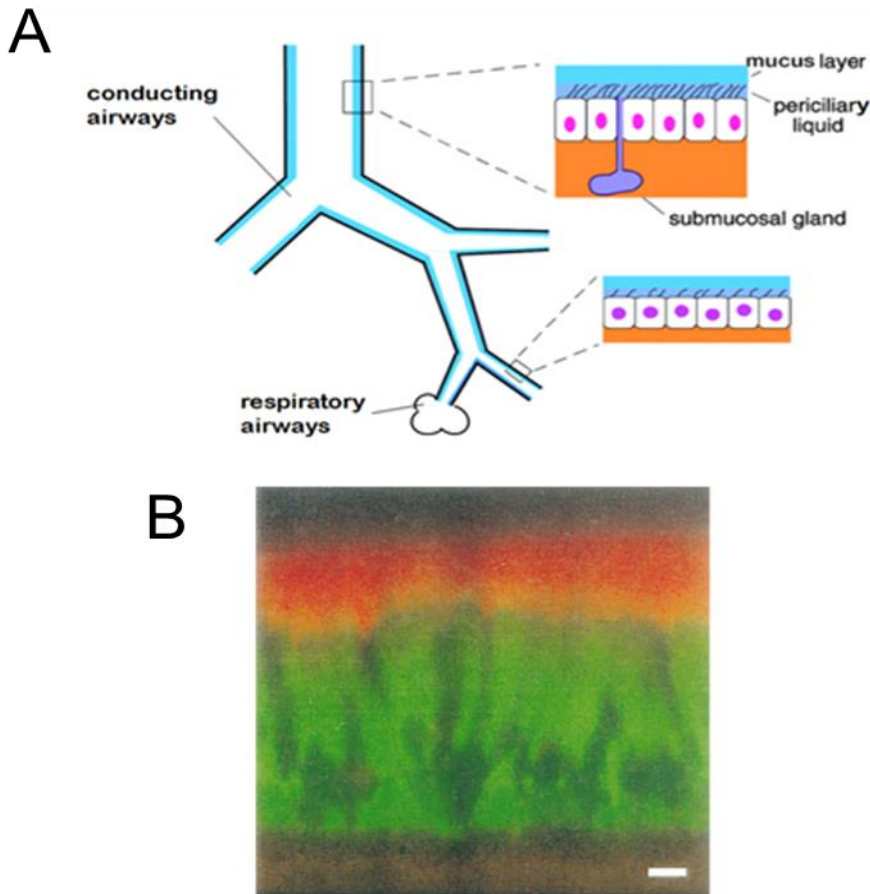


Figure 1.04: The conducting airways are covered with a thin layer of airway surface liquid (ASL). (A) is a cartoon representation of where the ASL is located in the airways. Figure adapted from Verkman (2002). (B) shows an *in vitro* image of human tracheobronchial epithelial cells stained green using 10 μ M calcein/AM and the overlying fluid stained using dextrans conjugated to Texas Red. Figure taken from Matsui *et al.* (1998) .

The ASL consists of two layers: the underlying periciliary layer and the overlying mucus layer. The mucus layer predominantly consists of water and mucins and is responsible for trapping inhaled pathogens, which are removed by subsequent mucociliary clearance (Matsui *et al.*, 1998; Knowles and Boucher, 2002). Airway mucins have been shown to bind a variety of pathogens, notably *Pseudomonas aeruginosa* (Vishwanath and Ramphal, 1984) and *Haemophilus influenzae* (Kubiet and Ramphal, 1995), and this forms part of the innate defence of the lung to inhaled pathogens. The periciliary layer consists of salts and water and both the volume and pH of the periciliary layer are important for efficient mucociliary clearance and maintenance of mucus properties (Bhaskar *et al.*, 1991; Tarran *et al.*, 2006). The importance of tight regulation of the ASL pH was demonstrated by Pezzulo *et al.* (2012)

who showed that killing of *Staphylococcus aureus* was impaired when porcine ASL pH was reduced from ~7.9 to ~7.4. Furthermore, airway antimicrobial peptide activity was also impaired at the lower pH. These findings demonstrate the importance of HCO_3^- in ASL, not only in accommodating efficient mucus expansion (as discussed in 1.5.) but also in regulation of pH-sensitive innate defence mechanisms of the airways. The traditional model of the ASL is that it exists as a “gel on liquid” form. However, this was recently challenged by Button *et al.* (2012) who suggested that the periciliary layer is a mesh due to the presence of mucins tethered to the cilia of epithelial cells that effectively form a periciliary brush (fig. 1.05) to prevent the overlying mucus from clogging the periciliary layer and impairing ciliary beat frequency.

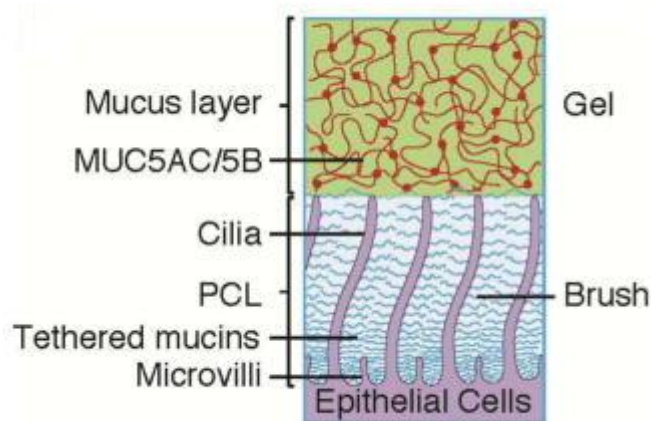


Figure 1.05: Schematic diagram of how the periciliary layer may exist as a mesh due to the presence of mucins tethered to the cilia of surface epithelia. Figure taken from Button *et al.* (2012).

In the upper airways, the periciliary layer composition and volume is primarily controlled by the submucosal glands which contain a subset of cells known as serous cells (fig. 1.06). These cells are able to secrete Cl^- , to provide a driving force for water transport, and HCO_3^- , to control both the volume and the pH of the secreted fluid. Ballard *et al.* (1999) provided clear evidence that the site for the majority of ASL secretion is from glands lying below the mucosal layer rather than surface epithelia itself by demonstrating that in porcine airways, acetylcholine-stimulated fluid secretion was unaffected when the surface epithelia was removed. Further *ex vivo* studies on intact submucosal glands from porcine, murine and human airways, show fluid secretion is increased in response to a variety of stimuli including

carbachol, VIP and forskolin (Joo *et al.*, 2002; Ianowski *et al.*, 2007). Whilst many studies have clearly shown SMGs to mediate fluid secretion, less attention has been paid to the composition of this fluid, specifically the role for HCO_3^- in the fluid. In 1992, Smith and Welsh were the first to suggest HCO_3^- is secreted across airway epithelia by demonstrating a reduction in forskolin-induced short-circuit current (I_{sc}) across human nasal epithelia in the absence of HCO_3^- (Smith and Welsh, 1992). *In vitro* studies on a model human serous cell line (Calu-3) have also revealed HCO_3^- to be a key component of the fluid secreted from these cells. Devor *et al.* (1999) used I_{sc} measurements to show that forskolin stimulated an I_{sc} across the Calu-3 cell that was reduced upon the removal of HCO_3^- from the bath solution suggesting HCO_3^- is secreted from the Calu-3 cell (Devor *et al.*, 1999). This supported previous work by Lee *et al.* (1998) who discovered that forskolin-stimulated I_{sc} in Calu-3 cell was not due to Cl^- or Na^+ flux and was reduced when HCO_3^- was removed suggesting that the majority of the forskolin-stimulated I_{sc} was due to HCO_3^- flux. Similarly, Garnett *et al.* (2011), Shan *et al.* (2012) and Huang *et al.* (2012) have all demonstrated that HCO_3^- secretion occurs in Calu-3 cells. This work indicates that serous cells possess the necessary machinery for both Cl^- and HCO_3^- secretion.

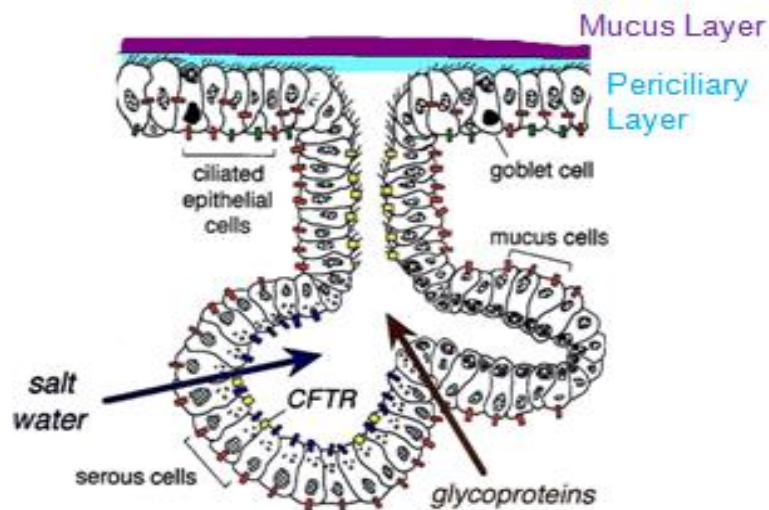


Figure 1.06: The submucosal gland is responsible for the majority of the airway surface liquid and mucus secretion. Serous cells of the submucosal gland are heavily involved in regulating the volume and the composition of the ASL due to their coordinated activity of surface ion transporters. Figure adapted from Salinas *et al.* (2005).

1.6.1. Role of CFTR and Anion Exchangers in HCO_3^- Secretion

Serous cells of the SMG express high levels of CFTR on the apical surface (Engelhardt *et al.*, 1994). CFTR is a Cl^- channel that belongs to the ATP-binding cassette (ABC) family of transporters and is expressed on the apical membrane of surface epithelia. CFTR consists of two transmembrane spanning domains, each containing 6 transmembrane spanning segments and 2 nucleotide binding domains (NBD1 and NBD2). The two transmembrane spanning domains are joined by a regulatory (R) domain which possesses 9 consensus sites for phosphorylation by PKA as well as sites for PKC phosphorylation (Riordan *et al.*, 1989; Picciotto *et al.*, 1992; Sheppard and Welsh, 1999). The 3D structure of CFTR is shown in figure 1.07A. Upon CFTR phosphorylation of the R domain, a conformational change occurs in the R domain which allows the two NBDs to interact and bind ATP causing the channel to open. Subsequent ATP hydrolysis at NBD2 results in channel closure (fig. 1.07B). The requirement for both CFTR phosphorylation as well as ATP in channel gating was shown by Anderson *et al.* (1991) who demonstrated that CFTR activity was dependent on PKA phosphorylation and the presence of MgATP.

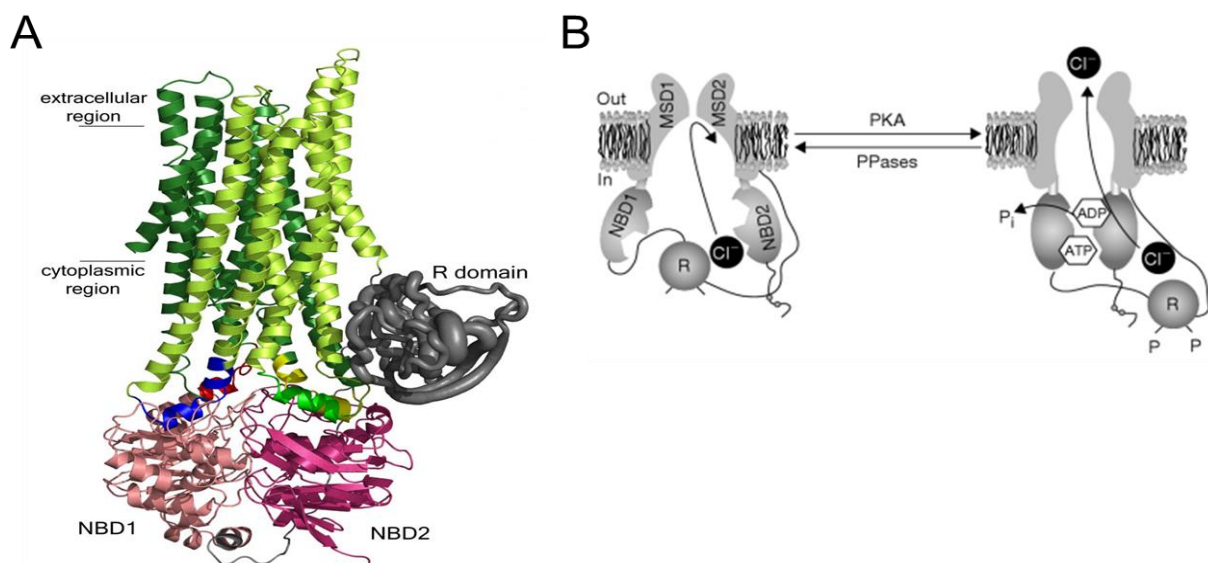


Figure 1.07: Structure and gating of CFTR. (A) shows a 3D homology model in which the two membrane spanning domains (MSDs) are shown in green and the two nucleotide binding domains (NBDs) are shown in pink. The regulatory (R) domain is shown in grey. Figure taken from Serohijos *et al.* (2008). (B) displays how PKA-dependent phosphorylation of the R domain facilitates a conformational change in CFTR to allow ATP to bind to the NBDs and induce channel opening and Cl^- secretion. ATP hydrolysis at NBD2 closes the channel. Figure taken from Chen *et al.* (2006).

The major signalling pathway that regulates CFTR activity is the cAMP/PKA pathway and activation of CFTR stimulates transepithelial Cl^- and fluid secretion in CFTR-expressing tissues (Cheng *et al.*, 1991; Haws *et al.*, 1994; Cobb *et al.*, 2002; Cobb *et al.*, 2003; Derand *et al.*, 2004; Hentchel-Franks *et al.*, 2004). The role of CFTR-dependent anion secretion and subsequent fluid secretion has been studied extensively in the airways. Joo *et al.* (2002) demonstrated that cAMP-elevating agonists, Vasoactive Intestinal Peptide (VIP) and forskolin, increased fluid secretion from submucosal glands which was absent in glands isolated from non CFTR-expressing tissue. Studies performed on Calu-3 cells revealed that treatment with a variety of phosphodiesterase inhibitors that increase cAMP levels activates electrogenic Cl^- secretion which is inhibitable by the non-specific CFTR inhibitor glybenclamide (Cobb *et al.*, 2002) whilst stimulation of Calu-3 cells with VIP induced efflux of I^- which was sensitive to H-89 and glybenclamide but not DIDS suggesting VIP activated PKA-regulated, CFTR-dependent I^- transport (Derand *et al.*, 2004). Similarly, Rollins *et al.* (2008) demonstrated that activation of the adenosine receptor subtype $\text{A}_{2\text{B}}$, a G_s coupled receptor that stimulates adenylyl cyclase and cAMP production, caused CFTR-dependent fluid secretion in primary human bronchial epithelia. Not only does CFTR stimulate Cl^- secretion but it also inhibits the epithelial Na^+ channel, ENaC, to prevent Na^+ reabsorption from the lumen of the airways and thereby further increasing the osmotic gradient for water transport (Mall *et al.*, 1999). Lee and Foskett (2010) have suggested an alternative mechanism of cAMP-dependent CFTR activation. Studies on primary porcine serous cells revealed that stimulation of cells with the cAMP agonists VIP and forskolin also induced an elevation in $[\text{Ca}^{2+}]_\text{i}$, a process that was PKA-dependent. The researchers suggested that this cAMP-induced increase in $[\text{Ca}^{2+}]_\text{i}$ caused Ca^{2+} activated K^+ channels to increase the electrochemical driving force for Cl^- secretion *via* CFTR. Furthermore, they showed mouse serous cells were unable to secrete fluid in response to cAMP agonists because there was no accompanying increase in $[\text{Ca}^{2+}]_\text{i}$ (Lee and Foskett, 2012). Only when Ca^{2+} -activated K^+ channels were activated with 1-EBIO did forskolin stimulate fluid secretion from mouse serous cells and highlights the importance of cAMP and Ca^{2+} crosstalk in order to regulate CFTR-dependent ion and fluid secretion. The role of CFTR in mediating fluid secretion has been well described but what is less well known is how it also regulates HCO_3^- secretion in the airways.

Although research has shown airway HCO_3^- secretion to be cAMP-activated and CFTR-dependent, how this HCO_3^- secretion is achieved is still controversial. Illek *et al.* (1997)

recorded I_{sc} in Calu-3 cells and demonstrated a cAMP-induced I_{sc} which possessed a HCO_3^- dependent component. The HCO_3^- induced I_{sc} was activated by the CFTR modulator genistein and inhibited by the CFTR blocker glybenclamide leading the researchers to conclude that CFTR directly mediates HCO_3^- efflux. This was supported by studies performed on pancreatic duct cells that showed CFTR to possess HCO_3^- transporting capabilities (Ishiguro *et al.*, 1996). Shan *et al.* (2012) also proposed that HCO_3^- is secreted through CFTR in the airways as they found HCO_3^- secretion to be blocked by the CFTR inhibitor GlyH-101, as well as by genetic knockdown of CFTR in Calu-3 cells. The importance of CFTR in regulating HCO_3^- secretion is highlighted when studying HCO_3^- transport in CF tissue. Impaired HCO_3^- secretion has been shown in a number of different CF tissue including CF canine airways (Smith and Welsh, 1992), CF murine intestinal epithelia (Xiao *et al.*, 2012), CF human nasal epithelia (Paradiso *et al.*, 2003) as well as in cell lines transfected with mutant CFTR (Choi *et al.*, 2001). Furthermore, Coakley *et al.* (2003) demonstrated that cultured primary human bronchial epithelia (HBEs) were able to secrete HCO_3^- in response to an acidic ASL, a process enhanced by intracellular cAMP elevations. However, HBEs isolated from CF patients were unable to alkalinize an acidic ASL in basal or cAMP elevated conditions, consistent with impaired CFTR-dependent HCO_3^- secretion in these cells. Similar findings were reported by Paradiso *et al.* (2003) who found that the rate of HCO_3^- secretion in primary nasal epithelia isolated from CF patients was significantly lower than that of non-CF nasal epithelia. In addition, forskolin was only able to increase the rate of HCO_3^- secretion in non-CF cells. Therefore, whilst it is clear CFTR plays a major role in HCO_3^- secretion, more recently it has been speculated, that in some tissue at least, CFTR may indirectly regulate HCO_3^- secretion due to the activation of associated Cl^-/HCO_3^- exchangers. Studies performed in kidney cells, intestinal cells and pancreatic duct cells have revealed that members of the SLC26 family of Cl^-/HCO_3^- exchangers, SLC26A3, SLC26A4 and SLC26A6, function to secrete HCO_3^- in these tissue (Soleimani *et al.*, 2001; Stewart *et al.*, 2011). Studies into SLC26 family members interactions with CFTR have shown that SLC26A9, a SLC26 family member transporter expressed in airway epithelia (Lohi *et al.*, 2002), acted as a cAMP-stimulated Cl^- channel when coexpressed with CFTR in HEK 293T cells and that SLC26A9 activity in HBE cells was also dependent on CFTR expression (Bertrand *et al.*, 2009). A recent study by Anagnostopoulou *et al.* (2012) showed that SLC26A9 played an important role in Cl^- secretion in response to IL-13 to prevent airway mucus obstruction in mice. In 2011, our laboratory revealed that the Cl^-/HCO_3^- exchanger SLC26A4 (pendrin) directly regulated HCO_3^- secretion in Calu-3 cells (Garnett *et al.*, 2011).

However, pendrin activity was markedly reduced in the presence of the CFTR inhibitor GlyH-101, and the PKA inhibitor H-89, as well as being reduced in CFTR KD cells, showing that CFTR regulated pendrin activity. However, how this is achieved is still not fully understood. SLC26 transporters physically and functionally interact with the phosphorylated R domain of CFTR *via* their STAS domain as described by Ko *et al.* (2004) and Avella *et al.* (2011) and illustrated in figure 1.08. Furthermore, most SLC26 transporters possess a PDZ binding domain; a protein-protein interaction module consisting of 80-100 amino acids (Lee and Zheng, 2010), which enable them to bind to PDZ binding scaffold proteins, for example CAP70 (Rossmann *et al.*, 2005) or NHERF1 (Lohi *et al.*, 2003). These scaffold proteins are also bound to CFTR, thus tethering both transporters within the same macromolecular complex. However, pendrin does not possess a C-terminal PDZ domain so therefore must associate with CFTR in an alternative, and as of yet unidentified, mechanism.

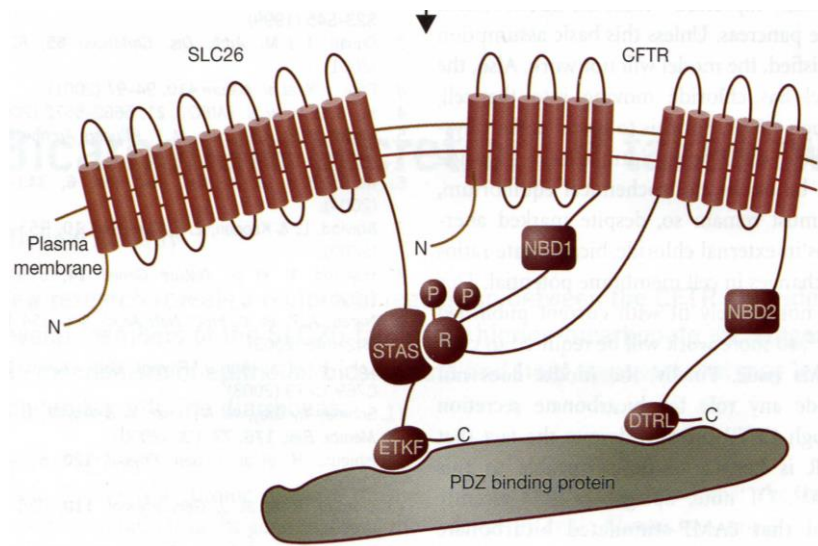


Figure 1.08: The physical and functional interaction between CFTR and SLC26 transporters. The phosphorylated R domain of CFTR binds to SLC26 transporters *via* their STAS domain to enables CFTR to directly regulate the activity of the SLC26 anion exchangers. Figure taken from Gray (2004).

1.6.1.2. CFTR is contained within a macromolecular complex

CFTR regulation by cAMP signalling is more complex than first believed. This is because CFTR is contained within a macromolecular complex at the apical membrane which forms a microdomain to localize the cAMP signalling machinery to the site of CFTR (fig 1.09). Sun *et al.*, (2000) demonstrated that at the apical membrane of Calu-3 cells, CFTR binds to the

PDZ binding protein Na⁺/H⁺ Exchanger regulatory factor 1 (NHERF1) (Sun *et al.*, 2000b). NHERF1 interacts with the anchor protein Ezrin which in turn is bound to actin to indirectly tether CFTR to the cytoskeleton. PKA also binds to Ezrin which enables PKA to be colocalized with CFTR to enable efficient CFTR activation (Sun *et al.*, 2000a). CFTR is able to be activated by compartmentalized cAMP signalling, as shown by Huang *et al.* (2001) who used cAMP measurements and patch-clamp experiments to show that although apical adenosine caused very little increase in total cellular cAMP compared to forskolin, the extent of CFTR activation between the two agonists was very similar. These findings suggest stimulation of adenosine receptors produces a highly compartmentalized cAMP signal which is sufficient to activate CFTR. Compartmentalization of cAMP signalling has also been proposed by Barnes *et al.* (2005) who showed that inhibition of phosphodiesterase 4D did not significantly increase total [cAMP]_i but was able to stimulate CFTR activity in Calu-3 cells. This suggests that inhibition of specific PDE activity only increases cAMP levels at a specific microdomain of the cell. In addition, inhibition of PKA reduced the activity of phosphodiesterase 4D which demonstrated the relationship that exists between cAMP signalling components. Furthermore, Penmatsa *et al.* (2010) demonstrated that, in HEK cells, phosphodiesterases are also located within a microdomain with CFTR by showing PDE3 coimmunoprecipitated with CFTR, an interaction which was increased after PKA activation. Together, these data show that the components required for cAMP signal transduction and termination are all contained within a microdomain to allow for efficient cAMP-regulated CFTR activation without affecting other cAMP-dependent processes in other parts of the cell.

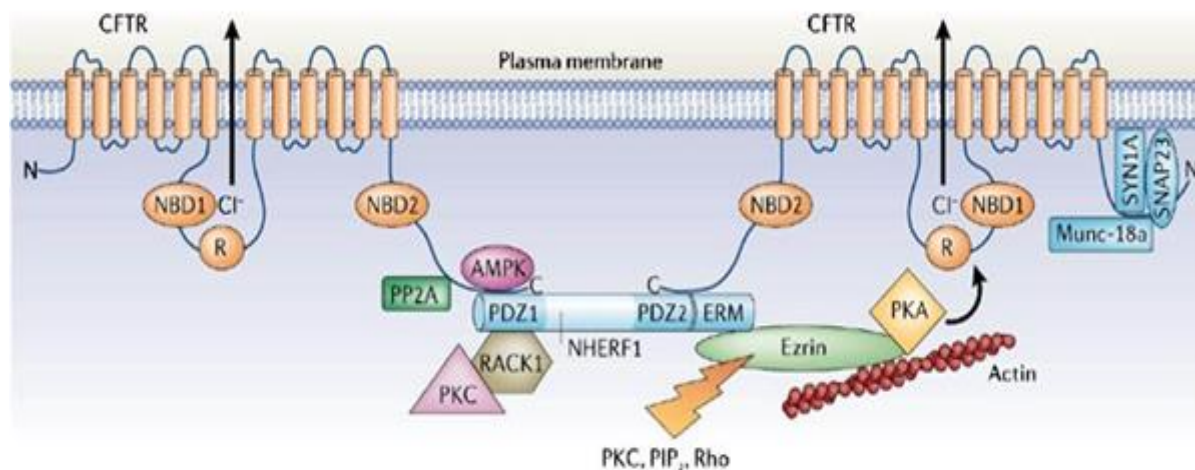


Figure 1.09. CFTR is contained within a macromolecular complex at the apical membrane of airway cells to allow compartmentalization of the cAMP signalling machinery. NHERF1 (Na⁺/H⁺ exchange regulatory factor 1) interacts with Ezrin to provide a scaffold for PKA as well as interacting with actin to tether the microdomain to the cytoskeleton. Figure taken from Guggino and Stanton (2006)

1.6.2. Sodium Bicarbonate Cotransporters

Whereas CFTR and Pendrin appear to mediate the apical efflux of HCO₃⁻ in human airway Calu-3 cells, HCO₃⁻ influx from the blood is believed to be controlled by NBCs. NBCs perform different functions depending on their expression in different tissue. For instance, an electrogenic Na⁺/HCO₃⁻ cotransporter expressed in the kidney (kNBCe1) mediates HCO₃⁻ reabsorption whereas the same transporter expressed in the pancreas mediates HCO₃⁻ secretion (Ruiz and Arruda, 1992; Jacob *et al.*, 2000) with the major difference between the two isoforms being the differences in stoichiometry of each transporter. In non HCO₃⁻ secreting tissue, NBCs act to regulate intracellular pH; for example in epididymal epithelium in which pH_i recovery from an acid load is both Na⁺ and HCO₃⁻-dependent and is prevented by non-specific pharmacological inhibition of NBC (Zuo *et al.*, 2011). However, in HCO₃⁻ secreting tissue, NBCs have another role; to transport HCO₃⁻ from the blood and accumulate it into the cell. Studies performed on rabbit colonic crypts have shown that Na⁺-dependent HCO₃⁻ uptake across the basolateral membrane was activated by forskolin and inhibited by the NBCe1 inhibitor S089 demonstrating the role of NBCe1 in cAMP-stimulated HCO₃⁻ transport (Bachmann *et al.*, 2003). Genetic knockdown of an electroneutral Na⁺/HCO₃⁻ cotransporter (NBCn1) in mice show a significant reduction in forskolin-stimulated HCO₃⁻ secretion in the duodenum and highlights the importance of these cAMP-regulated

transporters in HCO_3^- secreting epithelia (Chen *et al.*, 2012). In Calu-3 cells, Devor *et al.* (1999) demonstrated that forskolin-stimulated HCO_3^- secretion is markedly reduced when a) Na^+ is absent from the serosal solution and b) DNDS or ouabain are present at the basolateral membrane thus implicating a role for NBC in accumulation of intracellular HCO_3^- for secretion at the apical membrane. These findings are supported by Shan *et al.* (2012) who have also shown HCO_3^- secretion to be Na^+ -dependent in Calu-3 cells. Furthermore, Calu-3 cells also express both NBCe1 and NBCe2 on their basolateral membranes (Kreindler *et al.*, 2006). Studies on porcine bronchi show that removal of Na^+ from the serosal solution markedly inhibits forskolin-stimulated fluid secretion although, surprisingly, this has no effect on HCO_3^- concentration of the secreted fluid suggesting that basolateral NBC is responsible for mediating fluid secretion yet cells may possess other mechanisms to ensure that the pH of secreted fluid is maintained e.g. Na^+/H^+ exchangers (Ballard *et al.*, 1999). These findings demonstrate the importance of coordinating the activity of both apical and basolateral HCO_3^- transporters to achieve efficient HCO_3^- secretion in the airways and other HCO_3^- secretory tissue.

1.6.3. Model of anion secretion in Calu-3 cells

A current model for anion secretion in Calu-3 cells is shown in figure 1.10. The model includes the key pH_i regulatory transporters that have been shown to be expressed in Calu-3 cells. At the basolateral membrane, HCO_3^- enters the cell from the serosa due to the activity of the cAMP-regulated NBCs with a Na^+ gradient maintained by the basolateral Na^+/K^+ ATPase (not included in fig 1.10). At the apical membrane, activation of CFTR promotes Cl^- efflux as well as stimulation of the $\text{Cl}^-/\text{HCO}_3^-$ exchanger pendrin. This enables HCO_3^- secretion to occur across the apical membrane *via* pendrin, whilst Cl^- is recycled due to the coordinated activity of both CFTR and pendrin. Importantly, our laboratory has shown that increases in intracellular cAMP inhibit the basolateral $\text{Cl}^-/\text{HCO}_3^-$ exchanger (AE2) (Garnett *et al.*, 2011; Garnett *et al.*, 2013) to prevent loss of intracellular HCO_3^- across the basolateral membrane.

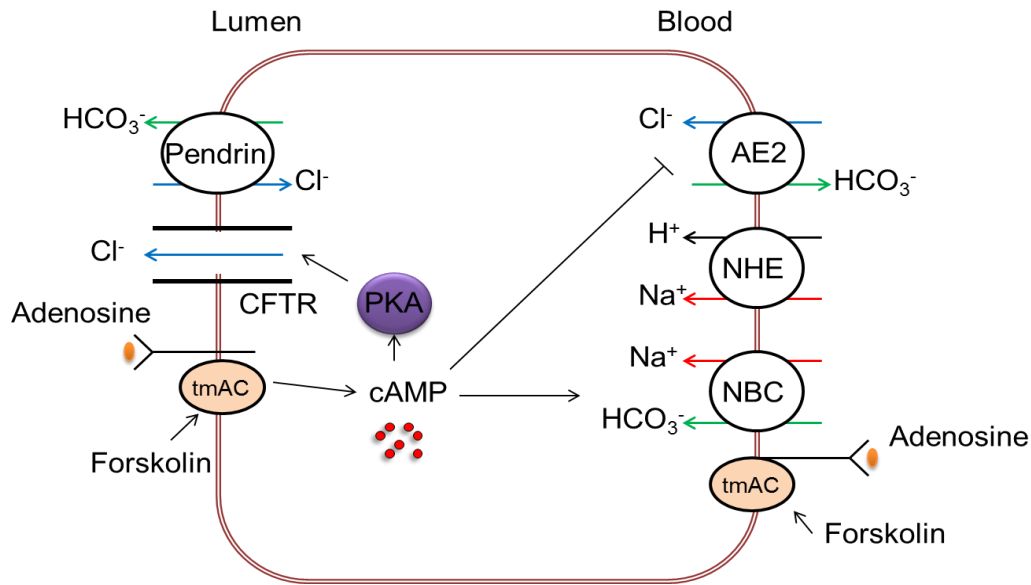


Figure 1.10: A model of anion secretion in the Calu-3. This model demonstrates how Calu-3 cells achieve HCO_3^- secretion upon stimulation by a cAMP agonist. CFTR = Cystic fibrosis transmembrane conductance regulator; NHE = Na^+/H^+ Exchanger; NBC = $\text{Na}^+/\text{HCO}_3^-$ Cotransporter; tmAC = transmembrane adenylyl cyclase; AE2 = anion exchanger 2.

1.7. Hypothesis and Aims

Given that hypercapnia has been shown to affect cAMP signalling in mammalian cells (Townsend *et al.*, 2009; Cook *et al.*, 2012) and knowing that cAMP plays a major role in the efficient secretion of HCO_3^- in airway epithelia, I hypothesise that hypercapnia will cause a dysregulation of cAMP-dependent HCO_3^- secretion in Calu-3 cells.

The major aim of the current study was to investigate the effect of acute and chronic hypercapnia on cAMP-regulated ion and fluid transport in a model human airway epithelial cell line.

The specific aims of this work were to:

- assess whether hypercapnia can affect intracellular cAMP levels in a model of human airway epithelial cells.

- study transepithelial ion and fluid transport in a polarised monolayer of human airway epithelia and deduce whether hypercapnia can alter the activity of known HCO_3^- transporters in these cells.
- understand the key signalling components involved in any CO_2 -induced alterations in ion and fluid transport.
- investigate the effects of chronic hypercapnia in a clinically-relevant setting by observing whether hypercapnia can alter the wound healing ability of Calu-3 cells.

Chapter 2: Methods

2.1. Cell Culture

All cell culture techniques were carried out in a class II vertical laminar flow hood (Jouan Ltd, UK). All equipment was sterilized prior to use and all consumables were pre-warmed to 37°C in a water bath prior to use. Calu-3 cells (ATCC HTB-55) (Shen *et al.*, 1994) were grown in 75cm² flasks (Corning) in 30mls of culture medium consisting of Eagle's Minimum Essential Medium (EMEM) supplemented with 10% fetal calf serum, 1% non-essential amino acids, 2mM L-Glutamine, 100Uml⁻¹ penicillin and 100µgml⁻¹ streptomycin. Cells were initially seeded at 3 x 10⁶ cells/flask and became confluent after 7 days. Cells were incubated at 37°C in humidified air containing 5% (v/v) CO₂ and were only used between passage 20 and passage 50. To subculture cells, the media was removed and cells were washed 3 times with sterile phosphate buffered saline (PBS). Cells were then incubated in 5ml of trypsin solution (0.05% trypsin and 0.02% ethylenediaminetetraacetic acid (EDTA) in Earle's balanced salt solution) for 20 minutes in a humidified incubator at 37°C. When approximately 50% of cells had detached, these cells were added to 10mls pre-warmed culture medium and a further 5ml of trypsin solution was added to the flask and incubated for another 20 minutes. This ensured the remaining cells detached and these cells were added to the culture medium. The resulting cell suspension was centrifuged at 1500g for 3 minutes. The supernatant was discarded and the cell pellet was re-suspended in 10 ml of media before cells were seeded as required.

2.2. Transepithelial Resistance Measurements

The transepithelial electrical resistance (TEER) was routinely measured using an epithelial voltohmmeter (World Precision Instruments, UK) to determine when cells had formed a polarized monolayer which generally occurred after 6 days as indicated by a transepithelial electrical resistance of above 600Ω cm⁻² (fig. 2.01). All resistance measurements presented in this work are corrected for the resistance of an empty transwell which was calculated as 111 ± 4 Ω cm⁻² (n=6).

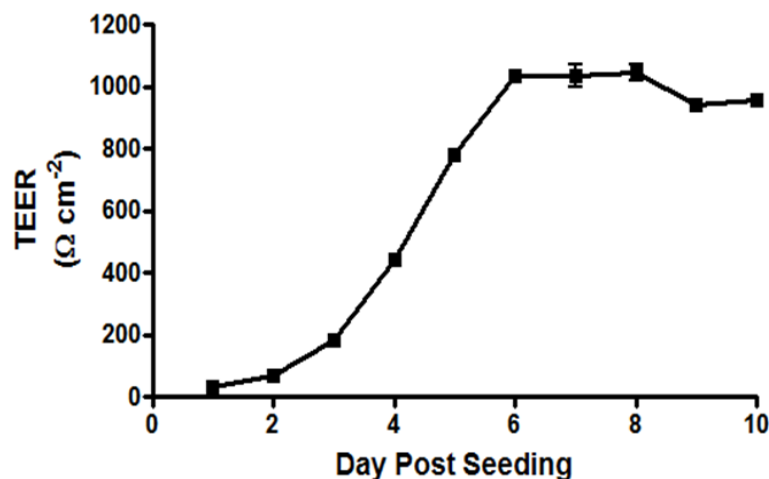


Figure 2.01: Change in the transepithelial electrical resistance (TEER) of Calu-3 cells grown as a polarised monolayer on permeable transwell supports. Each data point represents mean \pm S.E.M., $n = 6$ for each.

2.3. Short circuit current measurements using an Ussing Chamber

The Ussing Chamber, named after its founder Hans Ussing (Ussing and Zerahn, 1951), is a device that allows for the measurement of transepithelial ion transport across epithelial cells by recording the short-circuit current (I_{sc}) across a monolayer of epithelia. The I_{sc} is the current required to clamp the transepithelial voltage (V_{te}) to 0mV and thus changes in I_{sc} reflect changes in ion transport across the epithelial monolayer. Calu-3 cells were cultured on to 12 mm permeable Snapwell supports with 0.4 μ m pore polyester membrane insert (Corning, UK) at a seeding density of 2.5×10^5 cells/well and were studied 8-10 days post-seeding. Snapwells were mounted into the Ussing chamber in which each chamber was connected to a calomel voltage sensing electrode and a AgCl₂ current sensing electrode (both stored in 3M KCl) by 3M KCl salt bridges containing 3% Agar (fig. 2.02). The potential difference between the two chambers was offset prior to recording. Cells were bathed in 7.5mls of Krebs solution that were gassed with either 5% (v/v) CO₂/95% (v/v) O₂ for control conditions or 10% (v/v) CO₂/90% (v/v) O₂ to induce acute hypercapnia. Pharmacological agents were prepared as a concentrated stock solution and the appropriate amount of drug was added to the chamber in order to generate the desired working concentration. To measure the I_{sc} , the cells were clamped at 0mV using a DVC-1000 Voltage/Current Clamp (WPI) and a Powerlab 1200 feedback amplifier (AD Instruments) injected the appropriate current to keep V_{te} at 0mV. This was recorded as the I_{sc} . To monitor transepithelial resistance (R_{te}), a 2

second 10mV pulse was applied every 30 seconds and the resulting increase in current enabled R_{te} to be calculated using Ohms Law. V_{te} was recorded using Scope 3 software (AD Instruments).

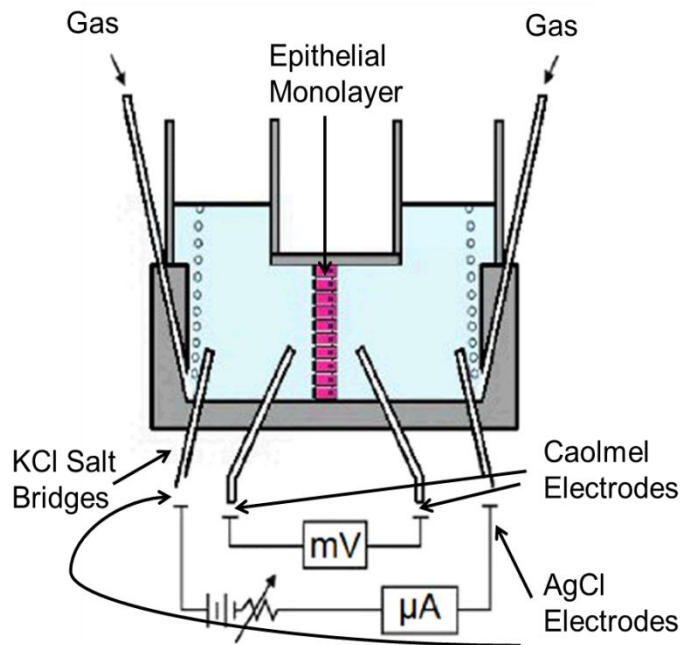


Figure 2.02: Diagram to show how short-circuit current was measured using an Ussing chamber. Calu-3 cells were grown as a polarised monolayer on permeable Snapwell supports, inserted into an Ussing chamber which was bathed in 7.5mls of Krebs solution. The chamber was connected to voltage sensing calomel electrodes and current sensing AgCl electrodes by KCl salt bridges. Figure adapted from Rasgado-Flores *et al.* (2013).

2.4. Intracellular pH Measurements

In order to investigate HCO_3^- transport in Calu-3 cells, real-time intracellular pH measurements were performed. Cells were cultured on 12mm permeable Transwell supports with 0.4 μm pore polyester membrane insert (Corning, UK) at an initial seeding density of 2.5×10^5 cells/well and were studied 8-12 days post-seeding. Cells were washed in NaHEPES solution and incubated for one hour in NaHEPES containing 10 μM 2'-7'-bis(carboxyethyl)-5(6)-carboxyfluorescein acetoxymethyl ester (BCECF-AM) added to the apical compartment. Cells were then mounted on to the stage of a Nikon fluor inverted microscope (magnification of x60 with a numerical aperture of 0.70) Krebs solutions were gassed with 5% (v/v) CO_2 /95% (v/v) O_2 for control conditions and this gas composition was altered to 10% (v/v) CO_2 /90% (v/v) O_2 to induce hypercapnia. Solutions were perfused across

the apical and basolateral compartments of the cell at 37°C at a speed of 3ml/min (apical) and 6ml/min (basolateral). pH_i was measured using a Life Sciences Microfluorimeter System. Cells were alternatively excited at 490 nm (H^+ -sensitive) and 440 nm (H^+ -insensitive) wavelengths every 1.024s by a 75W xenon short arc lamp (Osram, Germany) using a rainbow filter wheel (Life Sciences Resources, UK) and a dichroic mirror allowed omitted light to be collected at 510 nm. The ratio of 490 nm emission to 440 nm emission was recorded using PhoCal 1.6b software and was converted into a pH_i value using the standard curve obtained from the intracellular pH_i calibration (see section 2.4.1.). For analysis of pH_i measurements, ΔpH_i was determined by calculating the mean basal pH_i over a time period of 60 seconds before and after a solution change. This was then subtracted from the mean pH_i that results as a consequence of the solution change. Rate of pH_i change ($\Delta\text{pH}_i/\Delta t$) was determined by performing a linear regression over a period of no less than 30 seconds of data (see figure 2.03). The $\Delta\text{pH}_i/\Delta t$ was converted to transmembrane HCO_3^- efflux ($-J(\text{B})$) by multiplying $\Delta\text{pH}_i/\Delta t$ by total buffering capacity of the cell (β_{tot}). $\beta_{\text{tot}} = \beta_i + \beta_{\text{HCO}_3^-}$ where β_i represents the intrinsic buffering capacity and $\beta_{\text{HCO}_3^-}$ is the $\text{CO}_2\text{-HCO}_3^-$ buffer system-dependent buffering capacity (see section 2.4.2.).

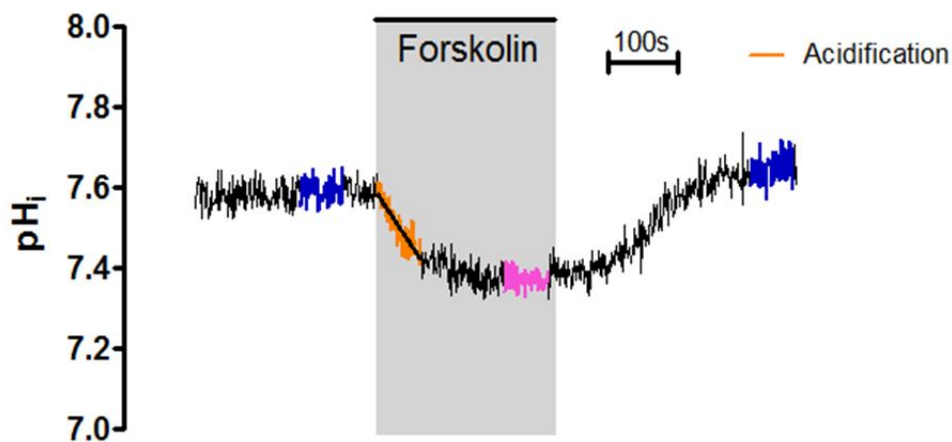


Figure 2.03. Analysis of pH_i experiments. Change in pH_i was measured by calculating the mean pH_i before and after treatment (navy blue areas) and subtracting the steady state pH_i resulting from treatment (pink area). To measure rate of pH change ($\Delta\text{pH}_i/\Delta t$), a linear regression was performed on at least 30seconds of data during pH change as shown in orange.

2.4.1. Intracellular pH Calibration

Cells were treated the same way as in *Intracellular pH Measurements* but this time were perfused with high K^+ solutions (120mM K^+) containing 10 μ M nigericin and each set to a known pH. Nigericin is a K^+/H^+ exchanger ionophore to activate K^+/H^+ exchange which allowed intracellular $[H^+]$ to equilibrate with extracellular $[H^+]$ (Hegyi *et al.*, 2003). 490/440 ratios were converted into a pH_i using the standard curve as shown in figure 2.04B. Several calibrations were performed throughout the duration of this work in order to routinely calibrate intracellular pH in different batches of Calu-3 cells.

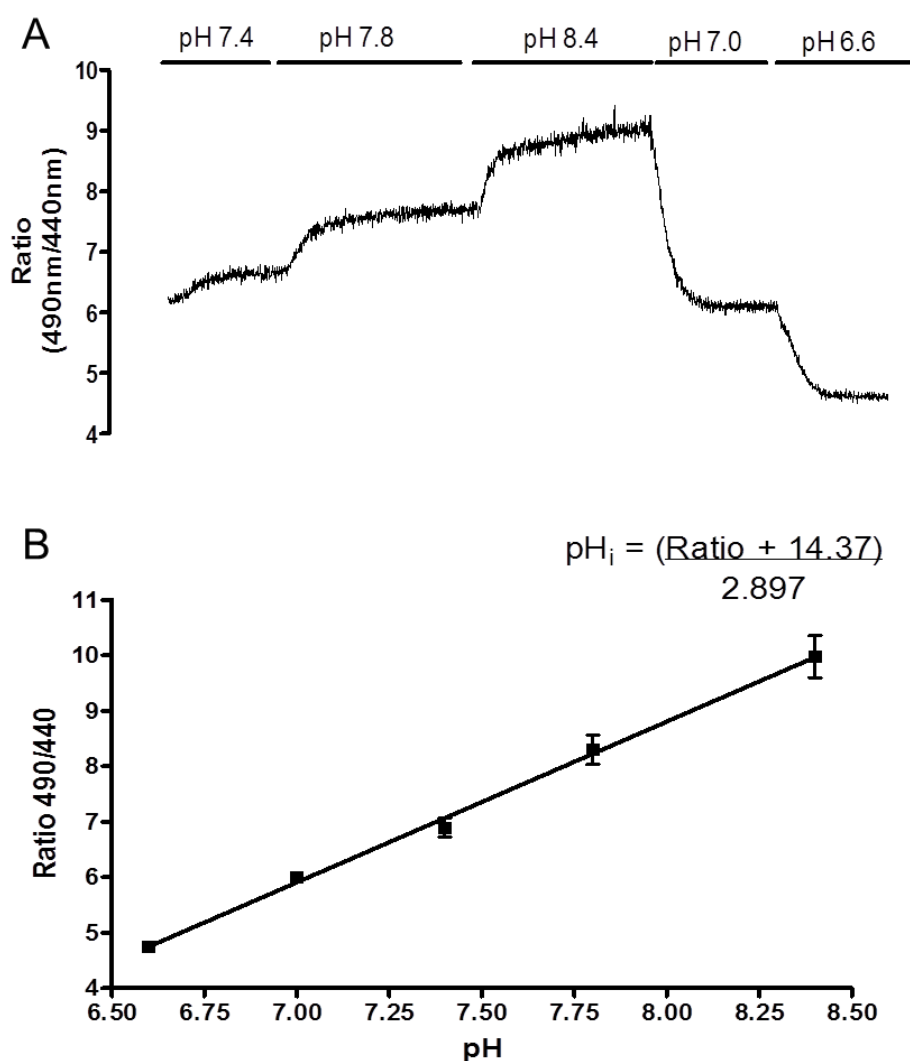


Figure 2.04: Intracellular pH_i calibration of Calu-3 cells. (A) shows a representative experiment in which Calu-3 cells were loaded for one hour with 10 μ M BCECF-AM and perfused with high K^+ solutions of known pH containing 10 μ M nigericin. (B) shows the resulting standard curve that was used to calculate pH_i from 490/440 ratios. Data represents mean \pm S.E.M.; $n = 4$, $r^2 = 0.954$.

2.4.2. Determining Intracellular Buffering Capacity

In order to determine the buffering capacity of cells (β_{tot}), the intrinsic buffering capacity (β_i) was added to the buffering capacity of the $\text{CO}_2\text{-HCO}_3^-$ buffer system ($\beta_{\text{HCO}_3^-}$). β_i was calculated using the NH_4^+ pulse technique (Roos and Boron, 1981). Here, cells were exposed to solutions containing differing amounts of NH_4Cl , ranging from 0mM NH_4Cl to 30mM NH_4Cl . NH_3 enters the cell and subsequently binds to free protons to form NH_4^+ and cause an alkalisation of pH_i . β_i is then calculated *via* the following equation:

$$\beta_i = \frac{\Delta[\text{NH}_4^+]_i}{\Delta\text{pH}_i}$$

$\beta_{\text{HCO}_3^-}$ is calculated using the formula:

$$\beta_{\text{HCO}_3^-} = 2.3 \times [\text{HCO}_3^-]_i$$

in which the Henderson Hasselbalch equation states:

$$[\text{HCO}_3^-]_i = \text{pCO}_2 \times 10^{(\text{pH} - \text{pK})}$$

The buffering capacity for Calu-3 cells at varying CO_2 concentrations is displayed in figure 2.05.

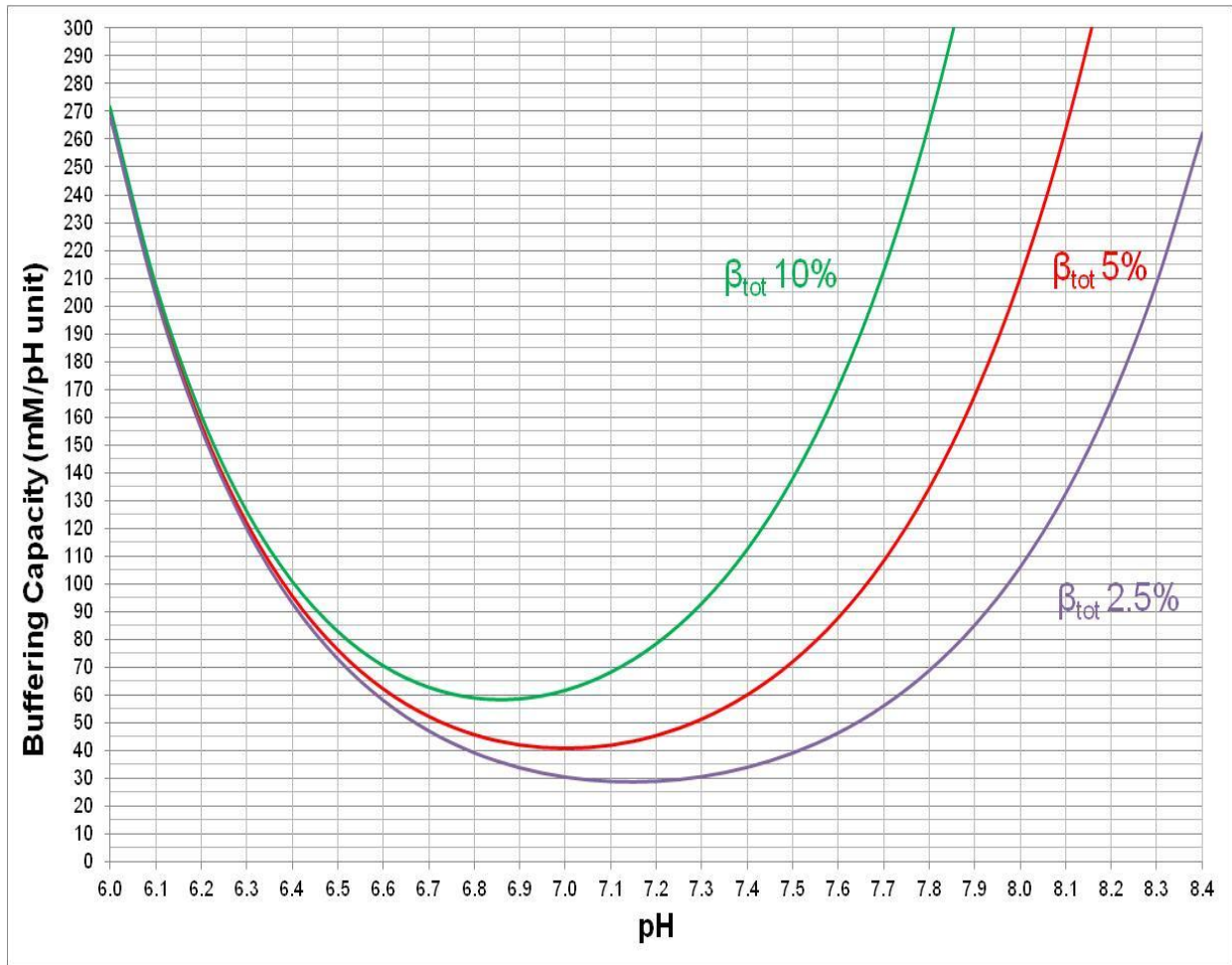


Figure 2.05: Buffering capacity of Calu-3 cells when exposed to different concentrations of CO₂. Total buffering capacity (β_{tot}) was calculated by adding the intrinsic buffering capacity of Calu-3 cells (β_i) to the buffering capacity of the CO₂/HCO₃⁻ buffer system ($\beta_{\text{HCO}_3^-}$). β_{tot} was calculated for cells exposed to 2.5% CO₂, 5% CO₂ and 10% CO₂. n = 6 for each.

2.5. Intracellular Ca²⁺ Measurements

Calu-3 cells were cultured on 25mm diameter glass coverslips (VWR) at an initial seeding density of 1×10^6 cells/coverslip and studied 3-4 days post seeding when cells were approximately 80% confluent. Cells were washed in NaHEPES and incubated with 5 μ M Fura-2 AM (Grynkiewicz *et al.*, 1985) for one hour before the dye was removed and cells were incubated for 15 minutes in NaHEPES to allow for de-esterification of the dye. Incomplete de-esterification of Fura-2 AM will lead to artefacts within the experiment as Fura-2 AM is fluorescent but Ca²⁺-insensitive. Cells were mounted onto a Nikon fluor oil immersion microscope (magnification of x40 with a numerical aperture of 1.3) and heated to 37°C. Krebs solutions were gassed with 5% (v/v) CO₂/95% (v/v) O₂ for control conditions

and this gas composition was altered to 10% (v/v) CO₂/90% (v/v) O₂ to induce hypercapnia. Solutions were perfused across cells at a speed of 3ml/min. To measure [Ca²⁺]_i, cells were alternatively excited at 340nm and 380nm wavelengths every 0.250s and emitted light collected at 510nm. Fluorescence at 340nm is sensitive to high [Ca²⁺]_i and fluorescence at 380nm is sensitive to low [Ca²⁺]_i. The ratio of 340 nm emission to 380 nm emission was recorded using InCyt PM-2 software.

2.6. Fluid Secretion Assays

The effects of chronic hypercapnia on Calu-3 cell physiology were assessed by fluid secretion assays in which the volume and composition of fluid secreted by cells over a 24 hour period was measured. Cells were first washed three times with PBS in order to remove any mucus that may have accumulated over time. Extra care was taken when removing the PBS to ensure no residual fluid remained in the transwell at the end of the washes. Solutions containing desired pharmacological agents were then added to the transwells (1ml basolaterally, 200µl apically) and cells were incubated at 37°C in humidified air containing 5% (v/v) CO₂ (control) or 10% (v/v) CO₂ (hypercapnia) for 24 hours. The apical fluid was then removed and its volume measured. 180µl was removed first and then the rest of the fluid was removed 1µl at a time to ensure high accuracy. Samples were collected in an Eppendorf tube and, after a brief incubation in the appropriate incubator, had the pH assessed using a micro pH probe. Samples were then stored at -20°C to allow for further analysis using the PAS Assay (see section 2.9.).

2.7. Radiolabelled cAMP Assay

Calu-3 cells were cultured in 12 well plates (Corning, UK) at an initial seeding density of 3 x 10⁵ cells/well and used 7 days post-seeding at approximately 80% confluency. Cells were treated with 100µl [³H]-adenine at a concentration of 2µCurie/ml and incubated for 2 hours at 37°C in humidified air containing 5% (v/v) CO₂. This ensured that at least some adenine-containing molecules synthesised after treatment would be labelled with the ³H isotope. Cells were then washed twice with PBS and incubated for a further 30 minutes at 37°C in humidified air containing 5% (v/v) CO₂/95% (v/v) O₂ (normocapnic controls) or 10% (v/v) CO₂/90% (v/v) O₂ (hypercapnia). Incubation was performed in normal growth medium that

had been pregassed with the appropriate CO₂ concentration and titrated to pH 7.4 using 1M NaOH. Incubation also took place in the presence of 1mM IBMX to prevent breakdown of any cAMP. Forskolin (5µM) was then added to the cells for 10 minutes before the assay was ended by removal of media and lysis of cells by adding 5% (w/v) trichloroacetic acid containing 1mM ATP and 1mM cAMP for one hour at 4°C.

cAMP levels in lysates were measured by the double column chromatography procedure described by Johnson *et al.* (1994). The lysate was added to columns containing 1ml anion exchange resin DOWEX 50 which had been prewashed with 1M HCl. This acidified DOWEX 50 traps any neutrally charged cAMP but does not trap the negatively charged adenine, adenosine, AMP, ADP or ATP, which flowed through the column and was collected in scintillation vials. The DOWEX 50 columns were then placed above columns containing Al₂O₃ and were washed through with ddH₂O. This caused cAMP to be washed off the DOWEX and trapped on the Al₂O₃ which becomes acidic in the presence of H₂O. Finally, the Al₂O₃ columns were washed with Tris-HCl (pH 7.5) to neutralize the Al₂O₃ and thus wash off the cAMP to collect in scintillation vials. 2.5mls of scintillation fluid was added to each vial and the radioactivity of each sample was measured using a scintillation liquid analyzer Tricab 2900 TR (PerkinElmer) in which radioactive particles emitting from the ³H isotope transferred energy to the scintillation fluid causing the emission of photons allowing for luminescence measurements. The radioactive counts were processed using QuantaSmart software and the ratio of the DOWEX 50 flow-through counts to the Al₂O₃ flow-through counts were used to normalize the amount of [³H]-cAMP to total cellular [³H]-adenine.

2.8. Measurements of extracellular ATP

Calu-3 cells, cultured on 12mm permeable Transwell supports and studied 10 days post seeding, were washed three times with PBS. For normocapnic controls, cells were incubated for 20 minutes in pregassed 25mM NaHCO₃ solution containing 10mM HEPES, 0.6mM NaOH and 15mM Mannitol (pH 7.4 when gassed with 5% (v/v) CO₂/95% (v/v) O₂) at 37°C in humidified air containing 5% (v/v) CO₂. For cells exposed to hypercapnia, they were incubated for 20 minutes in pregassed 25mM NaHCO₃ solution containing 10mM HEPES, 10mM NaOH (pH 7.4 when gassed with 10% (v/v) CO₂/90% (v/v) O₂) at 37°C in humidified air containing 10% (v/v) CO₂. The assay is highly sensitive to salts hence the reason to omit NaCl, KCl, MgCl₂ and CaCl₂. 50µl of solution was added to the apical compartment and

200µl of solution was added to the basolateral compartment. After incubation, both apical and basolateral solutions were very carefully removed to minimize mechanically-induced ATP release. Assays were performed by adding 15 µL of luciferin to 15 µL of sample in a black 96-well plate. A blank of 15 µL assay buffer with 15 µL luciferin was subtracted from the readings of samples. Luciferin and samples containing luciferin were kept out of contact with light due to the photosensitivity of the reagent

All luciferase assays were performed using the Roche Applied Science ATP bioluminescence assay kit HS II and read using a BioTek Flx800 multidetection microplate reader. The luminometer was set to record luminescence with a sensitivity of 125 and an integration time of 6s with no filter. All readings were taken 25s after the addition of luciferin to the samples.

2.9. PAS Assay

To measure the mucin content of secreted apical fluid, the periodic acid-Schiff's (PAS) assay was used. The PAS assay is used to detect glycoproteins which relies on a periodic acid/acetic acid mixture oxidizing hydroxyl groups in sugars to form aldehydes. These formed aldehydes then react with Schiff's reagent to form a purple colour which can then be analysed by spectrophotometry. To generate a standard curve, pig mucin (a gift from Prof. Jeff Pearson, Newcastle University) was diluted to (in µg/ml) 100, 50, 20, 10, 5, 2 and 1 and 100µl of standards were added to a 96 well plate in duplicate. 100µl of sample was made to 1ml by addition of deionised water and 100µl was added to wells in duplicate. 100µl of a periodic acid/acetic acid mix (made from 10µl periodic acid added to 7% acetic acid) was added to all standards and samples and the plate was incubated for 60 minutes at 37°C. In addition, 0.1g of sodium metabisulphate was added to 6mls of Schiff's reagent and this was also incubated for 30 minutes at 37°C before 100µl was added to all standards and samples. The plate was then incubated at room temperature for 30 minutes before absorbance was read at 550nm using a BioTek ELx808 Absorbance Microplate Reader. Absorbance was then converted to mucin concentration using the standard curve shown in figure 2.06.

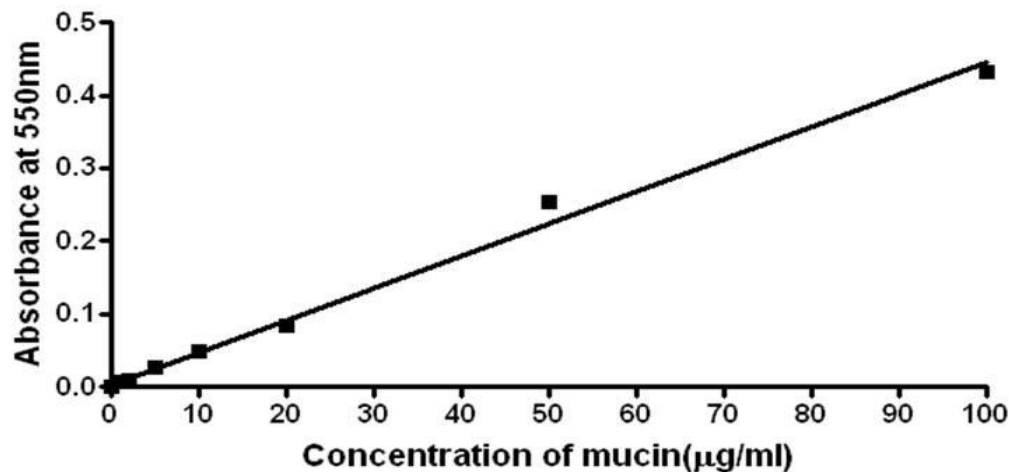


Figure 2.06: Standard curve generated for the Periodic acid Schiff's assay. Pig mucin samples of known concentration were added to a periodic acid/acetic acid mix before addition of Schiff's reagent and absorbance measured at 550nm using a BioTek ELx808 Absorbance Microplate Reader. Data represents mean of samples run in duplicate; $r^2 = 0.994$.

2.10. Wound Healing Assay

Calu-3 cells, cultured on 12mm permeable Transwell supports and studied 8-12 days post seeding, were exposed to a single scratch using a P200 pipette tip, washed three times in PBS and incubated for one hour at 37°C in humidified air containing 5% (v/v) CO₂ in air to bring the cells and plate up to temperature. Cells were placed in the Nikon BioStation CT at 37°C in humidified air containing 5% (v/v) CO₂ for normocapnia or 10% (v/v) CO₂ for hypercapnia and imaged under phase contrast at x4 magnification every four hours for 36 hours. Three different fields of view within one transwell were imaged and the area of the wound was calculated using ImageJ software as shown in figure 2.07.

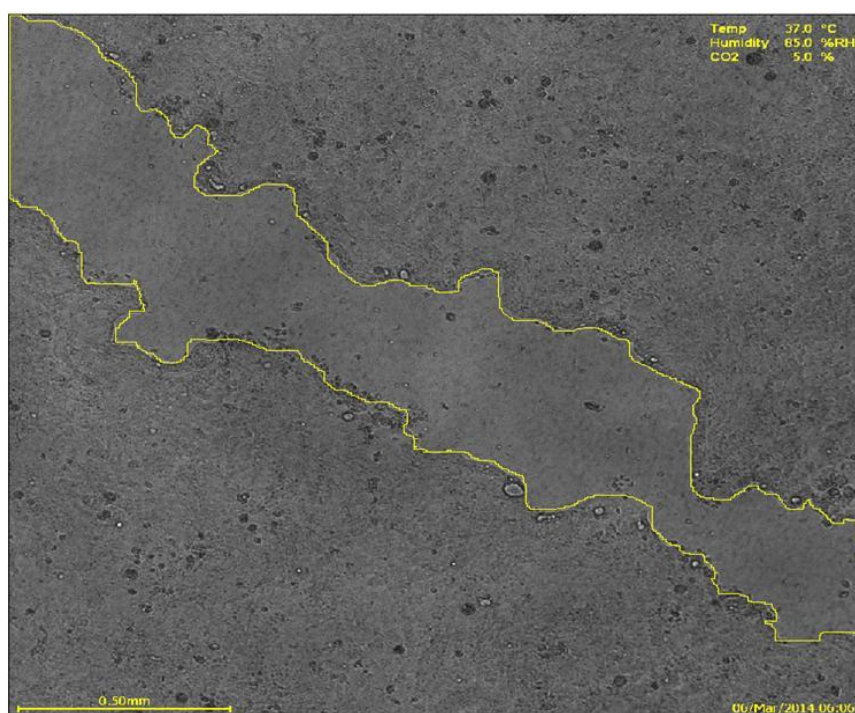


Figure 2.07: Example analysis of wound healing assay. The wound was drawn around using the polygon tool in ImageJ and the resulting area of wound size was calculated.

2.11. Confocal Microscopy

The actin cytoskeleton network was visualised using confocal microscopy. Calu-3 cells were cultured on 12mm permeable Transwell supports and studied 8-12 days post seeding. Media was removed and cells were incubated in pregassed high Cl^- Krebs solution for 20 minutes at 37°C in humidified air containing 5% (v/v) CO_2 (control) or 10% (v/v) CO_2 (hypercapnia) for 20 minutes before $5\mu\text{M}$ forskolin was added for 10 minutes. After treatment, cells were washed three times with PBS and then fixed by treating with 4% paraformaldehyde (PFA) for 10 minutes. Cells were then washed three times for 5 minutes with PBS before washing with 50mM NH_4Cl to quench any remaining PFA. Cells were permeabilized with 1% Triton X-100 in PBS for 5 minutes and then subsequently washed three times for 5 minutes with PBS. PBS containing 3% FCS and 0.1% azide was then added to block non-specific binding. At this point, the transwell membrane was cut out and placed in a 12 well plate with the apical side facing upwards. $200\mu\text{l}$ of PBS containing 3% FCS, 0.1% azide and 0.25% Phalloidin–Tetramethylrhodamine B isothiocyanate (Phalloidin-TRITC) (Sigma) was then added to cells for 30 minutes at room temperature before cells were washed twice with PBS. Cells were rinsed with PBS before $0.2\mu\text{g/ml}$ 4',6-diamidino-2-phenylindole (DAPI) was then added for

two minutes. After rinsing, cells were then mounted on slides using 1-2 drops of Vectashield mounting medium (Vector Laboratories, UK).

Cells were visualized using a Nikon A1R Confocal microscope at x60 magnification using a 0.1 DIC lens with a numerical aperture of 1.4. To visualize DAPI stained specimens, cells were excited with the DAPI excitation wavelength of 405nm and imaged at the emission wavelength of 450nm. To visualize TRITC stained specimens, cells were excited with the TRITC excitation wavelength of 595nm and imaged at the emission wavelength of 561nm. Z-stacks were taken at a rate of 15µm 2.5 seconds⁻¹. Data was analysed using ImageJ software.

2.12. End Point PCR

To assess the expression of proteins at the mRNA level, RNA was extracted from polarised Calu-3 cells using the QIAGEN RNeasy Mini Kit. Briefly, RNA was extracted using 1% β-mercaptoethanol and purified using spin technology as per manufacturer's instructions. RNA yield and purity was assessed using a Nanodrop 2000 (Thermo Scientific, UK). To remove any DNA that may contaminate the RNA, 4.5µg RNA was added to 4.5µl DNase (BioLine) and 2µl DNase Buffer (BioLine) made up to 20µl with Mill-Q H₂O. This was incubated at 37°C for 30 minutes before 4µl DNase stop buffer (BioLine) was added for 10 minutes at 65°C.

The purified RNA was reverse transcribed into cDNA using the following reaction mix:

10µl pure RNA
3.2µL 25mM Magnesium Chloride
10x Reaction Buffer, (BioLine)
16µl dNTPs (BioLine)
2µl of random Hexamers (10µM),
1µl Reverse Transcriptase (BioLine)
3.8µl Milli-Q H₂O

The reverse transcription reaction was then carried out as shown in table 2.01.

Step	Temperature (°C)	Duration (mins)	Number of Cycles
1	42	60	1
2	95	5	1
3	5	5	1

Table 2.01: Conditions for reverse transcription of mRNA into cDNA

To perform End Point PCR, the following reaction mix was used

0.8µl 50mM MgCl₂

4µl 10x Reaction Buffer (BioLine)

0.5µl Taq DNA Polymerase (BioLine)

20.7µl Milli-Q H₂O

2µl forward primer made to 10pmol/µl (Eurofins Genomics)

2µl reverse primer made to 10pmol/µl (Eurofins Genomics)

10µl cDNA

The End Point PCR reaction was then carried out according to table 2.02.

Step	Temperature (°C)	Duration (mins)	Number of Cycles
1	95	5	1
2	95	0.5	35
	Annealing Temp	0.5	
	72	0.5	
3	72	12	1

Table 2.02: Conditions for End Point PCR

8µl of PCR product was then combined with 2µl loading dye (BioLine) and run on a 1.5% Agarose TBE (54g Tris, 27.5g boric acid, 20ml 0.5M EDTA per 1L de-ionised water, pH 8.0) gel containing 0.006% Ethidium Bromide at 70V for one hour. 5µl of Hyperladder IV

(BioLine) was used as a molecular weight marker. The gel was viewed using the Bio Rad Gel Doc EZ Imager and Image Lab 4.0 software.

Primer sequences for PCR reactions are displayed in table 2.03

Gene	Sequence	Annealing Temp (°C)	Expected Product Size
CFTR	Fwd: 5'-AATGTAACAGCCTTCTGGGAG-3'	57.9	391
	Rev: 5'-GTTGGCATGCTTTGATGACGCTTC-3'	62.7	
NBCe1 (SLC4A4)	Fwd: 5'-GGTGTGCAGTTCATGGATCGTC-3'	62.1	336
	Rev: 5'-GTCAGTGTCCAGACTTCCCTTC-3'	62.1	
NBCe2 (SLC4A5)	Fwd: 5'-ATCTTCATGGACCAGCAGCTCAC-3'	60.6	468
	Rev: 5'-TGCTTGGCTGGCATCAGGAAG-3'	61.8	
NBCn1 (SLC4A7)	Fwd: 5'-CAGATGCAAGCAGCCTTGTGTG-3'	62.1	328
	Rev: 5'-GGTCCATGATGACCACAAGCTG-3'	62.1	
NDCBE1 (SLC4A8)	Fwd: 5'-GCTCAAGAAAGGCTGTGGCTAC-3'	62.1	243
	Rev: 5'-CATGAAGACTGAGCAGCCCATG-3'	62.1	
NCBE (SLC4A10)	Fwd: 5'-GCAGGTCAGGTTGTTTCTCCTC-3'	62.1	498
	Rev: 5'-TCTTCCTCTTCTCCTGGGAAGG-3'	62.1	
Pannexin 1	Fwd: 5'-AGAGCGAGTCTGGAAACC-3'	56.0	133
	Rev: 5'-CAAGTCTGAGCAAATATGAGG-3'	55.9	
Pannexin 2	Fwd: 5'-AAGCAGATCCAGTCCAAG-3'	53.7	82
	Rev: 5'-GGGCTCTTCTCCTTCTCC-3'	58.2	

Table 2.03: Primer sequences, annealing temperatures and expected product size for End Point PCR experiments. Primer sequences for NBC family members were obtained from Damkier *et al.* (2007) and primer sequences for pannexin family members were obtained from Ransford *et al.* (2009)

2.13. Western Blot

Western Blots were performed to investigate whether hypercapnia had any effects on protein expression, specifically on CFTR expression. Calu-3 cells were cultured on 12mm permeable Transwell supports and studied 8-12 days post seeding. For studies into acute hypercapnia, Calu-3 cells were incubated in pre-gassed high Cl⁻ Krebs solution at 37°C in humidified air containing 5% (v/v) CO₂ (normocapnic controls) or 10% (v/v) CO₂ (hypercapnic) for 20 minutes before addition of either agonist or vehicle for a further 10 minutes. For studies into chronic hypercapnia, Calu-3 cells were instead incubated for 24 hours prior to cell lysis. Cells were lysed with RIPA buffer consisting of (in mM) 150 NaCl, 1 Tris-HCl, 1% Deoxycholic Acid, 1% Triton X-100 and 0.1% SDS with a protease inhibitor tablet (Roche) added to 10mls of RIPA buffer. Cells were shaken at 4°C for 30 minutes before they were scraped

using a pipette tip to aid lysis. The lysate was collected in an Eppendorf tube which was then centrifuged for 20 minutes at 12,000 RPM at 4°C to remove the cell debris.

To quantify protein, the Pierce Assay was performed in which 10µl protein samples were added to 150µl 660 Pierce Reagent (Sigma Aldrich) in duplicate and absorbance was measured at 660nm using a BioTek ELx808 Absorbance Microplate Reader. Protein concentration was calculated from a standard curve generated from known concentrations of Bovine Serum Albumin (0, 0.0625, 0.125, 0.25, 0.5, 1 and 2mgs/ml) as shown in figure 2.08.

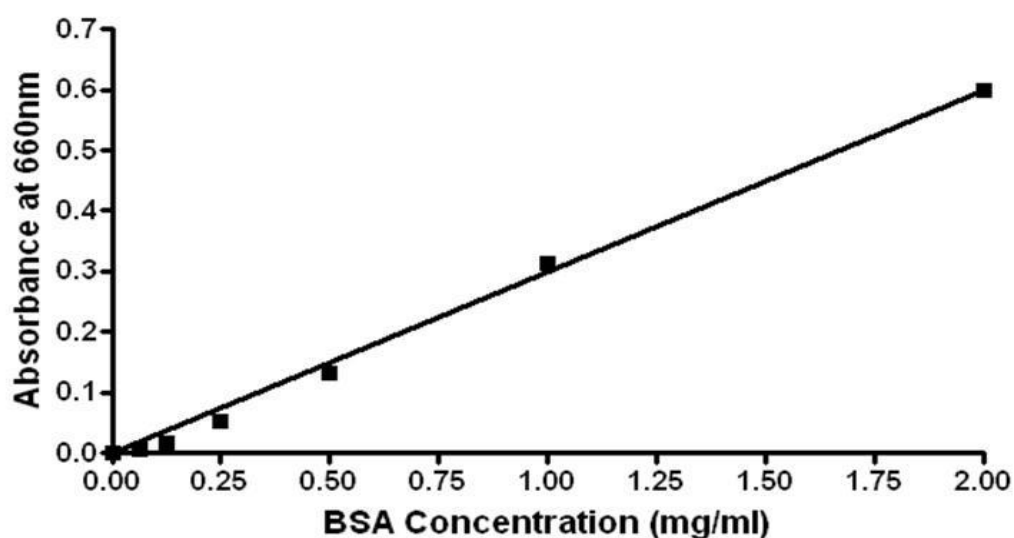


Figure 2.08. Standard curve for protein quantification generated using the Peirce Assay. BSA samples of known concentration were added to 660 Peirce Reagent (Sigma Aldrich) and absorbance measured at 660nm using a BioTek ELx808 Absorbance Microplate Reader. Data represents mean of samples ran in duplicate; $r^2 = 0.998$.

Gel electrophoresis was performed on NuPAGE precast 4-12% gels. 15µg protein was combined with 4µl NuPAGE Loading Buffer and 2µl NuPAGE reducing agent and heated to 70°C for 10 minutes prior to loading into the gel. 2µl of reference ladder (Novex) was also loaded into the gel. Electrophoresis was performed at 200V for 1 hour. The gel was then transferred to a nitrocellulose membrane at 400mA for 1 hour 30 minutes at 4°C. The membrane was blocked for one hour in blocking buffer consisting of PBS + 0.1% Tween 20 (PBST) containing 5% dried skimmed milk powder (Marvel) before primary 596 anti-CFTR monoclonal antibody was added overnight at 4°C at 1:3000 dilution in blocking buffer. The membrane was then washed using PBST before the anti-mouse Horse Radish Peroxidase (HRP) secondary antibody was added at 1:3000 dilution in blocking buffer for one hour. Any

unbound secondary antibody was then washed off with PBST. To detect any HRP activity, equal volumes of the enhanced chemiluminescent substrates Enhanced Luminol Reagent and the Oxidizing Reagent (Thermo Scientific) were added to the blot for 10 minutes before the blot was exposed to Kodak Scientific Imaging film for 1 minute. The film was developed and the band intensity was analysed using ImageJ software. To reprobe the blot, Restore Western Blot Stripping Buffer (Thermo Scientific) was added for 15 minutes at room temperature, the blot was then washed in PBST and blocked in blocking buffer for one hour before another immunoblot was performed. To detect β -actin expression, a monoclonal goat anti-actin antibody was added at a 1:2000 dilution in blocking buffer for 2 and a half hours. The membrane was then washed using PBST before an anti-goat HRP secondary antibody was added at 1:3000 dilution in blocking buffer for one hour and HRP activity was assessed as previously stated.

2.14. Solutions and Reagents

All reagents were purchased from Sigma Aldrich apart from forskolin, U73122, HC067047, H-1152, ouabain, dorsomorphin (R & D Systems); BCECF-AM, Fura-2 AM, H₂-DIDS, DIDS (Invitrogen) and SQ22536, GlyH-101, CFTR_{inh} 172 (Calbiochem). All gas cylinders were purchased from BOC and consisted of the following mixtures: 5% CO₂/95% O₂, 10% CO₂/90% O₂ and 2.5% CO₂/97.5% O₂.

NaHEPES solution consisted of (in mM) 130 NaCl, 5 KCl, 1 CaCl₂, 1 MgCl₂, 10 NaHEPES and 10 D-Glucose. 1M HCl was used to calibrate the solution to pH 7.6 at room temperature. High Cl⁻ Krebs solution consisted of (in mM) 25 NaHCO₃, 115 NaCl, 5 KCl, 1 CaCl₂, 1 MgCl₂ and 10 D-Glucose. For high Cl⁻, Na⁺ free solutions, NaHCO₃ was replaced with choline bicarbonate and NaCl was replaced with NMDG-Cl which was made by adding HCl to 1M NMDG solution until pH reached 7.2. Zero Cl⁻ Krebs solution consisted of (in mM) 25 NaHCO₃, 115 NaGluconate, 2.5 K₂SO₄, 1 CaGluconate, 1 MgGluconate and 10 D-Glucose. For zero Cl⁻, Na⁺ free solutions, NaHCO₃ was replaced with choline bicarbonate and Na Gluconate was replaced with NMDG-Gluconate which was made by adding gluconic acid to 1M NMDG until pH reached 7.2.

Intracellular pH_i calibration solutions consisted of (in mM) 5 NaCl, 130 KCl, 1 CaCl₂, 1 MgCl₂, 10 D-Glucose, 10 HEPES (for solutions set at pH 7.6 or below) or 10 TRIS (for solutions set at pH 7.8 or above) as well as 10μM nigericin. Solutions were set to desired pH by using 1M HCl or 1M NaOH.

Solutions used to determine intracellular buffering capacity consisted of (in mM) 4.5 KCl, 1 MgCl₂, 2 CaCl₂, 5 BaCl, 10 HEPES, 10 D-Glucose as well as varying concentrations of NH₄Cl/NMDG-Cl, ranging from 0 NH₄Cl/145 NMDG-Cl to 30 NH₄Cl/115 NMDG-Cl. All solutions were titrated to pH 7.4 at 37°C using 1M CsOH.

2.15. Statistical Analysis

Statistical analysis was performed using GraphPad Prism 4 software. Student's t-test, one way ANOVA (with Tukey's multiple comparison post-test) or two way ANOVA (with Bonferroni post-test) were carried out where applicable to determine statistical significance between measurements. A p value of <0.05 was considered statistically significant.

Chapter 3: Effect of acute hypercapnia on cAMP-dependent HCO₃⁻ transport in Calu-3 cells

3.1. Introduction

As already discussed in chapter 1, there exists a great body of evidence that demonstrates the role of the second messenger, cAMP, in the regulation of HCO₃⁻ secretion in a variety of human tissue, including airway epithelia. cAMP has been shown to stimulate HCO₃⁻ secretion *via* PKA-dependent phosphorylation of CFTR (Devor *et al.*, 1999; Hug *et al.*, 2003; Garnett *et al.*, 2011) and increase the activity of NBCs to accumulate HCO₃⁻ into the cell from the blood (Bachmann *et al.*, 2003; Bachmann *et al.*, 2008; Chen *et al.*, 2012). Our laboratory, and others, have used intracellular pH measurements to demonstrate that in Calu-3 cells, elevations in [cAMP]_i activated CFTR-dependent Cl⁻/HCO₃⁻ exchange and inhibited basolateral AE2 to favour a vectorial HCO₃⁻ transport from the blood to luminal membrane (Garnett *et al.*, 2011; Garnett *et al.*, 2013; Kim *et al.*, 2014). Furthermore, our laboratory has also described that acute hypercapnia significantly reduced both forskolin-stimulated and parathyroid hormone-stimulated cAMP levels in two renal cell lines: HEK-PR1 and OK cells which affected the cAMP-dependent activity of NHE3 (Cook *et al.*, 2012). Thus, should this effect of hypercapnia also be present in airway epithelia, it would be predicted that cAMP-dependent regulation of HCO₃⁻ transport would be impaired. This chapter details the investigations into the effects of acute hypercapnia on cAMP-regulated HCO₃⁻ transport in Calu-3 cells.

3.2. Acute hypercapnia attenuates forskolin-stimulated cAMP levels in Calu-3 cells

To investigate whether hypercapnia was able to modulate [cAMP]_i in Calu-3 cells, cells were stimulated with either vehicle (DMSO) or forskolin and [cAMP]_i was measured by a radiolabelled cAMP assay. Incubation solutions were buffered to pH 7.5 to eliminate any effects of extracellular pH (pH_e) on [cAMP]_i. Intracellular pH measurements revealed that exposure of Calu-3 cells to 10% CO₂ induced an intracellular acidosis of 0.18 ± 0.01 pH units (n=60) which recovered after ~20 minutes (fig 3.01A). Further investigations into the mechanisms underlying this recovery process are detailed in section 3.11. It is important to note that exposure of polarized Calu-3 cells to hypercapnia does not affect the integrity of the epithelial monolayer as measured by transepithelial electrical resistances (TEER). In

normocapnia, TEER was $671 \pm 42 \Omega \text{ cm}^{-2}$ ($n=3$) whilst in cells exposed to acute hypercapnia, TEER was $600 \pm 42 \Omega \text{ cm}^{-2}$ ($p>0.05$; $n=3$) and highlights that acute hypercapnia has no major effect on the ability of Calu-3 cells to form a highly resistive monolayer. Thus, cells were exposed to 10% CO_2 for 20 minutes prior to forskolin stimulation to ensure any effects of hypercapnia on $[\text{cAMP}]_i$ were due to CO_2 *per se* and not CO_2 -induced acidosis. In normocapnia (5% CO_2), forskolin stimulated a 3.3 ± 0.5 fold increase in intracellular cAMP levels ($p<0.001$; $n=6$; fig 3.01B). Although cells exposed to 10% CO_2 for 20 minutes also demonstrated a significant 2.3 ± 0.4 fold increase in intracellular cAMP levels ($p<0.05$ $n=6$; fig 3.01B), this increase in intracellular cAMP was $36 \pm 9\%$ lower than that observed in normocapnia ($p<0.05$) demonstrating that acute hypercapnia attenuates cAMP production in Calu-3 cells.

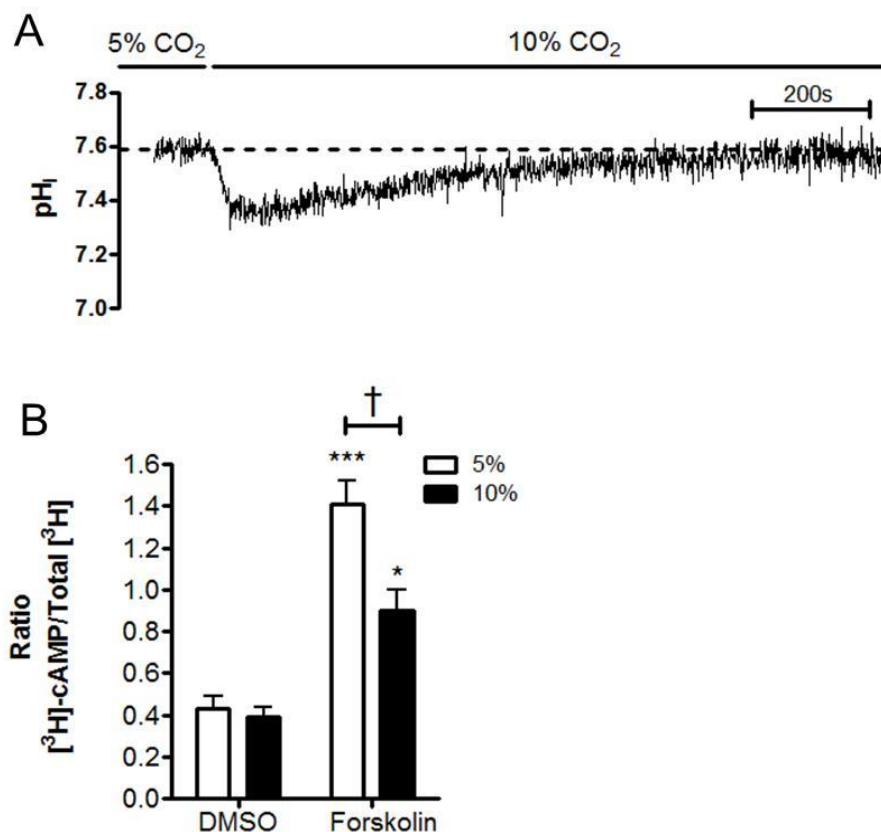


Figure 3.01: Acute hypercapnia attenuates forskolin-stimulated cAMP levels in Calu-3 cells. (A) shows the effect of hypercapnia (10% CO_2) on pH_i of Calu-3 cells and demonstrated cells recover pH_i from CO_2 -induced acidosis after ~20 minutes. (B) shows the effect of acute hypercapnia on intracellular cAMP in which cells were incubated for 20 minutes in either 5% CO_2 (v/v) in air or 10% CO_2 (v/v) in air before being stimulated with either vehicle (DMSO) or $5\mu\text{M}$ forskolin for a further 10 minutes. Intracellular cAMP levels were measured by measuring the amount of $[\text{H}^3]\text{-cAMP}$ molecules in each sample. *** = significant effect of forskolin ($p<0.001$; * = $p<0.05$); † = significant effect of hypercapnia ($p<0.05$). Data represents mean \pm S.E.M.; $n = 6$ for each.

3.3. Acute hypercapnia reduces forskolin-stimulated increases in short-circuit current

To assess whether the effects of acute hypercapnia on forskolin-stimulated elevations in $[cAMP]_i$ would lead to alterations in cAMP-regulated ion transport, the short circuit current (I_{sc}) of Calu-3 cells was measured in cells exposed to either 5% (v/v) $CO_2/95\%$ (v/v) O_2 (control) or 10% (v/v) $CO_2/90\%$ (v/v) O_2 for 20 minutes prior to recording. To measure electrogenic Cl^- secretion, cells were stimulated with 5 μ M forskolin in the presence of a basolateral to apical Cl^- gradient, achieved by reducing apical Cl^- to 40mM whilst maintaining basolateral Cl^- at 124mM. Figure 3.02A shows a representative I_{sc} recording under normocapnic conditions and figure 3.02B shows a representative I_{sc} recording under hypercapnic conditions. In normocapnia, prior to reducing the apical Cl^- concentration, Calu-3 cells displayed a basal I_{sc} of $5.2 \pm 0.4\mu A$ and further investigations showed that this basal I_{sc} was relatively insensitive to both basolateral bumetanide (25 μ M) and EIPA (3 μ M), whereas CFTR_{inh} 172 (20 μ M) was able to reduce basal I_{sc} by $48.5 \pm 4.2\%$ ($p < 0.01$; $n=3$) indicating low level CFTR activity mediated this I_{sc} . Interestingly, in cells exposed to 20 minutes hypercapnia, the basal I_{sc} was reduced to $1.3 \pm 1.3\mu A$ ($p < 0.01$ vs. normocapnia; $n=8$; fig. 3.02C) implying that acute hypercapnia inhibited CFTR in basal conditions. Forskolin induced an increase in I_{sc} which peaked after approximately 90s to a maximal level and then decreased slightly until a new steady state was reached. The forskolin-induced increase in I_{sc} was blocked by a combination of apical CFTR_{inh}-172 (20 μ M) and basolateral bumetanide (25 μ M) implying that CFTR mediated the increase in I_{sc} . The fact that CFTR_{inh} 172 did not completely block the response to forskolin alone suggests a CFTR-independent component to the response. However, other groups have reported that 50 μ M CFTR_{inh} 172 was required to inhibit CFTR in the Ussing chamber setup, and as such there maybe concentration-dependent issues evident here (Schwarzer *et al.*, 2010). The maximal forskolin-stimulated increase in I_{sc} (ΔI_{sc}) was $19.3 \pm 2.0\mu A\ cm^{-2}$ ($n=10$) in normocapnia compared to $14.1 \pm 1.1\mu A\ cm^{-2}$ in acute hypercapnia ($p=0.053$ vs. normocapnia; $n=8$; fig. 3.02D). The rate of forskolin-stimulated I_{sc} increase in normocapnia was $10.4 \pm 1.3\mu A\ cm^{-2}\ min^{-1}$ ($n=10$) which was reduced to $5.7 \pm 0.6\mu A\ cm^{-2}\ min^{-1}$ ($p < 0.01$ vs. normocapnia; $n=8$; fig. 3.02E) in cells exposed to acute hypercapnia. These findings suggest that the attenuation of forskolin-stimulated cAMP levels by acute hypercapnia were sufficient to reduce cAMP-regulated anion secretion in Calu-3 cells.

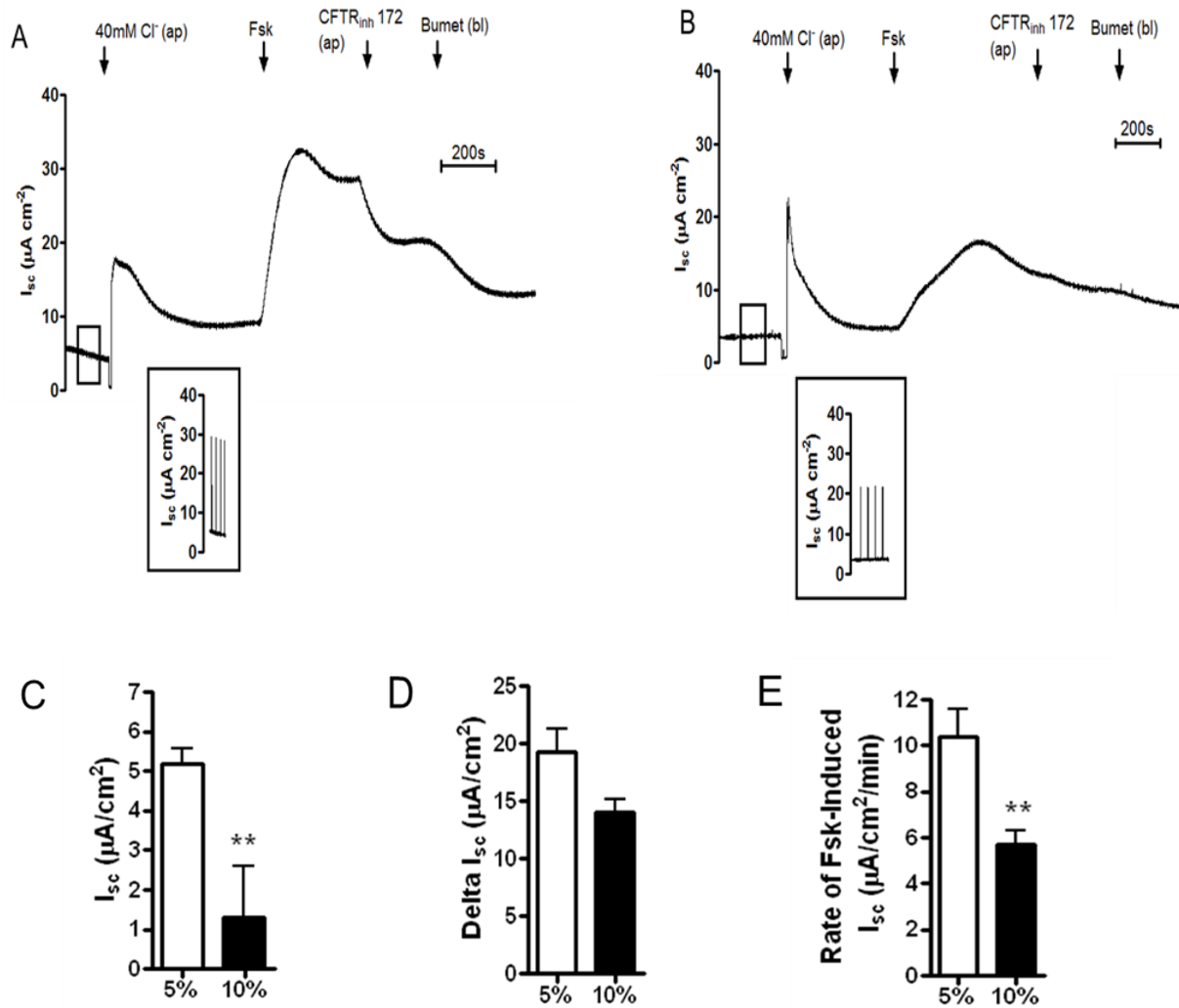


Figure 3.02: Acute hypercapnia reduces forskolin-stimulated I_{sc} in Calu-3 cells. Cells were grown on permeable Snapwell supports and forskolin-stimulated electrogenic Cl^- secretion was measured using an Ussing chamber. (A) shows a representative recording of a control experiment in which cells were exposed to 5% (v/v) CO_2 /95% (v/v) O_2 and (B) shows a representative recording of an in which cells were exposed to 10% (v/v) CO_2 /90% (v/v) O_2 for 20 minutes prior to being studied. Apical Cl^- was reduced to 40mM and cells were stimulated with forskolin (5μM) before addition of apical CFTR_{inh}-172 (20μM) and basolateral bumetanide (25μM) as indicated. The inset shows that a 2 second 10mV pulse was applied across the cells every 30 seconds to monitor transepithelial electrical resistance (TEER). These pulses were removed from the trace in order to display the effects of treatment more clearly. The basal I_{sc} (C), the maximal forskolin-stimulated increase in I_{sc} (D) and the rate of increase in forskolin-stimulated I_{sc} (E) are displayed. ** = significant effect of hypercapnia ($p < 0.01$). Data represents mean \pm S.E.M.; $n = 10$ for normocapnia and $n = 8$ for hypercapnia.

The response of Calu-3 cells to other cAMP agonists was also assessed. Adenosine (10 μ M) stimulated a maximal increase in I_{sc} of $25.2 \pm 3.6 \mu A cm^{-2}$ at a rate of $23.9 \pm 10.9 \mu A cm^{-2} min^{-1}$ (n=3) whilst dibutyryl cAMP (800 μ M) stimulated a maximal increase in I_{sc} of $16.4 \pm 3.7 \mu A cm^{-2}$ at a rate of $11.3 \pm 2.0 \mu A cm^{-2} min^{-1}$ (n=4). Figure 3.03 shows these values are comparable to forskolin-stimulated cells and suggest that forskolin-induced changes in I_{sc} are cAMP-dependent. Furthermore, preincubation of cells for one hour with the PKA inhibitor H-89 reduced the forskolin-stimulated maximal increase in I_{sc} by $62 \pm 7\%$ (n=4; $p < 0.05$; fig. 3.03A) and the rate of I_{sc} increase by $78 \pm 7\%$ (n=4; $p < 0.05$; fig. 3.03B) and implicates forskolin-stimulated changes in I_{sc} were due to cAMP activation of PKA and subsequent phosphorylation of CFTR to mediate electrogenic Cl^{-} secretion.

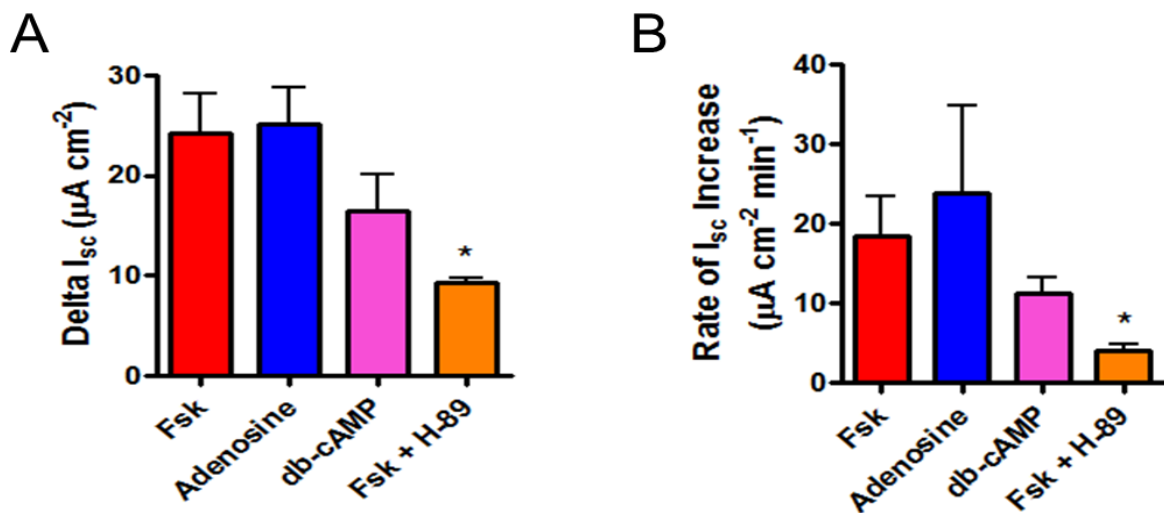


Figure 3.03: Forskolin-stimulated increases in I_{sc} are cAMP and PKA-dependent. The effect of the cAMP agonists adenosine (10 μ M) and dibutyryl cAMP (800 μ M) as well as the PKA inhibitor H-89 (50 μ M) on I_{sc} in Calu-3 cells were measured. The maximal increase in I_{sc} (A) and the rate of I_{sc} increase (B) induced by each agonist are displayed. * = significant effect of H-89 ($p < 0.05$). Data represents mean \pm S.E.M.; n=6 for forskolin, n=3 for adenosine and n=4 for dibutyryl cAMP and forskolin + H-89.

Although the reduced forskolin-stimulated CFTR-dependent I_{sc} measurements observed in acute hypercapnia were likely to be due to a result of CO_2 -induced reductions in $[cAMP]_i$, a reduced expression of CFTR at the apical membrane would also be predicted to cause this effect. Therefore, two independent western blots were carried out on cells that had been incubated for 20 minutes in pregassed high Cl^{-} Krebs solution exposed to either 5% CO_2 , 5%

CO₂ + 5 minute forskolin stimulation, 10% CO₂ or 10% CO₂ + 5 minute forskolin stimulation. Each time, the protein samples were generated in Newcastle but one Western Blot was performed by myself in Newcastle (figs. 3.04A and B) and another blot was performed in the laboratory of Professor Ursula Seidler in Hannover, Germany (figs. 3.04C and D). In each case, there appeared to be a trend for CFTR expression to be higher in cells that had been exposed to acute hypercapnia compared to the normocapnic controls. These data suggest, therefore, that the effect of hypercapnia on CFTR-dependent I_{sc} measurements is actually an underestimation of the degree by which hypercapnia can reduce CFTR activity although whether the effects of hypercapnia on CFTR expression translates to an increased membrane expression is unresolved at the present time.

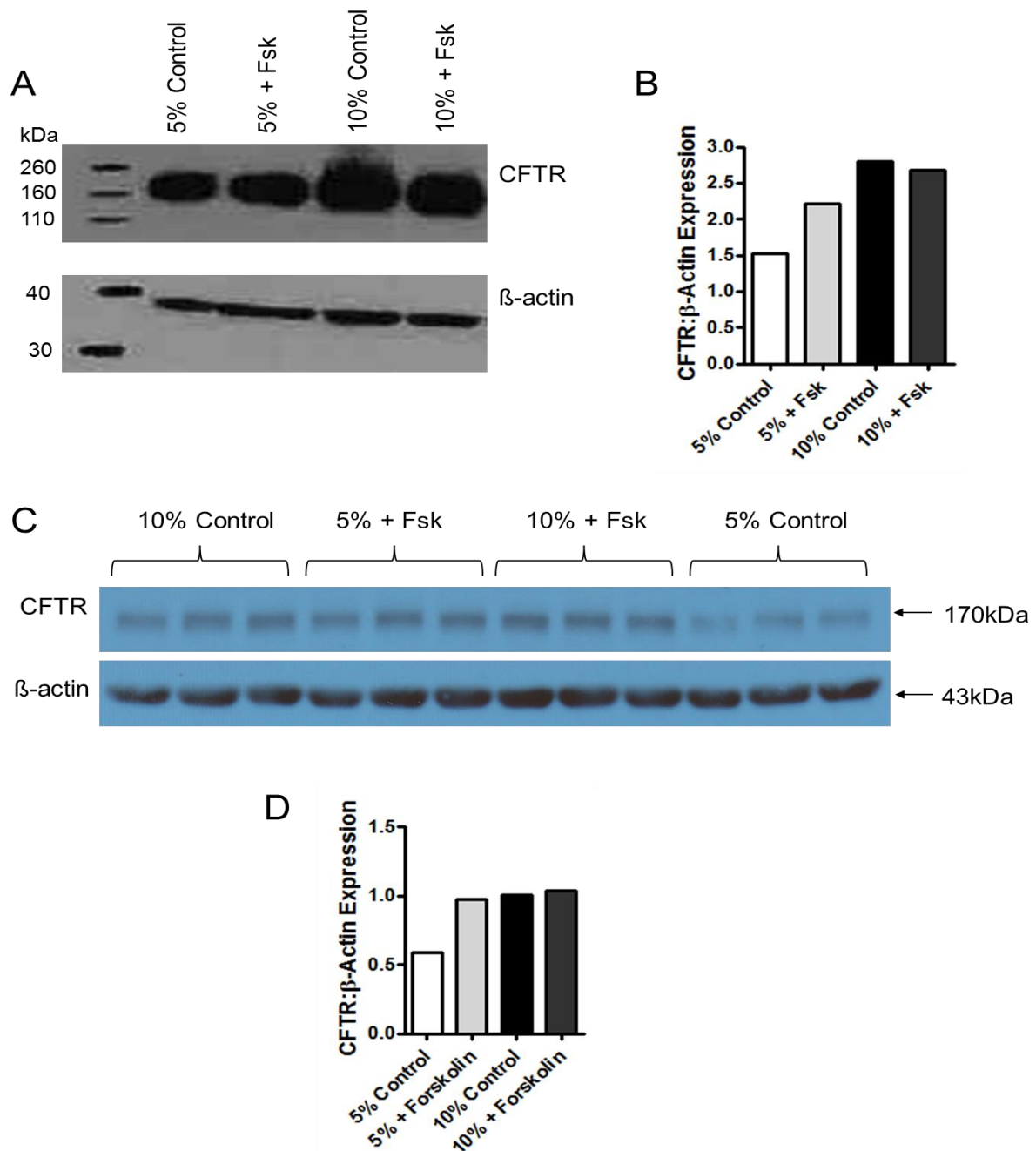


Figure 3.04: Acute hypercapnia increases total CFTR expression in Calu-3 cells. (A) shows the results from a Western Blot performed by myself in Newcastle, in which the effect of forskolin and acute hypercapnia on CFTR protein expression was assessed and normalized to actin expression. The data is summarized in (B). For each experimental condition, 3 lysates were generated from 3 separate transwell. These lysates were combined to produce one lysate for each experimental condition; thus data represents mean of n=1. (C) shows the results from a Western Blot in which the samples were generated in Newcastle but the Western Blot was performed in the laboratory of Prof. Ursula Seidler (Hannover, Germany). Here, for each experimental condition, 3 lysates were generated from 3 separate samples and each lysate was ran on the gel so that each sample was performed in triplicate. The data is summarized in (D). Data represents mean of triplicate sample; n=1 for each condition.

3.4. cAMP agonists produce an intracellular acidification in Calu-3 cells

Agonists that raise intracellular cAMP levels have previously been shown to induce HCO_3^- secretion in Calu-3 cells using short circuit current measurements or by measuring changes in secreted HCO_3^- via the pH stat technique (Devor *et al.*, 1999; Krouse *et al.*, 2004; Shan *et al.*, 2012). Here, real-time intracellular pH measurements were used to assess changes in HCO_3^- transport. As shown in figure 3.05A, in normocapnic conditions, addition of 5 μM forskolin induced an intracellular acidification in Calu-3 cells indicative of net HCO_3^- efflux from the cells until a new steady state pH_i was reached. This acidification was reversible after forskolin wash off. The magnitude of the acidification was 0.18 ± 0.01 pH units ($n=155$) and equated to a HCO_3^- flux of $9.4 \pm 0.5 \text{ mM HCO}_3^- \text{ min}^{-1}$ ($n=155$) when corrected for buffering capacity of the cells. 10 μM adenosine produced a similar intracellular acidification to forskolin. Adenosine caused pH_i to decrease by 0.16 ± 0.01 units ($n=14$) and induced a HCO_3^- flux at a rate of $7.9 \pm 1.1 \text{ mM HCO}_3^- \text{ min}^{-1}$ ($n=14$).

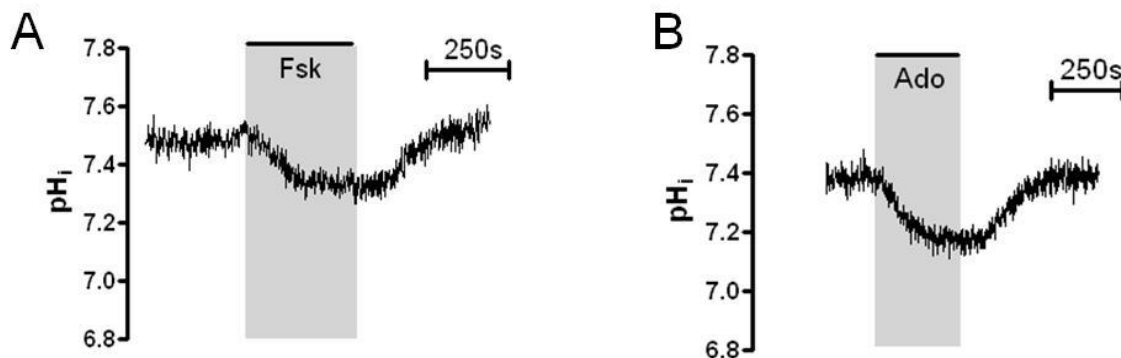


Figure 3.05: cAMP agonists induced a reversible intracellular acidification in Calu-3 cells. 5 μM apical forskolin (A) or 10 μM bilateral adenosine (B) were added to Calu-3 cells and the pH_i changes resulting from agonist stimulation were assessed.

3.5. Profile of cAMP-induced intracellular acidification

3.5.1. HCO_3^- Dependence

To verify that the intracellular acidification following stimulation of cells with a cAMP agonist was HCO_3^- dependent, 25mM NaHCO_3 was replaced with equimolar NaHEPES and cells were stimulated with forskolin (fig. 3.06A). In HCO_3^- containing conditions, forskolin

induced an intracellular acidification of 0.19 ± 0.02 pH units ($n=4$) with a HCO_3^- flux of $12.2 \pm 1.5 \text{ mM min}^{-1}$ ($n=4$). However, there was no observed intracellular acidification in the presence of NaHEPES. Here, forskolin induced a decrease in pH_i of 0.02 ± 0.003 ($p < 0.01$ vs. HCO_3^- containing conditions; $n=4$; fig. 3.06B) which produced no measureable HCO_3^- flux ($0.0 \pm 0.0 \text{ mM min}^{-1}$; $p < 0.01$ vs. HCO_3^- containing conditions; $n=4$; fig. 3.06C). These data imply that the cAMP-stimulated intracellular acidification is a result of HCO_3^- secretion from the cells.

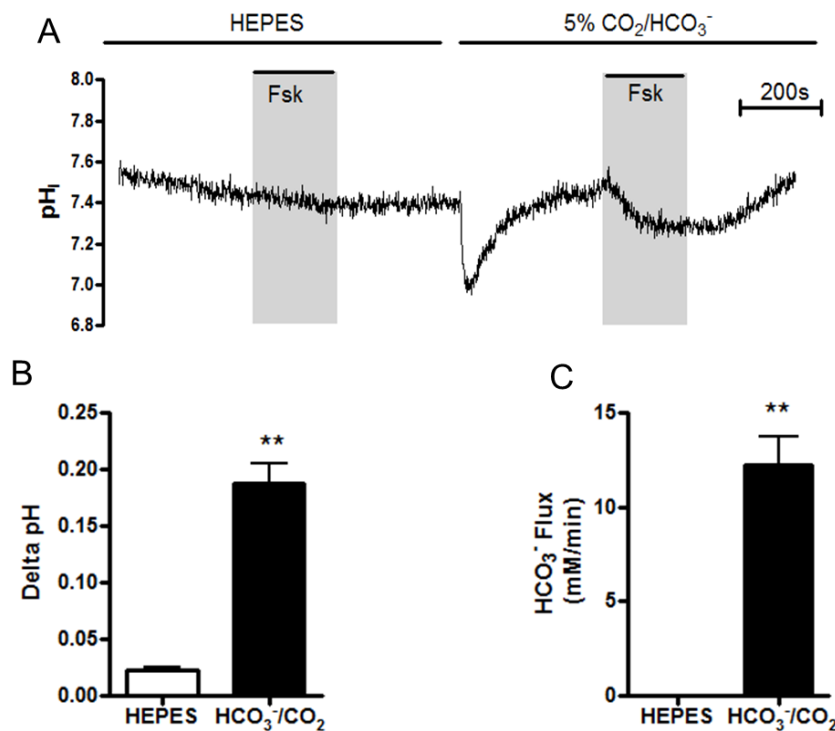


Figure 3.06: Forskolin-stimulated intracellular acidification is HCO_3^- dependent. (A) shows a representative experiment in which cells were stimulated with forskolin in either HEPES buffered solutions or HCO_3^- containing solutions buffered with 5% (v/v) $\text{CO}_2/95\%$ (v/v) O_2 . The ΔpH and the rate of HCO_3^- flux resulting from forskolin stimulation are shown in (B) and (C) respectively. ** = significant difference between HEPES and HCO_3^- containing conditions ($p < 0.01$). Data represents mean \pm S.E.M; $n=4$.

3.5.2. Effect of membrane potential

To further characterize the cAMP-induced intracellular acidification, cells were depolarized by perfusion with a modified high K^+ Krebs solution in which KCl was increased to 115mM and NaCl was reduced to 5mM to eliminate the electrical driving force for anion secretion. As figure 3.07 shows, in control conditions, addition of forskolin caused a decrease in pH_i of 0.14 ± 0.01 ($n=4$; fig. 3.07B) and a HCO_3^- flux of $4.6 \pm 0.4 mM \min^{-1}$ ($n=4$; fig. 3.07C). However, in the presence of high extracellular K^+ , forskolin addition caused a decrease in pH_i of 0.04 ± 0.01 ($p<0.001$ vs. control; $n=4$; fig. 3.07B) which produced no measureable HCO_3^- flux (HCO_3^- flux = $0.0 \pm 0.0 mM \min^{-1}$; $p<0.001$ vs. control; $n=4$; fig. 3.07C). This abolishment of forskolin-stimulated intracellular acidification in depolarized cells indicated that anion secretion (i.e. HCO_3^-) underlies the response to cAMP agonists.

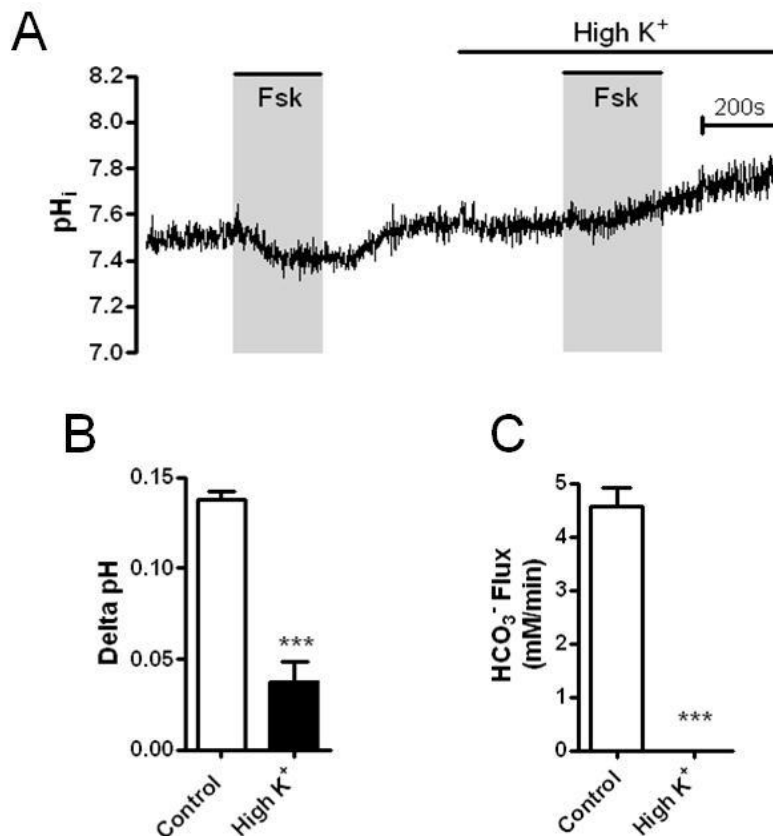


Figure 3.07: Depolarization of Calu-3 cells prevents forskolin-stimulated intracellular acidification. (A) shows a representative experiment in which the effect of high extracellular $[K^+]$ on the forskolin-stimulated intracellular acidification was assessed. The delta pH (B) and HCO_3^- flux (C) were compared between the control response and the response in the presence of 115mM extracellular K^+ . *** = significant effect of high extracellular $[K^+]$ ($p<0.001$). Data represents mean \pm S.E.M; $n = 4$ for each.

3.5.3. SQ 22,536 Sensitivity

Both forskolin and adenosine stimulate cAMP production *via* an activation of transmembrane adenylyl cyclase (tmAC) either directly, by forskolin, or due to activation of G-protein coupled receptors by adenosine. Therefore, it would be predicted that forskolin or adenosine-induced intracellular acidification would be blocked by inhibition of tmAC. Cells were preincubated for one hour with the tmAC inhibitor SQ 22,536 (500 μ M) and the response to 5 μ M forskolin was assessed immediately, and then after 20 minutes of inhibitor wash out (fig. 3.08A). As shown in figure 3.08B, SQ 22,536 had no effect on the delta pH resulting from forskolin stimulation (initial response = 0.21 ± 0.03 ; response after inhibitor wash out = 0.22 ± 0.02 ; $p > 0.05$; $n = 3$) but SQ 22,536 did appear to have an inhibitory effect on the rate of forskolin-stimulated HCO_3^- flux (initial response = $6.6 \pm 1.3 \text{ mM min}^{-1}$; response after inhibitor wash out = $14.3 \pm 1.7 \text{ mM min}^{-1}$; $p < 0.05$; $n = 3$; fig 3.08C). These findings suggested that inhibition of tmAC is able to impair cAMP-stimulated HCO_3^- transport and that the forskolin-stimulated increases in cAMP is dependent on the activity of tmAC.

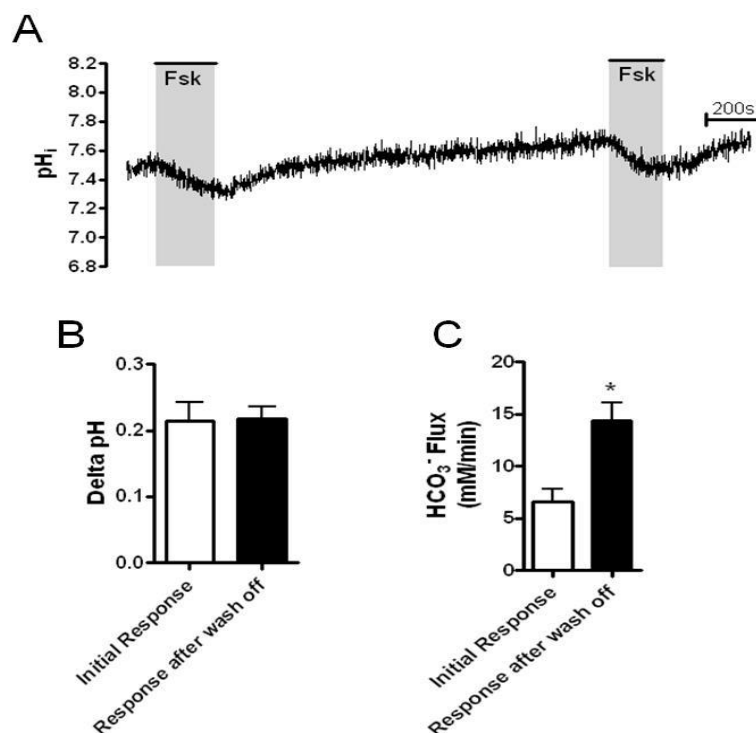


Figure 3.08: Preincubation of Calu-3 cells with SQ 22,536 causes a reversible decrease in the rate of the forskolin-stimulated intracellular acidification. (A) shows a representative experiment in which cells were preincubated with 500 μ M SQ22,536 for one hour and the response to 5 μ M forskolin was assessed immediately and then 20 minutes later. The delta pH (B) and HCO_3^- flux (C) were compared between the initial response to forskolin and the response after washing. * = significant difference after washing ($p < 0.05$). Data represents mean \pm S.E.M; $n = 3$.

3.5.4. H-89 Sensitivity

One of the major actions of cAMP is to activate PKA, which phosphorylates downstream targets (e.g. CFTR). Our laboratory has shown that inhibition of PKA, using H-89, blocked forskolin-stimulated CFTR-dependent anion exchange activity in Calu-3 cells, thus highlighting the importance of PKA in cAMP-regulated HCO_3^- transport (Garnett *et al.*, 2011). To assess whether the cAMP-induced intracellular acidification was PKA-dependent, cells were preincubated with 50 μM H-89 for one hour and the response to 10 μM adenosine was assessed immediately and then after 20 minutes of inhibitor wash out (fig. 3.09A). This was also compared to control experiments performed on the same day in which cells had not been treated with H-89. For control experiments, adenosine produced an HCO_3^- flux of $7.6 \pm 1.1 \text{ mM min}^{-1}$. In H-89 treated cells, the HCO_3^- efflux induced by immediate stimulation with adenosine was significantly reduced to $2.5 \pm 0.5 \text{ mM min}^{-1}$ ($p < 0.05$ vs. control cells; $n=4$; fig. 3.09C) implying that PKA was involved in producing the intracellular acidification in response to a cAMP agonist. However, it appeared that H-89 was reversible as in H-89 preincubated cells, after 20 minutes of inhibitor wash out, there was some recovery in the response to adenosine with adenosine-stimulated HCO_3^- flux increasing to $5.6 \pm 0.9 \text{ mM min}^{-1}$ which was not statistically significantly different to control conditions ($p > 0.05$ vs. control cells; $n=4$; fig 3.09C).

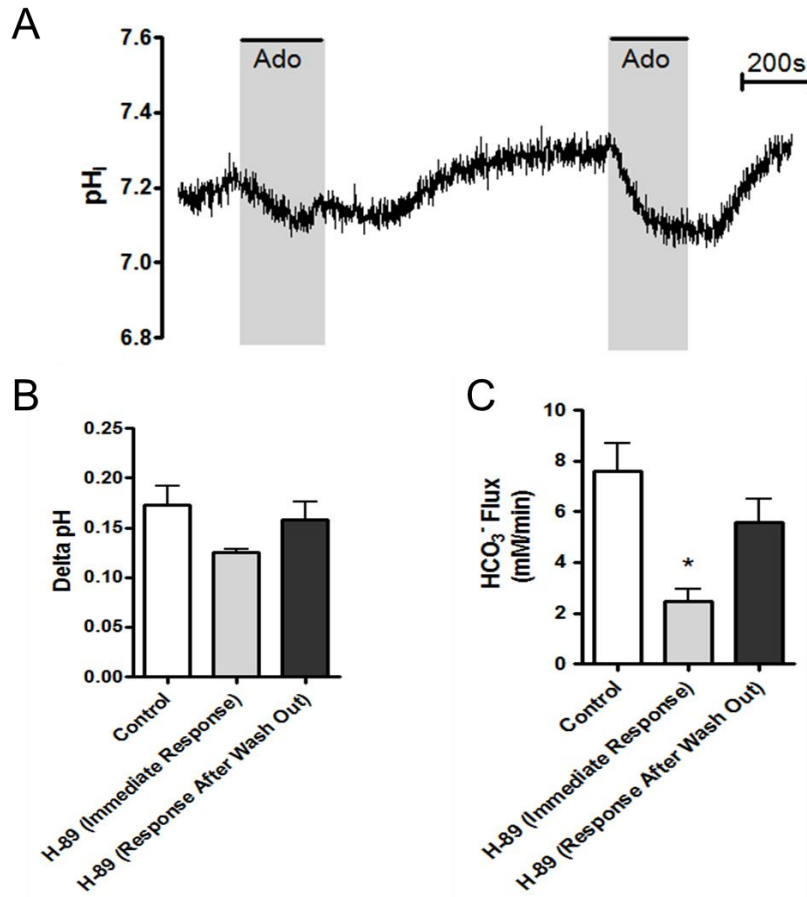


Figure 3.09: Preincubation of Calu-3 cells with H-89 causes a reversible decrease in the rate of the adenosine-stimulated intracellular acidification. (A) shows a representative experiment in which cells were preincubated with 50 μ M H-89 for one hour and the response to 10 μ M bilateral adenosine was assessed immediately and then 20 minutes later. The ΔpH (B) and HCO_3^- flux (C) were compared between the initial response to adenosine and the response after washing as well as untreated controls. * = significant effect of H-89 vs. untreated controls ($p < 0.05$). Data represents mean \pm S.E.M; $n = 8$ for untreated cells and $n = 4$ for H-89 treated cells.

3.5.5. GlyH-101 Sensitivity

Having shown that the cAMP-induced intracellular acidification was tmAC and PKA-dependent, it was important to assess whether the HCO_3^- efflux was mediated *via* CFTR. Cells were stimulated with forskolin in the presence or absence of the CFTR inhibitor GlyH-101 (Muanprasat *et al.*, 2004) as shown in figure 3.10A. In control conditions, forskolin induced a decrease in pH_i of 0.16 ± 0.03 units ($n=4$) and a HCO_3^- flux of $10.2 \pm 3.3 \text{ mM min}^{-1}$ ($n=4$). However, in the presence of GlyH-101, forskolin elicited a decrease in pH_i of 0.03 ± 0.02 units ($n=4$; $p < 0.05$ vs. control; fig. 3.10B) and a HCO_3^- flux of $2.2 \pm 0.5 \text{ mM min}^{-1}$ ($n=4$;

$p < 0.05$ vs. control; fig. 3.10C). Therefore, these data show that the forskolin-stimulated intracellular acidification resulting from HCO_3^- flux is almost completely CFTR-dependent.

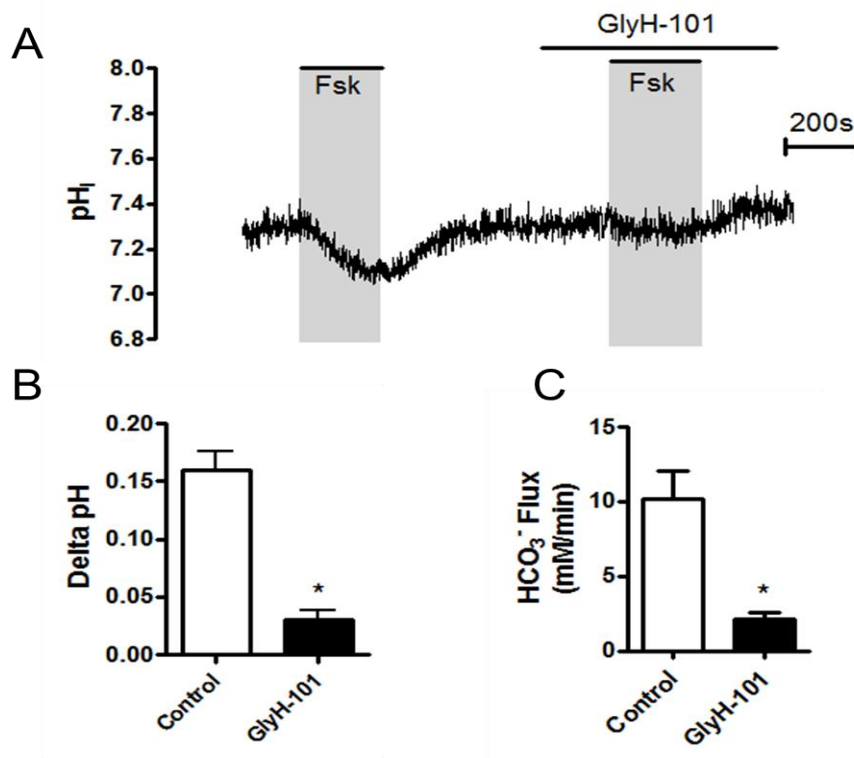


Figure 3.10: GlyH-101 inhibits forskolin-stimulated intracellular acidification. (A) shows an example pH_i trace in which the effect of GlyH-101 (10 μM) on the forskolin-stimulated intracellular acidification was assessed. The delta pH (B) and HCO_3^- flux (C) were compared between the control response and the response in the presence of GlyH-101. * = significant effect of GlyH-101 ($p < 0.05$). Data represents mean \pm S.E.M; $n = 4$ each.

3.6. Hypercapnia increases the magnitude and rate of cAMP-induced intracellular acidification

My results have shown that addition of agonists that elevate intracellular cAMP produced an intracellular acidification as a result of CFTR-dependent HCO_3^- secretion. Therefore, to investigate how acute hypercapnia affected cAMP-regulated HCO_3^- transport, cAMP agonists were added when cells were exposed to 10% CO_2 . As already shown in figure 3.01A, exposure of Calu-3 cells to 10% CO_2 caused an intracellular acidification which took approximately 20 minutes for cells to recover from. Therefore, cells were stimulated with cAMP agonist after pH_i recovery to eliminate any differences in pH_i affecting the response to agonist stimulation. This assay, illustrated in figures 3.11A and D, was used to investigate the

effect of acute hypercapnia on cAMP-stimulated HCO_3^- transport and is therefore used for a large part of this work. As shown in figure 3.11, both forskolin and adenosine-stimulated intracellular acidifications were significantly enhanced in hypercapnic conditions. In normocapnia, forskolin caused pH_i to decrease by 0.19 ± 0.01 and induced a HCO_3^- flux of $9.7 \pm 0.5 \text{ mM HCO}_3^- \text{ min}^{-1}$ ($n=130$). However, in hypercapnia forskolin caused pH_i to decrease by 0.35 ± 0.01 ($p<0.001$ vs. normocapnia; $n=130$; fig. 3.11B) and induced a HCO_3^- flux of $37.6 \pm 1.5 \text{ mM HCO}_3^- \text{ min}^{-1}$ ($p<0.001$ vs. normocapnia; $n=130$; fig. 3.11C) which corresponded to a 2.0 ± 0.04 fold increase in the magnitude of the acidification ($p<0.001$; $n=130$) and a 4.5 ± 0.2 fold increase in the rate of forskolin-stimulated HCO_3^- flux ($p<0.001$; $n=130$). Similarly, in normocapnia, adenosine caused pH_i to decrease by 0.16 ± 0.01 ($n=14$) and induced a HCO_3^- flux of $7.9 \pm 1.1 \text{ mM HCO}_3^- \text{ min}^{-1}$ ($n=14$). However, in hypercapnia adenosine caused pH_i to decrease by 0.27 ± 0.02 ($p<0.001$ vs. normocapnia; fig. 3.11E) and induced a HCO_3^- flux of $23.0 \pm 2.7 \text{ mM HCO}_3^- \text{ min}^{-1}$ ($p<0.001$ vs. normocapnia; fig. 3.11F) which corresponded to a 1.7 ± 0.1 fold increase of in the magnitude of the acidification ($p<0.001$; $n=14$) and a 3.2 ± 0.3 fold increase in the rate of adenosine-stimulated HCO_3^- flux ($p<0.001$; $n=14$). Therefore, these data showed that acute hypercapnia modulated cAMP-regulated HCO_3^- transport in Calu-3 cells.

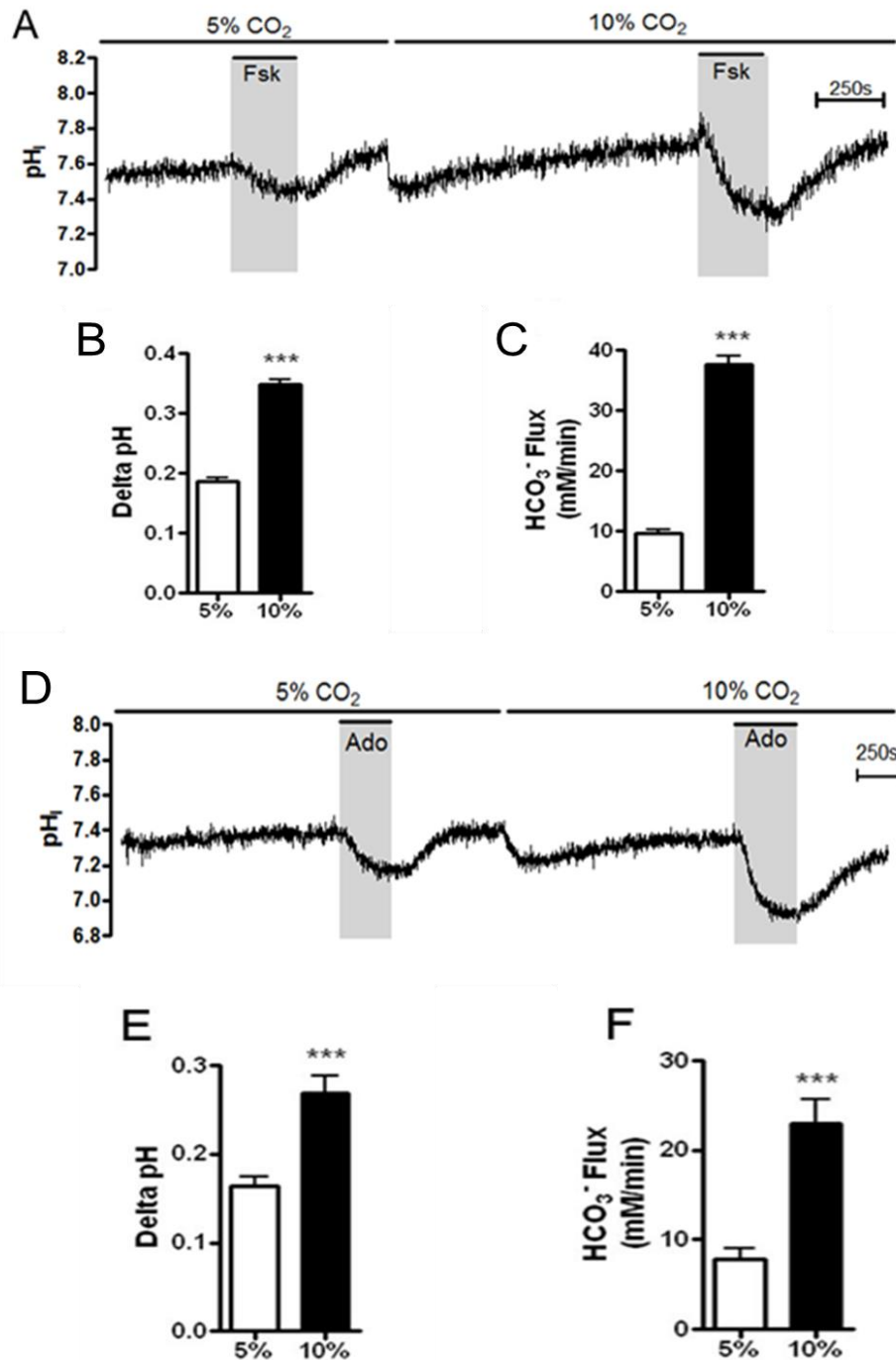


Figure 3.11: Acute hypercapnia increases the magnitude and rate of forskolin and adenosine-stimulated intracellular acidification. (A) shows a representative experiment in which Calu-3 cells were stimulated with 5 μ M forskolin in normocapnia and hypercapnia. The delta pH (B) and the HCO₃⁻ flux (C) resulting from forskolin stimulation are displayed. *** = significant effect of hypercapnia ($p < 0.001$). Data represents mean \pm S.E.M., $n = 130$ for each. (D) shows a representative experiment in which Calu-3 cells were stimulated with 10 μ M bilateral adenosine in normocapnia and hypercapnia. The delta pH (E) and the HCO₃⁻ flux (F) resulting from adenosine stimulation are displayed. *** = significant effect of hypercapnia ($p < 0.001$). Data represents mean \pm S.E.M., $n = 14$ for each.

A dose response curve of the forskolin-stimulated decrease in pH_i and the rate of forskolin-stimulated HCO_3^- flux are shown in figs 3.12A and 3.12B and respectively. In hypercapnic conditions, the forskolin-stimulated intracellular acidification was significantly enhanced at 3, 5, 10 and 30 μM forskolin ($p < 0.05$).

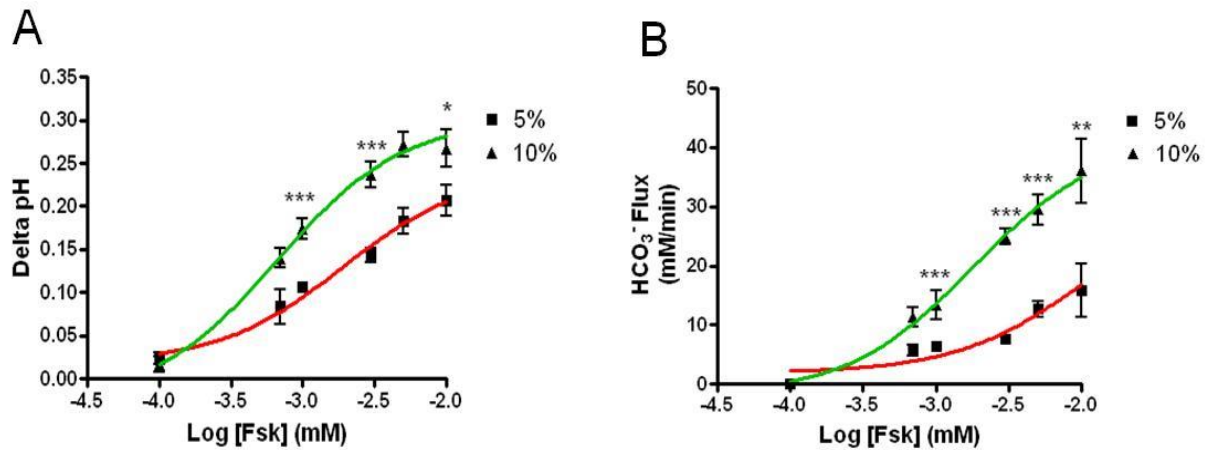


Figure 3.12: The effect of hypercapnia on the dose response of forskolin-stimulated acidification in Calu-3 cells. Cells were stimulated with increasing concentrations of forskolin and the delta pH (A) and rate of HCO_3^- efflux (B) were assessed in normocapnia and hypercapnia. * = significant effect of hypercapnia ($p < 0.05$; ** = $p < 0.01$; *** = $p < 0.001$). Data represents mean \pm S.E.M., $n = 3$ for each except for concentration of 3 μM and 5 μM in which $n = 6$.

3.7. CO_2 *per se* mediates the effects of hypercapnia

3.7.1. The effect of CO_2 -induced intracellular acidosis

As already discussed, Calu-3 cells were able to recover their pH_i within 20 in response to CO_2 -induced acidosis and therefore, differences in pH_i could be eliminated as the cause of the observed effect of hypercapnia. However, it could be argued that the CO_2 -induced intracellular acidification itself may induce changes in cAMP-regulated HCO_3^- transport. To test this, Calu-3 cells in normocapnia were exposed to an acid load by addition of 40mM sodium acetate (fig. 3.13A). This induced an intracellular acidification of 0.19 ± 0.04 pH units ($n=3$) which was comparable to the acidosis produced by 10% CO_2 in experiments performed on the same day (0.26 ± 0.05 pH units; $p > 0.05$ vs. sodium acetate; $n=3$; fig. 3.13B). Furthermore, Calu-3 cells were able to recover from sodium acetate-induced acidosis over 20 minutes to again mimic the effect of 10% CO_2 . In experiments where cells were exposed to hypercapnia, the forskolin-stimulated delta pH and HCO_3^- flux were significantly increased 1.8 ± 0.1 and 2.4 ± 0.2 fold respectively ($p < 0.05$ vs. normocapnia; $n=3$ for each;

figs 3.13C and D). However, this was not observed in cells exposed to 40mM sodium acetate; delta pH increased 1.4 ± 0.1 fold ($p>0.05$ vs. control; fig. 3.13C) and HCO_3^- flux increased 1.4 ± 0.5 fold ($p>0.05$ vs. control; fig. 3.13D). These data suggest the CO_2 -induced acidification of pH_i did not contribute to the effect of hypercapnia on the forskolin-stimulated intracellular acidification.

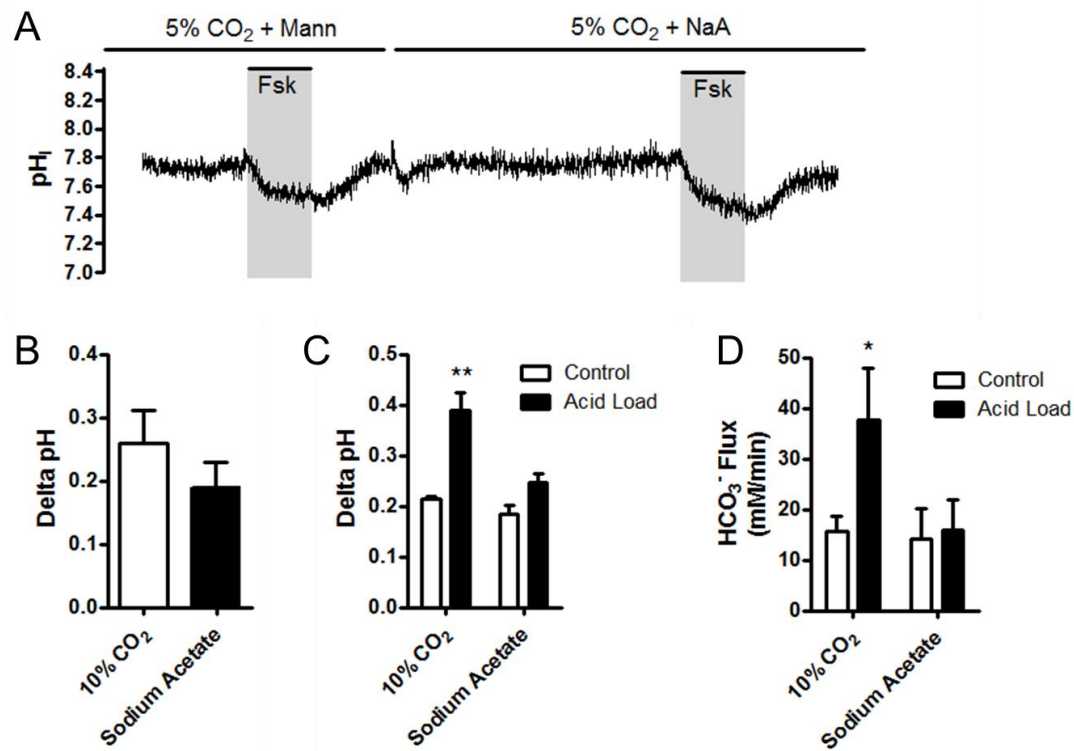


Figure 3.13: CO_2 -induced intracellular acidosis does not contribute to the effect of hypercapnia on cAMP-regulated HCO_3^- transport. (A) shows an example experiment in which cells were stimulated with $5\mu\text{M}$ forskolin in normocapnia with an acid load induced into the cells by the addition of 40mM Na Acetate. The magnitude of the acidification induced by 10% CO_2 and Na Acetate is shown in (B). The delta pH (C) and HCO_3^- flux (D) resulting from forskolin-stimulation were compared between cells exposed to 10% CO_2 and cells exposed to Na Acetate. * = significant effect of hypercapnia ($p<0.05$; ** = $p<0.01$). Data represents mean \pm S.E.M.; $n = 3$ for each.

3.7.2. The effect of CO₂-induced extracellular acidosis

The data from figure 3.13 revealed that CO₂-induced intracellular acidosis did not contribute to the effect of hypercapnia on cAMP-regulated HCO₃⁻ transport. However, the effects of extracellular pH (pH_e) still needed to be assessed. When Krebs solution containing 25mM HCO₃⁻ was gassed with 5% CO₂/95% O₂, the pH of the solution was 7.44 ± 0.02 (n=4). However, gassing with 10% CO₂/90% O₂ caused the pH of the solution to decrease to 7.13 ± 0.04 (n=3). Therefore differences in pH_e could be contributing to the observed effect of hypercapnia. In order to control for differences in pH_e, solutions needed to be at the same pH when gassed with either 5% or 10% CO₂ but without altering the HCO₃⁻ concentration. Therefore, Krebs solutions were modified and the compositions of the solutions used in the following experiments are given in table 3.01. To set pH to 7.44 in solutions gassed with 10% CO₂, 10mM HEPES and 10mM NaOH were added (solution C) whilst for solutions gassed with 5% CO₂, 10mM HEPES and 0.6mM NaOH was added to the solution along with 20mM mannitol to overcome the differences in osmolarity (solution B). When pH_e was maintained at 7.44, hypercapnia still significantly augmented both the adenosine-induced delta pH and HCO₃⁻ flux by 1.7 ± 0.1 and 4.3 ± 0.7 fold respectively (p<0.05 vs. normocapnia; n=3 for each) as shown in figure 3.14. This suggests that differences in pH_e do not contribute to the effect of hypercapnia on intracellular acidification.

	CO ₂	HEPES	NaOH	Mannitol	pH	Osmolarity
Solution A	5%	-	-	-	7.4	280
Solution B	5%	10mM	0.6mM	20mM	7.4	310
Solution C	10%	10mM	10mM	-	7.4	310
Solution D	5%	10mM	0.6mM		7.4	290
Solution E	5%	-	-	10mM	7.4	290
Solution F	5%	-	-	20mM	7.4	310

Table 3.01: Modifications to high Cl⁻ Krebs solution in order to assess the effects of hypercapnia when extracellular pH is equal in both normocapnic and hypercapnic conditions.

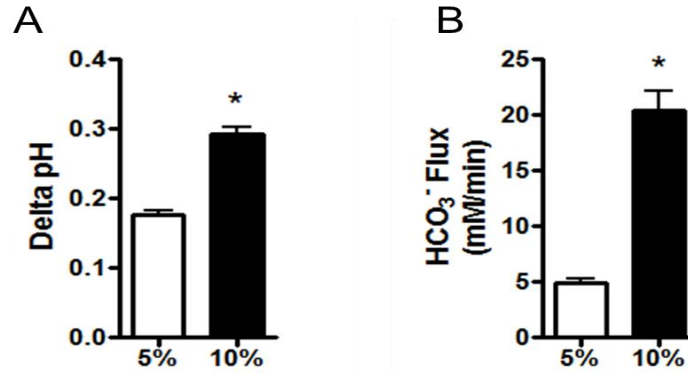


Figure 3.14: The effects of hypercapnia on the forskolin-stimulated intracellular acidification are not due to differences in extracellular pH. Modifications to high Cl⁻ Krebs solution allowed the pH of the solution to be set to pH 7.44 when gassed with either 5% CO₂/95% O₂ (v/v) or 10% CO₂/90% O₂ (v/v). The forskolin-stimulated decrease in pH_i (A) and HCO₃⁻ flux (B) are displayed. * = significant effect of hypercapnia (p<0.05). Data represents mean ± S.E.M., n=3 for each.

As the above experiments had been carried out using solutions containing NaOH and HEPES, it was necessary to ensure that the presence of HEPES and NaOH did not affect the responses to adenosine. Therefore, HEPES/NaOH-containing (solution D) and HEPES/NaOH-free solution containing mannitol (solution E) were compared to determine the effect, if any, of HEPES and NaOH. In control experiments, adenosine induced a decrease in pH_i of 0.26 ± 0.01 (n=3) and a HCO₃⁻ flux of $8.6 \pm 0.8 \text{ mM HCO}_3^- \text{ min}^{-1}$ (n=3). These responses were not significantly different to those observed in HEPES/NaOH-containing solutions; delta pH = 0.25 ± 0.02 (p>0.05 vs. controls) and HCO₃⁻ flux = $10.0 \pm 1.0 \text{ mM HCO}_3^- \text{ min}^{-1}$ (p>0.05 vs. control; n=3 for each) and shows that inclusion of HEPES and NaOH into the solutions did not alter the cells response to cAMP stimulation. Addition of HEPES and NaOH also inevitably increased osmolarity of the solutions and, as such, this parameter was also controlled for by comparing a standard solution of 280mOsm (solution A) to a high osmolarity solution of 310mOsm (solution F). In control experiments, adenosine induced a decrease in pH_i of 0.20 ± 0.03 (n=3) and a HCO₃⁻ flux of $6.0 \pm 0.9 \text{ mM HCO}_3^- \text{ min}^{-1}$ (n=3). These responses were not significantly different to those observed in hyperosmotic solutions; delta pH = 0.17 ± 0.03 (p>0.05 vs. controls; n=3) and HCO₃⁻ flux = $7.3 \pm 2.5 \text{ mM HCO}_3^- \text{ min}^{-1}$ (p>0.05 vs. control; n=3) and shows that the 30mOsm difference did not alter the cells response to cAMP stimulation. Finally, all previous experiments had been carried out by performing the 5% response first and the 10% response second. When attempting to do this the other way round, a change from 10% CO₂ to 5% CO₂ produced an alkalisation of pH_i

which did not subsequently recover. Therefore, in order to ensure there were no time-dependent effects on Calu-3 cells responses to cAMP stimulation, two responses to adenosine were measured with the second one measured 20 minutes after the first one to mimic the time points of the normal assay. In the first response, adenosine induced a decrease in pH_i of 0.18 ± 0.01 ($n=3$) and a HCO_3^- flux of $4.6 \pm 0.5 \text{ mM HCO}_3^- \text{ min}^{-1}$ ($n=3$). These responses were not significantly different to those observed in the second response 20 minutes later; $\Delta \text{pH} = 0.20 \pm 0.02$ ($p>0.05$ vs. first response; $n=3$) and HCO_3^- flux = $7.3 \pm 1.9 \text{ mM HCO}_3^- \text{ min}^{-1}$ ($p>0.05$ vs. first response; $n=3$) and shows that the effect of hypercapnia was not simply observed because it was always measured after stimulation of the cells in normocapnia.

3.7.3. The effect of carbonic anhydrase-dependent hydration of CO_2

Hypercapnia may produce a significant increase in cAMP-stimulated intracellular acidification due to the fact that increased intracellular CO_2 would favour an increased production of HCO_3^- due to the action of carbonic anhydrase catalysing the formation of carbonic acid. A higher intracellular $[\text{HCO}_3^-]$ would increase the driving force for HCO_3^- efflux and therefore may produce the increase in cAMP-induced acidification observed in hypercapnic conditions. Therefore, to test this possibility, cells were treated with the non-specific carbonic anhydrase inhibitor acetazolamide to assess whether increased intracellular HCO_3^- underlies the effect of hypercapnia. In control experiments, hypercapnia elicited a 2.0 ± 0.04 fold increase in the magnitude of the forskolin-stimulated intracellular acidification ($p<0.05$; $n=4$; fig. 3.15A) and a 3.1 ± 0.7 fold increase in the rate of forskolin-stimulated HCO_3^- flux ($p<0.05$; $n=4$; fig. 3.15B). In acetazolamide treated cells, hypercapnia induced a 1.5 ± 0.2 fold increase in the magnitude of the forskolin-stimulated intracellular acidification ($p<0.05$ vs. normocapnia; $p>0.05$ vs. control experiments; $n=4$; fig. 3.15A) and a 2.3 ± 0.3 fold increase in the rate of forskolin-stimulated HCO_3^- flux ($p<0.05$ vs. normocapnia; $p>0.05$ vs. control experiments; $n=4$; fig. 3.15B). These data suggest that a CO_2 -induced increase in HCO_3^- production *via* carbonic anhydrase activity does not underlie the effects of hypercapnia in Calu-3 cells.

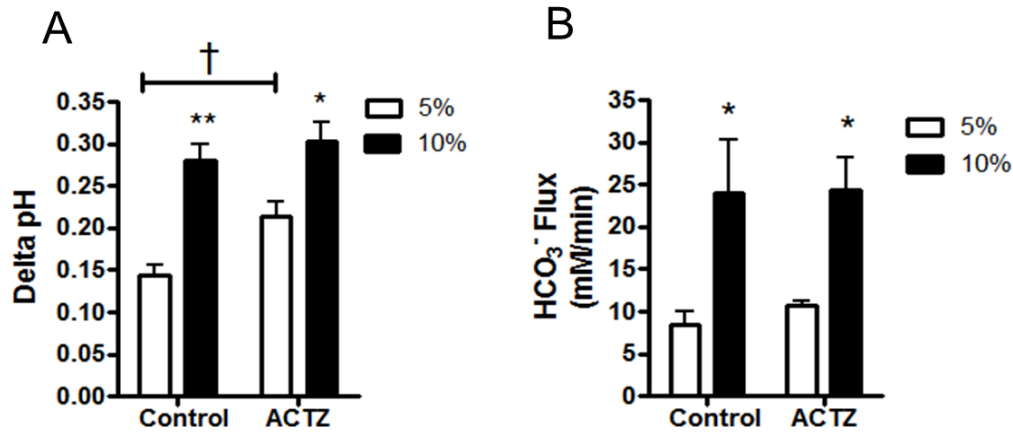


Figure 3.15: Acetazolamide does not block the effect of hypercapnia on the forskolin-stimulated acidification. Calu-3 cells were stimulated with 5 μM forskolin in normocapnic (5% CO₂) and hypercapnic (10% CO₂) in the presence or absence of 100 μM acetazolamide. The delta pH (A) and the HCO₃⁻ flux (B) resulting from forskolin stimulation are displayed. * = significant effect of hypercapnia (p < 0.05; ** = p < 0.01); † = significant effect of acetazolamide (p < 0.05). Data represents mean ± S.E.M.; n = 4 for each.

3.7.4. CO₂ does not mediate its effects on cAMP-regulated HCO₃⁻ transport *via* sAC

The findings displayed in figure 3.7 suggest that activation of tmAC is important for forskolin-stimulated HCO₃⁻ transport in Calu-3 cells. Although our laboratory has shown CO₂ can modulate tmAC activity (Townsend *et al.*, 2009; Cook *et al.*, 2012), CO₂ has also been shown to regulate sAC activity (Schmid *et al.*, 2010; Rahman *et al.*, 2013) and that sAC can regulate CFTR in Calu-3 cells (Wang *et al.*, 2008). Therefore, changes in sAC activity may underlie the effect of elevated CO₂ on cAMP-regulated HCO₃⁻ transport. To test this, the sAC inhibitor KH7 was used to see whether it could block the effect of hypercapnia. KH7 had a small but significant effect on the magnitude of the forskolin-stimulated intracellular acidification; in control conditions, hypercapnia increased the magnitude of the acidification 1.5 ± 0.1 fold (p < 0.05 vs. normocapnia; n = 4; fig 3.16A) but this was reduced to a 1.3 ± 0.03 fold increase of in KH7 treated cells (p > 0.05 vs. normocapnia; p > 0.05 vs. control experiments; n = 4; fig. 3.16A) and suggests there may be a small role of sAC in responses to hypercapnia. However, when looking at the rate of forskolin-stimulated HCO₃⁻ flux resulting from forskolin stimulation, hypercapnia caused this to increase 2.9 ± 0.03 fold in control experiments (p < 0.05; n = 4; fig. 3.16B) and 2.6 ± 0.3 fold in KH7 treated cells (p < 0.05 vs. normocapnia; p > 0.05 vs. control experiments; n = 4; fig 3.16B). Together, these data suggest

that sAC has a minimal role in mediating the effects of hypercapnia on cAMP-regulated HCO_3^- transport.

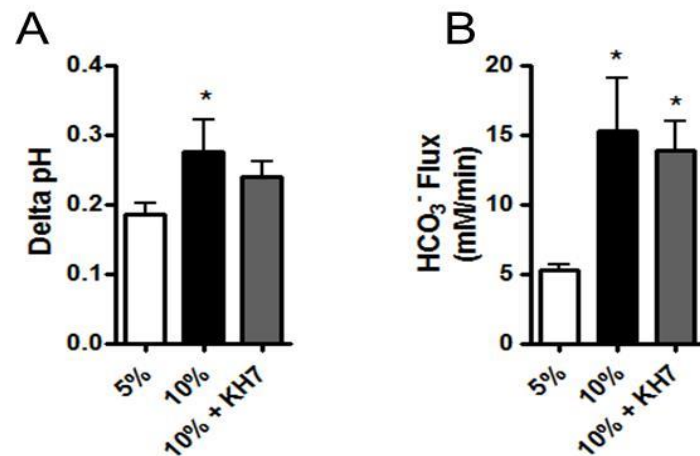


Figure 3.16: KH7 does not block the effect of hypercapnia on the forskolin-stimulated intracellular acidification. The effect of the sAC inhibitor KH7 (10 μM) on the forskolin-stimulated acidification was assessed in hypercapnic conditions. The delta pH (A) and the HCO_3^- flux (B) resulting from forskolin stimulation are displayed. * = significant effect of hypercapnia ($p < 0.05$). Data represents mean \pm S.E.M.; $n=4$ for each.

3.7.5. CO_2 does not mediate its effects on adenosine-stimulated HCO_3^- transport via regulation of PLA_2

Given that both adenosine and forskolin evoke very similar responses in Calu-3 cells that are both similarly modulated by hypercapnia, it strongly suggests that both are signalling *via* the same pathway i.e. by elevating intracellular cAMP levels. However, Cobb *et al.* (2002) have shown that adenosine can also activate phospholipase A_2 in Calu-3 cells when signalling *via* $\text{A}_{2\text{B}}$ receptors. Inhibition of PLA_2 activity reduced CFTR activity when expressed in cos-7 cells. Furthermore, activation of PLA_2 caused production of arachidonic acid which, when added exogenously, increased intracellular cAMP levels in Calu-3 cells. It was therefore important to know whether the CO_2 -mediated changes in adenosine-stimulated intracellular acidification were PLA_2 dependent. The PLA_2 inhibitor AACOCF₃ was unable to block the effect of hypercapnia on adenosine-stimulated cells; hypercapnia increased the magnitude of the adenosine-stimulated intracellular acidification 1.9 ± 0.2 fold in control conditions ($p < 0.01$; $n=4$) and 1.8 ± 0.2 fold in the presence of AACOCF₃ ($p < 0.01$; $n=4$; fig. 3.17A). Similarly, hypercapnia enhanced the rate of forskolin-stimulated HCO_3^- flux 4.0 ± 0.7 fold in control conditions ($p < 0.01$; $n=4$) and 4.2 ± 0.8 fold in the presence of AACOCF₃ ($p < 0.01$;

n=4; fig. 3.17B). These data suggest that (i) the adenosine-stimulated intracellular acidification is not dependent on PLA₂ and (ii) hypercapnia does not modulate the PLA₂ pathway to mediate its effects in adenosine-stimulated cells.

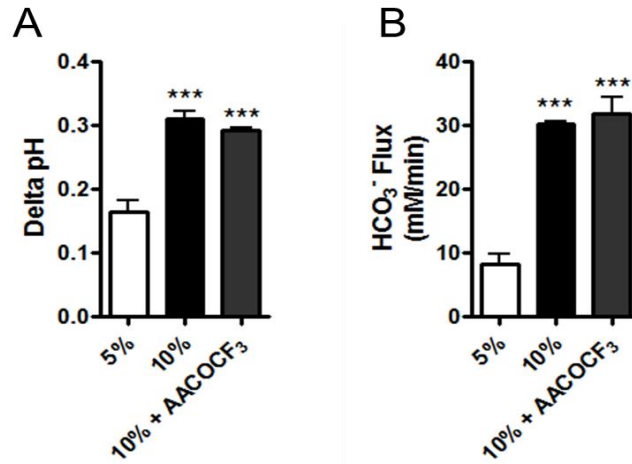


Figure 3.17: AACOCF₃ does not block the effect of hypercapnia on adenosine-stimulated intracellular acidification. The effect of PLA₂ inhibitor AACOCF₃ (20μM) on the adenosine-stimulated acidification was assessed in hypercapnic conditions. The delta pH (A) and the HCO₃⁻ flux (B) resulting from adenosine stimulation are displayed. *** = significant effect of hypercapnia (p<0.001). Data represents mean ± S.E.M.; n=4 for each.

3.8. Hypocapnia does not modulate cAMP-regulated HCO₃⁻ transport

To investigate the dose-response of cAMP-regulated HCO₃⁻ transport to CO₂, the effect of hypocapnia (2.5% CO₂) was assessed on the forskolin-stimulated intracellular acidification. As shown in figure 3.18A, exposure of cells to 2.5% CO₂ induced an intracellular alkalinisation of 0.25 ± 0.05 units (n=3) that did not recover after twenty minutes. This highlights that Calu-3 cells have adaptive mechanisms to recover from intracellular acidosis but not intracellular alkalinisation, perhaps suggesting Calu-3 cells are much more tolerant to increases in pH_i as opposed to decreases. When assessing the forskolin-stimulated intracellular acidification, hypocapnia actually caused a 4.9 ± 1.9 fold reduction in the magnitude of the acidification (p<0.05; n=3; fig. 3.18B). However, there was no effect of hypocapnia on the rate of forskolin-stimulated HCO₃⁻ flux compared to normocapnia. Here, hypocapnia induced a 0.7 ± 0.1 fold change in the rate of forskolin-stimulated HCO₃⁻ flux (p>0.05; n=3; fig. 3.18C) Together, these data suggest hypocapnia may have a small effect on regulation of cAMP-stimulated HCO₃⁻ transport, although whether this is due to the increased in pH_i or an effect of the lower CO₂ is still yet to be determined.

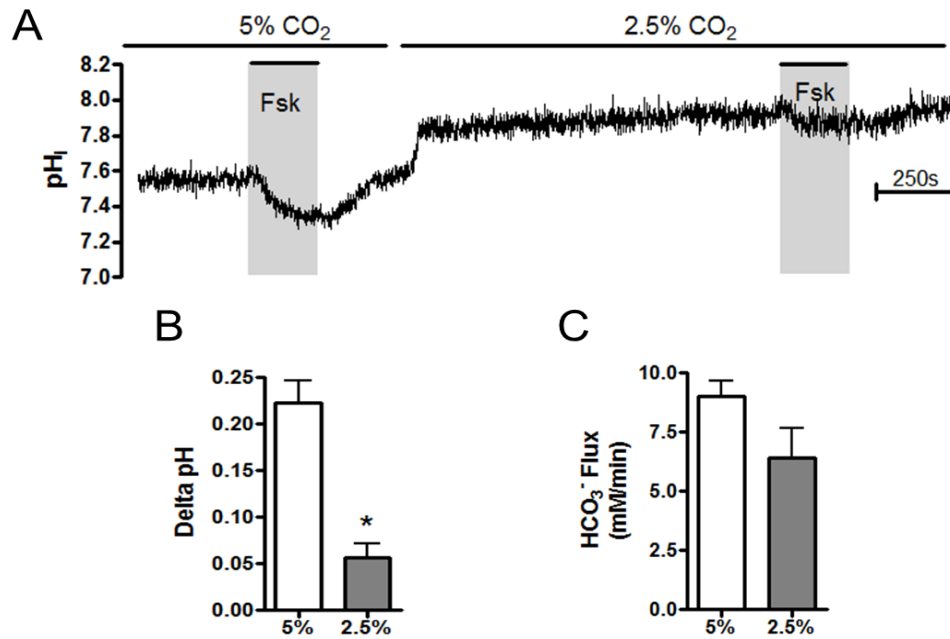


Figure 3.18: Hypocapnia does not modulate forskolin-stimulated HCO₃⁻ transport in Calu-3 cells. (A) shows a representative experiment in which cells were stimulated with 5μM forskolin in normocapnia (5% CO₂) and after 20 minutes exposure to hypocapnia (2.5% CO₂). The delta pH (B) and HCO₃⁻ flux (C) are summarized. * = significant effect of hypocapnia (p<0.05). Data represents mean ± S.E.M.; n=3 for each.

3.9. Permeability of Calu-3 Cells to CO₂

It was initially believed that gases crossed cell membranes passively and there was no requirement for carrier proteins. However, several studies have suggested that aquaporins mediate CO₂ transport into and out of cells. Expression of AQP1 in *Xenopus* oocytes significantly enhances their CO₂ permeability (Nakhoul *et al.*, 1998) whilst AQP1 mediates 60% of CO₂ transport across red blood cells (Endeward *et al.*, 2006). Musa-Aziz *et al.* (2009) showed that AQP4 and AQP5 were also CO₂ permeable when expressed in *Xenopus* oocytes and imply that CO₂ transport across the lipid bilayer is mediated by aquaporin-dependent facilitated diffusion. An alternative explanation of CO₂ permeability was suggested by Itel *et al.* (2012) who argued that the cholesterol content of the lipid bilayer was a major determinant of CO₂ permeability. In MDCK cells, increasing membrane cholesterol reduced CO₂ diffusion into the cell whereas the opposite was true when membrane cholesterol was decreased. This paper also reported that AQP1 expression enhanced CO₂ diffusion supporting findings from previously mentioned studies. A summary of the role of aquaporins in gas transport across cells is reviewed by Herrera and Garvin (2011).

To investigate the permeability of Calu-3 cells to CO₂, intracellular pH measurements were performed with the premise that when CO₂ enters the cells, an intracellular acidification would occur due to the formation of carbonic acid and subsequent dissociation into H⁺ and HCO₃⁻. Figure 3.19A shows that applying 10% CO₂ to both the apical and basolateral membrane elicited an intracellular acidification of 0.24 ± 0.02 units (n=6) which is reversible after 10% CO₂ is removed. Applying 10% CO₂ to the apical membrane caused an acidification of 0.22 ± 0.02 (n=6) units whilst applying 10% CO₂ to the basolateral membrane causes an acidification of 0.01 ± 0.01 units (p<0.001 vs. bilateral or apical 10% CO₂; n=6; fig. 3.19B). Therefore, these findings show that only the apical membrane of Calu-3 cells are CO₂-permeable and may indicate differences in cholesterol levels and/or aquaporin expression at each membrane. Physiologically, these findings are interesting given that serous cells may in fact be insensitive to changes in P_aCO₂ if CO₂ from the blood is unable to cross the basolateral membrane. To determine whether the asymmetry in CO₂ membrane permeability is specific for this gas, NH₃ transport was also assessed. AQP1 has also been reported to be permeable to NH₃ permeable and therefore any similarities between CO₂ and NH₃ permeability in Calu-3 cells would suggest AQP1 is responsible for transportation of CO₂ (Musa-Aziz *et al.*, 2009). 20mM NH₄Cl was added to either the apical membrane or basolateral membrane and the resulting pH_i changes that resulted were assessed. If membranes are permeable to NH₃, an alkalinisation will result from NH₃ entry into cells and association with H⁺ to form NH₄⁺. Addition of apical NH₄Cl caused a pH increase of 0.62 ± 0.10 units (n=4) whilst addition of basolateral NH₄Cl actually caused a pH decrease of 0.14 ± 0.04 units (n=4; p<0.001 vs apical NH₄Cl). Therefore, like with CO₂, there exists differences in membrane permeability to NH₃ and suggests differential expression of aquaporins may be responsible for this asymmetry.

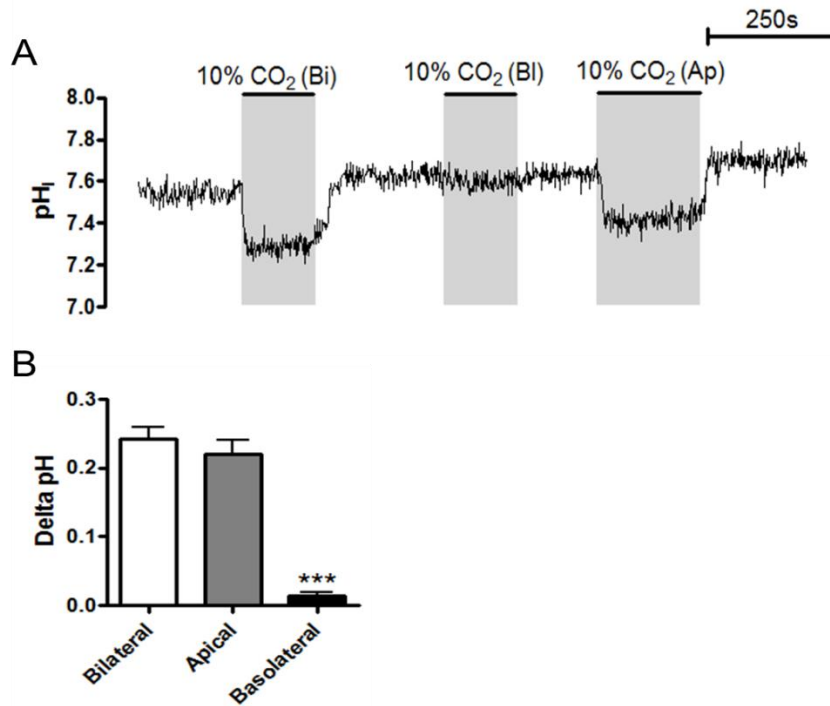


Figure 3.19: Only the apical membrane of Calu-3 cells is permeable to CO₂. (A) shows a representative experiment in which cells were exposed to 10% CO₂ either bilaterally (bi), basolaterally only (bl) or apically only (ap). The acidification that results from 10% CO₂ treatment is displayed in (B). *** = significant effect of administering 10% CO₂ to the basolateral membrane only ($p < 0.001$). Data represents mean \pm S.E.M.; $n = 6$ for each.

3.10. CO₂ elicits membrane specific effects

Given the asymmetry in membrane permeability to CO₂ in Calu-3 cells, it was interesting to see whether the effects of hypercapnia on cAMP-regulated HCO₃⁻ transport were also dependent on the site of CO₂ exposure. The response to forskolin was measured in normocapnia and then again in cells that had been exposed to either apical, basolateral or bilateral 10% CO₂. Bilateral 10% CO₂ increased the magnitude of the forskolin-stimulated intracellular acidification 1.7 ± 0.1 fold ($p < 0.05$ vs. normocapnia; $n = 3$) which was similar to the 2.2 ± 0.3 fold increase observed when 10% CO₂ was applied apically only ($p < 0.05$ vs. normocapnia; $n = 3$; figure 3.20A). However, in the presence of basolateral 10% CO₂, only a 1.3 ± 0.1 fold increase in the magnitude of the forskolin-stimulated intracellular acidification was observed which was not statistically significantly different from normocapnia ($p > 0.05$ vs. normocapnia; $n = 3$; fig 3.20A). Furthermore, when assessing the rate of forskolin-stimulated HCO₃⁻ flux, the fold increases in bilateral hypercapnia, apical hypercapnia and basolateral hypercapnia were 3.5 ± 0.6 ($p < 0.05$ vs. normocapnia; $n = 3$), 2.5 ± 0.3 ($p < 0.05$ vs.

normocapnia; n=3) and 1.6 ± 0.3 ($p > 0.05$ vs. normocapnia; n=3) respectively (fig. 3.20B). These data show that the effect of hypercapnia on cAMP-regulated HCO_3^- transport is dependent on CO_2 being applied to the apical membrane.

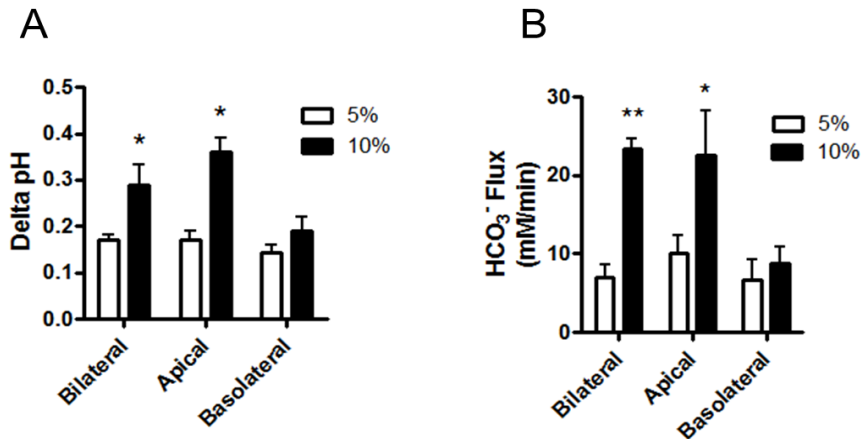


Figure 3.20: Only apical CO_2 induced modulations to forskolin-stimulated intracellular acidification. Calu-3 cells were stimulated with $5\mu\text{M}$ forskolin in normocapnia (5% CO_2) and hypercapnia (10% CO_2) with 10% CO_2 applied either to both membranes (bilateral) or only either the apical membrane or basolateral membrane. The delta pH (B) and the rate of HCO_3^- flux (C) resulting from forskolin stimulation are displayed. * = significant effect of hypercapnia ($p < 0.05$; ** = $p < 0.01$). Data represents mean \pm S.E.M.; n = 3 for each.

3.11. Recovery of pH_i from CO_2 -induced acidosis

It was interesting to understand more about the pH_i recovery that occurs after Calu-3 cells are exposed to 10% CO_2 and attempt to identify the CO_2 -sensitive mechanisms/transporters that facilitated pH_i recovery. The following equation was used to calculate % recovery from CO_2 -induced acidosis with the values obtained as indicated in figure 3.21A.

$$\% \text{ Recovery} = \frac{\text{pH}_i \text{ 10\% end} - \text{pH}_i \text{ 10\% start}}{\text{pH}_i \text{ 5\%} - \text{pH}_i \text{ 10\% start}} \times 100$$

In control experiments, cells exhibited a $96.3 \pm 3.0\%$ (n=70) recovery in pH_i from CO_2 -induced acidosis. However, when basolateral Na^+ was removed, recovery was significantly reduced to $-10.5 \pm 21.4\%$ (n=5; $p < 0.001$ vs. control; fig. 3.21B). This abolishment of pH_i recovery suggested this process was completely Na^+ -dependent. Removal of basolateral Cl^- or addition of basolateral DIDS ($100\mu\text{M}$) reduced recovery to $49.6 \pm 2.9\%$ ($p < 0.05$ vs.

control; n=3; fig. 3.4B) and $44.3 \pm 3.8\%$ ($p < 0.05$ vs. control; n=3; fig. 3.21B) respectively. Interestingly, inhibition of NHEs using $3\mu\text{M}$ EIPA had no effect on recovery (% recovery = $85.0 \pm 8.4\%$ ($p > 0.05$ vs. control; n=4; fig. 3.21B)) suggesting that H^+ efflux *via* NHEs did not underlie the increase in pH_i . Finally, increasing intracellular cAMP levels using forskolin reduced recovery to $0.4 \pm 7.9\%$ ($p < 0.001$ vs. control; n=3; fig. 3.21B) and suggested that the transporters involved in mediating recovery were negatively regulated by cAMP.

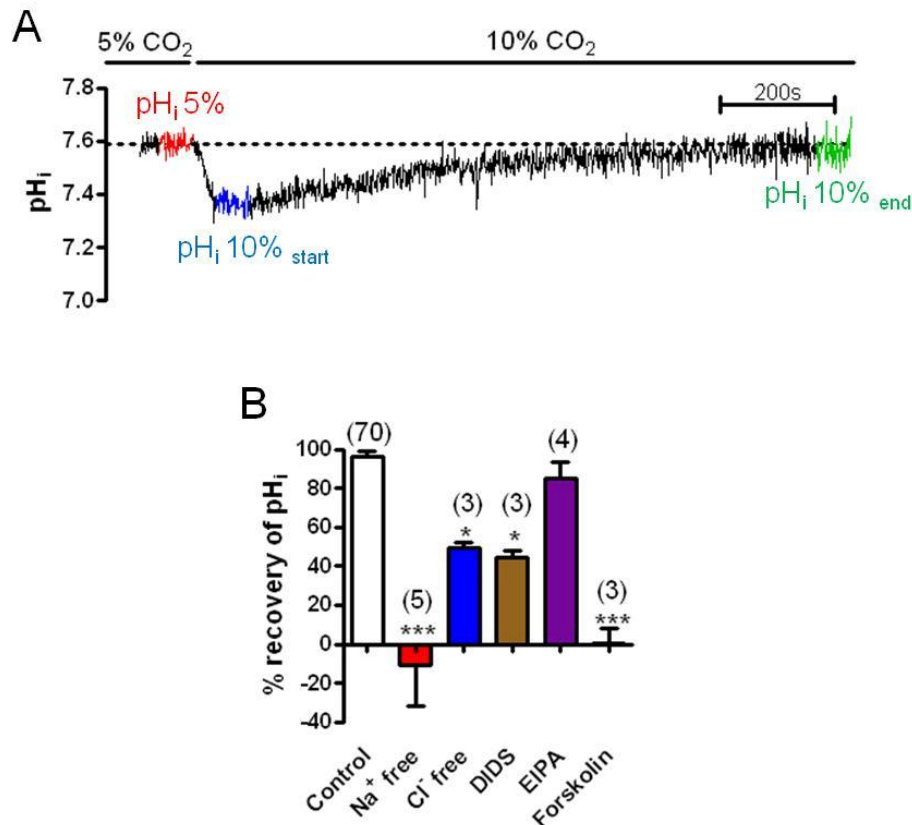


Figure 3.21: pH_i recovery after CO_2 -induced acidosis is Na^+ -dependent and inhibited by forskolin. (A) shows an example experiment in which the recovery of pH_i after CO_2 -induced acidosis can be quantified. (B) summarizes the effects of removal of basolateral Na^+ or Cl^- , addition of basolateral DIDS ($100\mu\text{M}$) or EIPA ($3\mu\text{M}$) or addition of $5\mu\text{M}$ forskolin on pH_i recovery. * = significant effect of treatment ($p < 0.05$; *** = $p < 0.001$). Data represents mean \pm S.E.M., n numbers displayed in parenthesis.

3.12. Effects of hypercapnia on other cAMP signalling agents

I have currently shown that the cAMP elevating agonists forskolin and adenosine both induce an intracellular acidification in Calu-3 cells that is due to cAMP-regulated, CFTR-dependent

HCO₃⁻ secretion. This acidification is modulated by hypercapnia and suggests a CO₂-induced change in intracellular cAMP levels may underlie this phenomenon. As both forskolin and adenosine increase intracellular cAMP *via* an activation of tmAC, it was worth investigating whether hypercapnia could modulate HCO₃⁻ transport when intracellular cAMP levels were raised independently of tmAC activity.

3.12.1. IBMX

Phosphodiesterases (PDEs) are the enzymes responsible for cAMP breakdown and it has been shown that inhibition of these enzymes increase intracellular cAMP sufficiently enough to activate CFTR-dependent I_{sc} in Calu-3 cells (Cobb *et al.*, 2003). For a detailed review of the biochemistry of PDEs, see Conti and Beavo (2007). Thus, hypercapnia may modulate cAMP-dependent processes due to effects on PDE activity in Calu-3 cells. To investigate this possibility, cells were stimulated with either forskolin (control) or IBMX, a non-specific PDE inhibitor, in normocapnia and hypercapnia. A representative experiment in which cells were stimulated with 1mM IBMX alone is shown in figure 3.22A. In control experiments performed on the same day in which cells were stimulated with forskolin, hypercapnia induced a 1.8 ± 0.2 fold increase in the magnitude of the forskolin-stimulated intracellular acidification ($p < 0.05$; $n = 3$; fig. 3.22B) and a 2.4 ± 0.4 fold increase in the rate of forskolin-stimulated HCO₃⁻ flux ($p < 0.05$; $n = 3$; fig. 3.22C). Stimulation of cells with IBMX did induce an intracellular acidification consistent with increases in [cAMP]_i underlying this process. However, hypercapnia only elicited a 1.3 ± 0.1 fold increase in the magnitude of IBMX-stimulated intracellular acidification ($p > 0.05$; $n = 3$; fig. 3.22B) and a 1.5 ± 0.1 fold increase in the rate of IBMX-stimulated HCO₃⁻ flux ($p > 0.05$; $n = 3$; fig. 3.22C). These data suggest that hypercapnia is unable to modulate intracellular cAMP levels when they are raised by phosphodiesterase inhibition as opposed to activation of tmAC.

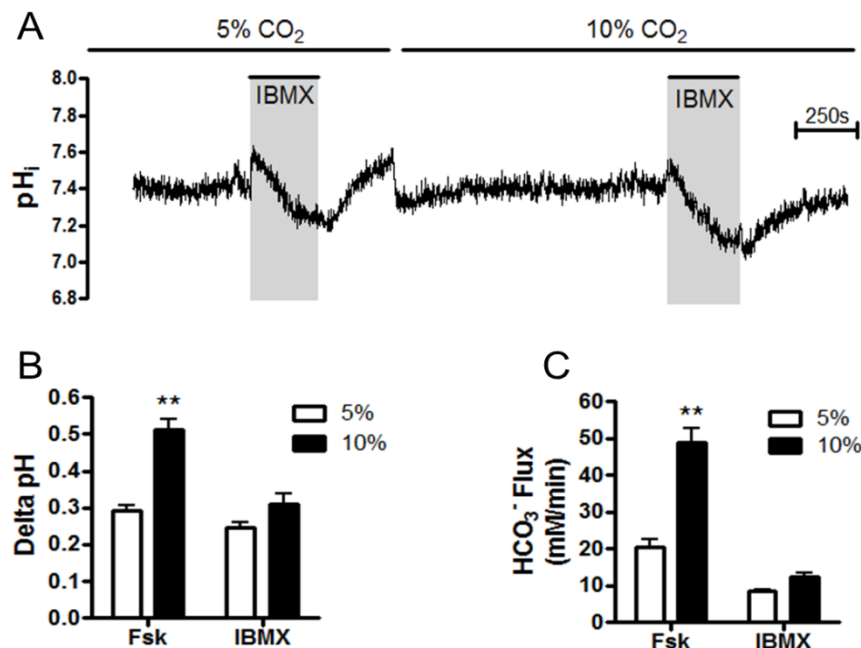


Figure 3.22: Hypercapnia does not alter the IBMX-stimulated intracellular acidification. (A) shows a representative experiment in which Calu-3 cells were stimulated with 1mM IBMX in normocapnia and after 20 minutes exposure to hypercapnia. Control experiments in which 5 μ M forskolin was used to stimulate intracellular acidification were performed on the same day. The delta pH (B) and the rate of HCO_3^- flux (C) resulting from forskolin stimulation or IBMX stimulation are displayed. ** = significant effect of hypercapnia ($p < 0.01$); Data represents mean \pm S.E.M.; $n = 3$ for each.

3.12.2. Dibutrylyl-cAMP

An alternative way to increase intracellular cAMP levels independently of tmAC activity is by using a membrane permeant cAMP analogue. Dibutrylyl-cAMP (db-cAMP) is one such analogue that, due to the presence of a dibutrylyl group, is cell permeable. To investigate whether hypercapnia could modulate exogenous cAMP signalling, the effect of db-cAMP signalling in normocapnia and hypercapnia was investigated. Ideally, these experiments would have been performed on the same transwell of cells. However, it was found that although db-cAMP did induce an intracellular acidification, consistent with this response being cAMP-regulated, the acidification was irreversible, implying that db-cAMP is unable to be broken down by endogenous phosphodiesterases. Therefore, repeated exposures to db-cAMP in the same experiment were impossible, so separate experiments for normocapnia and hypercapnia were performed. Figures 3.23A and 3.23B show example experiments carried out in normocapnia and hypercapnia respectively. Unpaired analysis of the forskolin-stimulated intracellular acidification showed that hypercapnia did not significantly enhance

the magnitude of the response, only increasing it 1.3 ± 0.2 fold ($p > 0.05$; $n = 3$; fig. 3.23C). This was also the case in db-cAMP-stimulated cells in which hypercapnia induced a 2.1 ± 0.8 fold increase in the magnitude of the acidification ($p > 0.05$; $n = 3$; fig. 3.23C). However, hypercapnia did significantly enhance the rate of HCO_3^- flux 2.4 ± 0.8 and 4.1 ± 1.9 fold in forskolin and db-cAMP-stimulated cells respectively ($p < 0.05$; $n = 3$; fig. 3.23D). Therefore, these data suggest that hypercapnia can modulate exogenous cAMP levels and therefore indicate that CO_2 is not only modulating tmAC activity in these cells as initially thought. However, given the unpaired nature of these experiments, the data is not as robust as it could be and alternative cAMP analogues should be explored before this data is deemed conclusive.

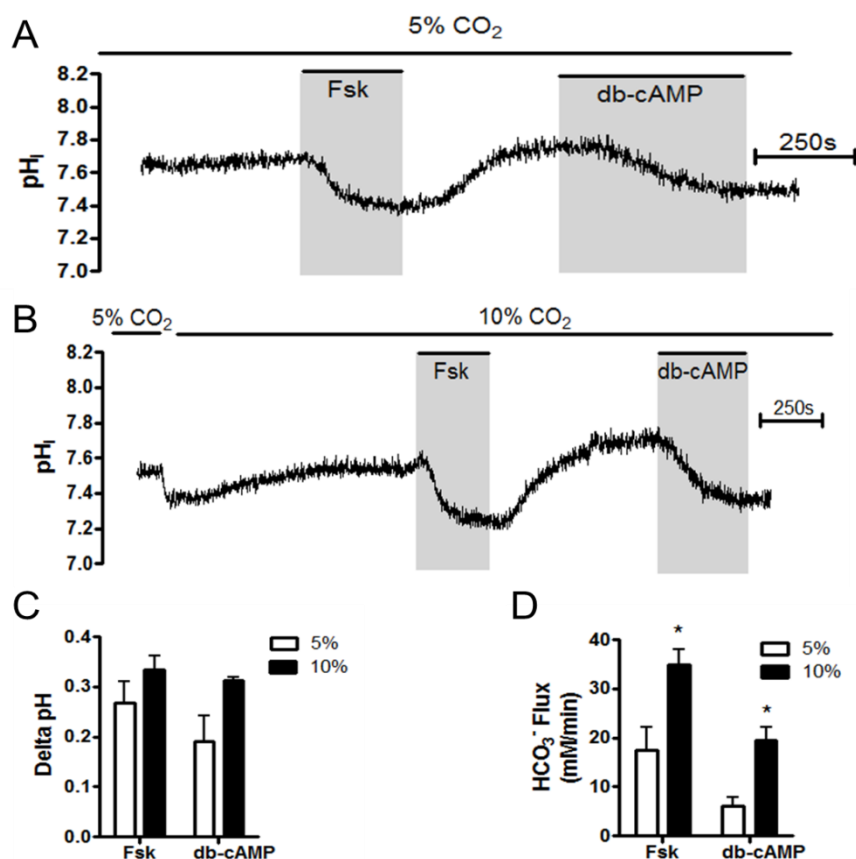


Figure 3.23: Hypercapnia is able to modulate dibutyryl-cAMP-stimulated intracellular acidification in Calu-3 cells. (A) shows an example experiment in which cells were stimulated with 5 μ M forskolin and then 800 μ M db-cAMP in normocapnia and (B) shows the same protocol repeated in cells exposed to 20 minutes hypercapnia. The delta pH (C) and the rate of HCO_3^- flux (D) resulting from forskolin or db-cAMP stimulation are displayed. * = significant effect of hypercapnia ($p < 0.05$); Data represents mean \pm S.E.M.; $n = 3$ for each.

3.12.3. Multidrug Resistance Proteins

The multidrug resistance proteins (MRPs) are a family of ABC transporters that have been shown to transport cyclic nucleotides in mammalian cells (Jedlitschky *et al.*, 2000; Chen *et al.*, 2001; van Aubele *et al.*, 2002). Inhibition of MRPs in T84 cells dose-dependently reduced forskolin-stimulated elevations in extracellular cAMP ($[cAMP]_e$) implicating the role of these transporters in regulating cAMP efflux from the cell (Xie *et al.*, 2011). Hamilton *et al.* (2001) have shown that MRP-1 is expressed on the basolateral membranes in Calu-3 cells and given their role in cAMP transport, it was important to test whether these transporters play a role in CO₂-induced changes in cAMP-regulated HCO₃⁻ transport. As shown in figure 3.24A, cells were treated with the MRP inhibitor MK-571 and the response to forskolin stimulation was assessed in normocapnia and hypercapnia and the data was compared to control experiments performed on the same day. In control experiments, hypercapnia induced a 2.4 ± 0.3 fold increase in the magnitude of the forskolin-stimulated intracellular acidification ($p < 0.05$; $n = 3$; fig. 3.24B) and a 5.7 ± 0.6 fold increase in the rate of forskolin-stimulated HCO₃⁻ flux ($p < 0.05$; $n = 3$; fig. 3.24C). However, in the presence of MK-571, the effect of hypercapnia was abolished. Here, hypercapnia induced a 1.0 ± 0.1 fold increase in the magnitude of the forskolin-stimulated intracellular acidification ($p > 0.05$; $n = 3$; fig. 3.24B) and a 1.1 ± 0.2 fold increase in the rate of forskolin-stimulated HCO₃⁻ flux ($p > 0.05$; $n = 3$; fig. 3.24C). What was also interesting was the fact that MK-571 abolished the recovery of pH_i from CO₂-induced acidosis (fig. 3.24D). These findings show that inhibition of MRPs prevent the effect of hypercapnia on cAMP-regulated HCO₃⁻ transport and suggest that hypercapnia may reduce $[cAMP]_i$ due to increased efflux *via* MRPs. Furthermore, the results also support the idea that elevations in intracellular cAMP prevents pH_i recovery from CO₂-induced acidosis, likely due to a downregulatory effect of cAMP on the transporter(s) responsible for this recovery, and implies that the MRPs are active during exposure to 10% CO₂.

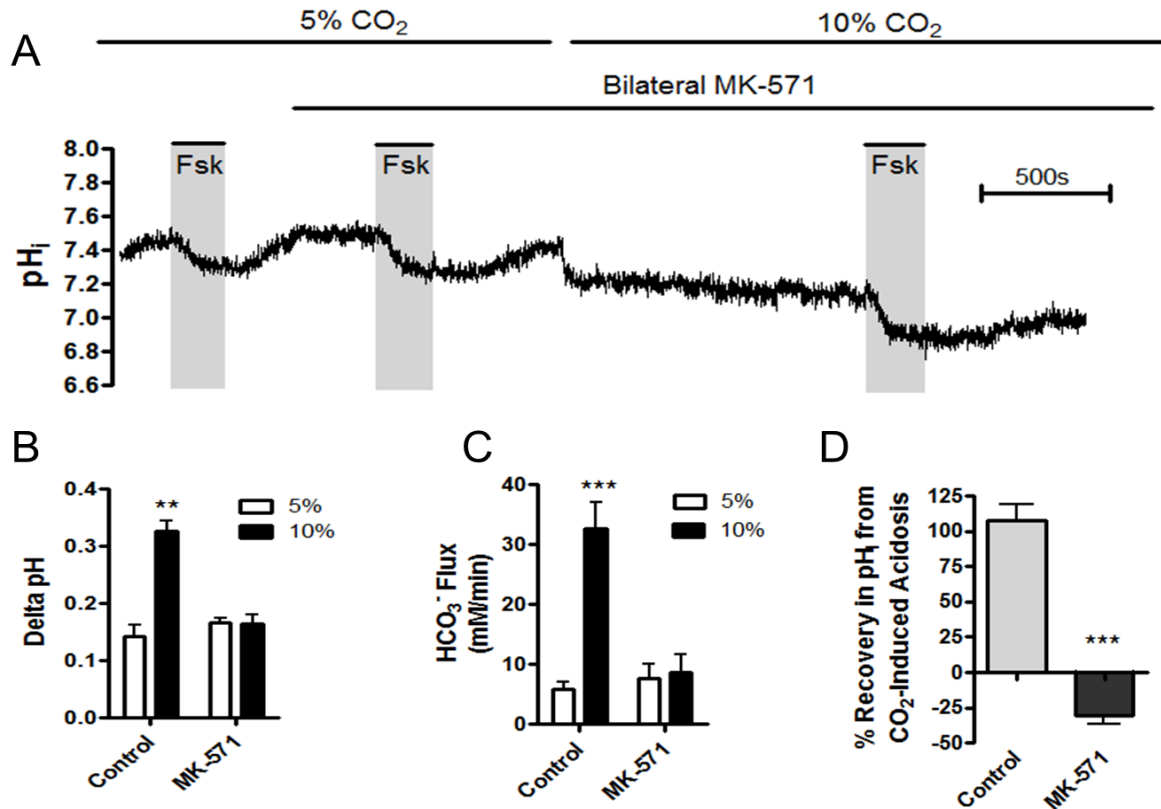


Figure 3.24: MK-571 blocks the effect of hypercapnia on the forskolin-stimulated intracellular acidification. (A) shows a representative experiment in which the effect of bilateral MK-571 (10 μ M) on forskolin-stimulated intracellular acidification in normocapnia and hypercapnia was assessed. The delta pH (B) and the HCO_3^- flux (C) resulting from forskolin stimulation in control cells or MK-571-treated cells are displayed. ** = significant effect of hypercapnia ($p < 0.01$); *** = $p < 0.001$). (D) shows the effect of MK-571 on the recovery in pH_i from CO_2 -induced acidosis. *** = significant effect of MK-571 ($p < 0.001$). Data represents mean \pm S.E.M.; $n=3$ for each.

In attempt to identify which membrane the apparent CO_2 -sensitive MRPs were expressed, MK-571 was added to one membrane only and the response to forskolin in normocapnia and hypercapnia was measured. Figure 3.25A shows the effect of apical MK-571 and figure 3.25B shows the effect of basolateral MK-571. As can be seen, distinct differences exist depending on which membrane MK-571 is applied. Firstly, apical MK-571 blocked recovery of pH_i from CO_2 -induced acidosis; a phenomenon which was not observed when MK-571 was applied basolaterally (fig 3.25E). Furthermore, only apical MK-571 was able to block the effect of hypercapnia on the forskolin-stimulated intracellular acidification. In control experiments performed on the same day and in basolateral MK-571 experiments, hypercapnia increased the magnitude of the forskolin-stimulated intracellular acidification 2.0 ± 0.2 fold and 2.0 ± 0.1 fold respectively ($p < 0.01$; $n=3$ for each; fig. 3.25C). Similarly, hypercapnia also

increased the rate of forskolin-stimulated HCO_3^- flux 4.9 ± 0.8 fold and 3.4 ± 0.6 fold respectively ($p < 0.05$; $n = 3$ for each; fig. 3.25D). However, in the presence of apical MK-571, the magnitude of forskolin-stimulated intracellular acidification and the rate of forskolin-stimulated HCO_3^- flux were only enhanced 0.9 ± 0.1 fold and 1.2 ± 0.3 fold respectively ($p > 0.05$; $n = 3$; figs 3.25C and D). This effect of apical MK-571 mimics the response to bilateral MK-571 and implies that the potential CO_2 -sensitive MRP transporters are located at the apical membrane.

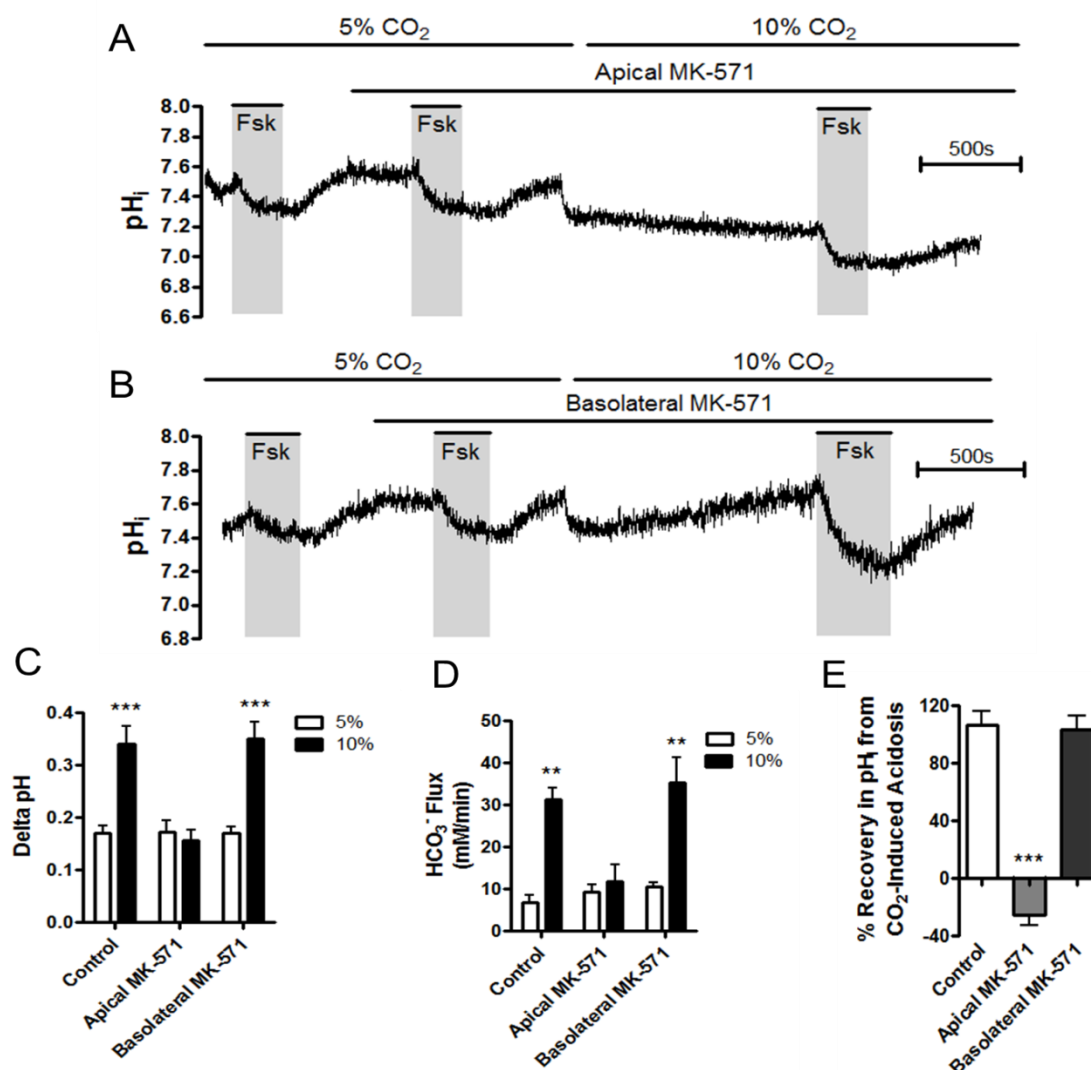


Figure 3.25: Apical but not basolateral MK-571 blocks the effect of hypercapnia on the forskolin-stimulated intracellular acidification. (A) shows a representative experiment in which MK-571 (10 μM) was applied apically and (B) shows a representative experiment in which MK-571 (10 μM) was applied basolaterally. The delta pH (C) and the HCO_3^- flux (D) resulting from forskolin stimulation in control cells or MK-571-treated cells are displayed. ** = significant effect of hypercapnia ($p < 0.01$; *** = $p < 0.001$). (E) shows the effect of MK-571 on the recovery in pH_i from CO_2 -induced acidosis. *** = significant effect of MK-571 ($p < 0.001$). Data represents mean \pm S.E.M.; $n = 3$ for each.

In attempt to quantify MRP activity in Calu-3 cells in normocapnia and hypercapnia, the rate of efflux of a MRP specific substrate was measured. Loading cells with the dye 5-chloromethyl-fluorescein diacetate (CMFDA) causes CMFDA to enter the cell where it is metabolized by intracellular esterases into glutathione-methylfluorescein (GSMF) which is a substrate for MRPs (Bogman *et al.*, 2003; Suda *et al.*, 2011). As GSMF is fluorescent, measuring the rate at which fluorescence decreased gave a measure of GSMF efflux from the cells. Cells were initially perfused with Krebs solution gassed with either 5% CO₂ or 10% CO₂ for 20 minutes before a 5 minute wash-in of probenecid to inhibit MRPs and thus prevent immediate efflux once the dye had loaded. Perfusion was then switched off and cells were loaded with 1µM CMFDA and fluorescence increased as GSMF accumulated inside the cell. After 20 minutes, perfusion was switched on to wash away the probenecid and fluorescence decreased as GSMF was transported out of the cell and washed away. The rate at which fluorescence decreased by 50% was measured by performing a linear regression between the maximal fluorescence and 50% of the maximal fluorescence as shown in figure 3.26A. In normocapnic conditions, fluorescence at 490nm decreased at a rate of 124 ± 32 counts sec⁻¹ (n=4) which was not statistically different than the fluorescent decrease of 192 ± 39 counts sec⁻¹ in hypercapnia (p>0.05; n=3) although there does appear to be a small trend for hypercapnia to increase GSMF efflux consistent with the idea that hypercapnia may activate MRPs and thus activate MRP-mediated cAMP efflux.

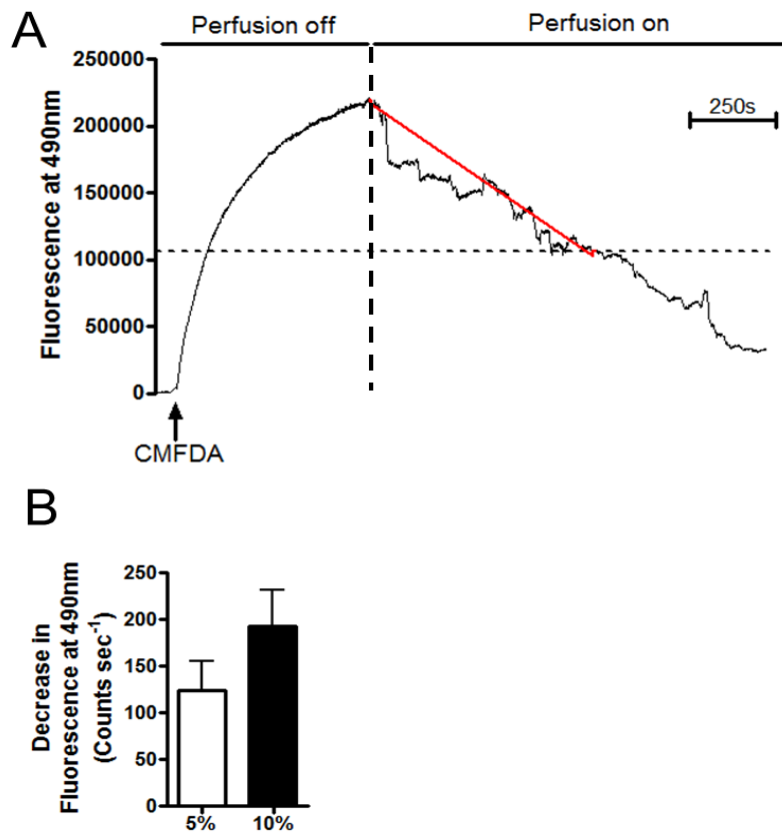


Figure 3.26: Acute hypercapnia has no effect on the rate of MRP-mediated GSMF efflux from Calu-3 cells. (A) shows a representative experiment in normocapnia in which the effect of CMFDA (1 μ M) on the fluorescence measured at 490nm was measured to assess the rate of MRP-mediated GSMF efflux. The red line demonstrates the linear regression calculated between the maximal 490nm counts and the time at which 490nm counts had decreased by 50%. (B) summarizes the effect of hypercapnia on the rate of decrease in 50% of the 490nm counts. Data represents mean \pm S.E.M., n=4 for normocapnia and n=3 for hypercapnia.

3.13. Disruption of compartmentalization of cAMP signalling does not prevent the effect of hypercapnia

As discussed in chapter 1, section 1.6.1.2, CFTR is contained within a macromolecular complex in epithelial cells that localizes the cAMP signalling machinery into a microdomain allowing for efficient signal transduction. The macromolecular complex is tethered to the actin cytoskeleton *via* scaffold proteins, including Ezrin, and the importance of the actin cytoskeleton integrity in CFTR regulation and cAMP compartmentalization was shown by Monterisi *et al.* (2012). Here, researchers demonstrated that pharmacological disruption of the actin cytoskeleton in human bronchial epithelial cells reduced membrane cAMP levels but increased cytosolic cAMP levels, suggesting a loss of cAMP compartmentalization. This

was accompanied by a reduction in CFTR-dependent Cl^- secretion, highlighting the importance of cAMP compartmentalization in efficient CFTR activation. Pharmacologically, the actin cytoskeleton can be disrupted by either latrunculin or cytochalasin D, each with a slight different mechanism of action. Latrunculin is able to bind to actin monomers and thus prevent depolymerisation into new F-actin filaments (Coue *et al.*, 1987; Morton *et al.*, 2000) whilst cytochalasin D binds to actin monomers and stimulates actin ATPase activity which initially increases the rate of actin polymerization. However, the accumulation of actin bound to ADP drastically impairs the polymerization of actin monomers into actin filaments (Sampath and Pollard, 1991). To assess whether hypercapnia mediated its effects on cAMP-dependent HCO_3^- transport by disrupting cAMP compartmentalization, Calu-3 cells were preincubated for one hour with either 10 μM latrunculin B or 10 μM cytochalasin D. To fully establish the effect of these compounds, confocal images of the actin cytoskeleton were taken as shown in figure 3.27A as well as transepithelial electrical resistance measurements to determine whether disruption of the actin cytoskeleton affected the monolayer integrity (fig. 3.27B). Figure 3.27A (far left panel) shows the cytoskeleton of untreated cells at the x-y focal plane. Cytochalasin D treatment (fig. 3.27A, left middle panel) caused a marked disruption of the cytoskeleton with the phalloidin staining appearing more punctate and much less organised. This is accompanied by a significant decrease in TEER that occurs within the first 30 minutes of treatment and persists over a 2 hour period (fig 3.27B). Interestingly, latrunculin B treatment (fig. 3.27A, middle right panel) did not appear to affect the overall global structure of the actin cytoskeleton, yet it induced a significant reduction in TEER, even more so than cytochalasin D (fig. 3.27B), indicating that the effects of latrunculin on actin cytoskeleton organization are much more subtle than the effects of cytochalasin D. Finally, it was worth noting that acute hypercapnia did not affect the gross organization of the actin cytoskeleton as highlighted in figure 3.27A (far right panel).

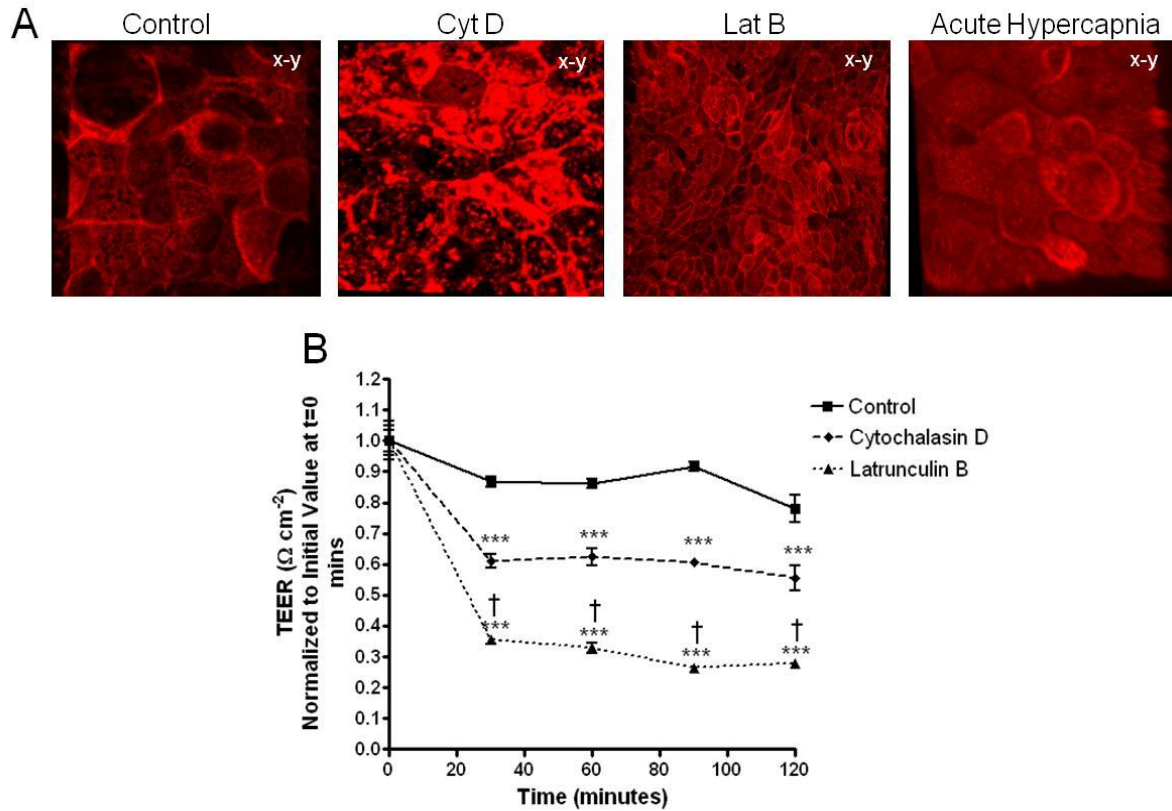


Figure 3.27: The effect of cytochalasin D and latrunculin B on actin cytoskeleton integrity and transepithelial electrical resistance in Calu-3 cells. (A) shows Calu-3 cells that were either untreated (far left panel) or either incubated for one hour with 10 μ M cytochalasin D (middle left panel) or 10 μ M latrunculin B (middle right panel) or incubated for 20 minutes in 10% CO₂ (far right panel) and stained with 0.25% Texas-Red Phalloidin to visualize F-actin using confocal microscopy. (B) displays the effects of 10 μ M cytochalasin D or 10 μ M latrunculin B on TEER measurements made every 30 minutes over a 2 hour period. *** = significant effect of treatment vs. control ($p < 0.001$); † = significant effect of Lat B vs. Cyt D ($p < 0.001$). Data represents mean \pm S.E.M.; $n = 3$ for each.

To assess whether disruption of the actin cytoskeleton affected the response to hypercapnia, Calu-3 cells were preincubated for one hour with either 10 μ M latrunculin B or 10 μ M cytochalasin D and compared to control experiments performed on the same day. Figure 3.28A shows the effect of cytochalasin D on the response to forskolin. In control experiments, hypercapnia caused a 1.7 ± 0.1 fold increase in the magnitude of the forskolin-stimulated intracellular acidification ($p < 0.05$; $n = 4$; fig. 3.28B) and increased the rate of forskolin-stimulated HCO₃⁻ flux 3.4 ± 0.1 fold ($p < 0.01$; $n = 4$; fig. 3.28C). In cytochalasin D treated cells, hypercapnia caused a 1.5 ± 0.1 fold increase in the magnitude of the forskolin-stimulated intracellular acidification ($p < 0.05$; $n = 4$) and increased the rate of forskolin-stimulated HCO₃⁻ flux 3.8 ± 0.6 fold ($p < 0.01$ $n = 4$). Thus, even though cytochalasin D caused

a clear disruption of the actin cytoskeleton, this had no effect on the CO₂ modulation of the forskolin-stimulated intracellular acidification suggesting that compartmentalized cAMP is not essential for mediating the response to hypercapnia. Similarly, latrunculin B treatment did not prevent the effect of hypercapnia. In these experiments, the magnitude of the forskolin-stimulated intracellular acidification and the rate of forskolin-stimulated HCO₃⁻ flux were increased 1.9 ± 0.1 fold (p<0.05; n=3; fig. 3.29B) and 2.7 ± 0.4 fold (p<0.05; n=3; fig. 3.29C) respectively in control experiments and increased 1.6 ± 0.2 fold (p<0.05; n=3; fig. 3.29B) and 3.0 ± 0.7 fold (p<0.05; n=3; fig. 3.29C) respectively in latrunculin B treated cells. Latrunculin B treatment did appear to increase the rate of forskolin-stimulated HCO₃⁻ flux in both normocapnia and hypercapnia, with these difference significant in hypercapnic conditions (p<0.05). This likely reflects the fact that latrunculin B treated monolayers were very leaky such was the pronounced effect of latrunculin B on TEER.

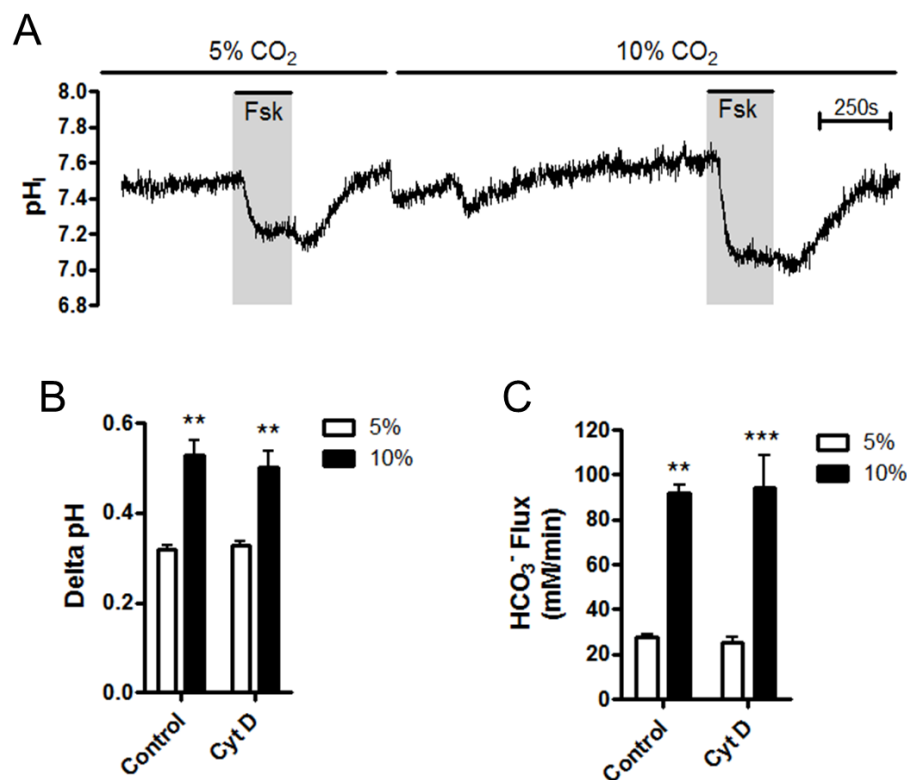


Figure 3.28: Cytochalasin D does not block the effects of hypercapnia on the forskolin-stimulated intracellular acidification. (A) shows a representative experiment in which Calu-3 cells were preincubated for one hour with cytochalasin D (10μM) and stimulated with 5μM forskolin in normocapnia and hypercapnia. The delta pH (B) and HCO₃⁻ flux (C) resulting from forskolin stimulation are summarized. ** = significant effect of hypercapnia (p<0.01; *** = p<0.001); Data represents mean ± S.E.M.; n=4 for each.

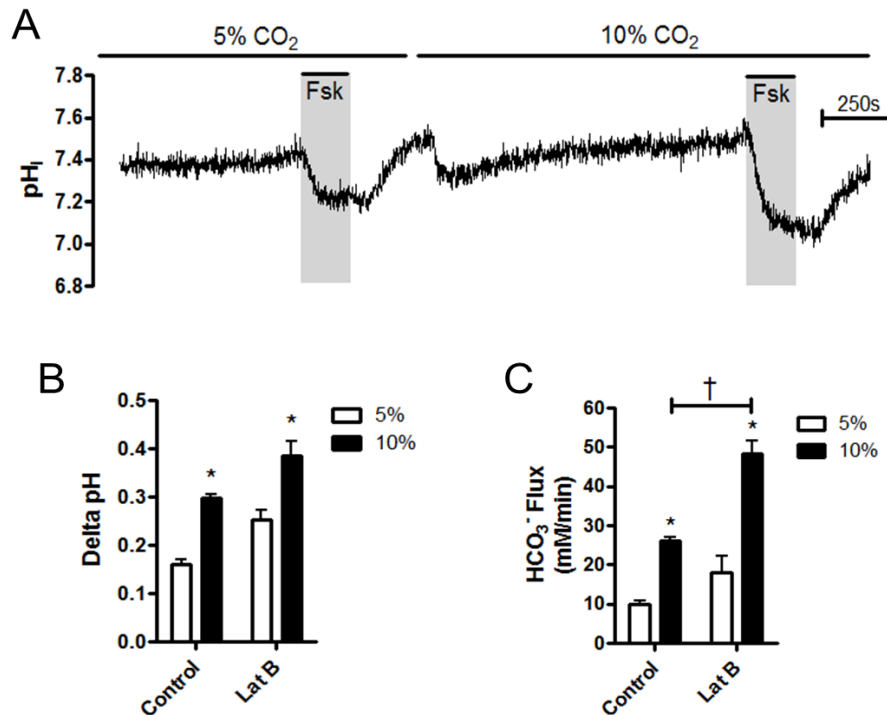


Figure 3.29: Latrunculin B does not block the effects of hypercapnia on the forskolin-stimulated intracellular acidification. (A) shows a representative experiment in which Calu-3 cells were preincubated for one hour with latrunculin B (10 μM) and stimulated with 5 μM forskolin in normocapnia and hypercapnia. The delta pH (B) and HCO_3^- flux (C) resulting from forskolin stimulation are summarized. * = significant effect of hypercapnia ($p < 0.05$); † = significant effect of latrunculin B treatment ($p < 0.05$). Data represents mean \pm S.E.M.; $n=3$ for each.

3.14. Effects of acute hypercapnia on specific H^+/HCO_3^- transporters

3.14.1. Apical HCO_3^- efflux

The forskolin-stimulated intracellular acidification, used as an assay to measure cAMP-regulated HCO_3^- transport, is the result of at least two components of HCO_3^- transport: apical HCO_3^- efflux and basolateral HCO_3^- influx. The fact that elevations in intracellular cAMP induced an intracellular acidification suggests that, during that period, HCO_3^- efflux is greater than HCO_3^- influx until a new steady state in pH_i is reached. The modulation of the response by hypercapnia suggests CO_2 is either increasing HCO_3^- efflux or, conversely, inhibiting HCO_3^- influx, or indeed both. Therefore, it was important to measure the activity of HCO_3^- transporters at each membrane in an attempt to understand how CO_2 was able to modulate cAMP-regulated HCO_3^- transport. One approach to study HCO_3^- transport at each membrane was by using the inhibitor stop technique (Hegyí *et al.*, 2003). Here, inhibition of basolateral

pH_i regulatory transporters (i.e. NBC, NHE and AE2) allowed for the study of apical HCO₃⁻ efflux only. As shown in figure 3.30A, cells were stimulated with 5μM forskolin and an acidification occurred until a new steady state pH_i was reached. At this point, 500μM DIDS and 3μM EIPA was added to the basolateral membrane to inhibit NBC, AE2 and NHE. Addition of these inhibitors induced a secondary intracellular acidification as together they prevented HCO₃⁻ influx across the basolateral membrane but HCO₃⁻ efflux across the apical membrane could continue and as such, this acidification represents a measure of apical CFTR-dependent HCO₃⁻ efflux only. Basolateral inhibitors and forskolin were washed off and the process was repeated in hypercapnia. The forskolin-stimulated intracellular acidification was significantly enhanced 1.7 ± 0.3 fold and 3.1 ± 0.1 fold in both magnitude of intracellular acidification and in rate of HCO₃⁻ flux respectively (p<0.05; n=3 for each; figs 3.30B and C). However, there was no effect of hypercapnia on the acidification produced when DIDS and EIPA were added to the basolateral membrane. Hypercapnia induced a 0.7 ± 0.1 fold increase in the magnitude of this acidification (p>0.05; n=3; fig. 3.30B) and a 1.3 ± 0.3 fold increase of in the rate of HCO₃⁻ efflux across the apical membrane (p>0.05; n=3; fig. 3.30C). These data suggest that apical HCO₃⁻ transport is unaffected by hypercapnia and implies that the increased acidification seen in hypercapnic conditions is more likely the result of a reduction in basolateral HCO₃⁻ influx. The same findings were also observed when adenosine was used to stimulate cAMP-regulated HCO₃⁻ transport.

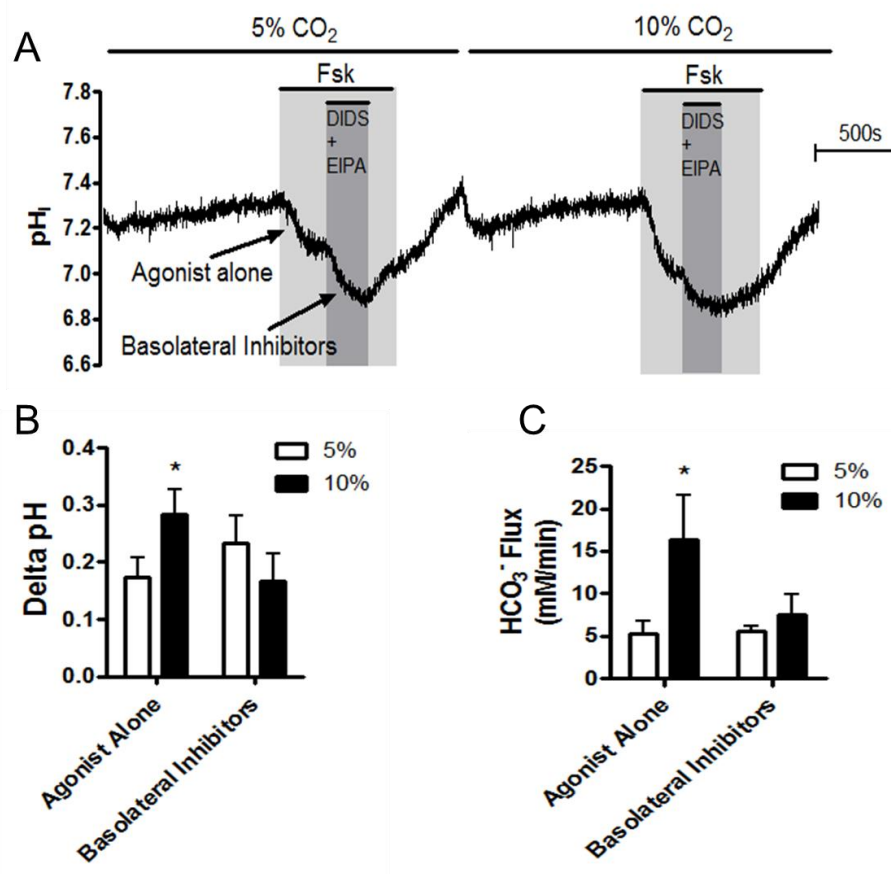


Figure 3.30: Apical HCO_3^- efflux is unaffected by acute hypercapnia. (A) shows a representative experiment in which the effect of hypercapnia on 5 μ M forskolin-stimulation and subsequent addition of H_2 -DIDS (500 μ M) and EIPA (3 μ M) to inhibit basolateral pH_i regulatory transporters was assessed. The delta pH_i (B) and the HCO_3^- flux (C) resulting from forskolin stimulation and subsequent addition of basolateral inhibitors are displayed. * = significant effect of hypercapnia ($p < 0.05$). Data represents mean \pm S.E.M.; $n=3$ for each.

To further investigate the effects of acute hypercapnia on CFTR-dependent HCO_3^- efflux across the apical membrane, CFTR-dependent anion exchange was assessed in normocapnia and hypercapnia. Garnett *et al.* (2011) showed that Calu-3 cells express the Cl^-/HCO_3^- exchanger pendrin on the apical membrane and that it is regulated by CFTR. Removal of Cl^- from the apical membrane reverses the exchanger such that HCO_3^- accumulates within the cell and an alkalisation occurs. Reintroduction of apical Cl^- allows the exchanger to function in its normal direction and HCO_3^- leaves the cell. The resulting reacidification can be used to measure CFTR-dependent HCO_3^- secretion at the apical membrane and, thus, this was measured in normocapnia and hypercapnia, as shown in figure 3.31A. In normocapnia, removal of apical Cl^- caused pH_i to increase by 0.79 ± 0.01 ($n=3$) units whilst in hypercapnia this increase in pH_i was 0.85 ± 0.07 ($p > 0.05$; $n=3$ fig. 3.31B). Furthermore, reintroduction of

apical Cl^- caused pH_i to reacidify at a rate of 0.49 ± 0.04 pH units min^{-1} in normocapnia and 0.48 ± 0.04 pH units min^{-1} in hypercapnia ($p > 0.05$; $n=3$; fig. 3.31C) which was calculated as a HCO_3^- efflux of $138 \pm 8 \text{ mM HCO}_3^- \text{ min}^{-1}$ and $204 \pm 33 \text{ mM HCO}_3^- \text{ min}^{-1}$ respectively ($p > 0.05$; $n=3$; fig. 3.31D). These data show that CFTR-dependent anion exchange activity was unaffected by acute hypercapnia and support the findings from the inhibitor stop experiments that HCO_3^- transport across the apical membrane is insensitive to changes in CO_2 .

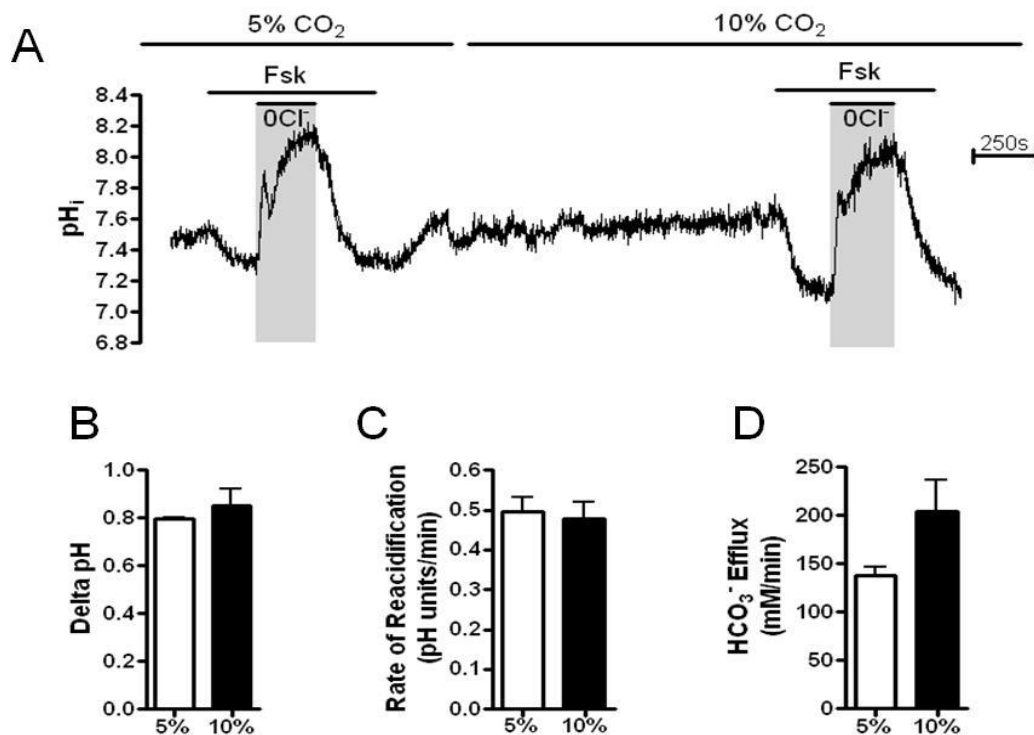


Figure 3.31: CFTR-dependent anion exchange activity is unaffected by acute hypercapnia. (A) shows a representative experiment in which the effect of acute hypercapnia on forskolin-stimulated, CFTR-regulated apical HCO_3^- transport was assessed by removal and subsequent readdition of apical Cl^- . The delta pH in response to removal of Cl^- is shown in (B). The reacidification and the HCO_3^- flux resulting from readdition of apical Cl^- are shown in (C) and (D) respectively. Data represents mean \pm S.E.M.; $n=3$ for each.

3.14.2. Basolateral HCO_3^- Influx

Members of the $\text{Na}^+/\text{HCO}_3^-$ Cotransporter (NBC) family serve as the major HCO_3^- importers in HCO_3^- secreting tissue (Bachmann *et al.*, 2003) and therefore changes in NBC activity will impact on HCO_3^- secretion across HCO_3^- secretory epithelia. End-point PCR revealed that both SLC4A4 (electrogenic $\text{Na}^+/\text{HCO}_3^-$ Cotransporter 1) and SLC4A7 (electroneutral $\text{Na}^+/\text{HCO}_3^-$ Cotransporter 1) were expressed in Calu-3 cells (fig. 3.32). SLC4A4 favours a stoichiometry of 2 HCO_3^- : 1 Na^+ (Romero *et al.*, 1997) whilst SLC4A7, being electroneutral, has a stoichiometry of 1 HCO_3^- : 1 Na^+ (Pushkin *et al.*, 1999).

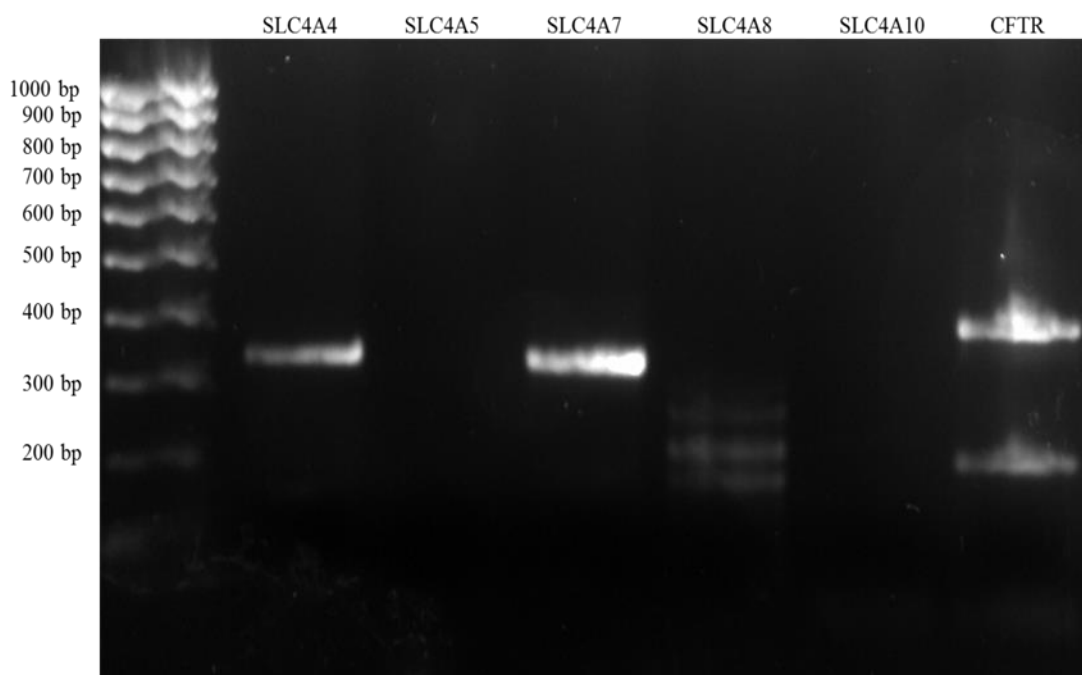


Figure 3.32: Members of the NBC family, SLC4A4 and SLC4A7, are expressed in Calu-3 cells. End-Point PCR on RNA samples extracted from Calu-3 cells grown as a polarized monolayer were analysed for the expression of members of the NBC family of HCO_3^- transporters. CFTR expression was also analysed as a positive control.

To determine whether CO_2 alters cAMP-regulated HCO_3^- transport by altering the activity of NBC, NBC activity was assessed using the technique employed by Yang *et al.*, (2009). Here, removal of basolateral Na^+ causes pH_i to decrease due to inhibition of NBC-dependent HCO_3^- influx whilst subsequent reintroduction of basolateral Na^+ reactivates NBC and the subsequent alkalinisation is a result of NBC-dependent HCO_3^- influx and can therefore be used as a measure of NBC activity. Experiments were carried out in the presence of EIPA to inhibit the Na^+/H^+ exchanger. Firstly, it was necessary to determine whether NBC activity in

Calu-3 cells was cAMP-dependent. Figure 3.33A shows an example trace in which the effect of forskolin on NBC activity was assessed. 5 μ M forskolin stimulated a 2.3 ± 0.4 fold increase in NBC activity ($n=3$; $p<0.05$), whilst other cAMP agonists, adenosine (10 μ M) and IBMX (1mM), stimulated a 2.5 ± 0.5 ($n=3$; $p<0.05$) and 2.3 ± 0.5 ($n=3$; $p<0.05$) fold increase in NBC activity respectively (fig. 3.33B). These findings indicate that NBC activity in Calu-3 cells is cAMP-regulated and therefore could be affected by acute hypercapnia.

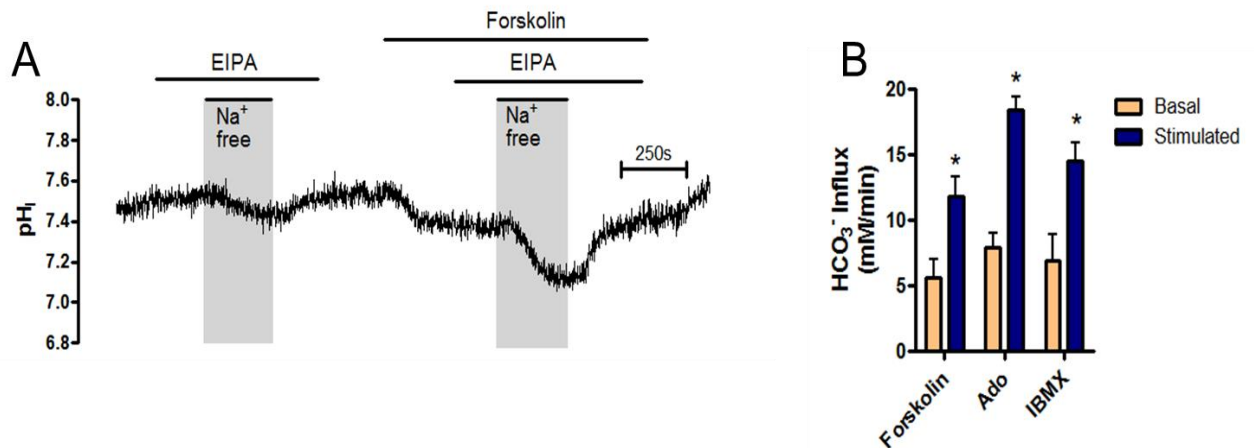


Figure 3.33: cAMP agonists stimulate Na⁺-dependent HCO₃⁻ import in Calu-3 cells. (A) shows a representative experiment in which NBC activity was assessed under basal and forskolin-stimulated conditions by removal and subsequent reintroduction of basolateral Na⁺ to inhibit and reactivate NBC-mediated HCO₃⁻ transport. EIPA (3 μ M) was present to inhibit the Na⁺/H⁺ exchanger. (B) shows the effect of the cAMP agonists forskolin (5 μ M), adenosine (10 μ M) and IBMX (1mM) on NBC-dependent HCO₃⁻ influx. * = significant effect of agonist stimulation; ($p<0.05$). Data represents mean \pm S.E.M.; $n=3$ for each.

The effect of acute hypercapnia on cAMP-regulated NBC activity was next assessed. Here, NBC activity was measured in normocapnic conditions or after cells had been exposed to 20 minutes hypercapnia as shown in figures 3.34A and B respectively. In normocapnia, forskolin stimulated a NBC-dependent HCO₃⁻ influx of 12.5 ± 1.8 mM min⁻¹ ($n=7$) whilst in hypercapnia, forskolin-stimulated NBC-dependent HCO₃⁻ influx was 11.3 mM min⁻¹ \pm 1.7 ($n=7$; $p>0.05$ vs. normocapnia; fig. 3.34C). These findings suggest that acute hypercapnia does not affect cAMP-stimulated NBC activity.

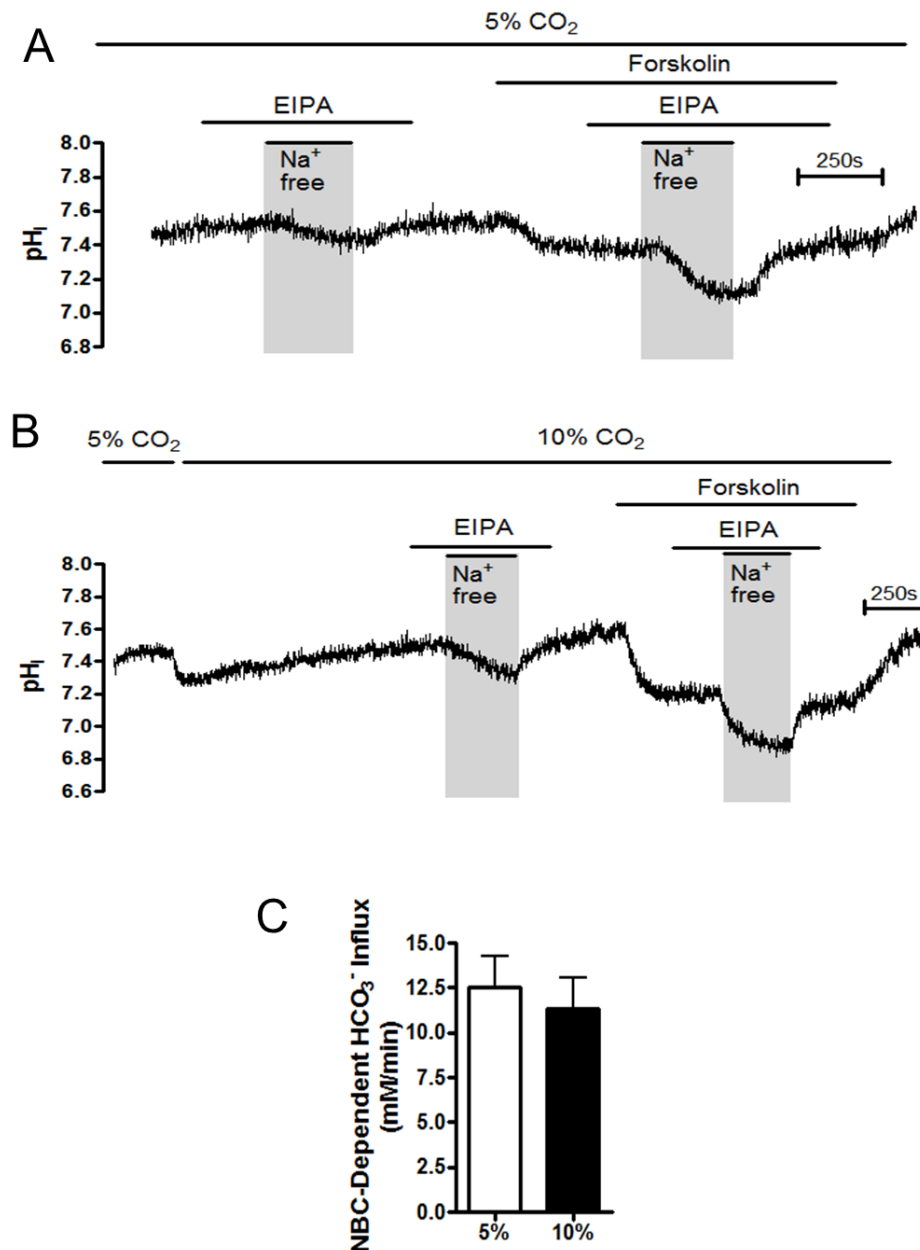


Figure 3.34: Acute hypercapnia does not affect forskolin-stimulated NBC activity. Example experiments to assess forskolin-stimulated NBC activity in normocapnia (A) and hypercapnia (B) are shown. Measurements were carried out in the presence of 3 μ M EIPA. The effect of acute hypercapnia on forskolin-stimulated NBC-dependent HCO₃⁻ influx is summarized in (C). Data represents mean \pm S.E.M.; n=7.

Similar findings were observed when the cAMP agonist was changed to adenosine. These sets of experiments were performed in a paired manner, with responses in both normocapnia and hypercapnia measured on the same transwell (fig. 3.35A). In normocapnia, adenosine (10 μ M) stimulated a NBC-dependent HCO₃⁻ influx of $12.5 \pm 1.8 \text{ mM min}^{-1}$ (n=4) whilst in

hypercapnia, adenosine-stimulated NBC-dependent HCO_3^- influx was $14.6 \pm 1.6 \text{ mM min}^{-1}$ ($n=4$; $p>0.05$; fig. 3.35B). These findings support the notion that although hypercapnia can modulate intracellular cAMP levels and cAMP-dependent HCO_3^- transport, this is not related to a change in NBC activity.

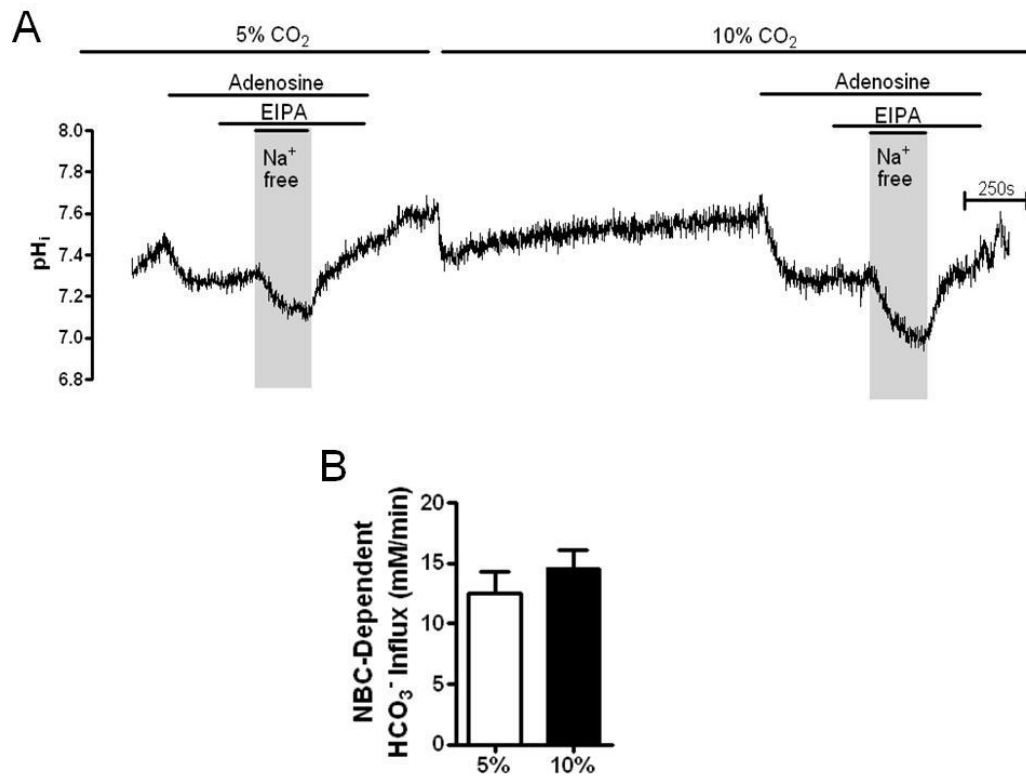


Figure 3.35: Acute hypercapnia does not affect adenosine-stimulated NBC activity. (A) shows a representative experiment in which adenosine-stimulated NBC activity was assessed in normocapnia (5% CO_2) and hypercapnia (10% CO_2) in the presence of $3 \mu\text{M}$ EIPA. The effect of acute hypercapnia on adenosine-stimulated NBC-dependent HCO_3^- influx is summarized in (B). Data represents mean \pm S.E.M.; $n=4$.

The current assay used to measure basolateral Na^+ -dependent HCO_3^- import could be influenced by CFTR-dependent HCO_3^- export occurring across the apical membrane simultaneously and, as such, it was important to measure NBC-mediated HCO_3^- import in a more isolated manner. To do this, NBC activity was measured in the presence of $10 \mu\text{M}$ GlyH-101 to inhibit cAMP-stimulated, CFTR-dependent apical HCO_3^- efflux (fig. 3.36A). As shown in figure 3.36B, in the presence of GlyH-101, Na^+ -dependent HCO_3^- influx increased 1.7 ± 0.3 fold in normocapnia ($n=4$; $p<0.05$) and 2.0 ± 0.3 fold in hypercapnia ($n=4$; $p<0.05$). These findings are to be expected given there is no longer an apical efflux pathway for HCO_3^- .

and thus realkalinisation of pH_i would occur much faster as HCO_3^- accumulated within the cell. However, even in the presence of GlyH-101, the rate of Na^+ -dependent HCO_3^- influx was unchanged in acute hypercapnia compared to normocapnia ($22.4 \pm 1.7 \text{ mM min}^{-1}$ vs. $21.8 \pm 3.0 \text{ mM min}^{-1}$ respectively; $n=4$; $p>0.05$; fig. 3.36B). These findings again provide strong evidence that cAMP-stimulated NBC activity is unaffected by changes in CO_2 .

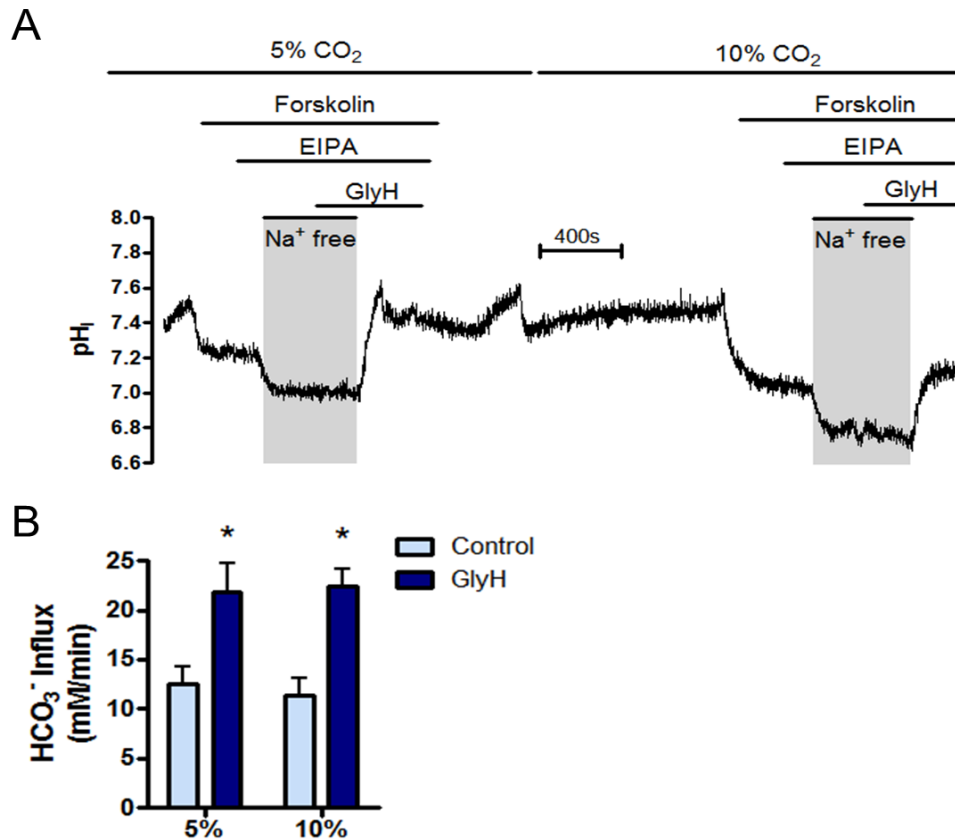


Figure 3.36: Acute hypercapnia does not affect the activity of $\text{Na}^+/\text{HCO}_3^-$ Cotransporters when measured in the presence of GlyH-101. (A) displays a representative experiment in which $5 \mu\text{M}$ forskolin was used to stimulate basolateral Na^+ -dependent HCO_3^- influx whilst GlyH-101 ($10 \mu\text{M}$) was added to the apical membrane to prevent CFTR-dependent apical HCO_3^- efflux. (B) summarizes the effect of hypercapnia on NBC-dependent HCO_3^- influx with and without GlyH-101. * = significant effect of GlyH-101 ($p<0.05$). Data represents mean \pm S.E.M.; $n = 7$ for non GlyH-101 treated cells and $n=4$ for GlyH-101 treated cells.

Although end point PCR revealed that SLC4A10 (a Na^+ -dependent $\text{Cl}^-/\text{HCO}_3^-$ exchanger) was not expressed in Calu-3 cells, it was interesting to assess the Cl^- dependence of Na^+ -dependent HCO_3^- transport. Figures 3.37A and B show example experiments used to measure Na^+ -dependent, Cl^- independent HCO_3^- influx in normocapnia and hypercapnia respectively, in which forskolin-stimulated Na^+ -dependent HCO_3^- transport was compared to Na^+ -

dependent HCO_3^- transport in the absence of basolateral Cl^- . Interestingly, in both normocapnia and hypercapnia, the rate of Na^+ -dependent HCO_3^- influx was significantly increased when basolateral Cl^- was removed. In normocapnia, removal of basolateral Cl^- increased Na^+ dependent HCO_3^- influx 1.8 ± 0.2 fold ($n=5$; $p<0.05$) whilst in hypercapnia, this increase was 2.0 ± 0.1 fold ($n=5$; $p<0.01$; fig. 3.37C). These findings suggested that there may exist a Na^+ -dependent $\text{Cl}^-/\text{HCO}_3^-$ exchanger in Calu-3 cells that acts to recycle HCO_3^- across the basolateral membrane in normal conditions, which, in the absence of basolateral Cl^- , favours HCO_3^- influx to contribute to the greater realkalinisation rate observed. Nevertheless, the rate of Na^+ -dependent HCO_3^- influx in Cl^- free conditions was unchanged in hypercapnia relative to normocapnia ($23.4 \pm 3.8\text{mM min}^{-1}$ vs. $19.8 \pm 2.19\text{mM min}^{-1}$ respectively; $p>0.05$; $n=5$; fig. 3.37C) implying that a putative Na^+ -dependent $\text{Cl}^-/\text{HCO}_3^-$ exchanger was also insensitive to changes in CO_2 and therefore does not underlie the CO_2 -induced changes in cAMP-regulated HCO_3^- transport.

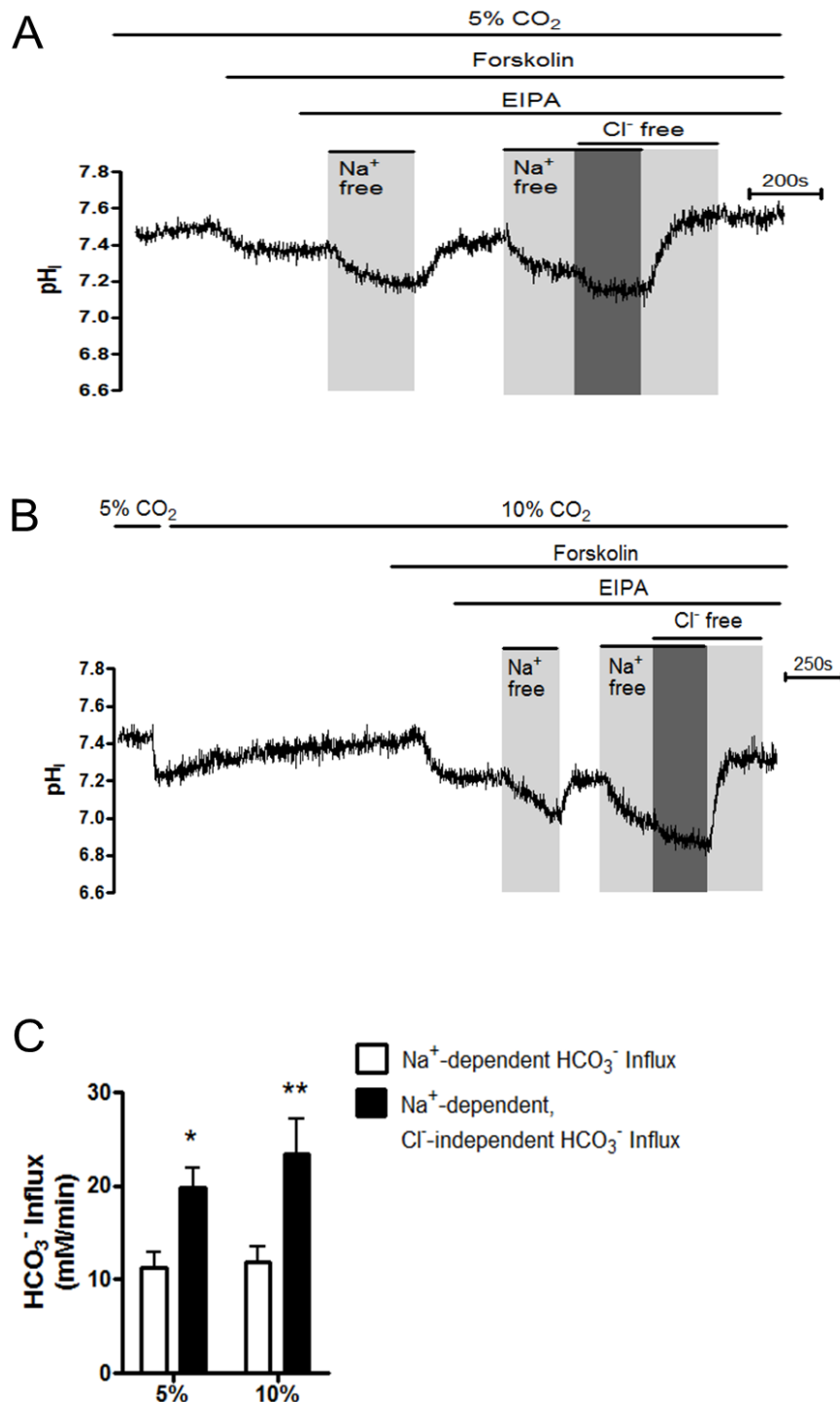


Figure 3.37: Acute hypercapnia does not alter the activity of a putative Na⁺-dependent Cl⁻/HCO₃⁻ exchanger. (A) shows a representative experiment in which Na⁺-dependent HCO₃⁻ influx was assessed in basolateral Cl⁻ containing and basolateral Cl⁻ free conditions after 5 μ M forskolin-stimulation in 5% CO₂. 3 μ M EIPA was present to inhibit Na⁺/H⁺ exchange. The same approach was used in cells exposed to acute hypercapnia (B). (C) displays the effect of basolateral Cl⁻ removal on the Na⁺-dependent HCO₃⁻ influx as well as the effect of hypercapnia; * = significant effect of basolateral Cl⁻ removal ($p < 0.05$; ** = $p < 0.01$) Data represents mean \pm S.E.M. $n = 5$ for each.

To further verify that cAMP-stimulated NBC activity was unaffected by hypercapnia, cells were stimulated with forskolin in the absence of basolateral Na^+ (fig. 3.38A). If NBC activity was altered by hypercapnia then inhibition of its activity by removal of basolateral Na^+ should prevent the CO_2 effect. However, even in the absence of basolateral Na^+ , there was still a significant 1.9 ± 0.2 fold increase in the magnitude of the forskolin-stimulated intracellular acidification ($p < 0.05$; $n = 3$; fig. 3.38B) and a significant 2.6 ± 0.5 fold increase in the rate of forskolin-stimulated HCO_3^- flux ($p < 0.05$; $n = 3$; fig. 3.38C). Thus, this supports previous data that shows hypercapnia did not alter cAMP-stimulated NBC activity in order to produce its alterations in forskolin-stimulated HCO_3^- transport.

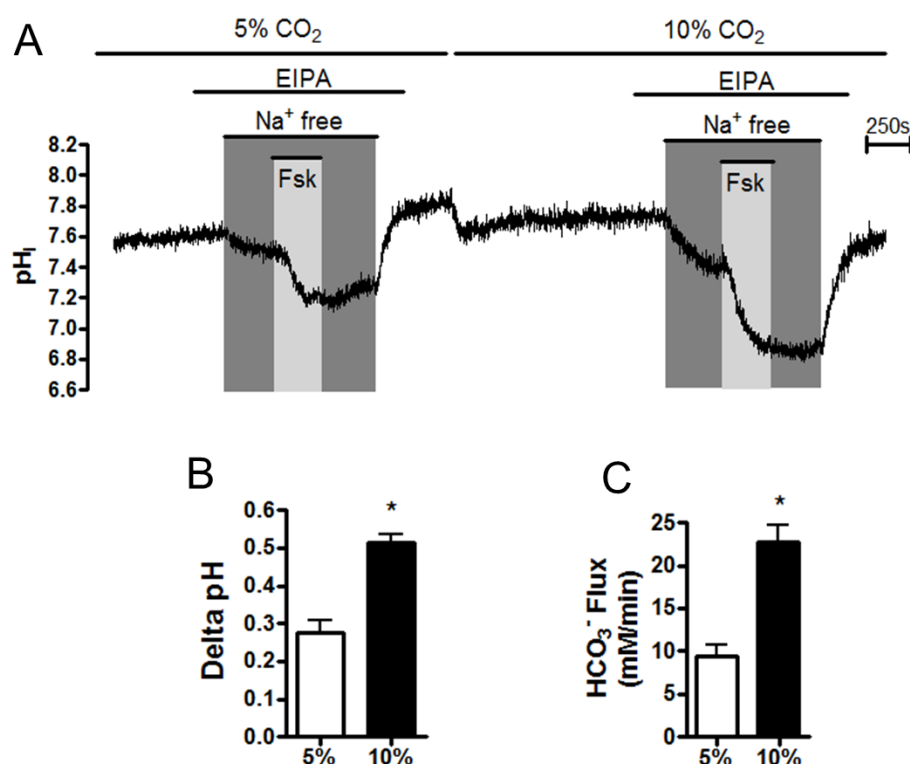


Figure 3.38: Hypercapnia augments forskolin-stimulated intracellular acidification even in absence of basolateral Na^+ . (A) shows a representative experiment in which Calu-3 cells were stimulated with $5\mu\text{M}$ forskolin in normocapnic (5% CO_2) and hypercapnic (10% CO_2) in the absence of basolateral Na^+ . The delta pH (B) and the HCO_3^- flux (C) resulting from forskolin stimulation are displayed. * = significant effect of hypercapnia ($p < 0.05$). Data represents mean \pm S.E.M.; $n = 3$ for each.

One interesting observation from the previous experiments was the effect of hypercapnia on the magnitude of the acidification when basolateral Na^+ was removed under basal conditions. This difference can be seen clearly in figure 3.38A. Further analysis revealed that, in

normocapnia, the magnitude of this acidification was 0.09 ± 0.02 whilst in hypercapnia it was 0.26 ± 0.05 ($p < 0.05$ vs. normocapnia; $n=3$). These findings imply that basal NBC activity (i.e. in the absence of cAMP stimulation) was enhanced by hypercapnia, and this was further explored in the next set of experiments. Both basal and stimulated NBC activity was assessed in either normocapnia (fig. 3.39A) or hypercapnia (fig. 3.39B). In normocapnia, basolateral Na^+ removal in non-stimulated cells caused pH_i to decrease by 0.13 ± 0.01 units ($n=5$) whilst this decrease in pH_i was enhanced to 0.24 ± 0.03 in hypercapnia ($p < 0.01$ vs. normocapnia; $n=6$; fig. 3.39C). Furthermore, the rate of basal NBC-dependent HCO_3^- influx in normocapnia was $4.8 \pm 0.2 \text{ mM HCO}_3^- \text{ min}^{-1}$ ($n=5$) which was significantly enhanced to $11.9 \pm 1.6 \text{ mM HCO}_3^- \text{ min}^{-1}$ in hypercapnia ($p < 0.05$ vs. normocapnia; $n=6$ fig. 3.39D). These data show that hypercapnia elevated basal NBC activity, likely as a mechanism to recover pH_i from CO_2 -induced acidosis. As a result, forskolin-stimulation only increases NBC activity 1.4 ± 0.2 fold in hypercapnia ($n=6$) compared to the 2.5 ± 0.5 fold increase in normocapnia ($p < 0.05$; $n=5$; fig. 3.39E). Therefore, under hypercapnic conditions, it appeared that cAMP was unable to significantly enhance NBC activity, because it was already at a maximal rate due to the effect of high CO_2 and this may contribute to impaired HCO_3^- transport in acute hypercapnic conditions.

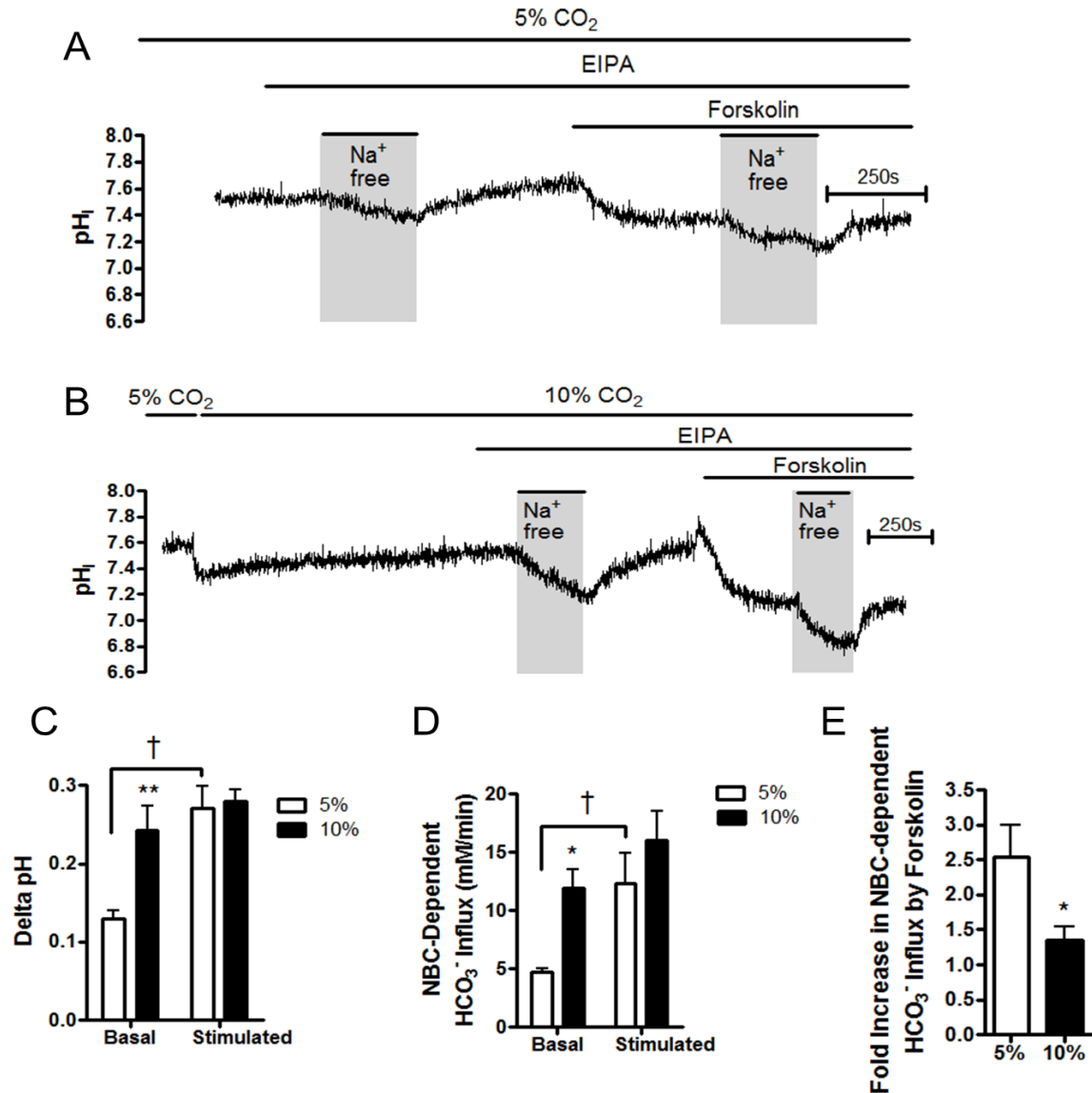


Figure 3.39: Hypercapnia increases Na⁺/HCO₃⁻ Cotransporter activity in basal conditions. (A) and (B) show representative experiments in which basal and forskolin-stimulated NBC activity was assessed in normocapnia and hypercapnia respectively. The delta pH resulting from basolateral Na⁺ removal (C) and NBC-dependent HCO₃⁻ influx (D) are displayed. (E) displays the fold increase in NBC activity by 5μM forskolin. * = significant effect of hypercapnia (p<0.05; ** = p<0.01); † = significant difference between basal and forskolin stimulated NBC activity. Data represents mean ± S.E.M.; n = 5 for normocapnia experiments and n=6 for hypercapnia experiments.

Recently, investigations into NBC activity in both transfected cell lines and in primary murine pancreatic ductal cells have shown that the proteins belonging to the With No Lysine kinase (WNK) family and the Ste20p-related proline alanine-rich kinase (SPAK) family are able to regulate NBC activity. Yang *et al.* (2011a) described NBCe1-dependent HCO₃⁻

transport was increased when WNK1, 3 or 4 or SPAK were knocked down in mouse pancreatic duct cells and decreased when WNK1 or 4 or SPAK were overexpressed. The effects of WNK and SPAK appeared to be a reduction in NBCe1 membrane expression given that overexpression of SPAK or WNK1 reduced NBCe1 surface expression in transfected HEK cells. The researchers showed that WNK acted as a scaffold for SPAK which phosphorylated NBCe1 causing a reduction in its surface expression. Given I have found hypercapnia upregulated NBC activity in Calu-3 cells, it was interesting to assess whether CO₂ was able to modulate WNK/SPAK expression. Therefore, a western blot was carried out to measure expression of WNK4, SPAK or phosphorylated SPAK (p-SPAK) in cells that had been incubated for 20 minutes in pregassed high Cl⁻ Krebs solution exposed to either 5% CO₂, 5% CO₂ + 5 minute forskolin stimulation, 10% CO₂ or 10% CO₂ + 5 minute forskolin stimulation. Figure 3.40 shows the results of the Western blots. Although only representative of n=2 experiments, the data suggests that under basal conditions, acute hypercapnia decreases the expression of WNK4 but has no major effects on either SPAK or p-SPAK expression. Furthermore, forskolin appears to have no major effect on either WNK4, SPAK or p-SPAK expression.

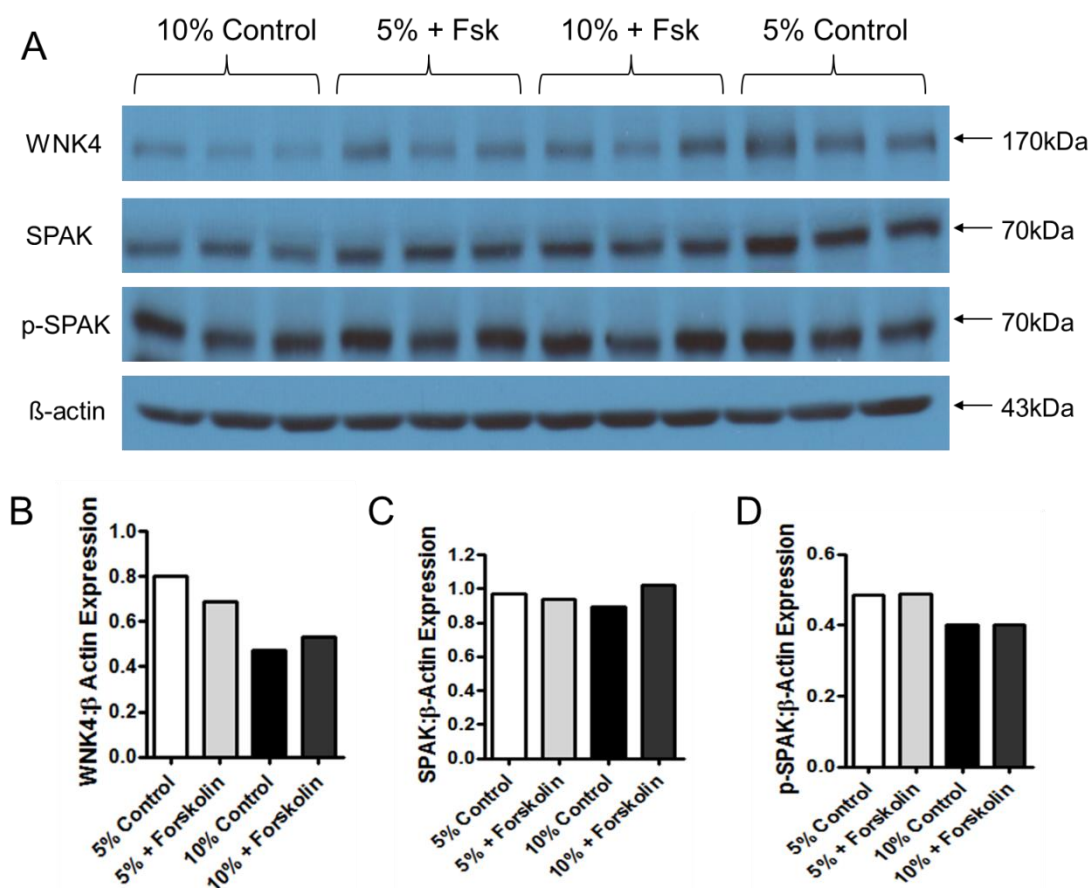


Figure 3.40. Acute hypercapnia reduces WNK4 expression under basal conditions in Calu-3 cells. (A) shows the results from a Western Blot in which the effect of forskolin (5 μ M) and acute hypercapnia on WNK4, SPAK and phosphorylated SPAK (p-SPAK) expression was assessed and normalized to β -actin expression. For each experimental condition, 3 lysates were generated from 3 separate samples and each lysate was ran on the gel so that each sample was performed in triplicate. The data for WNK4, SPAK and p-SPAK are summarized in (B), (C) and (D) respectively. Data represents mean of triplicate samples performed on n=2 independent samples. The protein extraction was carried out by myself but the Western Blots were performed in the laboratory of Professor Ursula Seidler, (Hannover, Germany).

3.14.3. Src kinase

The findings that acute hypercapnia activated NBC activity in basal conditions, and therefore reduced the ability of cAMP to enhance its activity, may impact upon cAMP-regulated HCO_3^- transport in hypercapnic conditions. Several studies have shown that the Src family kinases influence HCO_3^- transport in human epithelial by regulation of NBCs, and are potentially sensitive to changing levels of CO_2 . Ruiz *et al.* (1999) measured NBC activity in rabbit proximal tubule cells by measuring pH_i recovery after removal and then reapplication of external Na^+ . They found that CO_2 enhanced NBC activity in these cells but this effect was

blocked by herbimycin, a Src family kinase inhibitor. Furthermore, overexpression of Csk, a negative regulator of Src kinase, also prevented NBC activation by CO₂. Espiritu *et al.* (2002) also studied NBC activity in proximal tubule epithelium. They also demonstrated 10% CO₂ increased NBC activity in a Ca²⁺/Calmodulin-dependent manner. Furthermore, 10% CO₂ also increased Pyk2 phosphorylation which enhanced its interaction with Src kinase. These findings showed that Src family kinases were involved in the CO₂-dependent upregulation of NBC activity in kidney epithelia and suggest Src family kinases are involved in CO₂ signal transduction. To test the role of Src kinase in mediating the response to hypercapnia in airway epithelia, Calu-3 cells were preincubated for one hour with Src kinase Inhibitor 1 (SKI-1) and perfused with SKI-1 for the duration of the experiment. As shown in figure 3.41A, the responses of cells to forskolin in normocapnia and hypercapnia were measured and compared to control experiments performed on the same day. In control experiments, hypercapnia caused a 1.9 ± 0.1 fold increase in the magnitude of the forskolin-stimulated intracellular acidification ($p < 0.05$; $n = 3$; fig. 3.41B) and increased the rate of forskolin-stimulated HCO₃⁻ flux 4.2 ± 0.2 fold ($p < 0.05$; $n = 3$; fig. 3.41C). Although the raw data displayed in figure 3.41 shows SKI-1 caused a reduction in the forskolin-stimulated intracellular acidification, these reductions were not sufficient enough to significantly affect the fold changes in the forskolin-stimulated intracellular acidification by hypercapnia. In SKI-1 treated cells hypercapnia caused a 1.8 ± 0.3 fold increase in the magnitude of the forskolin-stimulated intracellular acidification ($p < 0.05$ vs. normocapnia; $p > 0.05$ vs. control experiments; fig. 3.41B) and increased the rate of forskolin-stimulated HCO₃⁻ flux 4.0 ± 1.1 fold ($p < 0.05$ vs. normocapnia; $p > 0.05$ vs. control experiments; fig. 3.41C). Therefore, these data show that Src kinases have no role in the CO₂-mediated modulation of cAMP-regulated HCO₃⁻ transport in Calu-3 cells.

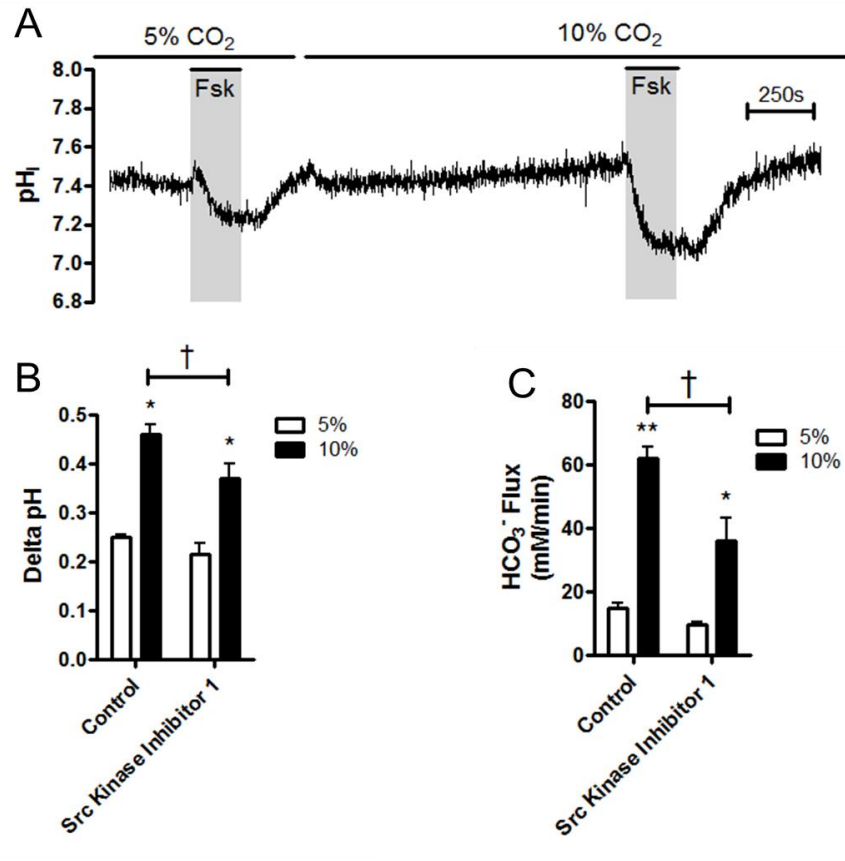


Figure 3.41: Src kinase inhibition does not block the effects of hypercapnia on the forskolin-stimulated intracellular acidification. (A) shows a representative experiment in which Calu-3 cells were preincubated for one hour with Src kinase inhibitor 1 (SKI-1) (2 μ M) and perfused with SKI (2 μ M) for the duration of the experiment. Cells were stimulated with 5 μ M forskolin in normocapnia and hypercapnia. The delta pH (B) and HCO₃⁻ flux (C) resulting from forskolin stimulation are summarized. * = significant effect of hypercapnia (p<0.05; ** = p<0.01); † = significant effect of SKI-1 (p<0.05). Data represents mean \pm S.E.M.; n=3 for each.

3.14.4. PI3 Kinase

Another study that investigated CO₂ upregulation of NBC activity in the proximal tubule was performed by Bernardo *et al.* (2003). Here, the researchers suggested that CO₂-induced increase in NBC proximal tubule activity was caused by increased NBC expression at the plasma membrane, a process dependent on PI3 Kinase – an enzyme involved in protein trafficking and, interestingly, able to interact with Src kinase. To test whether PI3 Kinase was involved in mediating the effects of hypercapnia in Calu-3 cells, cells were preincubated with the irreversible PI3 Kinase inhibitor wortmannin. As shown in figure 3.42, in control experiments, hypercapnia caused a 2.0 ± 0.1 fold increase in the magnitude of the forskolin-stimulated intracellular acidification (p<0.001; n=3; fig. 3.42B) and increased the rate of

forskolin-stimulated HCO_3^- flux 4.0 ± 0.7 fold ($p < 0.05$; $n=3$; fig. 3.42C). In wortmannin treated cells, hypercapnia caused a 1.8 ± 0.1 fold increase in the magnitude of the forskolin-stimulated intracellular acidification ($p < 0.001$; $n=3$; fig. 3.42B) and increased the rate of forskolin-stimulated HCO_3^- flux 3.6 ± 0.3 fold ($p < 0.05$; $n=3$; fig. 3.42C). Therefore, these findings suggest PI3 Kinase is not involved in transducing the effect of hypercapnia in Calu-3 cells.

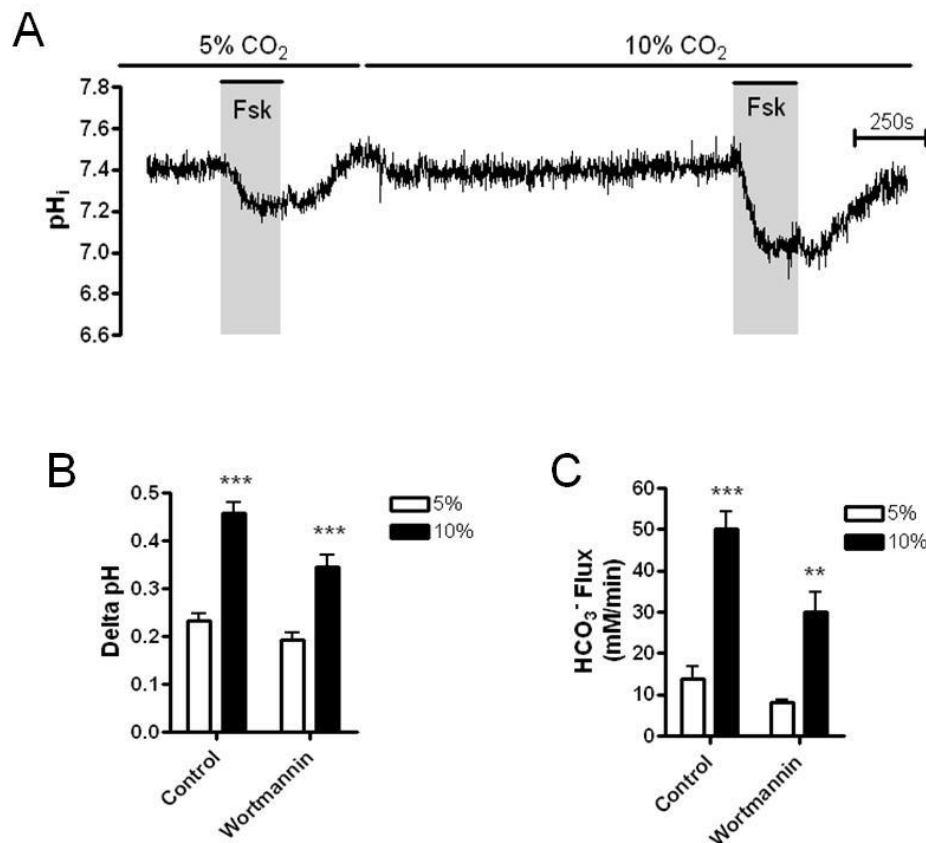


Figure 3.42: PI3 Kinase inhibition does not block the effects of hypercapnia on the forskolin-stimulated intracellular acidification. Calu-3 cells were preincubated with the PI3 Kinase inhibitor wortmannin (10 μ M) and stimulated with 5 μ M forskolin in normocapnia and hypercapnia as shown in (A). The delta pH (B) and HCO_3^- flux (C) resulting from forskolin stimulation are summarized. ** = significant effect of hypercapnia ($p < 0.01$; *** = $p < 0.001$); Data represents mean \pm S.E.M.; $n=3$ for each.

3.14.5. Basolateral AE2 activity

Both Garnett *et al.* (2011) and Kim *et al.* (2014) have shown that AE2 activity is reduced when intracellular cAMP levels increase in Calu3 cells, likely to prevent loss of HCO_3^- across the basolateral membrane when cells are stimulated to secrete HCO_3^- . Thus, one would

predict that CO₂-induced changes in intracellular cAMP may impact upon AE2 activity. AE2 activity was measured by the method described in figure 3.31. This was done in both basal and forskolin-stimulated conditions in normocapnia and hypercapnia. In basal conditions, removal of basolateral Cl⁻ caused pH to increase by 0.26 ± 0.01 in normocapnia (n=5) but this was significantly reduced to 0.09 ± 0.02 in conditions of hypercapnia (p<0.001; n=6; fig. 3.43B) Similarly, reintroduction of basolateral Cl⁻ induced a HCO₃⁻ flux of $28.7 \pm 9.3\text{mM HCO}_3^- \text{ min}^{-1}$ (n=5) in normocapnia but this was significantly reduced to $17.8 \pm 6.2\text{mM HCO}_3^- \text{ min}^{-1}$ (p<0.05; n=5; fig. 3.43C) in hypercapnic conditions. These data suggest that acute hypercapnia modulates the activity of AE2 in non-stimulated conditions, implying CO₂ is able to regulate AE2 in a cAMP-independent manner. In forskolin-stimulated conditions, AE2 activity was abolished as already reported by our laboratory (Garnett *et al.*, 2011; Garnett *et al.*, 2013). In normocapnia, removal of basolateral Cl⁻ caused pH to increase by 0.01 ± 0.01 (n=5) and reintroduction of basolateral Cl⁻ did not induce any measureable HCO₃⁻ efflux. In hypercapnia, identical results were observed. Removal of basolateral Cl⁻ caused pH to increase by 0.01 ± 0.01 (p>0.05; n=5) and reintroduction of basolateral Cl⁻ did not induce any measureable HCO₃⁻ efflux. These findings demonstrated that although acute hypercapnia reduces forskolin-stimulated cAMP levels in Calu-3 cells, the reductions are not sufficient to relieve the cAMP-induced inhibition of AE2 activity. Thus differences in AE2 activity cannot explain the CO₂-induced modulation of cAMP-stimulated HCO₃⁻ transport in Calu-3 cells.

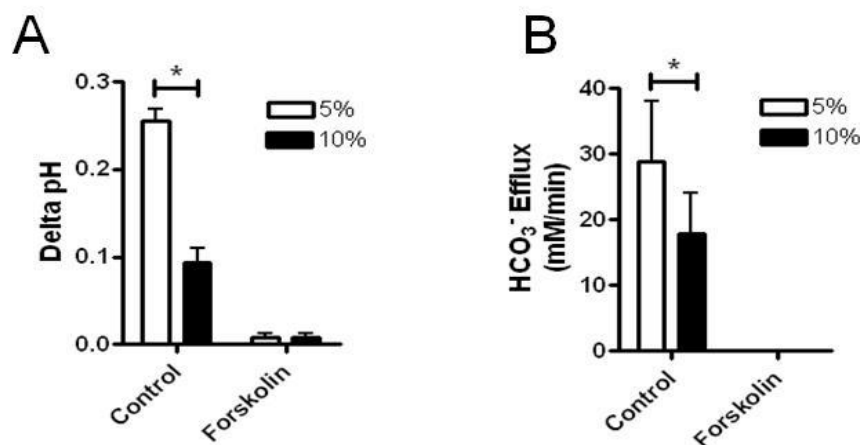


Figure 3.43: Acute hypercapnia is unable to relieve the cAMP-induced inhibition of basolateral AE2 but does reduce AE2 activity in basal conditions. AE2 activity was assessed by removal and subsequent readdition of basolateral Cl⁻ in basal or forskolin-stimulated conditions. The delta pH resulting from basolateral Cl⁻ removal (A) and the rate of HCO₃⁻ efflux after basolateral Cl⁻ readdition (B) are summarized. * = significant effect of hypercapnia (p<0.05). Data represents mean \pm S.E.M.; n = 5 for each.

3.14.6. Na⁺/H⁺ Exchangers

The NHE family of transporters may contribute to the forskolin-stimulated intracellular acidification and therefore could be the site of CO₂ modulation. Although the forskolin-stimulated intracellular acidification appears to be the result of CFTR-dependent HCO₃⁻ efflux across the apical membrane, changes in H⁺ transport would also contribute to changes in intracellular pH. To test whether NHEs were involved in mediating the response to hypercapnia on the forskolin-stimulated intracellular acidification, experiments were performed in the presence of the NHE inhibitor EIPA as shown in figure 3.44A. EIPA did not significantly alter the response to forskolin in normocapnia: delta pH was 0.38 ± 0.03 and 0.40 ± 0.01 ($p > 0.05$; $n=4$; fig. 3.44B) and HCO₃⁻ efflux was $25.8 \pm 3.4 \text{ mM HCO}_3^- \text{ min}^{-1}$ and $34.0 \pm 1.3 \text{ mM HCO}_3^- \text{ min}^{-1}$ ($p > 0.05$; $n=4$; fig. 3.44C) in control and EIPA-treated conditions, respectively. Furthermore, in the presence of EIPA, hypercapnia caused a significant 1.5 ± 0.1 fold increase in the magnitude of the forskolin-stimulated intracellular acidification ($p < 0.01$; $n=4$; fig. 3.44B) and a significant 3.2 ± 0.3 fold increase in the rate of forskolin-stimulated HCO₃⁻ flux ($p < 0.01$; $n=4$; fig. 3.44C). These data show that NHE transporters are not involved in mediating the effect of the forskolin-stimulated intracellular acidification in hypercapnia.

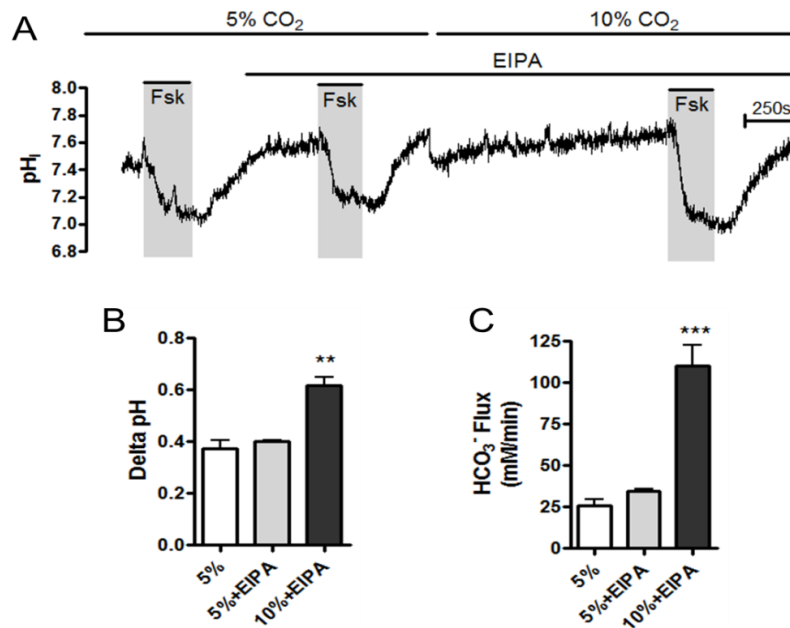


Figure 3.44: CO₂-induced modulation of forskolin-stimulated intracellular acidification is not due to changes in Na⁺/H⁺ Exchanger activity. (A) shows a representative experiment in which cells were stimulated with 5 μM forskolin in the presence of 3 μM EIPA in normocapnia (5% CO₂) and hypercapnia (10% CO₂). The delta pH (B) and the HCO₃⁻ flux (C) resulting from forskolin stimulation are displayed. ** = significant effect of hypercapnia (p<0.01; *** = p<0.001). Data represents mean ± S.E.M.; n=4 for each.

3.14.7. Na⁺-K⁺-Cl⁻ cotransporter

The Na⁺-K⁺-Cl⁻ cotransporter 1 (NKCC1) is a transporter that facilitates the influx of Na⁺, K⁺ and 2 Cl⁻ ions in secretory epithelia and has been found to be expressed in Calu-3 cells (Liedtke *et al.*, 2001). Furthermore, data from the Ussing chamber experiments (fig. 4.2) show that NKCC1 has a role in forskolin-stimulated ion transport in Calu-3 cells. Changes in NKCC1-mediated ion transport would affect intracellular [Na⁺], [K⁺] and [Cl⁻] and therefore could contribute to changes in HCO₃⁻ transport due to possible effects on membrane potential and/or CFTR-dependent Cl⁻/HCO₃⁻ exchange. Therefore, the response to forskolin in hypercapnia was assessed in the presence of bumetanide. As shown in figure 3.45, bumetanide did not significantly alter the response to forskolin in normocapnia: delta pH was 0.19 ± 0.04 in control conditions and 0.15 ± 0.01 in the presence of bumetanide (p>0.05; n=3; fig. 3.45B) whilst HCO₃⁻ efflux was 8.9 ± 1.1 mM HCO₃⁻ min⁻¹ in control conditions and 8.6 ± 1.5 mM HCO₃⁻ min⁻¹ in the presence of bumetanide (p>0.05; n=3; fig. 3.45C). Furthermore, in the presence of bumetanide, hypercapnia caused a significant 2.0 ± 0.1 fold increase in the magnitude of the forskolin-stimulated intracellular acidification (p<0.01; n=3; fig. 3.45B) and

a 4.5 ± 1.0 fold increase in the rate of forskolin-stimulated HCO_3^- flux ($p < 0.05$; $n = 3$; fig. 3.45C). These data show that NKCC1 is not involved in mediating the effects of hypercapnia on the forskolin-stimulated intracellular acidification.

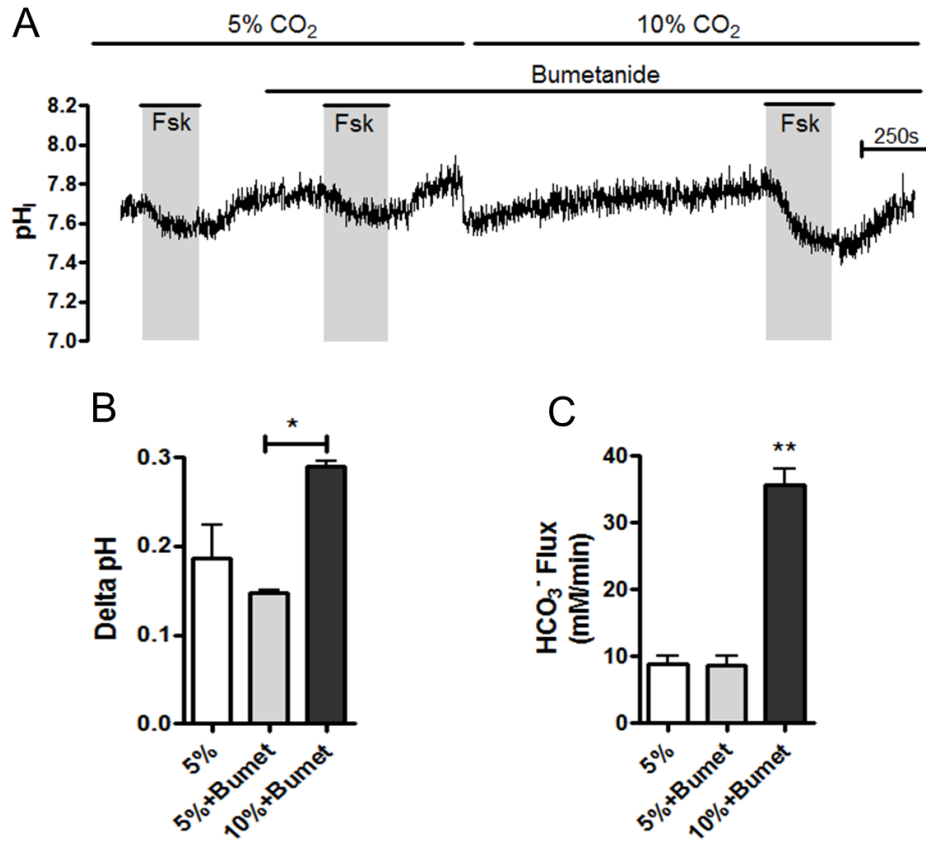


Figure 3.45: CO_2 -induced modulation of forskolin-stimulated intracellular acidification is not due to changes in $\text{Na}^+\text{-K}^+\text{-Cl}^-$ Cotransporter activity. (A) shows a representative experiment in which cells were stimulated with $5\mu\text{M}$ forskolin in the presence of $25\mu\text{M}$ bumetanide in normocapnia (5% CO_2) and hypercapnia (10% CO_2). The delta pH (B) and the HCO_3^- flux (C) resulting from forskolin stimulation are displayed. * = significant effect of hypercapnia ($p < 0.05$; ** = $p < 0.01$). Data represents mean \pm S.E.M.; $n = 3$ for each.

3.14.8. $\text{Na}^+/\text{K}^+\text{-ATPase}$

It has previously been shown that $\text{Na}^+/\text{K}^+\text{-ATPase}$ activity is reduced by hypercapnia in alveolar type II cells due to a CO_2 -induced endocytosis of the α subunit of $\text{Na}^+/\text{K}^+\text{-ATPase}$ which led to a reduction in Na^+ reabsorption (Briva *et al.*, 2007). Given the $\text{Na}^+/\text{K}^+\text{-ATPase}$ has been shown to be regulated by CO_2 in other human airway epithelial cells, it was important to assess whether CO_2 could modulate $\text{Na}^+/\text{K}^+\text{-ATPase}$ activity in Calu-3 cells. Changes in $\text{Na}^+/\text{K}^+\text{-ATPase}$ activity will alter intracellular $[\text{Na}^+]$ and $[\text{K}^+]$ and therefore could

affect membrane potential which could alter the driving force for HCO_3^- transport. Thus, the forskolin-stimulated intracellular acidification in both normocapnia and hypercapnia was assessed in the presence of the Na^+/K^+ -ATPase inhibitor ouabain (fig. 3.46A) and compared to control experiments performed on the same day. Ouabain has no effect on the magnitude of the forskolin-stimulated intracellular acidification, nor on the rate of forskolin-stimulated HCO_3^- flux measured in normocapnia as shown in figures 3.46B and 3.46C respectively. However, in the presence of basolateral ouabain, hypercapnia only elicited a 1.3 ± 0.5 fold increase in the magnitude of the forskolin-stimulated intracellular acidification ($p > 0.05$ vs. normocapnia; $n=3$; figs. 3.46B and D) and a 1.8 ± 0.4 fold increase in the rate of forskolin-stimulated HCO_3^- flux ($p > 0.05$ vs. normocapnia; $n=3$; fig. 3.46C and E). When compared to control experiments performed on the same day, in which hypercapnia caused a 2.1 ± 0.1 fold increase in the magnitude of the forskolin-stimulated intracellular acidification ($p < 0.05$ vs. normocapnia; $n=3$; fig. 3.46D) and a 5.7 ± 0.8 fold increase in the rate of forskolin-stimulated HCO_3^- flux ($p < 0.05$ vs. normocapnia; $n=3$; fig. 3.46E), it showed that ouabain was able to prevent the effect of hypercapnia on cAMP-regulated HCO_3^- transport. Furthermore, cells treated with ouabain only exhibited a $5.1 \pm 7.3\%$ ($p < 0.001$ vs. control; $n=3$; fig. 3.46F) in pH_i recovery from CO_2 -induced acidosis, suggesting that the Na^+/K^+ -ATPase plays a major role in this recovery process.

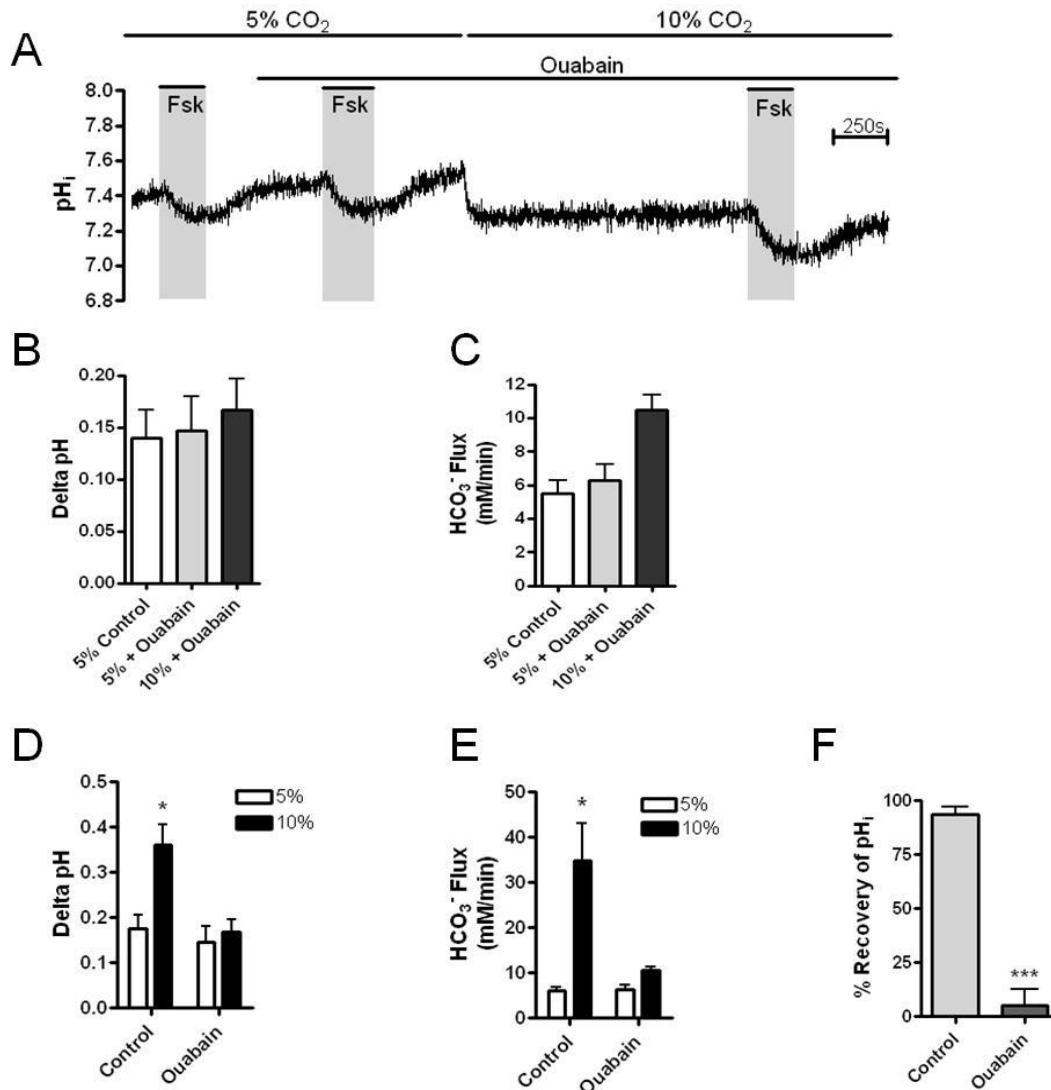


Figure 3.46: Ouabain treatment blocks the effect of acute hypercapnia on the forskolin-stimulated intracellular acidification. (A) shows a representative experiment in which cells were stimulated with $5\mu M$ forskolin in the presence of $100\mu M$ ouabain in normocapnia and hypercapnia. The ΔpH (B) and the HCO_3^- flux (C) resulting from forskolin stimulation are displayed. The ΔpH (D) and the HCO_3^- flux (E) resulting from forskolin stimulation in control experiments performed on the same day are displayed and compared to measurements made in the presence of ouabain. * = significant effect of hypercapnia ($p < 0.05$). (F) displays the effect of ouabain on recovery of pH_i from CO_2 -induced acidosis. *** = significant effect of ouabain ($p < 0.001$). Data represents mean \pm S.E.M.; $n=3$ for each.

3.14.9. AMP Kinase

Given that the effect of acute hypercapnia on cAMP-regulated HCO_3^- transport was prevented by treatment of cells with the Na^+/K^+ -ATPase inhibitor ouabain, it suggested Na^+/K^+ -ATPase was sensitive to CO_2 . This supports findings by Briva *et al.* (2007) who also

demonstrated that the Na^+/K^+ -ATPase is sensitive to CO_2 in rat alveolar type II cells and led to a decrease in alveolar fluid reabsorption. Further investigations into this phenomena revealed that the effect of hypercapnia on Na^+/K^+ -ATPase was blocked by inhibition of AMP Kinase and that AMP Kinase was activated by CO_2 *per se* (Vadasz *et al.*, 2008). Therefore, the role of AMP Kinase in transducing the CO_2 signal in Calu-3 cells was tested. Calu-3 cells were preincubated for one hour with the AMPK inhibitor dorsomorphin and perfused with dorsomorphin for the duration of the experiment as shown in figure 3.47A. In control experiments, hypercapnia caused a 1.8 ± 0.1 fold increase in the magnitude of the forskolin-stimulated intracellular acidification ($p < 0.05$; $n=4$; fig. 3.47B) and increased the rate of forskolin-stimulated HCO_3^- flux 4.2 ± 0.3 fold ($p < 0.001$; $n=4$; fig. 3.47C). Dorsomorphin treatment did not alter the effect of hypercapnia on cAMP-regulated HCO_3^- transport. In dorsomorphin treated cells, hypercapnia caused a 1.7 ± 0.3 fold increase in the magnitude of the forskolin-stimulated intracellular acidification ($p < 0.05$; $n=4$; fig. 3.47B) and increased the rate of forskolin-stimulated HCO_3^- flux 3.4 ± 0.4 fold ($p < 0.001$; $n=4$; fig. 3.47C). Therefore, these data show that AMPK has no role in the CO_2 -mediated modulation of cAMP-regulated HCO_3^- transport in Calu-3 cells.

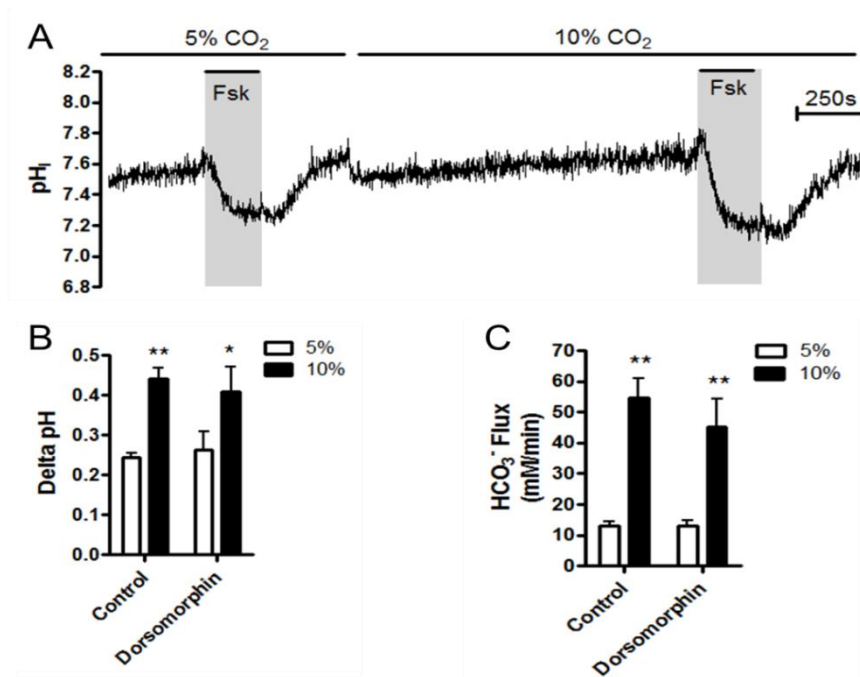


Figure 3.47. AMP Kinase inhibition does not block the effects of hypercapnia on the forskolin-stimulated intracellular acidification. Calu-3 cells were preincubated for one hour with the AMPK inhibitor dorsomorphin (1 μM) and perfused dorsomorphin (1 μM) for the duration of the experiment. Cells were stimulated with 5 μM forskolin in normocapnia and hypercapnia as shown in (A). The delta pH (B) and HCO_3^- flux (C) resulting from forskolin stimulation are summarized. * = significant effect of hypercapnia ($p < 0.05$; ** = $p < 0.01$); Data represents mean \pm S.E.M.; $n=3$ for each.

3.15. Discussion

3.15.1. The effects of hypercapnia on Calu-3 cells

Administration of 10% CO₂ to Calu-3 cells induced an intracellular acidosis which was found to recover after ~20 minutes showing that cells possess mechanisms in which they can sense and respond to acute hypercapnia. Characterizing the pH_i recovery process showed it to be completely Na⁺-dependent yet unaffected by inhibition of NHEs suggesting that recovery is mediated *via* Na⁺-dependent HCO₃⁻ influx as opposed to Na⁺-dependent H⁺ efflux. To support this, the NBC inhibitor DIDS was found to reduce recovery, implying this transporter does have an important role in pH_i recovery. The effect of basolateral Cl⁻ removal to reduce recovery by ~50% was interesting. Should there be a role for AE2-dependent HCO₃⁻ influx in pH_i recovery, removal of basolateral Cl⁻ would be predicted to enhance recovery not reduce it. Therefore, the effect of basolateral Cl⁻ removal may be an indirect effect on NBC; for instance, although removal of basolateral Cl⁻ would stimulate AE2-mediated HCO₃⁻ influx in Calu-3 cells, this would reduce the electrochemical driving force for NBC-dependent HCO₃⁻ influx and it may be such that recovery is specifically mediated by NBC-dependent HCO₃⁻ influx as opposed to AE2-dependent HCO₃⁻ influx. However, it was found that forskolin, as well as MK-571, blocked pH_i recovery, suggesting that the transporter(s) underlying pH_i recovery are negatively regulated by cAMP and thus argue against the identity of these transporters being members of the NBC family, given that these transporters are cAMP-activated (Devor *et al.*, 1999; Bachmann *et al.*, 2003; Bachmann *et al.*, 2008). However, it is possible that elevations in [cAMP]_i inhibited pH_i recovery because of an activation of CFTR-dependent HCO₃⁻ efflux preventing HCO₃⁻ accumulation within the cell and performing the same experiments in the presence of a CFTR inhibitor may yield different results.

Calu-3 cells displayed an asymmetry in membrane permeability to CO₂, with only the apical membrane being CO₂ permeable. This asymmetry has also been reported in human retinal pigment epithelia (Adijanto *et al.*, 2009) in which only the apical membrane is CO₂ permeable, and in human parietal cells, in which only the basolateral membrane is CO₂ permeable (Boron *et al.*, 1994) and suggests a differential expression of CO₂ transporters, of which aquaporins have been largely implicated (Nakhoul *et al.*, 1998; Endeward *et al.*, 2006; Musa-Aziz *et al.*, 2009), may be responsible for this. Kreda *et al.* (2001) found that AQP5 was expressed on the apical membrane of Calu-3 cells and AQP5 has been found to be CO₂ permeable when expressed in *Xenopus* oocytes (Musa-Aziz *et al.*, 2009). Alternatively, CO₂

permeability may be determined by the cholesterol content of the lipid bilayer as suggested by Itel *et al.* (2012). Therefore, it would be of interest to assess both the expression of aquaporins and the cholesterol content at each membrane to gain further insights into CO₂ permeability across human cell membranes.

3.15.2. Acute hypercapnia modulated [cAMP]_i and cAMP-regulated anion secretion

Stimulation of Calu-3 cells with the cAMP agonists forskolin and adenosine resulted in a multitude of measureable responses which were all affected by acute hypercapnia. Firstly, forskolin-induced increases in intracellular cAMP were significantly blunted by 20 minutes exposure to 10% CO₂. The incubation media in these experiments were buffered to pH 7.5 and cells were allowed to recover pH_i from CO₂-induced acidosis prior to agonist stimulation. Therefore, this shows that the effect of hypercapnia was due to CO₂ *per se* and not due to CO₂-induced acidosis. Given that these experiments were performed in the presence of 1mM IBMX, it would suggest that hypercapnia was affecting cAMP synthesis due to effects on tmAC activity as opposed to its breakdown by phosphodiesterases and our laboratory has already shown tmAC *per se* to be sensitive to changes in CO₂ (Townsend *et al.*, 2009). Interestingly, hypercapnia did not affect cAMP production in non-stimulated cells. This implies that, in order for hypercapnia to mediate its effects on tmAC, tmAC needs to be in an active state. Zhang *et al.* (1997) have described the presence of hydrophobic forskolin binding pockets within tmAC and forskolin binding at these sites induces a conformational change allowing for dimerization of the two catalytic subunits of tmAC. Thus, it seems likely that CO₂ can only modulate tmAC activity when it is held within this “forskolin-bound” state. Similar conformational changes within tmAC are induced when G_{as} coupled proteins bind to the enzyme, implying CO₂ modulates tmAC activity *via* the same mechanism when cells are stimulated with G-protein receptor agonists (Tesmer *et al.*, 1997). It is worth noting that intracellular cAMP measurements were performed on non-polarized Calu-3 cells and therefore, it will be important to attempt these experiments on polarized monolayers in order to replicate conditions for pH_i and I_{sc} measurements.

This hypercapnia-induced reduction in forskolin-stimulated cAMP levels also had major implications for cAMP-regulated ion transport across Calu-3 cells. In the presence of a basolateral to apical Cl⁻ gradient, forskolin, as well as adenosine and dibutyryl-cAMP, caused an increase in I_{sc} which reached an initial peak and then plateaued to a steady state. The forskolin-stimulated increase in I_{sc} was significantly reduced by PKA inhibition and was

reversed by the combination of apical CFTR_{inh}-172 and basolateral bumetanide. These data showed that elevations in intracellular cAMP induced CFTR-dependent electrogenic anion secretion in Calu-3 cells. In cells that had been exposed to 20 minutes hypercapnia, the rate of forskolin-stimulated increases in I_{sc} was significantly reduced by ~45% implying that CO₂-induced reductions in intracellular cAMP were sufficient enough to reduce CFTR activity. Another interesting observation from the Ussing chamber studies was that acute hypercapnia significantly reduced basal I_{sc} in Calu-3 cells. Given basal I_{sc} was sensitive to CFTR_{inh} 172, it suggested a large component of basal I_{sc} was mediated by CFTR and also suggested that acute hypercapnia reduced the activity of non-stimulated CFTR. The I_{sc} data is even more surprising given that acute hypercapnia appears to increase the total CFTR protein levels in Calu-3 cells. Whether this translates to an increased membrane expression remains to be seen but if acute hypercapnia does increase CFTR expression yet reduces cAMP-stimulated CFTR-dependent Cl⁻ secretion, it shows that the effect of hypercapnia on CFTR activity is more pronounced than first believed and that the I_{sc} data is actually an underestimation of the extent of hypercapnia-induced inhibition of CFTR activity.

3.15.2. How does a CO₂-induced reduction in [cAMP]_i lead to an apparent increase in cAMP-regulated HCO₃⁻ transport?

To focus on the effects of acute hypercapnia on HCO₃⁻ transport in Calu-3 cells, intracellular pH measurements were performed to indirectly measure HCO₃⁻ transport. Addition of the cAMP elevating agonists forskolin, adenosine, dibutyryl-cAMP or IBMX, all induced an intracellular acidification in Calu-3 cells before a new steady state pH_i was reached. This intracellular acidification was sensitive to inhibition of tmAC, PKA and CFTR and did not occur in HCO₃⁻-free conditions or in depolarised cells. Together these data show that elevations in cAMP stimulated CFTR-dependent HCO₃⁻ secretion that, temporarily, occurred at a greater rate than HCO₃⁻ influx across the basolateral membrane; hence an acidification was observed. Interestingly, acute hypercapnia significantly increased both the magnitude and rate of forskolin and adenosine-stimulated intracellular acidification which was independent of differences in pH_i, pH_e and did not occur due to an increased formation of intracellular HCO₃⁻ due to CO₂ hydration by carbonic anhydrase. Thus CO₂ *per se* was able to modulate cAMP-regulated HCO₃⁻ transport, likely due to reduced intracellular cAMP levels. Furthermore, the effect of hypercapnia was dependent on 10% CO₂ being applied to

the apical membrane. Basolateral 10% CO₂ was unable to modulate cAMP-regulated HCO₃⁻ transport and, given I have found the basolateral membrane to be CO₂ impermeable, suggests that in order for CO₂ to mediate its effects upon cAMP signalling, it needs to be able to get into the cell. Consequentially, should CO₂ indeed directly modulate tmAC, it would imply that the CO₂-sensitive sites of tmAC are located on intracellular domains. Conversely, there may be different isoforms of tmAC expressed at each membrane, of which only the isoforms expressed at the apical membrane are CO₂-sensitive. To get a clearer understanding of this, the specific isoforms of tmAC expressed in Calu-3 cells need to be identified.

At first, one would assume that a larger forskolin-stimulated intracellular acidification in the presence of hypercapnia was a result of CO₂ stimulating CFTR-dependent HCO₃⁻ secretion across the apical membrane. However, this would not be expected given that hypercapnia has been shown to reduce intracellular cAMP levels and CFTR-dependent Cl⁻ secretion. An alternative explanation was that hypercapnia was reducing cAMP-regulated HCO₃⁻ influx across the basolateral membrane which would also produce the same effect on intracellular acidification. This is supported by the fact that (i) CFTR-dependent Cl⁻/HCO₃⁻ exchange was unaffected by acute hypercapnia and (ii) the CO₂ effect was blocked by inhibition of pH_i regulatory transporters at the basolateral membrane. End-point PCR revealed that two members of the cAMP-regulated HCO₃⁻ importers belonging to the Na⁺/HCO₃⁻ Cotransporter family, SLC4A4 and SLC4A7, were expressed in Calu-3 cells yet, crucially, cAMP-stimulated Na⁺-dependent HCO₃⁻ influx was unaffected by acute hypercapnia. Thus, although hypercapnia clearly modulates cAMP-regulated HCO₃⁻ transport in Calu-3 cells, this does not appear to be mediated by altering the activity of cAMP-stimulated HCO₃⁻ transporters and raises the question as to the identity of the CO₂ target(s). One important finding from studies on NBC activity was the fact that hypercapnia actually stimulated NBC activity under basal conditions. This likely is an adaptive mechanism in Calu-3 cells to increase HCO₃⁻ uptake into the cell in response to CO₂-induced acidosis. However, as a result of this, NBC activity was not able to be further enhanced in response to cAMP stimulation as it was already at near maximal activity. This, therefore, could underlie the effect of elevated CO₂ and contribute to the greater forskolin-stimulated intracellular acidification observed in hypercapnic conditions. In normocapnia, elevations in cAMP stimulate both apical HCO₃⁻ efflux and basolateral HCO₃⁻ influx with HCO₃⁻ efflux temporarily occurring at a greater rate than HCO₃⁻ influx, hence an acidification is observed until the two processes are equal. However, in hypercapnia, elevations in cAMP stimulated apical HCO₃⁻ efflux but due to NBC activity

already being near maximal, did not stimulate increased basolateral HCO_3^- influx. This would therefore increase the difference between apical HCO_3^- efflux and basolateral HCO_3^- influx in response to cAMP stimulation and thus cause a greater intracellular acidification to occur. How hypercapnia activates NBC activity could be explained by the apparent reduction in WNK4 expression observed under basal, hypercapnic conditions as measured by Western blot. WNK4, together with SPAK, have been implicated in reducing surface expression of NBCe1 in pancreatic duct cells and thus a CO_2 -induced reduction in WNK-4 would alleviate this inhibitory effect of WNK-4/SPAK signalling increasing NBC activity. However, more repeats of the Western blot need to be performed before it can be concluded this is a real effect of hypercapnia in Calu-3 cells.

An alternative hypothesis to explain the effect of acute hypercapnia on the forskolin-stimulated intracellular acidification could be provided by the effect of ouabain. Ouabain had two major effects in Calu-3 cells; (i) it blocked the effect of acute hypercapnia on the forskolin-stimulated intracellular acidification and (ii) it prevented pH_i recovery from CO_2 -induced acidosis. These findings suggest that Na^+/K^+ -ATPase may be CO_2 sensitive, a finding which has already been reported in rat alveolar type II cells (Briva *et al.*, 2007). How Na^+/K^+ -ATPase may contribute to pH changes within Calu-3 cells could be explained by recent work by Vedovato and Gadsby (2014). Here, researchers demonstrated Na^+/K^+ -ATPase can act as a H^+ importer, with H^+ replacing a K^+ during the pump cycle. Therefore, CO_2 may uncouple the Na^+/K^+ -ATPase to increase H^+ influx across the basolateral membrane and therefore produce the greater intracellular acidification observed and hence explain why ouabain is able to block the CO_2 effect. Several studies have implicated that cAMP regulates Na^+/K^+ -ATPase activity with Dagenais *et al.* (2001), Bertorello *et al.* (1999) and Suzuki *et al.* (1995), demonstrating elevations in $[\text{cAMP}]_i$ activated Na^+/K^+ -ATPase in rat ATII cells due to an increased insertion of the α subunit at the basolateral membrane whilst Carranza *et al.* (1996) showed forskolin and db-cAMP activated Na^+/K^+ -ATPase in a PKA-dependent manner. Thus, if CO_2 is able to modulate Na^+/K^+ -ATPase activity, it would appear to be independent of its effects on $[\text{cAMP}]_i$. Vadasz *et al.* (2008), demonstrated that CO_2 inhibited Na^+/K^+ -ATPase in rat ATII cells *via* a mechanism involving AMPK but this does not appear to underlie the effect of hypercapnia in Calu-3 cells given the lack of effect of AMPK inhibition.

Ouabain also prevented pH_i recovery from CO_2 -induced acidosis, likely due to the fact that inhibition of Na^+/K^+ -ATPase would abolish the inward Na^+ gradient required to maintain NBC activity. It is interesting that two pharmacological agents that blocked pH_i recovery, ouabain and MK-571, also blocked the effect of hypercapnia on the forskolin-stimulated intracellular acidification suggesting that the transporters involved in pH_i recovery also underlie the effect of hypercapnia on the forskolin-stimulated intracellular acidification. Thus, prevention of CO_2 -induced upregulation of basal NBC activity without activation of CFTR-dependent HCO_3^- efflux, either by ouabain (due to an abolishment of the basolateral inward Na^+ gradient) or MK-571 (due to elevated $[\text{cAMP}]_i$ activating NBC and CFTR simultaneously) blocks the effect of hypercapnia on the forskolin-stimulated intracellular acidification and suggests this process plays a major role in the effect of acute hypercapnia on cAMP-regulated HCO_3^- transport in Calu-3 cells.

The roles of other basolateral transporters in mediating the effect of hypercapnia were also assessed. Although AE2 activity was reduced by hypercapnia in basal conditions, the fact that hypercapnia was unable to relieve the cAMP-induced inhibition of AE2 suggests that hypercapnia was not able to reduce forskolin-stimulated cAMP levels to the extent required for inhibition to be reversed. As a consequence, AE2 can be eliminated from having any contribution to the effects of hypercapnia on cAMP-regulated HCO_3^- transport. Similarly, inhibition of both NHE and NKCC1 did not affect the response to hypercapnia suggesting that hypercapnia was not modulating H^+ transport *via* NHE or having indirect effects on other HCO_3^- transporters by altering intracellular Na^+ , K^+ or Cl^- concentrations.

3.15.2. CO_2 exhibits differential effects on cAMP-elevating agonists

To further understand the mechanism of CO_2 modulation of cAMP signalling, Calu-3 cells were stimulated with agents that increase cAMP independently of tmAC. Hypercapnia had no effect on IBMX-induced intracellular acidification yet was able to augment dibutyryl-cAMP stimulated intracellular acidification. The absence of an effect of hypercapnia when cAMP levels are raised by inhibition of phosphodiesterases suggested that CO_2 does not reduce $[\text{cAMP}]_i$ by increasing its breakdown and therefore appeared to target cAMP production *via* tmACs. However, the effect of CO_2 on db-cAMP-stimulated intracellular acidification also suggested that CO_2 could modulate cAMP signalling independent of tmAC yet how this occurs is still unclear. One possible explanation could be *via* effects on MRPs. The MRP

inhibitor, MK-571, blocked the effect of hypercapnia on cAMP-regulated HCO_3^- transport and raised the intriguing possibility that hypercapnia reduced intracellular cAMP by activating MRP-mediated cAMP efflux as opposed to inhibition on tmAC. Thus preventing this reduction in $[\text{cAMP}]_i$ in hypercapnia maintained the activity of cAMP-regulated HCO_3^- transporters. Li *et al.* (2007) have described that MK-571 reduced cAMP efflux in gut epithelia and was able to significantly increase glybenclamide-sensitive I_{sc} measurements implying prevention of cAMP efflux *via* MRPs is important in regulation of CFTR-dependent anion secretion. Only apical MK-571 was able to block the effect of hypercapnia, implying that any putative CO_2 -sensitive MRPs were located at the apical membrane and may explain why only apical CO_2 modulates cAMP-regulated HCO_3^- transport. In an attempt to quantify MRP activity in normocapnia and hypercapnia, the rate of MRP-dependent efflux of the fluorescent metabolite of CMFDA, GSMF was measured in Calu-3 cells. Although the rate of dye efflux was not statistically significant between normocapnic and hypercapnic conditions, there did appear to be a small trend for hypercapnia to increase MRP activity, consistent with a CO_2 -induced activation of MRP-dependent cAMP efflux. Another aspect of cAMP signalling which was investigated was its dependence on compartmentalization. Latrunculin B and cytochalasin D, two pharmacological agents that disrupt F-actin polymerization and therefore predicted to disrupt organization of the actin cytoskeleton, were found to significantly reduce TEER suggesting these agents affected actin sufficiently to modulate tight junction properties. Furthermore, confocal images revealed a pronounced effect of cytochalasin D on the organization of the actin cytoskeleton. However, neither drug was able to prevent the effect of acute hypercapnia on cAMP-regulated HCO_3^- transport. Given that forskolin still elicited an intracellular acidification suggested that cAMP compartmentalization wasn't necessary in order to produce this response. This is somewhat surprising if you consider that Monterisi *et al.* (2012) demonstrated latrunculin B significantly reduced cAMP-stimulated CFTR activity in HBE cells and perhaps suggests that (i) important differences in actin cytoskeleton organization exist between Calu-3 cells and HBE cells or (ii) forskolin is able to raise $[\text{cAMP}]_i$ to such an extent that even a reduction in cAMP in specific microdomains is not sufficient to reduce the activity of cAMP-regulated transporters. In a similar vein, although acute hypercapnia reduced total $[\text{cAMP}]_i$, the fact that cytochalasin D or latrunculin B were unable to block the effect of acute hypercapnia on cAMP-regulated HCO_3^- transport would suggest CO_2 does not mediate its effects *via* disruption of the actin cytoskeleton. Further investigations into the effects of hypercapnia on cAMP signalling, in particular cAMP compartmentalization and whether hypercapnia only

modulates $[cAMP]_i$ at specific microdomains, could involve performing FRET analysis, a powerful microscopy technique to assess the relative levels of labelled molecules in different cellular regions.

The major findings of this chapter are summarized below and in figure 3.48.

- Acute hypercapnia induced an intracellular acidosis in Calu-3 cells which activated Na^+ -dependent HCO_3^- influx to recover pH_i
- Acute hypercapnia significantly attenuated forskolin-stimulated increases in intracellular cAMP and reduced CFTR-dependent electrogenic anion secretion.
- CO_2 -induced reductions in cAMP may be due to effects on tmAC activity *per se* and/or CO_2 may activate cAMP efflux *via* apically located MRPs.
- Acute apical hypercapnia modulated cAMP-stimulated, CFTR-dependent HCO_3^- transport in Calu-3 cells which is not due to an effect on cAMP-regulated HCO_3^- transporters but instead appeared to be mediated *via* an upregulation of basal NBC activity and/or activation of Na^+/K^+ -ATPase-dependent H^+ import.
- CO_2 upregulated NBC activity was due to an apparent reduction in WNK4 levels, thus reducing WNK4-mediated downregulation of NBCe1.

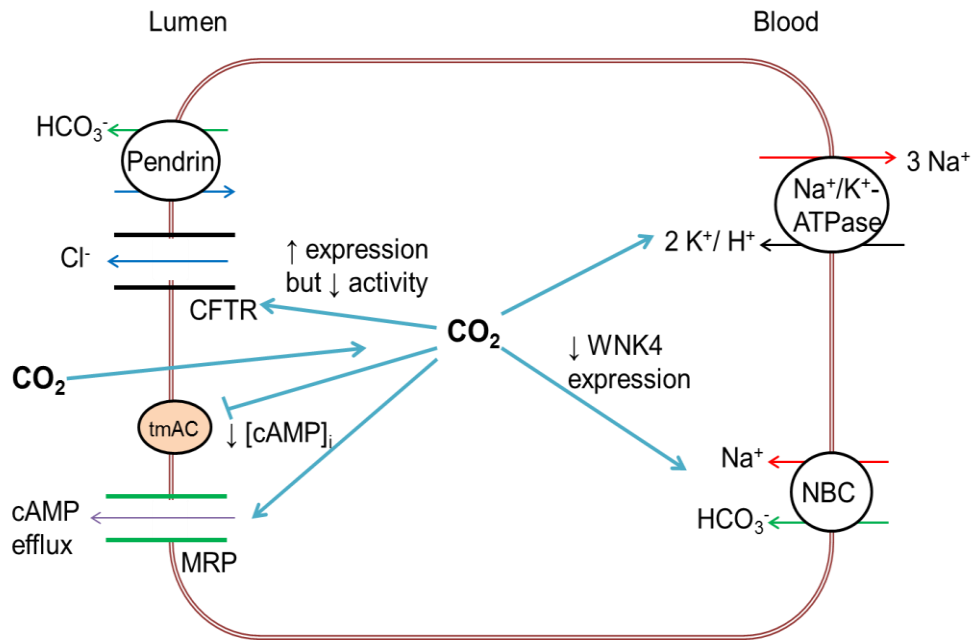


Figure 3.48. Major effects of acute hypercapnia on cAMP-dependent HCO_3^- transport in Calu-3 cells. Apical CO_2 enters the cell and is able to modulate intracellular cAMP levels $[\text{cAMP}]_i$ due to a reduction in tmAC activity and/or an increased efflux of cAMP *via* MRPs. This reduction in $[\text{cAMP}]_i$ reduces CFTR-dependent anion secretion. CO_2 also appears to reduce WNK4 expression to activate NBC under basal conditions to stimulate pH_i recovery from CO_2 -induced acidosis as well as increasing Na^+/K^+ -ATPase activity to increase H^+ influx.

Chapter 4: The role of Ca²⁺/ATP signalling in underlying the effects of hypercapnia

4.1. Introduction

As shown in chapter 3, acute hypercapnia modulated forskolin-stimulated increases in intracellular cAMP as well as reduced CFTR-dependent anion secretion in Calu-3 cells. The data suggested CO₂ reduced intracellular cAMP due to effects on tmAC activity *per se* and/or cAMP transport through multidrug resistance proteins (MRPs). The aim of this chapter was to ascertain whether hypercapnia was also modulating other cell signalling cascades to contribute to, or underlie, the effects of hypercapnia on cAMP signalling with particular focus on the role of Ca²⁺ signalling. Crosstalk between cAMP and Ca²⁺ signalling has been well described for the regulation of CFTR activity in airway epithelia (Lee and Foskett, 2010) and investigations into the molecular mechanisms behind cAMP and Ca²⁺ crosstalk have provided some very interesting data. Tovey *et al.* (2010) showed cAMP to increase the sensitivity of IP₃ receptors to IP₃ in HEK cells, allowing cAMP agonists to potentiate the Ca²⁺ release induced by the Ca²⁺ elevating agonist carbachol. Recently, work from Aldebaran Hofer's laboratory has described a STIM-1 dependent increase in cAMP levels in response to depletion of Ca²⁺ stores from the endoplasmic reticulum (ER). They describe this phenomenon as store operated cAMP signalling (socAMPs) and believe STIM-1 may be able to activate adenylyl cyclase 3 in certain cell types (Lefkimmiatis *et al.*, 2009; Maiellaro *et al.*, 2012). Schwarzer *et al.* (2010) believe socAMPs underlies the activation of CFTR-dependent Cl⁻ secretion in Calu-3 cells by a molecule secreted from *Pseudomonas aeruginosa*. Conversely, Jiang *et al.* (2011) have shown that trichosanthin-induced elevations in [Ca²⁺]_i decrease [cAMP]_i in HeLa cells due to an inhibition of adenylyl cyclases. Finally, our laboratory has also published data implicating a CO₂-induced, IP₃-dependent Ca²⁺ release was required for alterations to cAMP-dependent regulation of NHE3 in renal cells (Cook *et al.*, 2012). Therefore it was important to assess the relationship between hypercapnia, Ca²⁺ signalling and cAMP-dependent HCO₃⁻ transport in Calu-3 cells.

4.2. The role of Ca^{2+} signalling in response to hypercapnia

4.2.1. Inhibition of intracellular Ca^{2+} signalling

It has been reported that elevated CO_2 can affect $[\text{Ca}^{2+}]_i$, with both Briva *et al.* (2011) and Bouyer *et al.* (2003) showing hypercapnia caused an increase in $[\text{Ca}^{2+}]_i$ in epithelial cells. Furthermore, our laboratory has shown that acute hypercapnia reduced intracellular cAMP levels in renal epithelia through a mechanism involving CO_2 -induced IP_3 -dependent Ca^{2+} release (Cook *et al.*, 2012). Therefore, it was important to assess whether the CO_2 -induced changes to cAMP-regulated HCO_3^- transport I have demonstrated were dependent on changes in $[\text{Ca}^{2+}]_i$. In order to do this, cells were preincubated for one hour with the Ca^{2+} chelator BAPTA-AM and the responses to forskolin in both normocapnia and hypercapnia assessed and compared to control experiments performed on the same day. Figure 4.01A shows a representative experiment of BAPTA-AM treated cells. In control experiments, hypercapnia increased the magnitude of the forskolin-stimulated intracellular acidification 1.5 ± 0.1 fold ($p < 0.05$; $n=5$; fig. 4.01B) and increased the rate of forskolin-stimulated HCO_3^- flux 3.3 ± 0.2 fold ($p < 0.05$; $n=5$; fig. 4.01C). However, in BAPTA-AM treated cells, the effect of hypercapnia was abolished. In these experiments, hypercapnia increased the magnitude of the forskolin-stimulated intracellular acidification 1.0 ± 0.1 fold ($p > 0.05$; $n=5$; fig. 4.01B) and increased the rate of forskolin-stimulated HCO_3^- flux 1.5 ± 0.3 fold ($p > 0.05$; $n=5$; fig. 4.01C). In addition, BAPTA-AM was also found to prevent the effect of acute hypercapnia on $[\text{cAMP}]_i$ (fig. 4.01D). Together, these data implied that alterations in intracellular Ca^{2+} were required in order for hypercapnia to mediate its effects on cAMP-regulated HCO_3^- transport in Calu-3 cells. In addition, figure 4.01A clearly shows that BAPTA-AM loaded cells were only able to partially recover their pH_i after CO_2 -induced acidosis (recovery = $36.9 \pm 6.8\%$; $p < 0.001$; $n=5$; fig. 4.07) implying that intracellular Ca^{2+} appears to be important for the regulation of pH_i recovery.

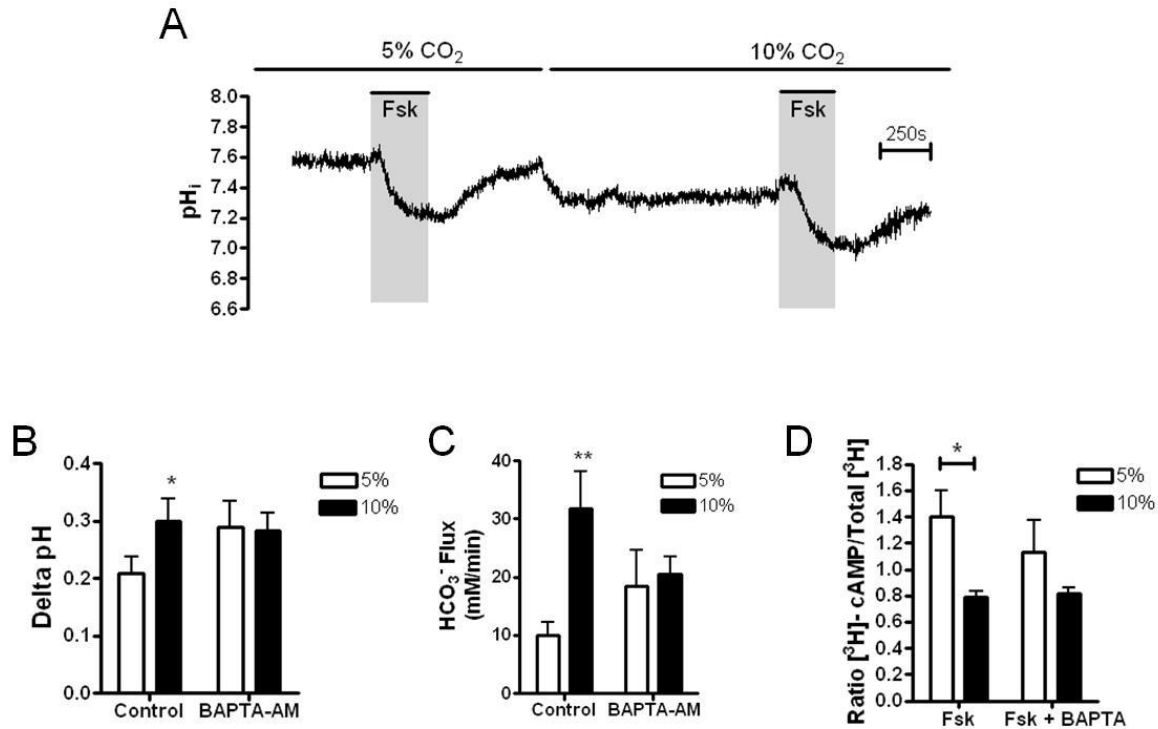


Figure 4.01. Preincubation of cells with BAPTA-AM blocks the effect of hypercapnia on the forskolin-stimulated intracellular acidification. (A) shows a representative experiment in which Calu-3 cells were preincubated with 50 μ M BAPTA-AM for one hour and the response to 5 μ M forskolin was assessed in normocapnia and hypercapnia. The delta pH (B) and HCO₃⁻ flux (C) resulting from forskolin stimulation are summarized. * = significant effect of hypercapnia ($p < 0.05$; ** = $p < 0.01$). Data represents mean \pm S.E.M.; $n = 5$ for each. (D) summarizes the effect of acute hypercapnia on forskolin-stimulated intracellular cAMP levels +/- BAPTA-AM (50 μ M). * = significant effect of hypercapnia ($p < 0.05$). Data represents mean \pm S.E.M; $n = 3$ for each.

As our group have already shown that hypercapnia was able to modulate IP₃-mediated Ca²⁺ release (Cook *et al.*, 2012), the effect of the phospholipase C (PLC) inhibitor U73122 (Bleasdale *et al.*, 1990) was assessed. Activation of PLC allows phosphatidylinositol 4,5-bisphosphate (PIP₂) to be hydrolysed into diacylglycerol (DAG) and IP₃ whereupon IP₃ can bind to IP₃ receptors on the ER to trigger Ca²⁺ release. Therefore, should CO₂ mediate its effects on cAMP-regulated HCO₃⁻ transport *via* modulation of the PLC/IP₃ signalling pathway, inhibition of PLC should prevent the effect of hypercapnia. Calu-3 cells were preincubated for one hour with U73122 and perfused with U73122 for the duration of the experiment (fig. 4.02A). The responses to forskolin in normocapnia and hypercapnia were measured and compared to control experiments performed on the same day. In control experiments, hypercapnia induced a 1.6 ± 0.1 fold increase in the magnitude of the forskolin-

stimulated intracellular acidification ($p < 0.05$; $n = 3$; fig. 4.2B) and a 2.3 ± 0.5 fold increase in the rate of forskolin-stimulated HCO_3^- flux ($p < 0.05$; $n = 3$; fig. 4.2C). However, in U73122-treated cells, hypercapnia only increased the magnitude and rate of forskolin-stimulated HCO_3^- flux 1.3 ± 0.3 fold ($p > 0.05$; $n = 3$; fig. 4.2B) and 1.5 ± 0.7 fold ($p > 0.05$; $n = 3$; fig. 4.2C) respectively. These findings implied that increases in Ca^{2+} , *via* IP_3 mediated Ca^{2+} release, were important for the effects of hypercapnia on cAMP signalling in Calu-3 cells. Interestingly, treatment with U73122 also affected pH_i recovery, with cells only recovering pH_i by $24.2 \pm 9.0\%$ after CO_2 -induced acidosis ($p < 0.001$; $n = 3$; fig. 4.7). These findings are similar to those observed in BAPTA-AM loaded cells and imply that the pH_i recovery was dependent on Ca^{2+} mobilization *via* activation of the PLC signalling pathway.

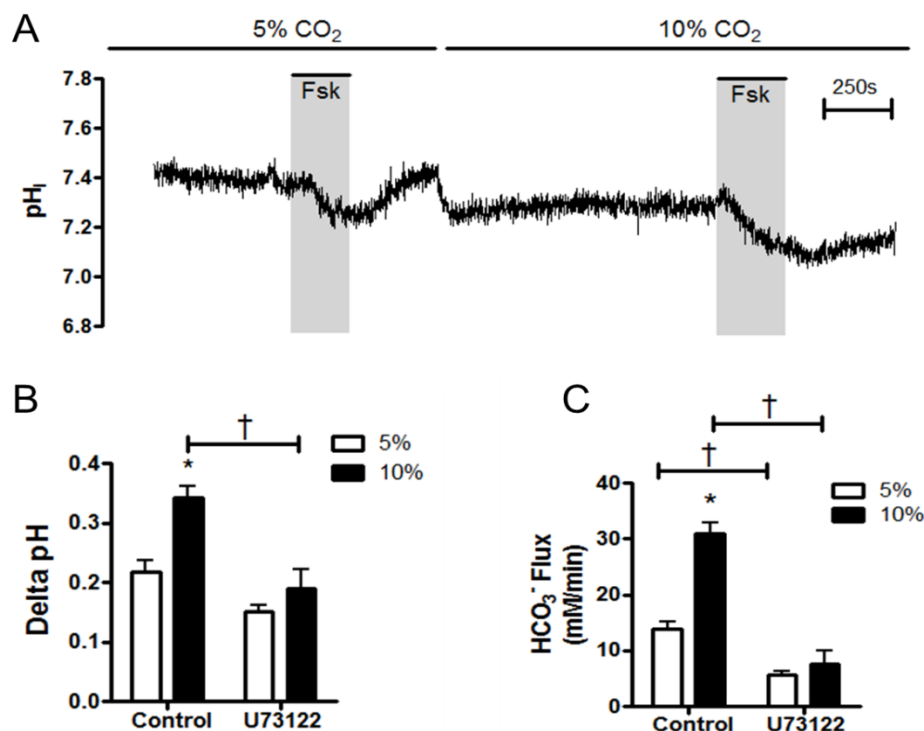


Figure 4.02: Inhibition of phospholipase C blocks the effect of hypercapnia on the forskolin-stimulated intracellular acidification. Calu-3 cells were preincubated for one hour and perfused with the PLC inhibitor U73122 (10 μ M) and the response to 5 μ M forskolin was assessed in normocapnia and hypercapnia as shown in (A). The delta pH (B) and HCO_3^- flux (C) resulting from forskolin stimulation are summarized. * = significant effect of hypercapnia ($p < 0.05$); † = significant effect of U73122 ($p < 0.01$). Data represents mean \pm S.E.M.; $n = 3$ for each.

Given that both BAPTA-AM and U73122 prevented the effect of hypercapnia on cAMP-regulated HCO_3^- transport suggested that the effect of hypercapnia involved IP_3 -dependent Ca^{2+} release. To further investigate whether this was the case, the effect of the IP_3 R inhibitor 2-APB (Maruyama *et al.*, 1997) was assessed. Peppiatt *et al.* (2003) demonstrated that 2-APB inhibited histamine-induced increases in cytosolic Ca^{2+} in HeLa cells but that the effect of 2-APB was poorly reversible. As a result, the effects of 2-APB in normocapnia and hypercapnia were assessed in separate experiments to negate the irreversible nature of 2-APB influencing the results. Figures 4.03A and B show representative experiments demonstrating the effects of 2-APB on the forskolin-stimulated intracellular acidification in normocapnia and hypercapnia respectively. In normocapnia, forskolin stimulated a HCO_3^- flux of $9.3 \pm 1.5 \text{ mM HCO}_3^- \text{ min}^{-1}$ (n=4) but this was reduced to $5.7 \pm 1.4 \text{ mM HCO}_3^- \text{ min}^{-1}$ (n=4) by 2-APB which although was calculated as a $37.6 \pm 12.1\%$ inhibition in HCO_3^- flux, was statistically not significant ($p > 0.05$; n=4). In hypercapnia, forskolin stimulated a HCO_3^- flux of $42.0 \pm 10.7 \text{ mM HCO}_3^- \text{ min}^{-1}$ (n=4) but this was reduced to $16.6 \pm 1.3 \text{ mM HCO}_3^- \text{ min}^{-1}$ by 2-APB (n=4) which was calculated as a $53.7 \pm 9.5\%$ inhibition ($p < 0.05$; n=4). Although the extent of the inhibition by 2-APB was not statistically significantly different between normocapnia and hypercapnia ($p > 0.05$), when assessing the fold changes in the rate of forskolin-stimulated HCO_3^- flux, figure 4.03E shows that, in control conditions, acute hypercapnia caused a 4.5 ± 0.8 fold increase in the rate of forskolin-stimulated HCO_3^- flux ($p < 0.01$; n=4), but in the presence of 2-APB, this fold increase in rate of HCO_3^- flux was significantly reduced to 1.9 ± 0.3 ($p < 0.05$; n=4). In addition, 2-APB also blocked the effect of acute hypercapnia on forskolin-stimulated intracellular cAMP levels (fig. 4.03F). Therefore, these findings show that 2-APB is able to block the effects of hypercapnia on cAMP-regulated HCO_3^- transport and supports previous findings from BAPTA-AM and U73122 experiments that implicate IP_3 -dependent Ca^{2+} release is required to produce the effects of acute hypercapnia.

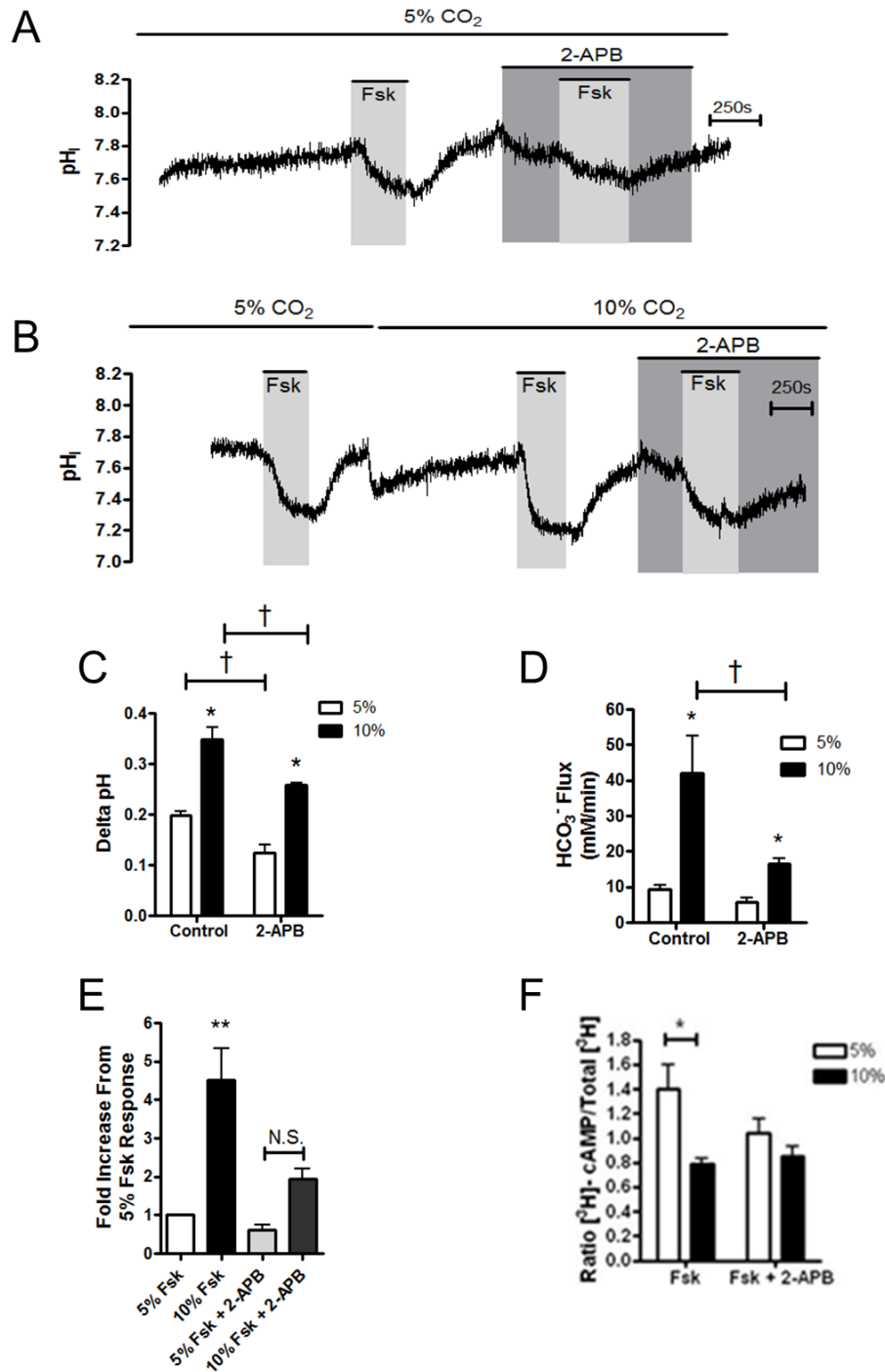


Figure 4.03: 2-APB blocks the effect of acute hypercapnia on the forskolin-stimulated intracellular acidification. (A) and (B) show representative experiments in which the effect of 2-APB (100μM) on the response to stimulation by forskolin (5μM) was assessed in normocapnia and hypercapnia respectively. The delta pH (C) and HCO₃⁻ flux (D) resulting from forskolin stimulation are summarized. (E) summarizes the effect of 2-APB on the fold increase in the rate of forskolin-stimulated HCO₃⁻ flux by acute hypercapnia. * = significant effect of hypercapnia (p<0.05; ** = p<0.01). † = significant effect of 2-APB (p<0.05). Data represents mean ± S.E.M.; n=4 for each. (F) displays the effect of acute hypercapnia on forskolin-stimulated intracellular cAMP levels +/- 2-APB (100μM). * = significant effect of hypercapnia (p<0.05). Data represents mean ± S.E.M., n=3 for each.

One potential important player in CO₂-induced changes in cAMP-stimulated HCO₃⁻ transport could be the IP₃R binding protein released with IP₃ (IRBIT). As its name suggests, IRBIT, when phosphorylated, binds to IP₃ receptors and outcompetes IP₃ binding in non-stimulated states. Elevations in IP₃ displace IRBIT, allowing for IP₃-dependent release from IP₃Rs of the ER (Ando *et al.*, 2003; Yang *et al.*, 2011b). The free IRBIT has then been shown to have major roles in regulating HCO₃⁻ secretion. Yang *et al.* (2009) demonstrated that IRBIT activated both NBCe1 and CFTR in mouse pancreatic duct cells to coordinate the secretion of HCO₃⁻. IRBIT KD cells displayed a significant reduction in NBCe1 and CFTR activity. Furthermore, Hong *et al.* (2013) have suggested that PIP₂-induced activation of NBCe1 is not only the result of IP₃-dependent Ca²⁺ release increasing Ca²⁺-dependent kinase phosphorylation of NBCe1, but also due to the increased concentration of cytosolic IRBIT able to modulate NBCe1 activity. Thus, it is apparent that IRBIT may have a major role in cAMP-regulated HCO₃⁻ transport should CO₂ mediate its effects *via* the elevation of IP₃/Ca²⁺. Therefore, the effect of hypercapnia on IRBIT and phosphorylated IRBIT was assessed by a Western Blot. The expression of IRBIT and p-IRBIT normalized to β-actin expression is shown in figure 4.04. Although only representative of n=2 experiments, it appeared that hypercapnia had no effect on IRBIT expression but it did induce a reduction in the amount of phosphorylated IRBIT. Therefore, these data suggested that hypercapnia may reduce the amount of IRBIT bound to the IP₃ receptor, possibly because hypercapnia had induced elevations in intracellular IP₃. Thus, these findings would support the notion that raised CO₂ induced IP₃-dependent Ca²⁺ release present in Calu-3 cells which acts to modulate cAMP-regulated HCO₃⁻ transport.

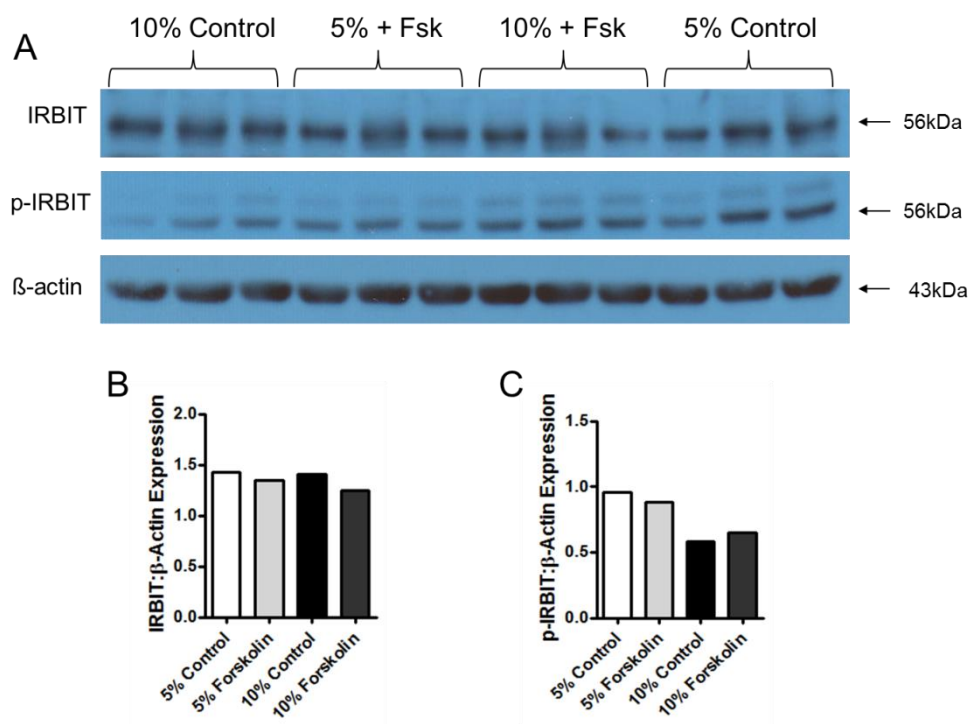


Figure 4.04: Acute hypercapnia reduces p-IRBIT expression in Calu-3 cells. (A) shows the results from a Western Blot in which the effect of forskolin (5 μ M) and acute hypercapnia on the expression of IRBIT and phosphorylated IRBIT (p-IRBIT) was assessed normalized to expression of β -actin. The data for IRBIT and p-IRBIT are summarized in (B) and (C) respectively. For each experimental condition, 3 lysates were generated from 3 separate transwells. Data represents mean of triplicate samples performed on n=2 independent samples. The protein extraction was carried out by myself but the Western Blots were performed in the laboratory of Professor Ursula Seidler, Hannover, Germany.

Currently, the data suggests that hypercapnia utilized intracellular Ca^{2+} signalling to mediate its effects on cAMP-regulated HCO_3^- transport. To assess whether this apparent effect of hypercapnia was linked to activation of downstream targets of Ca^{2+} , cells were preincubated for one hour with the CaM Kinase Kinase (CaMKK) inhibitor STO-609. CaMKK is activated by binding of the Ca^{2+} /calmodulin complex and is therefore activated in response to increases in cytosolic Ca^{2+} . An example experiment is shown in figure 4.05A. In control experiments, hypercapnia induced a 2.5 ± 0.3 fold increase in the magnitude of the forskolin-stimulated intracellular acidification ($p < 0.05$; $n=3$; fig. 4.05B) and a 4.4 ± 1.7 fold increase in the rate of forskolin-stimulated HCO_3^- flux ($p < 0.05$; $n=3$; fig. 4.05C). This effect of hypercapnia remained in STO-609 treated cells. Here, hypercapnia increased the magnitude of the forskolin-stimulated intracellular acidification and rate of forskolin-stimulated HCO_3^- flux 2.9 ± 0.4 fold ($p < 0.05$; $n=3$; fig. 4.05B) and 9.5 ± 3.7 fold ($p < 0.05$; $n=3$; fig. 4.05C) respectively. Therefore, CO_2 does not mediate its effects by a Ca^{2+} -dependent activation of CaMKK and

suggested that the role of Ca^{2+} is to either activate other downstream targets or directly influence cAMP signalling itself.

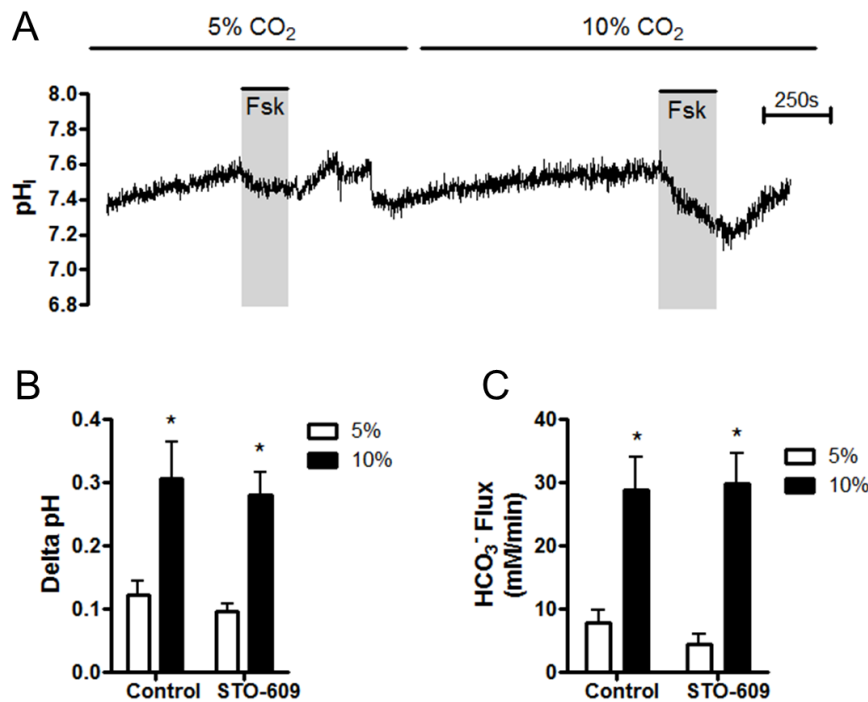


Figure 4.05: Inhibition of CaM Kinase Kinase does not block the effect of hypercapnia. (A) shows a representative experiment in which Calu-3 cells were preincubated for one hour with the CaM Kinase Kinase inhibitor STO-693 (20 μM) and the response to 5 μM forskolin was assessed in normocapnia and hypercapnia. The delta pH (B) and HCO_3^- flux (C) resulting from forskolin stimulation are summarized. * = significant effect of hypercapnia ($p < 0.05$). Data represents mean \pm S.E.M.; $n=3$ for each

The current data suggested that hypercapnia mediated its effects on cAMP-regulated HCO_3^- transport via an IP_3 -dependent Ca^{2+} release. IP_3 -dependent increases in Ca^{2+} are caused by Ca^{2+} release from the ER and, as such, depletion of the ER Ca^{2+} stores would be predicted to eliminate the CO_2 effect. Therefore, intracellular ER Ca^{2+} stores were depleted by exposing the cells to 200nM thapsigargin, a sarco/endoplasmic reticulum calcium ATP-ase (SERCA) inhibitor, whilst perfusing cells with a Ca^{2+} -free Krebs solution in which CaCl_2 was replaced with MgCl_2 and 0.5mM EGTA added to chelate any remaining Ca^{2+} . Measurements of intracellular Ca^{2+} in Calu-3 cells reveal that, in these conditions, exposing cells to 200nM thapsigargin in the absence of extracellular Ca^{2+} depletes $[\text{Ca}^{2+}]_i$ causes an initial increase in $[\text{Ca}^{2+}]_i$ due to an inhibition of Ca^{2+} reuptake into the ER. However, as $[\text{Ca}^{2+}]_i$ increase, Ca^{2+} leaves the cell along its concentration gradient and, consequentially, $[\text{Ca}^{2+}]_i$ decreases (see

fig. 4.09A). An example pH_i experiment is shown in figure 4.06A. In control experiments performed on the same day, hypercapnia increased the magnitude of the forskolin-stimulated intracellular acidification 2.0 ± 0.3 fold ($p < 0.05$; $n = 4$; fig. 4.06B) and increased the rate of forskolin-stimulated HCO_3^- flux 2.7 ± 0.5 fold ($p < 0.05$; $n = 4$; fig. 4.06C). In cells pre-treated with thapsigargin and perfused with a Ca^{2+} free Krebs solution, hypercapnia increased the magnitude of the forskolin-stimulated intracellular acidification 1.7 ± 0.1 fold ($p < 0.05$; $n = 4$; fig. 4.06B) and increased the rate of forskolin-stimulated HCO_3^- flux 2.8 ± 0.3 fold ($p < 0.01$; $n = 4$; fig. 4.06C). Therefore, these data suggest that if CO_2 does modulate intracellular Ca^{2+} , this is through a thapsigargin-insensitive store. Another interesting finding of these experiments was that intracellular Ca^{2+} depleted cells only exhibited a $25.2 \pm 8.1\%$ in pH_i recovery from CO_2 -induced acidosis ($p < 0.001$; $n = 4$; fig. 4.08). These findings support the results from BAPTA-AM and U73122 treated cells and provide further evidence of a Ca^{2+} -dependence to the pH_i recovery observed after CO_2 -induced acidosis.

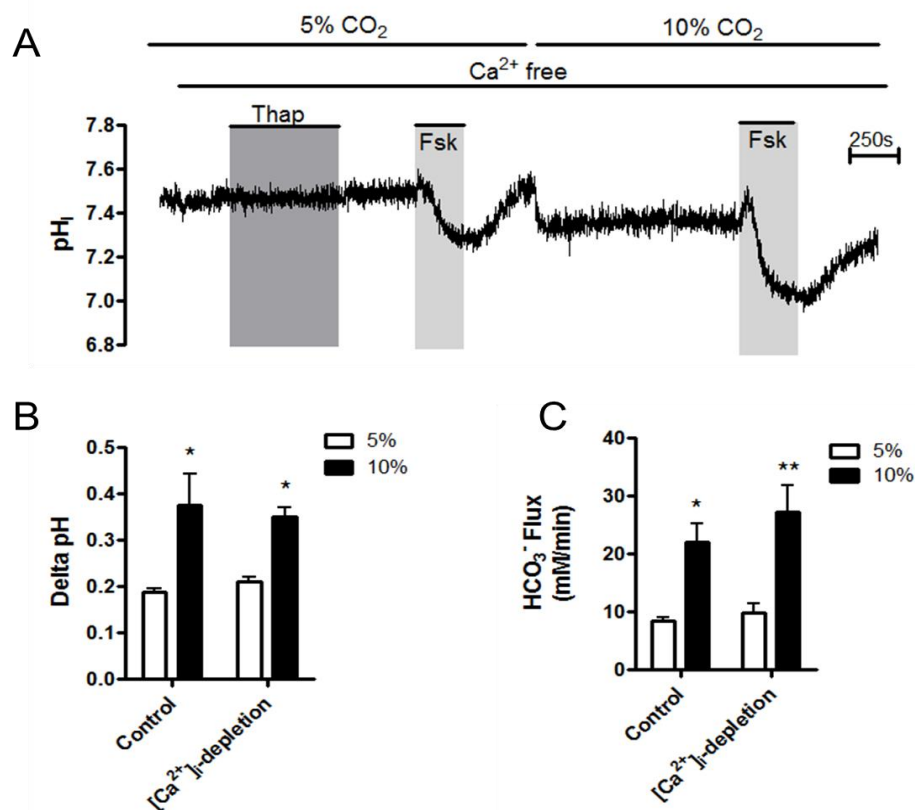


Figure 4.06: Depletion of intracellular Ca^{2+} does not alter the effect of hypercapnia. (A) shows a representative experiment in which Calu-3 cells were treated with 200nM thapsigargin whilst being perfused with Ca^{2+} free solution to deplete intracellular Ca^{2+} stores and the response to 5 μM forskolin was assessed in normocapnia and hypercapnia. The delta pH (B) and HCO_3^- flux (C) resulting from forskolin stimulation are summarized. * = significant effect of hypercapnia ($p < 0.05$; ** = $p < 0.01$). Data represents mean \pm S.E.M.; $n = 4$ for each.

Although in the previous set of experiments, cells had been perfused with a Ca^{2+} free solution, these experiments were designed to test the effect of depletion of intracellular Ca^{2+} stores rather than study the effects of extracellular Ca^{2+} *per se*. Therefore, it was of interest to test the effect of removal of external Ca^{2+} without thapsigargin treatment to determine whether CO_2 was able to modulate intracellular Ca^{2+} without extracellular Ca^{2+} . Cells were perfused with a Ca^{2+} -free solution containing 0.5mM EGTA and stimulated with forskolin in normocapnia and hypercapnia as shown in figure 4.07A. In control experiments performed on the same day, hypercapnia increased the magnitude of the forskolin-stimulated intracellular acidification 1.5 ± 0.1 fold ($p < 0.05$; $n=3$; fig. 4.07B). However, due to large variability on the day, the 2.2 ± 0.4 fold increase in the rate of forskolin-stimulated HCO_3^- flux in hypercapnia was not statistically significant although a clear trend existed ($p > 0.05$; $n=3$; fig. 4.07C). This was also the case when external Ca^{2+} was removed. Hypercapnia increased the magnitude of the forskolin-stimulated intracellular acidification fold 1.3 ± 0.1 ($p < 0.05$; $n=3$; fig. 4.07B) but again, due to large variability, the 2.1 ± 0.6 fold increase in the rate of forskolin-stimulated HCO_3^- flux in hypercapnia was not statistically significant although a clear trend did exist ($p > 0.05$; $n=3$; fig. 4.07C). Therefore, although it cannot be conclusively deduced that external Ca^{2+} has no role in mediating the effects of hypercapnia, the trend for hypercapnia to still increase forskolin-stimulated intracellular acidification in Ca^{2+} free conditions does suggest this to be the case. Consistent with a role for Ca^{2+} in mediating pH_i recovery from CO_2 -induced acidosis, removal of extracellular Ca^{2+} caused cells to only exhibit a $36.8 \pm 10.7\%$ in pH_i recovery ($p < 0.001$; $n=3$; fig. 4.08) suggesting that both extracellular and intracellular Ca^{2+} are important for the pH_i recovery process.

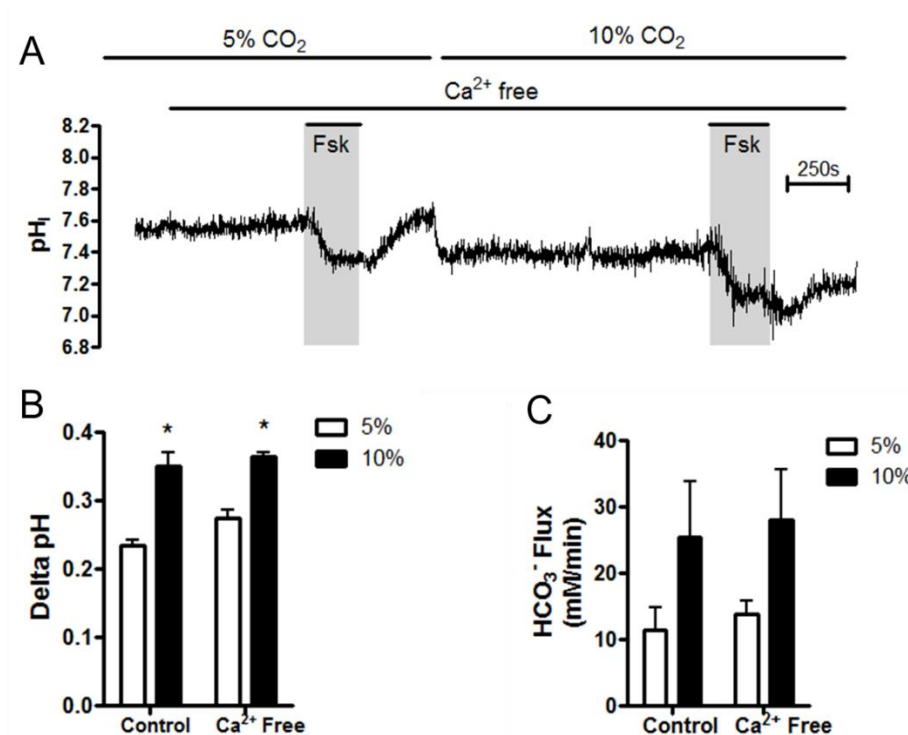


Figure 4.07: Removal of extracellular Ca^{2+} does not alter the effect of hypercapnia on the forskolin-stimulated intracellular acidification. (A) shows a representative experiment in which Calu-3 cells were perfused with a Ca^{2+} free solution and the response to 5 μ M forskolin was assessed in normocapnia and hypercapnia. The ΔpH (B) and HCO_3^- flux (C) resulting from forskolin stimulation are summarized. * = significant effect of hypercapnia ($p < 0.05$). Data represents mean \pm S.E.M.; $n=3$ for each.

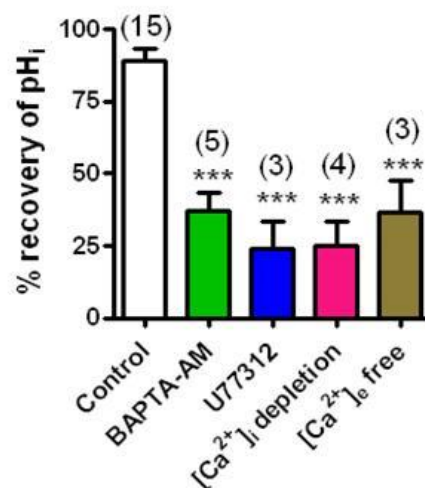
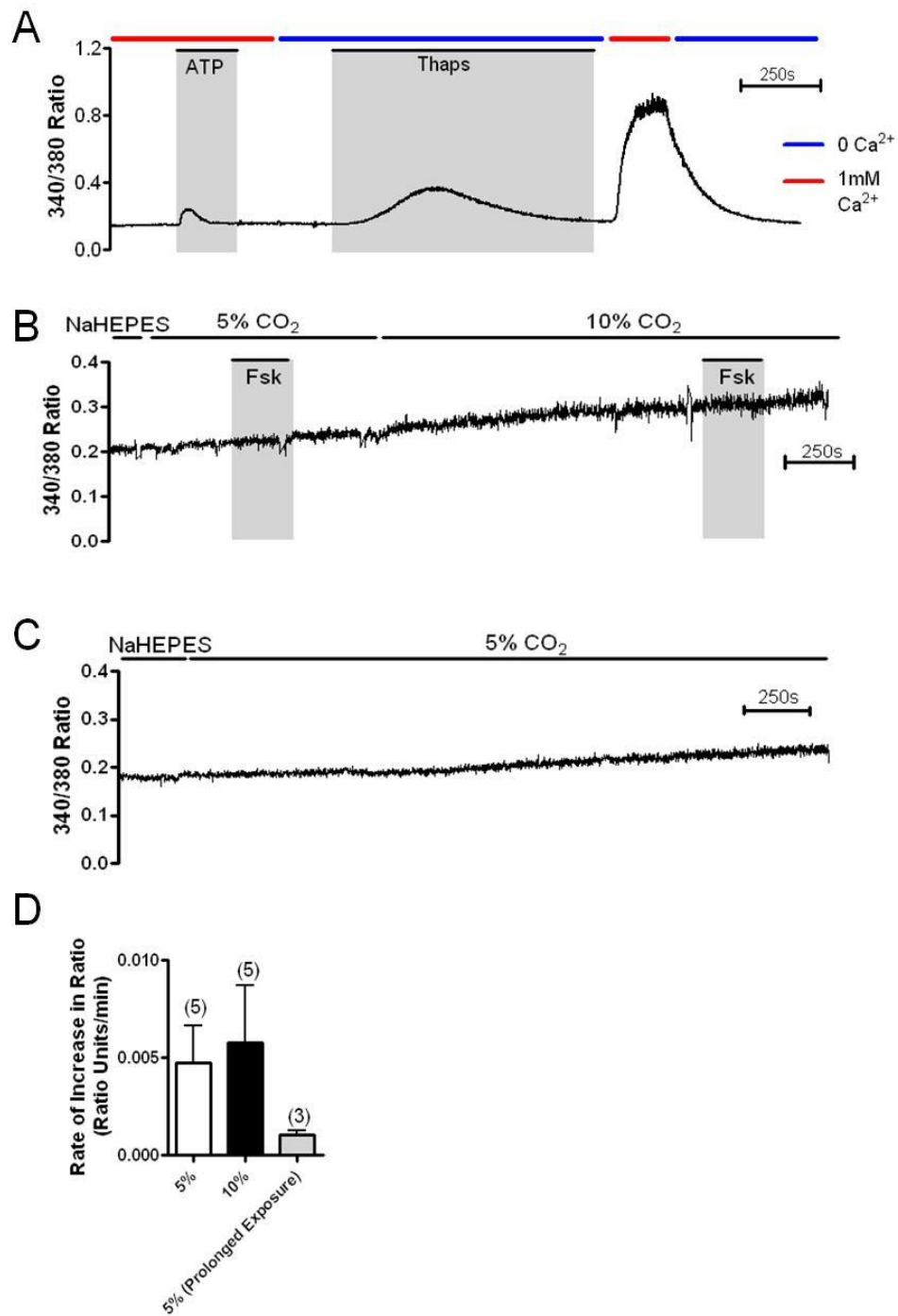


Figure 4.08: Ca^{2+} plays a role in mediating the intracellular pH recovery in response to CO_2 -induced acidosis. % recovery of pH_i was measured as described in chapter 3, section 3.11. *** = significant effect of treatment ($p < 0.001$). Data represents mean \pm S.E.M.; n numbers displayed in parenthesis.

4.2.2. Effect of CO₂ on intracellular Ca²⁺

The current data implied that there was a role for Ca²⁺ signalling in the CO₂-induced effect on cAMP-regulated HCO₃⁻ transport in Calu-3 cells, with the possibility that hypercapnia elicited an IP₃-dependent Ca²⁺ release which, not only could crosstalk with cAMP signalling pathways, but was also important for pH_i recovery from CO₂-induced acidosis. To ascertain whether hypercapnia induced a rise in intracellular Ca²⁺, Calu-3 cells were grown on glass coverslips and loaded with the Ca²⁺-sensitive dye, Fura-2-AM. To show that changes in [Ca²⁺]_i could be detected in non-polarised Calu-3 cells, cells were stimulated with ATP in the presence of 1mM Ca²⁺ and thapsigargin in the absence of extracellular Ca²⁺ and both agents induced an increase in the 340/380 ratios, indicative of elevated [Ca²⁺]_i (fig. 4.09A). Furthermore, reintroduction of extracellular Ca²⁺ after thapsigargin treatment induced a large rise in 340/380 ratio, indicative of store-operated Ca²⁺ entry (fig. 4.09A). Calu-3 cells were next perfused with high Cl⁻ Krebs solution gassed with either 5% CO₂/95% O₂ (v/v) or 10% CO₂/90% O₂ (v/v). As shown in figure 4.09B, there appeared to be a slow increase in [Ca²⁺]_i and therefore a liner regression was performed over the data points collected in 5% and 10% CO₂ to monitor whether CO₂ had any effect on this apparent increase in intracellular Ca²⁺. In normocapnia, the 340/380 ratio increased by 0.005 ± 0.002 units/min (n=5; fig. 4.09D). However, in hypercapnia, there was no significant difference in the rate of 340/380 ratio increase; here ratio increased by 0.006 ± 0.003 units/min (p>0.05 vs. normocapnia; n=5; fig. 4.09D). Therefore, these data suggested that hypercapnia did not induce an increase in total intracellular Ca²⁺. To confirm that the slow increase in 340/380 ratio was a feature of these experiments, cells were perfused with high Cl⁻ Krebs solution gassed with 5% CO₂/95% O₂ over an equivalent time course (fig. 4.09C). Again, a slow increase in 340/380 ratio was observed which was calculated as 0.001 ± 0.0002 units/min (n=3) which, although smaller than that observed in previous experiments in which the effects of hypercapnia was investigated, was not statistically significantly different (p>0.05), suggesting that the observed slow rise in 340/380 counts was a common feature of these experiments. To confirm that non-polarized Calu-3 cells responded to hypercapnia in a similar fashion to polarized cells, Calu-3 cells were grown on coverslips and pH_i was measured in response to 10% CO₂ (fig. 4.09E). Cells displayed a pH_i decrease of 0.19 ± 0.04 in response to hypercapnia (n=3; fig. 4.09F) which recovered by 110 ± 42.9% after 20 minutes (n=3; fig. 4.09G). These responses to hypercapnia were not different to those observed in polarized

monolayers of Calu-3 cells (figs. 4.09F and 4.09G) suggesting similar responses to hypercapnia exist between polarized and non-polarized Calu-3 cells



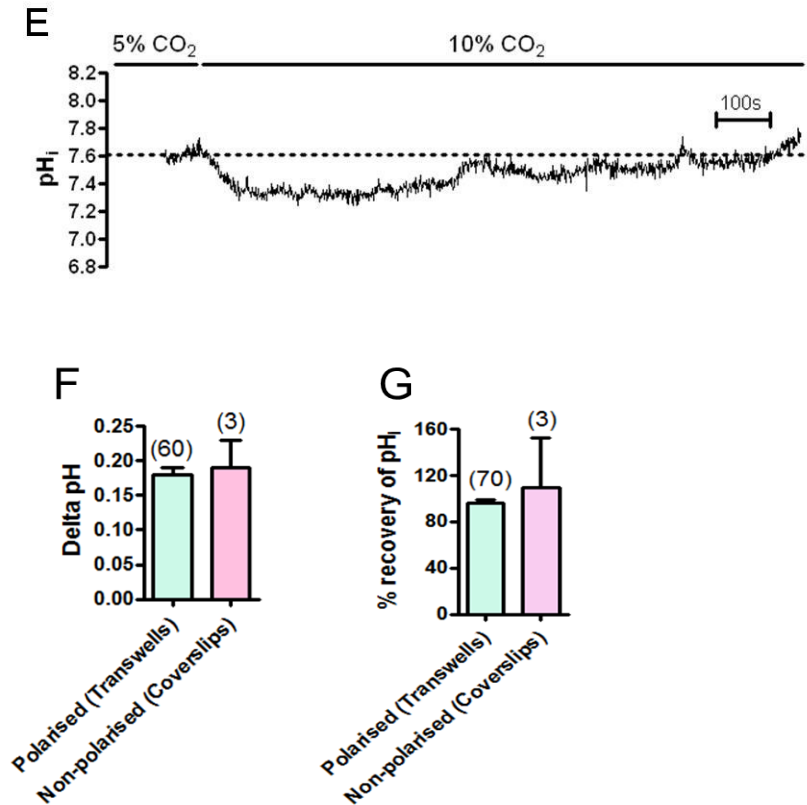


Figure 4.09: Acute hypercapnia does not cause an increase in intracellular Ca^{2+} in Calu-3 cells. Cells were grown as a non-polarised monolayer on glass coverslips and loaded with the Ca^{2+} -sensitive dye Fura-2-AM ($10\mu M$). (A) shows a representative experiment in which cells were stimulated with ATP ($100\mu M$) and thapsigargin ($200nM$) in the absence of extracellular Ca^{2+} before extracellular Ca^{2+} was reintroduced as indicated. These experiments were performed by my colleague Waseema Patel. (B) shows an example experiment in which cells were perfused with high Cl^- Krebs solution gassed with either 5% $CO_2/95\% O_2$ (v/v) or 10% $CO_2/90\% O_2$ (v/v). (C) shows an example experiment in which cells were perfused with high Cl^- Krebs solution gassed with either 5% $CO_2/95\% O_2$ (v/v). (D) summarizes the rate of increase in 340/380 ratio in normocapnia, hypercapnia and in normocapnia over a longer time course. Data represents mean \pm S.E.M., n numbers are displayed in parenthesis. (E) shows a representative experiment in which the effect of 10% CO_2 on pH_i of Calu-3 cells grown on glass coverslips was assessed. The magnitude of the pH_i decrease in response to hypercapnia and the extent of the recovery of pH_i are summarized in (F) and (G) respectively. Data represents mean \pm S.E.M., n numbers are displayed in parenthesis.

4.2.3. Activation of intracellular Ca^{2+} signalling

Although my experiments revealed that hypercapnia did not induce an increase in intracellular Ca^{2+} , the fact that these experiments were performed on non-polarised monolayers did limit the data and as a result, it cannot be concluded that CO_2 does not induce

a Ca^{2+} release in polarised monolayers of Calu-3 cells. Should CO_2 mediate its effects on cAMP-regulated HCO_3^- transport by mobilization of intracellular Ca^{2+} , it would be predicted that increasing intracellular Ca^{2+} in normocapnia may mimic the effect of hypercapnia. To investigate this possibility, cells were stimulated with forskolin in the absence or presence of Ca^{2+} elevating agonists that increase intracellular Ca^{2+} via two distinctly different mechanisms. Thapsigargin was used to inhibit SERCA to prevent Ca^{2+} reuptake into the endoplasmic reticulum and carbachol was used to activate cell surface cholinergic receptors and increase intracellular Ca^{2+} via phospholipase C-dependent IP_3 -mediated release from the ER. Figure 4.10A shows that addition of thapsigargin to Calu-3 cells grown on coverslips and loaded with the Ca^{2+} -sensitive dye Fura-2 caused a large increase in the 340/380 ratio, indicative of a large increase in $[\text{Ca}^{2+}]_i$. To investigate whether an increase in $[\text{Ca}^{2+}]_i$ mimicked the effect of hypercapnia on the forskolin-stimulated intracellular acidification, thapsigargin was added for 5 minutes prior to addition of forskolin in normocapnia as shown in figure 4.10B. Thapsigargin did not significantly alter the response to forskolin; the magnitude of the pH_i change and the rate of HCO_3^- flux was increased 1.1 ± 0.1 fold ($p > 0.05$; $n=3$; fig 4.10C) and 1.4 ± 0.4 fold ($p > 0.05$; $n=3$; fig. 4.10D) respectively by thapsigargin. These data show that increasing intracellular Ca^{2+} by thapsigargin did not mimic the effect of hypercapnia and suggests that if CO_2 does modulate intracellular Ca^{2+} , it is from thapsigargin-insensitive store.

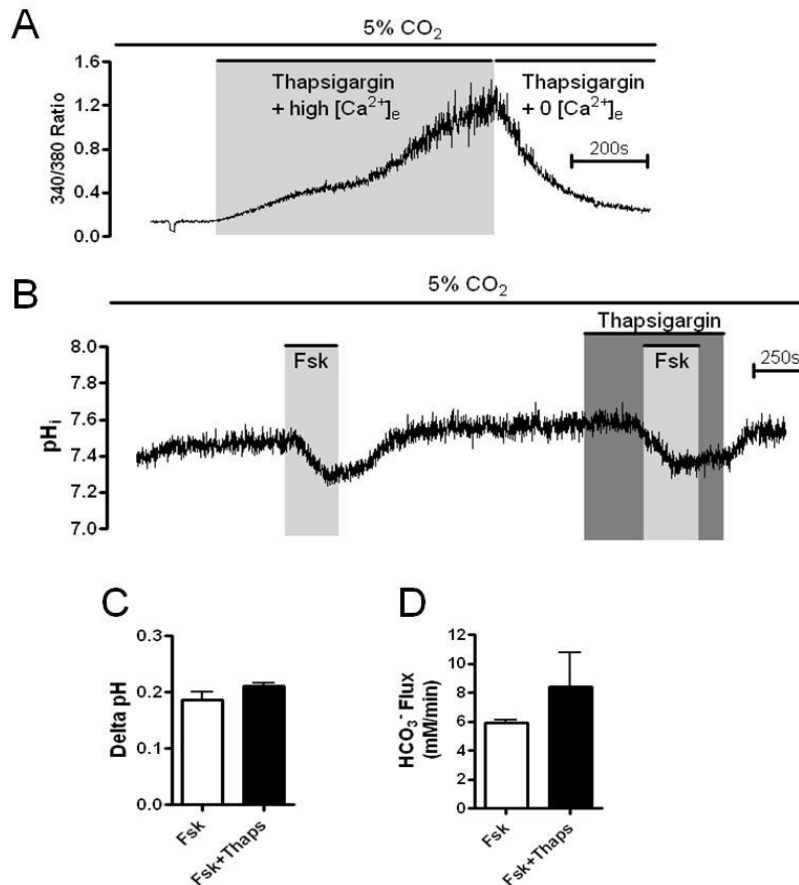


Figure 4.10: Thapsigargin treatment does not mimic the effect of hypercapnia on the forskolin-stimulated intracellular acidification. (A) shows a representative experiment in which the effects of thapsigargin (200nM) on [Ca²⁺]_i was assessed in Calu-3 cells grown on coverslips. (B) shows a representative experiment in which pH_i was measured in Calu-3 cells when stimulated with 5μM forskolin or 5μM forskolin in the presence of 200nM thapsigargin in normocapnia. The delta pH (C) and HCO₃⁻ flux (D) resulting from agonist stimulation are summarized. Data represents mean ± S.E.M.; n=3 for each.

In contrast to thapsigargin, carbachol had an effect at both membranes but basolateral carbachol had the most pronounced effect on the forskolin-stimulated intracellular acidification. Apical carbachol increased the magnitude of the forskolin-stimulated intracellular acidification 1.0 ± 0.1 fold ($p > 0.05$; $n = 4$; fig. 4.11B) and increased the rate of forskolin-induced HCO₃⁻ flux 2.1 ± 0.2 fold ($p < 0.01$; $n = 4$; fig. 4.11C). Basolateral carbachol increased the magnitude of the forskolin-stimulated intracellular acidification 1.4 ± 0.02 fold ($p < 0.01$ vs. forskolin alone; $p < 0.01$ vs. forskolin + apical carbachol; $n = 4$; fig. 4.11B) and increased the rate of forskolin-induced HCO₃⁻ flux 3.9 ± 0.2 fold ($p < 0.001$ vs. forskolin alone; $p < 0.01$ vs. forskolin + apical carbachol; $n = 4$; fig. 4.11C). Furthermore, the effect of

basolateral carbachol was blocked by atropine verifying that the effect of carbachol was due to signalling *via* cholinergic receptors and subsequent activation of the PLC/IP₃ signalling pathway (fig. 4.11D). Therefore, activation of the phospholipase C pathway and IP₃-dependent Ca²⁺ mobilization by carbachol mimics the effect of hypercapnia. This supports the findings that showed the effect of hypercapnia was dependent on PLC activity and also supports the findings by Cook *et al.* (2012) that showed hypercapnia affected cAMP signalling due to IP₃-dependent Ca²⁺ release.

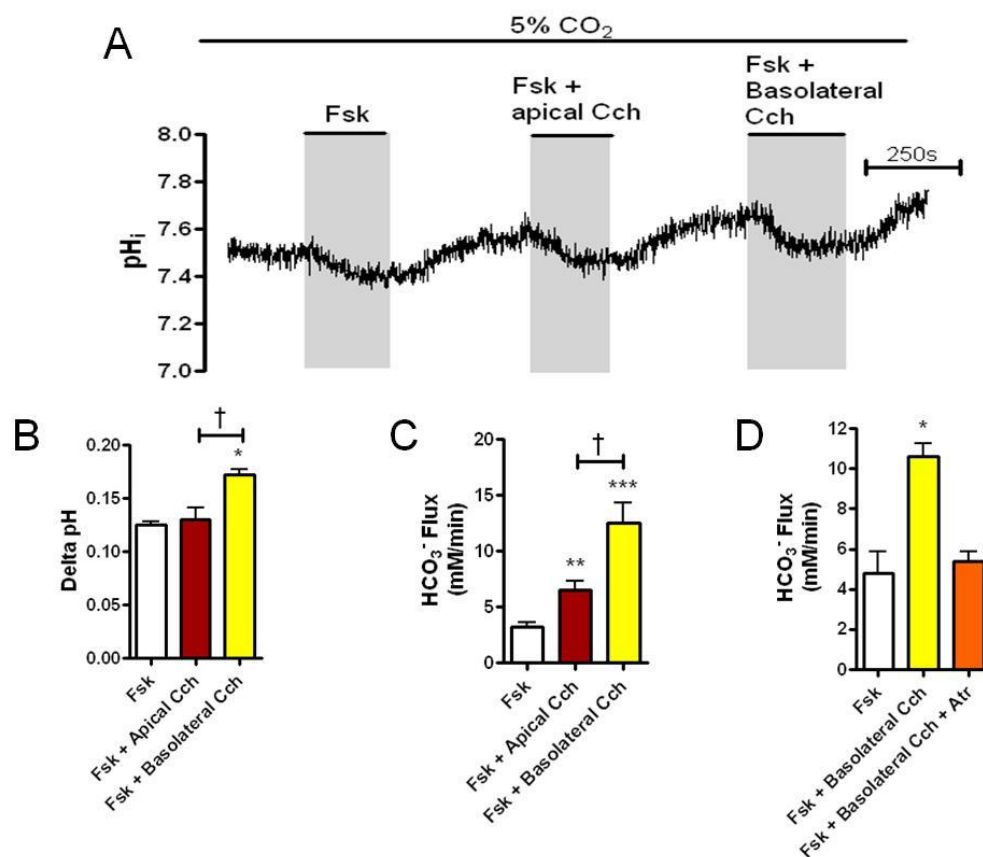


Figure 4.11: Basolateral carbachol mimics the effect of hypercapnia on the forskolin-stimulated intracellular acidification. (A) shows a representative experiment in which Calu-3 cells were stimulated with 5μM forskolin, 5μM forskolin + apical carbachol (20μM) or 5μM forskolin + basolateral carbachol (20μM). The delta pH (B) and HCO₃⁻ flux (C) resulting from agonist stimulation are summarized. The sensitivity of the effect of carbachol to atropine (10μM) is summarized in (D). * = significant effect of carbachol (p<0.05; ** = p<0.01; *** = p<0.001); † = significant difference between apical carbachol and basolateral carbachol (p<0.05). Data represents mean ± S.E.M.; n=4 for each

4.3. The effect of exogenous ATP

Given that hypercapnia has been shown to induce ATP release in brain tissue (Huckstepp *et al.*, 2010b) and that ATP signals *via* purinergic receptors to mobilize intracellular Ca^{2+} and regulate ion transport in airway epithelia (Homolya *et al.*, 2000; Son *et al.*, 2004), it was possible that CO_2 may induce ATP release from Calu-3 cells to activate purinergic receptors *via* an autocrine signalling mechanism and induce elevations in $[\text{Ca}^{2+}]_i$. If this was the case, addition of exogenous ATP in normocapnia should mimic the effect of hypercapnia. Carbachol was able to somewhat mimic the effect of hypercapnia, thus implicating activation of G_q -coupled receptors may underlie the effects of hypercapnia on cAMP-regulated HCO_3^- transport. Before the effects of ATP on the forskolin-stimulated intracellular acidification were assessed, the effect of ATP alone was first measured. As shown in figure 4.12A, addition of exogenous ATP caused a fast, transient acidification. In normocapnia, the magnitude of the acidification was 0.16 ± 0.03 (n=4) and was 0.22 ± 0.04 in hypercapnia ($p > 0.05$; n=4; fig. 4.12C). Interestingly, the rate of ATP-stimulated HCO_3^- flux was significantly enhanced 6.8 ± 2.6 fold from $16.0 \pm 6.8 \text{ mM HCO}_3^- \text{ min}^{-1}$ (n=4) in normocapnia to $60.0 \pm 15.3 \text{ mM HCO}_3^- \text{ min}^{-1}$ in hypercapnia ($p < 0.05$; n=4; fig. 4.12D). Further investigations revealed that the ATP-induced intracellular acidification was almost completely abolished by BAPTA-AM, as shown in figs 4.12B, C and D. Therefore, ATP utilizes Ca^{2+} signalling in order to mediate its effects in Calu-3 cells which is supported by figure 4.09A which showed a small but detectable Ca^{2+} transient after stimulation of Calu-3 cells with exogenous ATP.

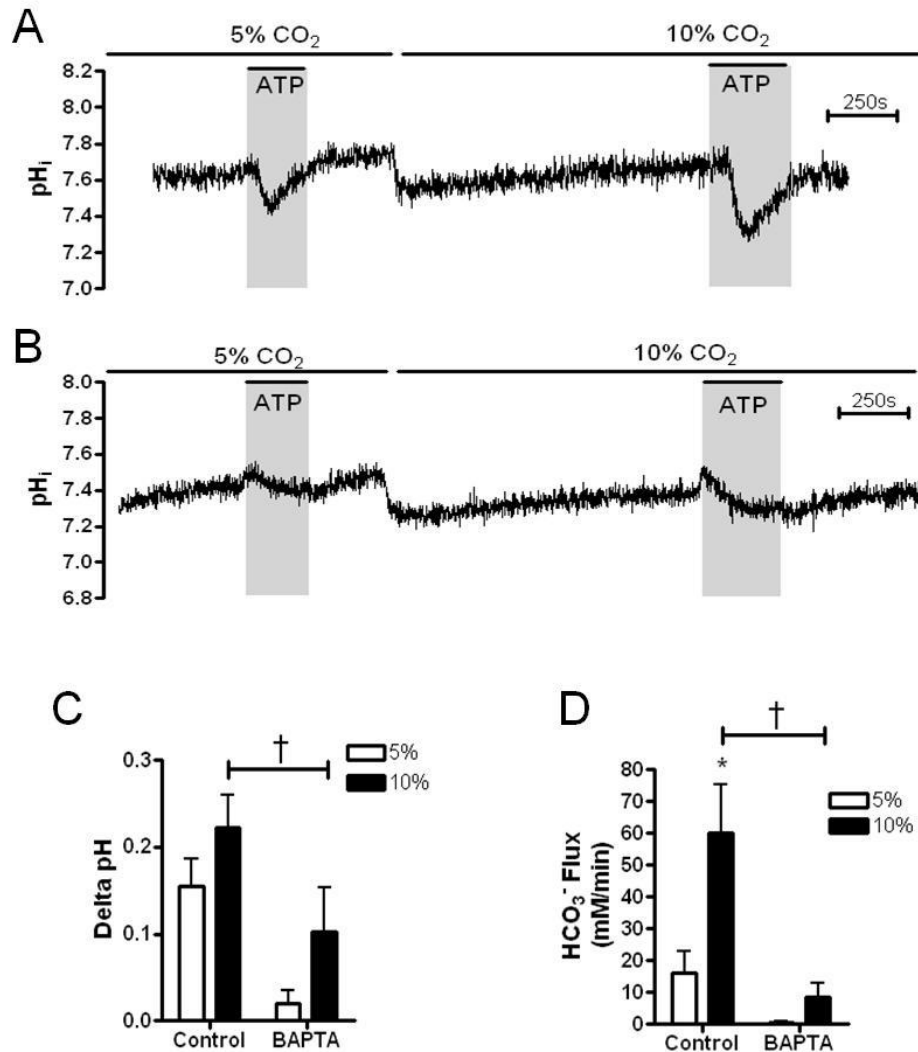


Figure 4.12: Exogenous ATP induces a Ca²⁺-dependent, transient intracellular acidification which is modulated by acute hypercapnia. (A) and (B) show representative experiments in which Calu-3 cells were stimulated with bilateral ATP (100μM) in normocapnia and hypercapnia in control and BAPTA-AM (50μM) loaded cells respectively. The delta pH (C) and HCO₃⁻ flux (D) resulting from ATP stimulation are summarized. * = significant effect of hypercapnia (p<0.05); † = significant effect of BAPTA-AM (p<0.05). Data represents mean ± S.E.M.; n=4 for each.

To assess how ATP-induced elevations in Ca²⁺ affected the forskolin-stimulated intracellular acidification, cells were stimulated with either forskolin alone or forskolin and bilateral ATP simultaneously in normocapnia and hypercapnia (fig. 4.13A). In normocapnia, ATP increased the magnitude of the forskolin-stimulated intracellular acidification 1.5 ± 0.1 fold (p<0.001 vs. forskolin alone; n=6; fig. 4.13B) which was similar, but significantly smaller, than hypercapnia, which increased the magnitude of the forskolin-stimulated intracellular acidification 2.2 ± 0.1 fold (p<0.001 vs. normocapnia; p<0.001 vs. ATP in normocapnia; n=6;

fig. 4.13B). Furthermore, ATP increased the rate of the forskolin-stimulated HCO_3^- flux 4.3 ± 0.5 fold in normocapnia ($p < 0.01$ vs. forskolin alone; $n = 6$; fig. 4.13C) which again was similar but significantly smaller than the 6.9 ± 0.8 fold increase in the forskolin-stimulated HCO_3^- flux observed in hypercapnia ($p < 0.001$ vs. normocapnia; $p < 0.05$ vs. ATP in normocapnia; $n = 6$; fig. 4.13C). The effect of exogenous ATP in hypercapnia was also assessed. ATP induced a non-significant 1.0 ± 0.1 fold increase in the magnitude of the forskolin-stimulated intracellular acidification in hypercapnia ($p > 0.05$ vs. forskolin alone; $n = 6$; fig. 4.13B) but did induce a 1.9 ± 0.2 fold increase in the rate of forskolin-stimulated HCO_3^- flux in hypercapnia ($p < 0.01$ vs. forskolin alone; $n = 6$; fig. 4.13C). Together, these data imply that (i) exogenous ATP mimics the effect of hypercapnia but does not modulate the cAMP-regulated HCO_3^- transport to the same extent as CO_2 and (ii) ATP and hypercapnia together are able to further enhance forskolin-stimulated HCO_3^- transport and suggests that if hypercapnia is mediating its effects by causing an ATP release, the ATP levels released by 10% CO_2 are not high enough to saturate the purinergic receptors.

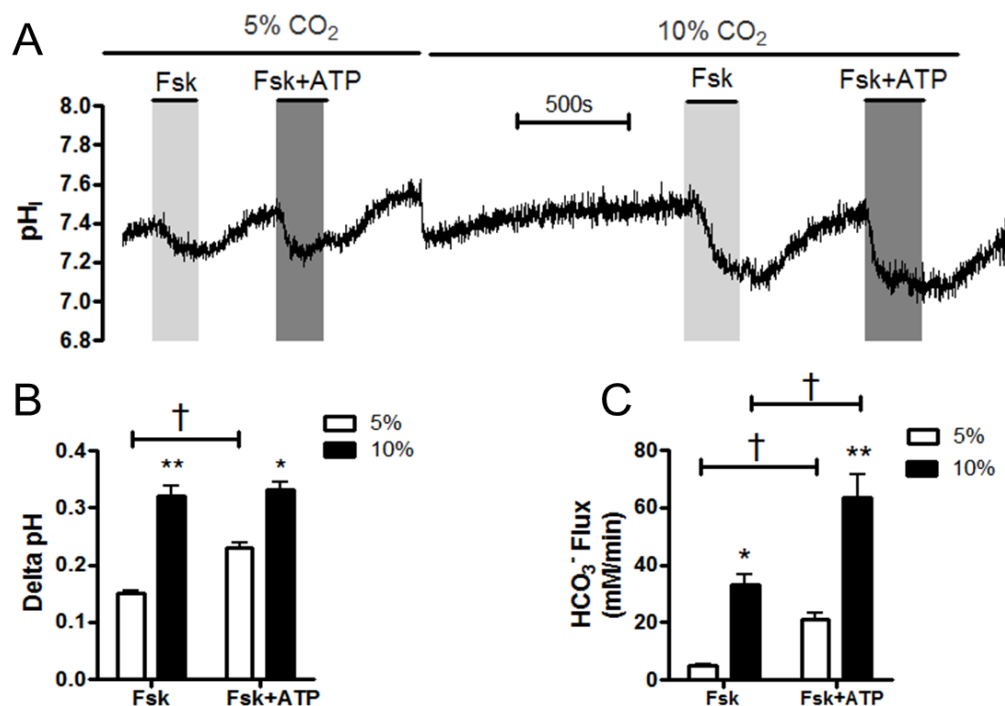


Figure 4.13: Exogenous ATP mimics the effect of hypercapnia on the forskolin-stimulated intracellular acidification. (A) shows a representative experiment in which Calu-3 cells were stimulated with either 5 μM forskolin or 5 μM forskolin + 100 μM bilateral ATP in normocapnia and hypercapnia. The delta pH (B) and HCO_3^- flux (C) resulting from agonist stimulation are summarized. * = significant effect of hypercapnia ($p < 0.05$; ** = $p < 0.01$). † = significant effect of ATP. Data represents mean \pm S.E.M.; $n = 6$ for each.

To determine whether exogenous ATP was mediating its effects on either apical or basolateral purinergic receptors, exogenous ATP was applied unilaterally. Figure 4.14A shows an example experiment in which ATP was added apically and figure 4.15A shows an example experiment in which ATP was added basolaterally. Apical ATP increased the magnitude of the forskolin-stimulated intracellular acidification 1.2 ± 0.1 fold ($p > 0.05$ vs. forskolin alone; $n=3$) compared to hypercapnia which induced a 1.6 ± 0.1 fold increase in the magnitude of the forskolin-stimulated intracellular acidification ($p < 0.01$ vs. normocapnia; $n=3$; fig. 4.14B). However, although apical ATP significantly enhanced the rate of forskolin-stimulated HCO_3^- flux 2.0 ± 0.1 fold ($p < 0.05$ vs. forskolin alone; $n=3$), this was significantly lower than the 4.7 ± 0.8 fold increase in forskolin-stimulated HCO_3^- flux induced by hypercapnia ($p < 0.05$ vs. normocapnia; $p < 0.05$ vs. apical ATP; $n=3$; fig. 4.14C). Basolateral ATP increased the magnitude of the forskolin-stimulated intracellular acidification 1.3 ± 0.3 fold ($p > 0.05$ vs. forskolin alone; $n=3$) compared to hypercapnia which induced a 1.9 ± 0.2 fold increase in the magnitude of the forskolin-stimulated intracellular acidification ($p < 0.05$ vs. normocapnia; $n=3$; fig. 4.15B). However, basolateral ATP appeared to have a greater effect than apical ATP on the rate of forskolin-stimulated HCO_3^- flux as it significantly enhanced this parameter 3.8 ± 0.7 fold ($p < 0.01$ vs. forskolin alone; $n=3$), which is not significantly different to the 5.4 ± 0.8 fold increase in forskolin-stimulated HCO_3^- flux induced by hypercapnia ($p < 0.01$ vs. normocapnia; $p > 0.05$ vs. basolateral ATP; $n=3$; fig. 4.15C). As summarized in figure 4.16, bilateral ATP has a significantly greater effect on the rate of forskolin-stimulated HCO_3^- flux compared to apical ATP ($p < 0.05$) but there was no difference between the effect of bilateral ATP compared to basolateral ATP. Together, these data suggested that although apical ATP did produce a small, but significant, effect on forskolin-stimulated HCO_3^- transport, the more pronounced effect of basolateral ATP implied that any CO_2 -induced ATP release occurred predominantly across the basolateral membrane.

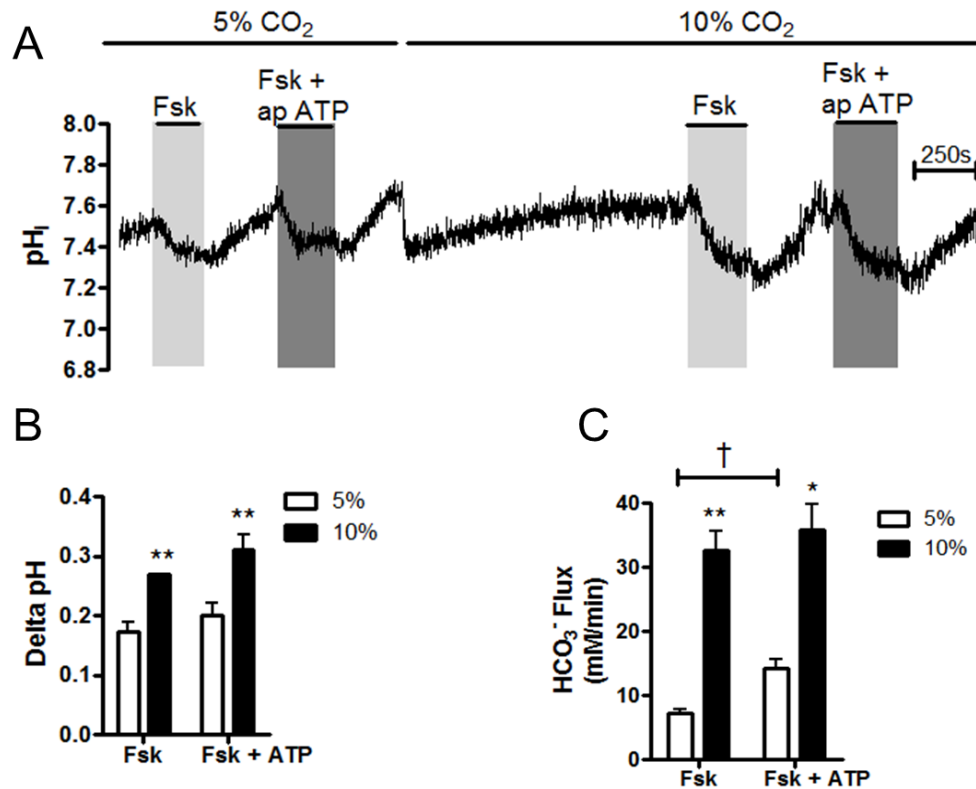


Figure 4.14: Exogenous apical ATP has a small effect on the forskolin-stimulated intracellular acidification. (A) shows a representative experiment in which Calu-3 cells were stimulated with either 5 μ M forskolin or 5 μ M forskolin + 100 μ M apical ATP in normocapnia and hypercapnia. The delta pH (B) and HCO₃⁻ flux (C) resulting from agonist stimulation are summarized. * = significant effect of hypercapnia (p<0.05; ** = p<0.01). † = significant effect of ATP. Data represents mean \pm S.E.M.; n=3 for each.

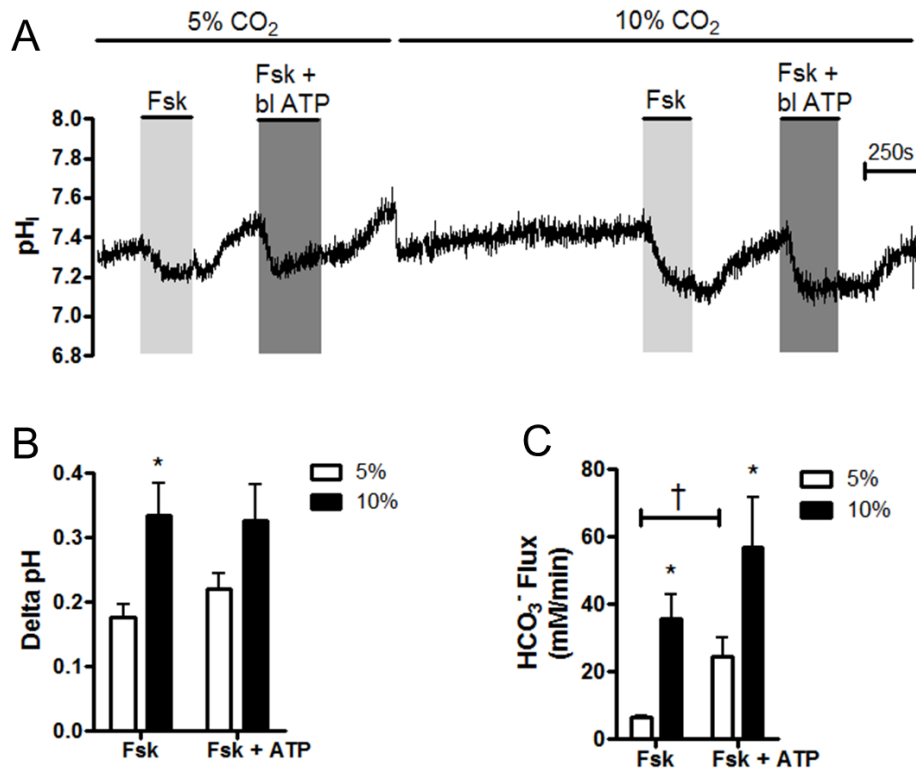


Figure 4.15: Exogenous basolateral ATP mimics the effect of hypercapnia on the forskolin-stimulated intracellular acidification. (A) shows a representative experiment in which Calu-3 cells were stimulated with either 5 μ M forskolin or 5 μ M forskolin + 100 μ M basolateral ATP in normocapnia and hypercapnia. The ΔpH (B) and HCO_3^- flux (C) resulting from agonist stimulation are summarized. * = significant effect of hypercapnia ($p < 0.05$). † = significant effect of ATP. Data represents mean \pm S.E.M.; $n=3$ for each.

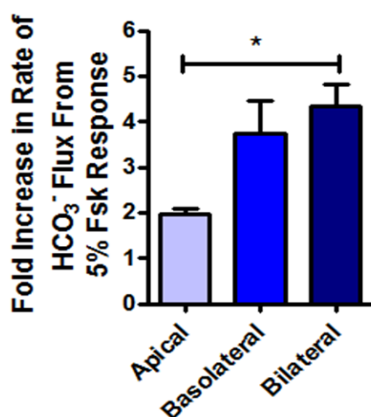


Figure 4.16: The effect of exogenous ATP on the forskolin-stimulated intracellular acidification is predominantly basolateral. * = significant effect of bilateral ATP vs apical ATP ($p < 0.05$). Data represents mean \pm S.E.M.; $n=6$ for bilateral ATP; $n=3$ for apical and basolateral ATP.

Next, the effect of ATP was tested for its Ca^{2+} dependence. Calu-3 cells were preincubated with BAPTA-AM for one hour before being stimulated with forskolin or forskolin + bilateral ATP simultaneously in normocapnia and hypercapnia. An example experiment is shown in figure 4.17A. In control experiments performed on the same day, exogenous ATP caused a 1.5 ± 0.1 fold increase in the magnitude of the forskolin-stimulated intracellular acidification ($p < 0.01$; $n=3$; figs. 4.17B and D) and a 3.8 ± 0.3 fold increase in the rate of forskolin-stimulated HCO_3^- flux ($p < 0.01$; $n=3$; figs. 4.17C and E). However, this effect of ATP was blocked in cells that had been treated with BAPTA-AM. Here, addition of exogenous ATP in normocapnia caused a 1.0 ± 0.1 fold increase in the magnitude of the forskolin-stimulated intracellular acidification ($p > 0.05$; $n=3$; figs. 4.17B and D) and a 1.3 ± 0.04 fold increase in the rate of forskolin-stimulated HCO_3^- flux ($p > 0.05$; $n=3$; figs. 4.17C and E). These findings demonstrated that the effect of ATP is Ca^{2+} -dependent and implicates G-protein coupled purinergic receptors in mediating the ATP effects. Given that the effect of hypercapnia is also Ca^{2+} -dependent, it shows that ATP and CO_2 are potentially signalling *via* the same common pathway and provides further indication that CO_2 may elicit its effects *via* a release of ATP.

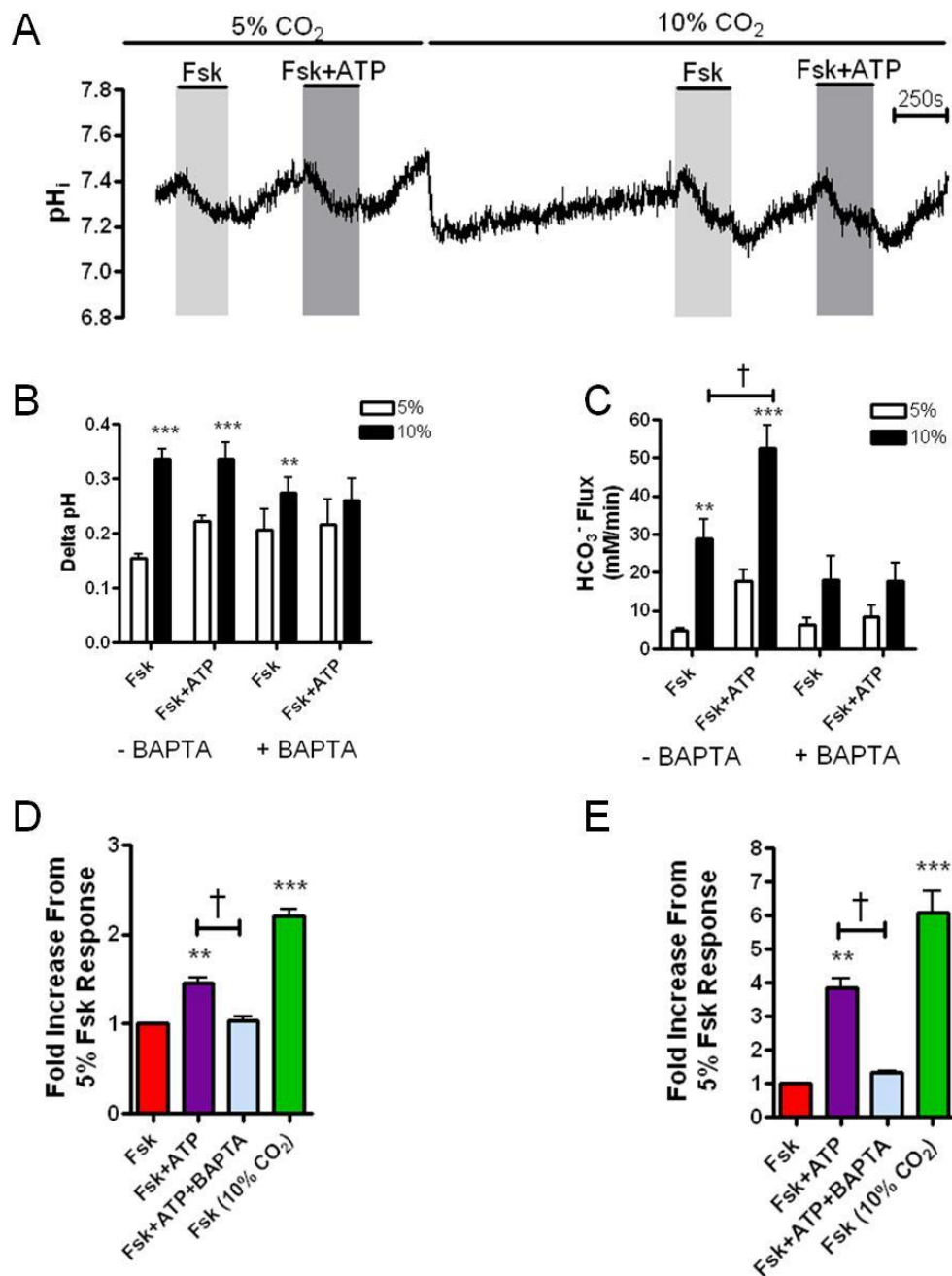


Figure 4.17: The effect of ATP on the forskolin-stimulated intracellular acidification is Ca²⁺-dependent. (A) shows a representative experiment in which Calu-3 cells were preincubated with BAPTA-AM (50μM) for one hour before being stimulated with either 5μM forskolin or 5μM forskolin + 100μM ATP in normocapnia and hypercapnia. The delta pH (B) and HCO₃⁻ flux (C) resulting from agonist stimulation are summarized and compared to non-BAPTA-AM loaded control experiments performed on the same day. ** = significant effect of hypercapnia (p<0.01; *** = p<0.001). † = significant effect of ATP (p<0.05). The fold increase in the delta pH (D) and HCO₃⁻ flux (E) from the forskolin response in normocapnia are summarized. ** = significant of treatment vs forskolin alone (p<0.01; *** = p<0.001); † = significant effect of BAPTA-AM (p<0.05). Data represents mean ± S.E.M., n=3 for each.

To verify that exogenous ATP was signalling *via* purinergic receptors, the non-specific P₂ receptor antagonist, suramin, was used to block purinergic receptor activation and an example experiment is shown in figure 4.18A. Exogenous ATP increased the magnitude of the forskolin-stimulated intracellular acidification 1.7 ± 0.1 fold ($p < 0.01$; $n = 4$; fig. 4.18B) but this effect of ATP was abolished in the presence of suramin as, in these conditions, ATP only increased the magnitude of the forskolin-stimulated intracellular acidification 0.8 ± 0.1 fold ($p > 0.05$ vs. forskolin alone; $p < 0.05$ vs. forskolin + ATP; $n = 4$; fig. 4.18B). Similarly, ATP increased the rate of forskolin-stimulated HCO₃⁻ flux 3.1 ± 0.6 fold ($p < 0.05$; $n = 4$; fig. 4.18C) but this was reduced to a 1.5 ± 0.2 fold increase in the presence of suramin ($p > 0.05$ vs. forskolin alone; $p < 0.05$ vs. forskolin + ATP; $n = 4$; fig. 4.18C). These findings imply that ATP elicits its effects on forskolin-stimulated HCO₃⁻ transport due to activation of purinergic receptors. It is worth noting that suramin treatment alone induced a pH_i decrease of 0.21 ± 0.03 units ($n = 4$) suggesting that suramin treatment alone modified HCO₃⁻/H⁺ transport which does slightly complicate experiments in which this drug was used.

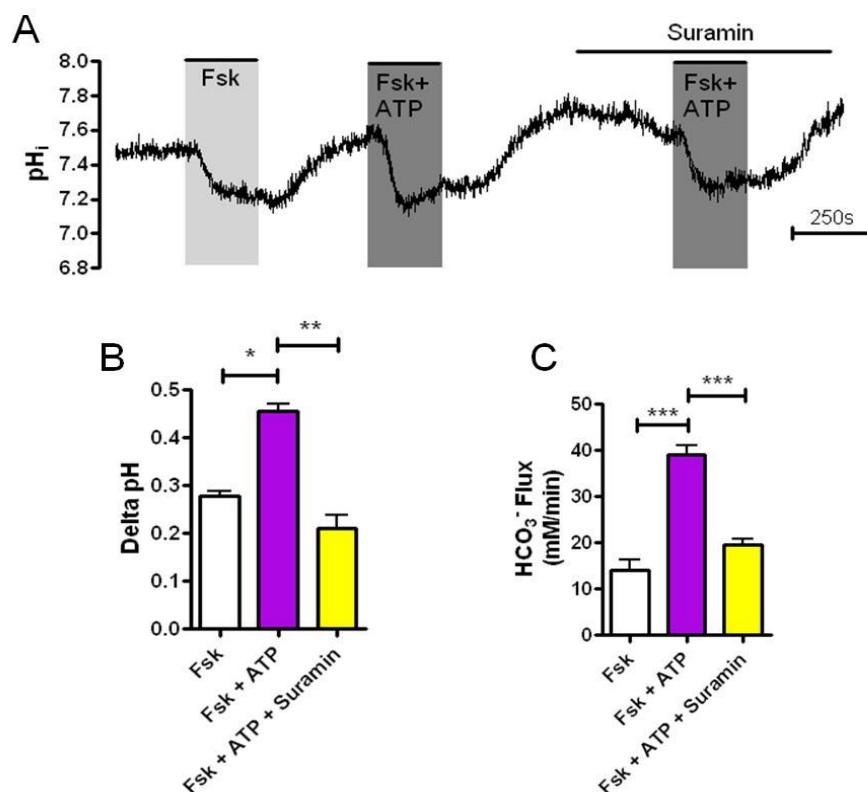


Figure 4.18: Suramin prevents ATP-mediated augmentation of forskolin-stimulated intracellular acidification. (A) shows a representative experiment in Calu-3 cells were stimulated with 5μM forskolin + 100μM bilateral ATP +/- suramin in normocapnia. The delta pH (B) and HCO₃⁻ flux (C) resulting from agonist stimulation are summarized. * = significant effect of hypercapnia ($p < 0.05$). Data represents mean \pm S.E.M.; $n = 4$ for each.

To determine whether the effect of ATP was specific or whether other nucleotides induced similar effects, the response to UTP was also assessed. UTP has been shown to act as a signalling molecule in the airways with both Namkung *et al.* (2010) and Bove *et al.* (2010) demonstrating UTP stimulated, Ca^{2+} and CFTR-dependent increases in I_{sc} in primary human bronchial epithelia and alveolar type II cells, respectively. Figure 4.19A shows an example experiment in which cells were stimulated with forskolin or forskolin and exogenous, bilateral UTP simultaneously in normocapnia and hypercapnia. In normocapnia, exogenous UTP increased the magnitude of the forskolin-stimulated intracellular acidification 1.5 ± 0.1 fold ($p < 0.001$ vs. forskolin alone; $n=4$) which was similar but significantly smaller than hypercapnia which increased the magnitude of the forskolin-stimulated intracellular acidification 2.1 ± 0.1 ($p < 0.001$ vs. normocapnia; $p < 0.01$ vs. UTP in normocapnia; $n=4$; fig. 4.19B). Furthermore, UTP increased the rate of forskolin-stimulated HCO_3^- flux 3.1 ± 0.9 fold in normocapnia ($p < 0.05$ vs. forskolin alone; $n=4$) which was significantly smaller than the 7.4 ± 0.2 fold increase in HCO_3^- flux observed in hypercapnia ($p < 0.001$ vs. normocapnia; $p < 0.01$ vs. UTP in normocapnia; $n=6$; fig. 4.19C). These data suggested that UTP, like ATP, can also modulate forskolin-stimulated HCO_3^- transport in a similar, but not as pronounced, fashion to hypercapnia. The UTP-induced 3.1 ± 0.9 fold ($n=4$) increase in the rate of forskolin-stimulated HCO_3^- transport in normocapnia was not statistically different to the 4.3 ± 0.5 fold increase induced by bilateral ATP ($p > 0.05$; $n=6$).

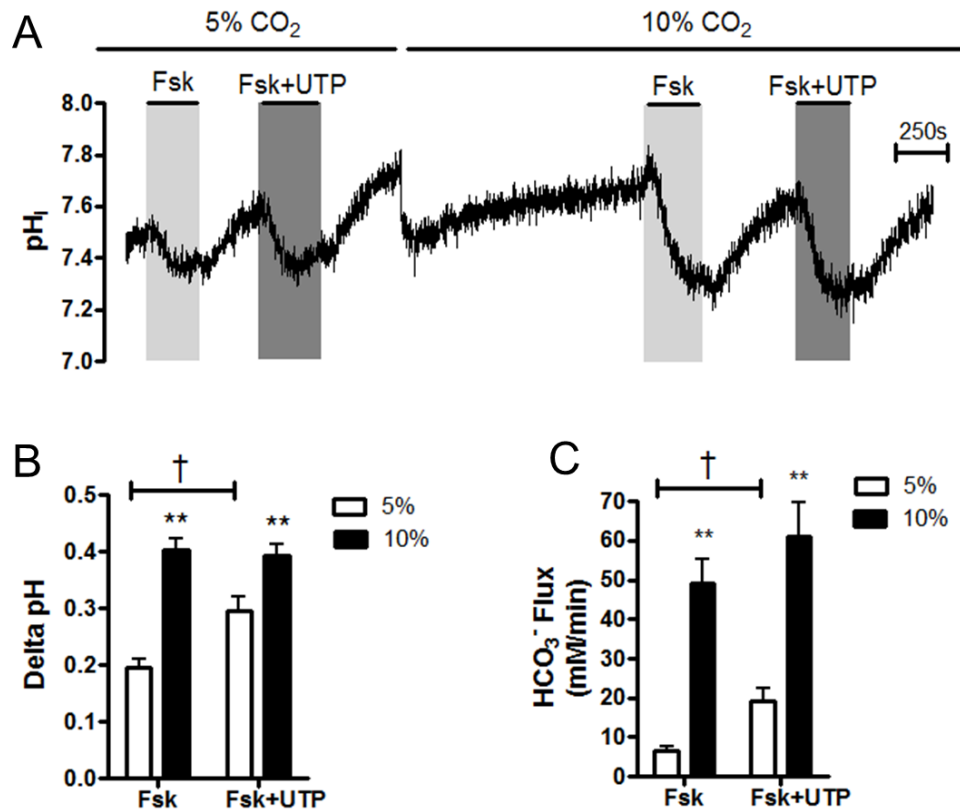


Figure 4.19: Exogenous UTP partially mimics the effect of hypercapnia on the forskolin-stimulated intracellular acidification. (A) shows a representative experiment in which Calu-3 cells were stimulated with either 5 μ M forskolin or 5 μ M forskolin + 100 μ M UTP in normocapnia and hypercapnia. The delta pH (B) and HCO₃⁻ flux (C) resulting from agonist stimulation are summarized. ** = significant effect of hypercapnia ($p < 0.01$); † = significant effect of UTP. Data represents mean \pm S.E.M.; $n=4$ for each.

Should hypercapnia induce a release of purinergic signalling molecules (i.e. ATP, UTP or both), inhibition of purinergic receptors would be predicted to prevent the effect of hypercapnia on cAMP-regulated HCO₃⁻ transport. To this end, suramin was used to block purinergic receptor activation and the response of Calu-3 cells to forskolin in normocapnia and hypercapnia was assessed, as shown in figure 4.20A. Suramin treatment did not affect the response to forskolin in 5% CO₂; in control conditions, the magnitude of the forskolin-stimulated intracellular acidification was 0.17 ± 0.01 ($n=3$) and the rate of forskolin-stimulated HCO₃⁻ flux was 5.6 ± 1.0 mM HCO₃⁻ min⁻¹ ($n=3$) whilst in the presence of suramin, the magnitude of the forskolin-stimulated intracellular acidification was 0.20 ± 0.02 ($p > 0.05$ vs. control; $n=3$; fig. 4.20B) and the rate of forskolin-stimulated HCO₃⁻ flux was 9.1 ± 1.9 mM HCO₃⁻ min⁻¹ ($p > 0.05$ vs. control; fig. 4.20C). Importantly, suramin treatment did

not affect the response to forskolin in hypercapnia. In control experiments, hypercapnia induced a 2.1 ± 0.2 fold increase in the forskolin-stimulated intracellular acidification ($p < 0.01$; $n=4$; fig. 4.20D) and a 7.9 ± 0.8 fold increase in the rate of forskolin-stimulated HCO_3^- flux ($p < 0.001$; $n=4$; fig. 4.20E). Similarly, in the presence of suramin, hypercapnia induced a 2.2 ± 0.2 fold increase in the forskolin-stimulated intracellular acidification ($p < 0.01$; $n=3$; fig. 4.20D) and a 5.6 ± 0.6 fold increase in the rate of forskolin-stimulated HCO_3^- flux ($p < 0.01$; $n=3$; fig. 4.20E). These data suggest that if CO_2 is inducing a release of ATP or UTP from Calu-3 cells, they are not signalling *via* purinergic receptors to induce changes in cAMP-regulated HCO_3^- transport.

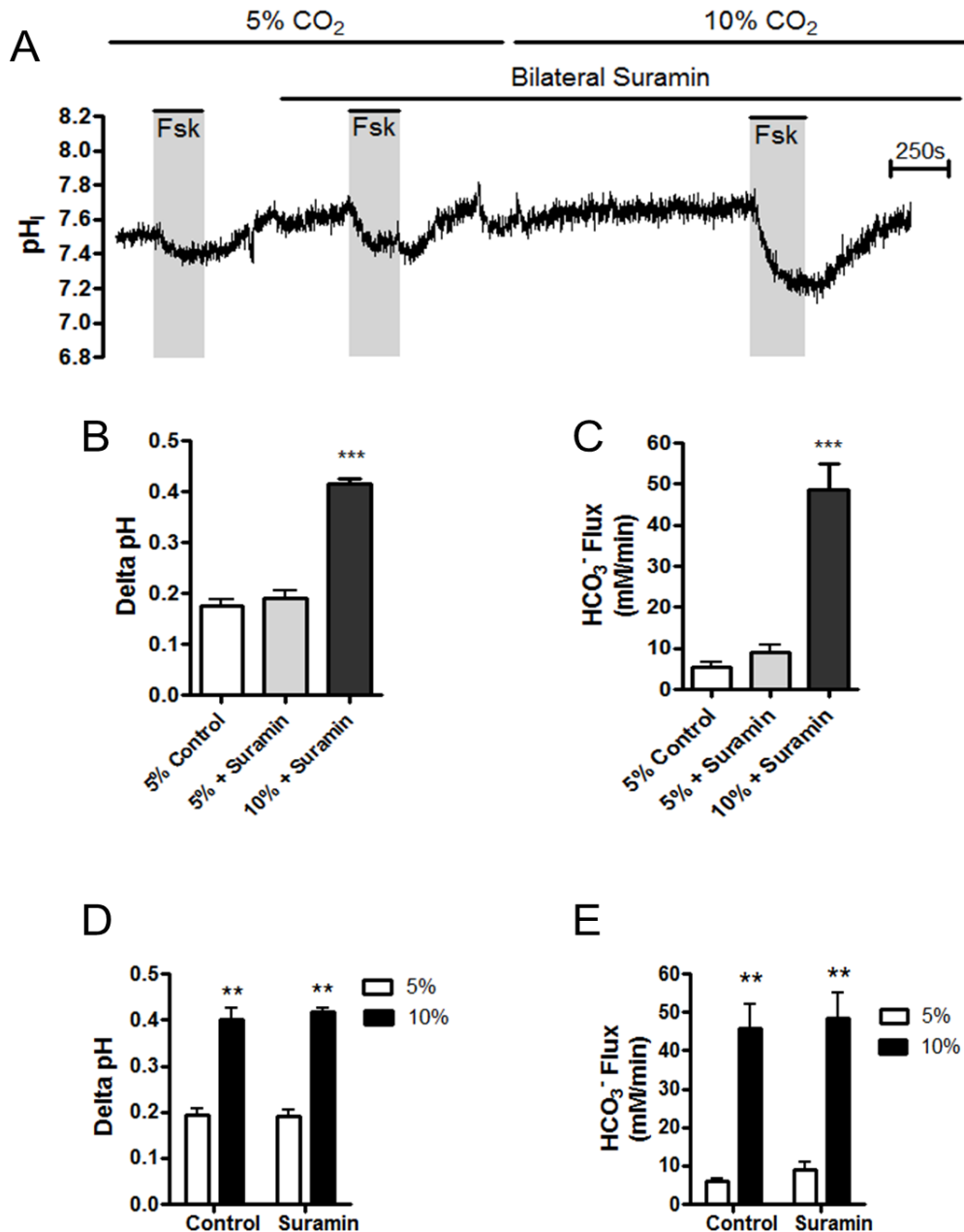


Figure 4.20: Suramin does not block the effect of hypercapnia on the forskolin-stimulated intracellular acidification. (A) shows a representative experiment in which Calu-3 cells were stimulated with 5 μ M forskolin alone or 5 μ M forskolin in the presence of 10 μ M suramin in normocapnia and hypercapnia. The effect of suramin on the delta pH (B) and HCO₃⁻ flux (C) resulting from forskolin stimulation is summarized. *** = significant effect of hypercapnia (p<0.001). The effect of suramin on the delta pH and HCO₃⁻ flux resulting from forskolin stimulation was also compared to control experiments performed on the same day as shown in (D) and (E) respectively. ** = significant effect of hypercapnia (p<0.01). Data represents mean \pm S.E.M.; n=3 for each.

An alternative way to deduce whether release of ATP mediated the effects of hypercapnia was to stimulate ATP hydrolysis by adding exogenous apyrase. Should ATP be mediating the effects of hypercapnia, metabolism of ATP should eliminate the CO₂ effect. Calu-3 cells were stimulated with forskolin in normocapnia and hypercapnia and then stimulated once more with forskolin in hypercapnia in the presence of apyrase (fig. 4.21A). Ideally, apyrase would have been added prior to exposing the cells to hypercapnia. However, perfusion of apyrase over a longer time frame was cost inefficient. Hypercapnia caused a 2.0 ± 0.2 fold increase in the magnitude of the forskolin- stimulated intracellular acidification ($p < 0.01$; $n = 3$; fig. 4.21B) and a 4.9 ± 1.8 fold increase in the rate of forskolin-stimulated HCO₃⁻ flux ($p < 0.05$; $n = 3$; fig. 4.21C) This was unchanged in the presence of apyrase; here hypercapnia caused a 2.0 ± 0.2 fold increase in the magnitude of the forskolin- stimulated intracellular acidification ($p < 0.01$ vs. normocapnia; $p > 0.05$ vs. hypercapnia; $n = 3$; fig. 4.21B) and a 4.4 ± 0.9 fold increase in the rate of forskolin-stimulated HCO₃⁻ flux ($p < 0.01$ vs. normocapnia; $p > 0.05$ vs. hypercapnia; $n = 3$; fig. 4.21C). Therefore, these data suggested ATP was not mediating the effects of hypercapnia.

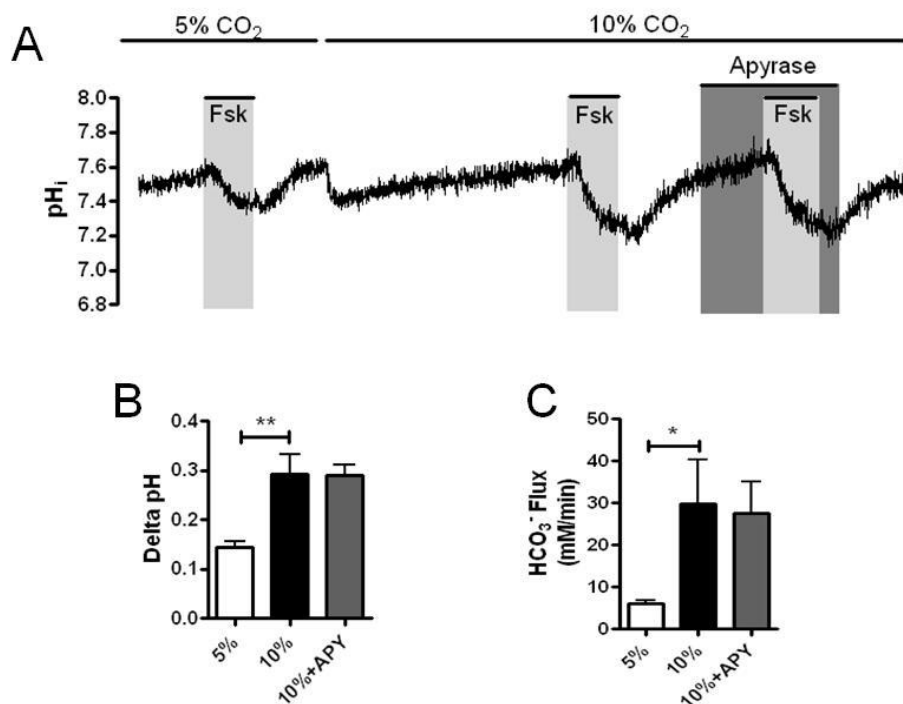


Figure 4.21: Apyrase does not block the effect of hypercapnia on the forskolin-stimulated intracellular acidification. (A) shows a representative experiment in which Calu-3 cells were stimulated with 5 μ M forskolin in normocapnia and hypercapnia and 5 μ M forskolin in the presence of apyrase (1U/ml) in hypercapnia. The effect of hypercapnia on the delta pH (B) and HCO₃⁻ flux (C) resulting from forskolin stimulation is summarized. * = significant effect of hypercapnia ($p < 0.05$; ** = $p < 0.01$). Data represents mean \pm S.E.M.; $n = 3$ for each.

Given that the data from experiments using suramin and apyrase implied ATP was not be signalling *via* purinergic receptors to mediate its effects, it was possible that ATP may have been broken down into adenosine by extracellular 5' nucleotidases (Arch and Newsholme, 1978) and that adenosine signalling could underlie the response in hypercapnia. Therefore, to assess whether adenosine signalling mediated the effect of hypercapnia, adenosine receptors were blocked using the non-specific adenosine receptor antagonist, CGS-15943. Figure 4.22A shows that treatment of cells with CGS-15943, prevented the adenosine-induced intracellular acidification in a non-reversible manner. In control conditions, adenosine induced an intracellular acidification of 0.18 ± 0.03 pH units ($n=3$) and a HCO_3^- flux of $5.9 \pm 1.3 \text{ mM HCO}_3^- \text{ min}^{-1}$ ($n=3$). However, in the presence of CGS-15943, the adenosine-stimulated intracellular acidification was 0.01 ± 0.02 pH units ($p<0.05$; $n=3$) with no measureable HCO_3^- flux ($0 \pm 0 \text{ mM HCO}_3^- \text{ min}^{-1}$ ($p<0.05$; $n=3$)). These data show that CGS-15943 was an appropriate inhibitor to use when studying the effects of adenosine signalling in Calu-3 cells. Figure 4.22B shows an example experiment used to assess the effects of hypercapnia on the forskolin-stimulated intracellular acidification in the presence of CGS-15943. CGS-15943 treatment alone did not affect the response to forskolin in normocapnia as shown in figs 4.22C and D. In control experiments performed on the same day, hypercapnia caused a 2.3 ± 0.1 fold increase in the magnitude of forskolin-stimulated intracellular acidification ($p<0.05$; $n=3$; fig. 4.22E) and a 5.0 ± 0.5 fold increase in the rate of forskolin-stimulated HCO_3^- flux ($p<0.001$; $n=3$; fig. 4.22F). In the presence of CGS-15943, hypercapnia caused a 2.4 ± 0.4 fold increase in the magnitude of forskolin-stimulated intracellular acidification ($p<0.05$; $n=3$; fig. 4.22D) and a 4.1 ± 0.1 fold increase in the rate of forskolin-stimulated HCO_3^- flux ($p<0.001$; $n=3$; fig. 4.22E). Therefore, these data imply that the effect of hypercapnia was not due to increases in extracellular adenosine (as a result of ATP metabolism) signalling *via* adenosine receptors to modulate cAMP-dependent HCO_3^- transport.

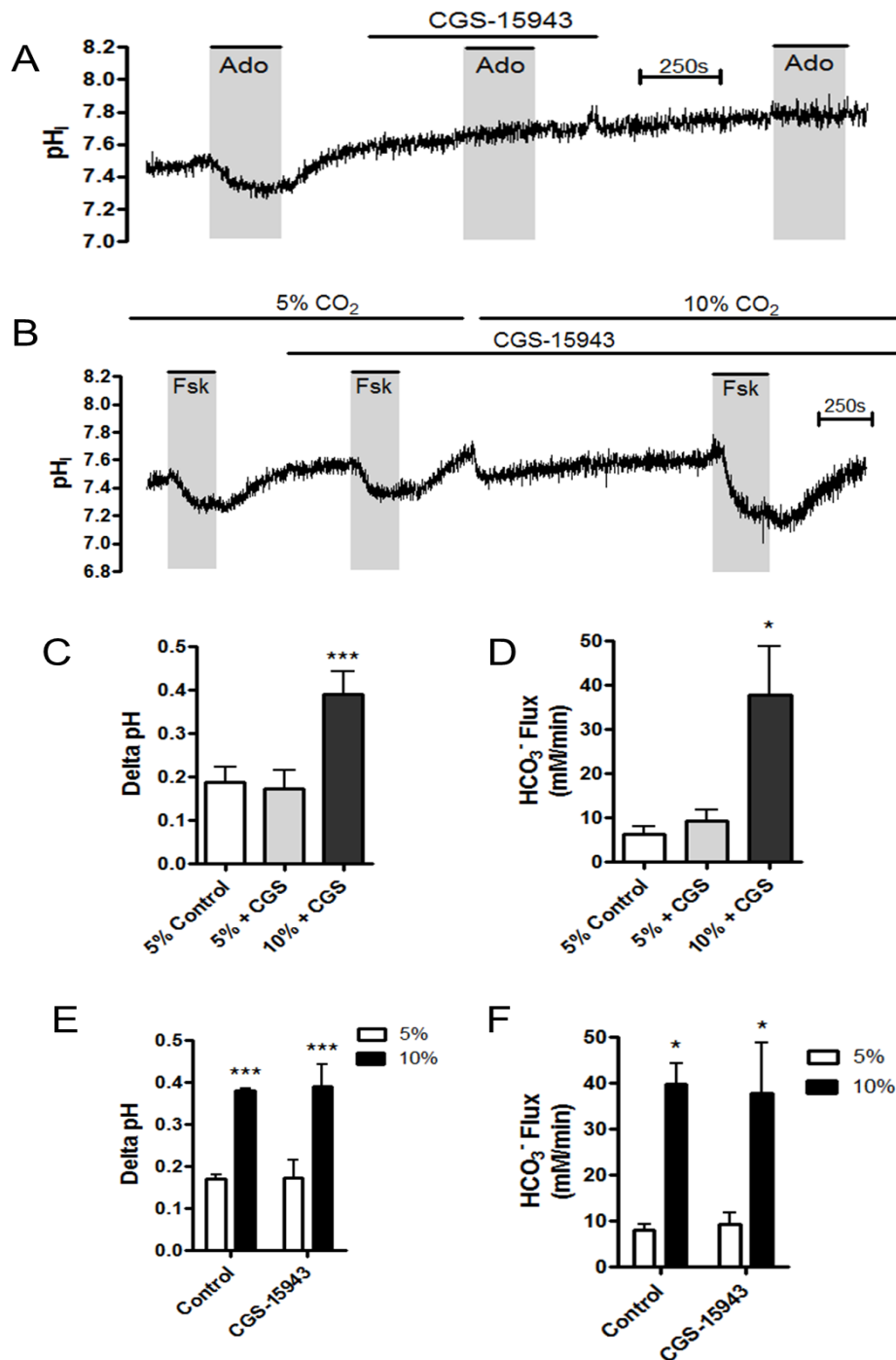


Figure 4.22: CGS-15943 does not block the effect of hypercapnia on the forskolin-stimulated intracellular acidification. (A) shows a representative experiment in which Calu-3 cells were stimulated with 10 μ M adenosine alone or in the presence of 500nM CGS-15943 as shown in (A). Calu-3 cells were stimulated with 5 μ M forskolin alone or 5 μ M forskolin in the presence of 500nM CGS-15943 in normocapnia and hypercapnia as shown in (B). The effect of hypercapnia on the delta pH (B) and HCO₃⁻ flux (C) resulting from forskolin stimulation is summarized. * = significant effect of hypercapnia ($p < 0.05$; *** = $p < 0.001$). The effect of CGS-15943 on the delta pH and HCO₃⁻ flux resulting from forskolin stimulation was also compared to control experiments performed on the same day as shown in (D) and (E) respectively. * = significant effect of hypercapnia ($p < 0.05$; *** = $p < 0.001$). Data represents mean \pm S.E.M.; $n = 3$ for each.

4.4. Possible mechanisms for CO₂-Induced ATP release

4.4.1. Connexins

The previously reported data suggests that exogenous ATP mimicked the effect of hypercapnia and implies CO₂ may mediate its effects by causing a release of ATP. Although the evidence for ATP release at this stage was minimal, the hypothesis would support the work done by Huckstepp *et al.* (2010b) who attributed a CO₂-induced ATP release as a mechanism for the regulation of ventilation in medulla oblongata of rats. Here, they showed the ATP release was due to CO₂-induced opening of connexin hemichannels, specifically connexin 26. Connexins are proteins possessing four membrane spanning domains and two extracellular loops containing cysteine residues. 6 connexins associate to form a connexon which forms a channel on the cell membrane. The extracellular cysteine residues interact with connexins on neighbouring cells to form a gap junction, capable of shuttling small molecules between adjacent cells. For a review of connexin hemichannels, see Matsuuchi and Naus (2013). Calu-3 cells have been reported to express connexins 32 and 43 (Go *et al.*, 2006; Scheckenbach *et al.*, 2011; Losa *et al.*, 2014) with Cx43 actually believed to be important in CFTR regulation by prostaglandins (Scheckenbach *et al.*, 2011). Thus, to determine whether connexins were involved in transduction of the CO₂ signal, the effect of hypercapnia on the forskolin-induced acidification was tested in the presence of the connexin inhibitors carbenoxolone, cobalt and proadifen.

Carbenoxolone has been shown to inhibit connexins in a variety of cell types (Sagar and Larson, 2006; Huckstepp *et al.*, 2010b) and figure 4.23A shows an example experiment of carbenoxolone treated cells. Interestingly, in conditions of normocapnia, carbenoxolone treatment alone increased both the magnitude of the forskolin-stimulated intracellular acidification and the rate of forskolin-stimulated HCO₃⁻ flux compared to the response in the absence of carbenoxolone. This is summarized in figures 4.23B and C. This suggests carbenoxolone treatment alone is able to modulate cAMP-regulated HCO₃⁻ transport. In control experiments performed on the same day, hypercapnia increased the magnitude of the forskolin-stimulated intracellular acidification 2.1 ± 0.1 fold ($p < 0.001$; $n = 4$; fig. 4.23D) and the rate of forskolin-stimulated HCO₃⁻ flux 5.8 ± 0.3 fold ($p < 0.001$; $n = 4$; fig. 4.23E). However, in the presence of carbenoxolone, hypercapnia was not able to significantly alter the forskolin-stimulated intracellular acidification. Here, hypercapnia increased the magnitude of the forskolin-stimulated intracellular acidification 0.8 ± 0.1 fold ($p > 0.05$; $n = 4$;

fig. 4.23D) and the rate of forskolin-stimulated HCO_3^- flux 1.1 ± 0.3 fold ($p > 0.05$; $n = 4$; fig. 4.23E). These data suggested that CO_2 may alter cAMP-regulated HCO_3^- transport by a modulation of connexin activity. Furthermore, cells treated with carbenoxolone were unable to recover their pH_i in response to CO_2 -induced acidosis and actually displayed a $-35.3 \pm 8.0\%$ in pH_i recovery ($p < 0.001$ vs. control; $n = 4$; fig. 4.26) demonstrating that cells actually further acidified after CO_2 -induced acidosis. Thus, connexins may also be important in the mechanisms of pH_i recovery from CO_2 -induced acidosis.

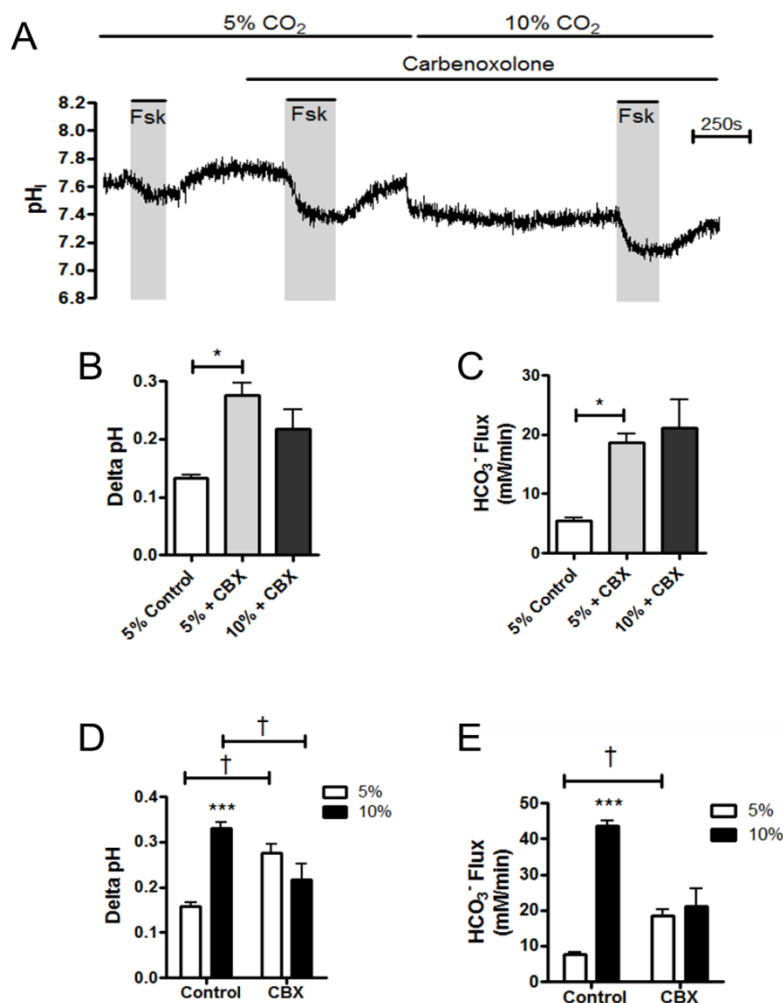


Figure 4.23: Carbenoxolone treatment blocks the effect of hypercapnia on the forskolin-stimulated intracellular acidification. (A) shows a representative experiment in which Calu-3 cells were stimulated with 5 μM forskolin alone or 5 μM forskolin in the presence of 100 μM carbenoxolone in normocapnia and hypercapnia. The effect of carbenoxolone on the ΔpH (B) and HCO_3^- flux (C) resulting from forskolin stimulation is summarized. * = significant effect of carbenoxolone in normocapnia ($p < 0.05$). The effect of carbenoxolone on the ΔpH and HCO_3^- flux resulting from forskolin stimulation was also compared to control experiments performed on the same day as shown in (D) and (E) respectively. *** = significant effect of hypercapnia ($p < 0.001$); † = significant effect of carbenoxolone ($p < 0.05$). Data represents mean \pm S.E.M.; $n = 4$ for each.

To verify that carbenoxolone was specifically targeting connexins, the effect of another reported connexin inhibitor was also tested. Cobalt has been shown to inhibit gap junctions in several studies performed on brain tissue (Huckstepp *et al.*, 2010b; Wenker *et al.*, 2012). Figure 4.24A shows an example experiment of cells treated with cobalt chloride. A notable difference between cobalt and carbenoxolone is the inability of cobalt to modulate the forskolin-stimulated intracellular acidification in normocapnia, as summarized in figures 4.24B and 4.23C. Furthermore, cobalt had no effect on the pH_i recovery from CO_2 -induced acidosis with cells demonstrating a $120.5 \pm 40.6\%$ recovery of pH_i ($p > 0.05$ vs. control; $n=3$; fig. 4.26). In control experiments performed on the same day, hypercapnia increased the magnitude of the forskolin-stimulated intracellular acidification 2.2 ± 0.1 fold ($p < 0.001$; $n=4$; fig. 4.24D) and the rate of forskolin-stimulated HCO_3^- flux 3.6 ± 0.5 fold ($p < 0.001$; $n=4$; fig. 4.24E). Unlike carbenoxolone, cobalt did not prevent the CO_2 -mediated increase of the forskolin-stimulated intracellular acidification. Here, hypercapnia increased the magnitude of the forskolin-stimulated intracellular acidification 2.1 ± 0.1 fold ($p < 0.01$; $n=4$; fig. 4.24D) and the rate of forskolin-stimulated HCO_3^- flux 5.0 ± 0.6 fold ($p < 0.001$; $n=4$; fig. 4.24E). These data suggest that either the effects of carbenoxolone were off target or that carbenoxolone and cobalt inhibit different members of the connexin family of which only the carbenoxolone-sensitive ones were CO_2 -sensitive.

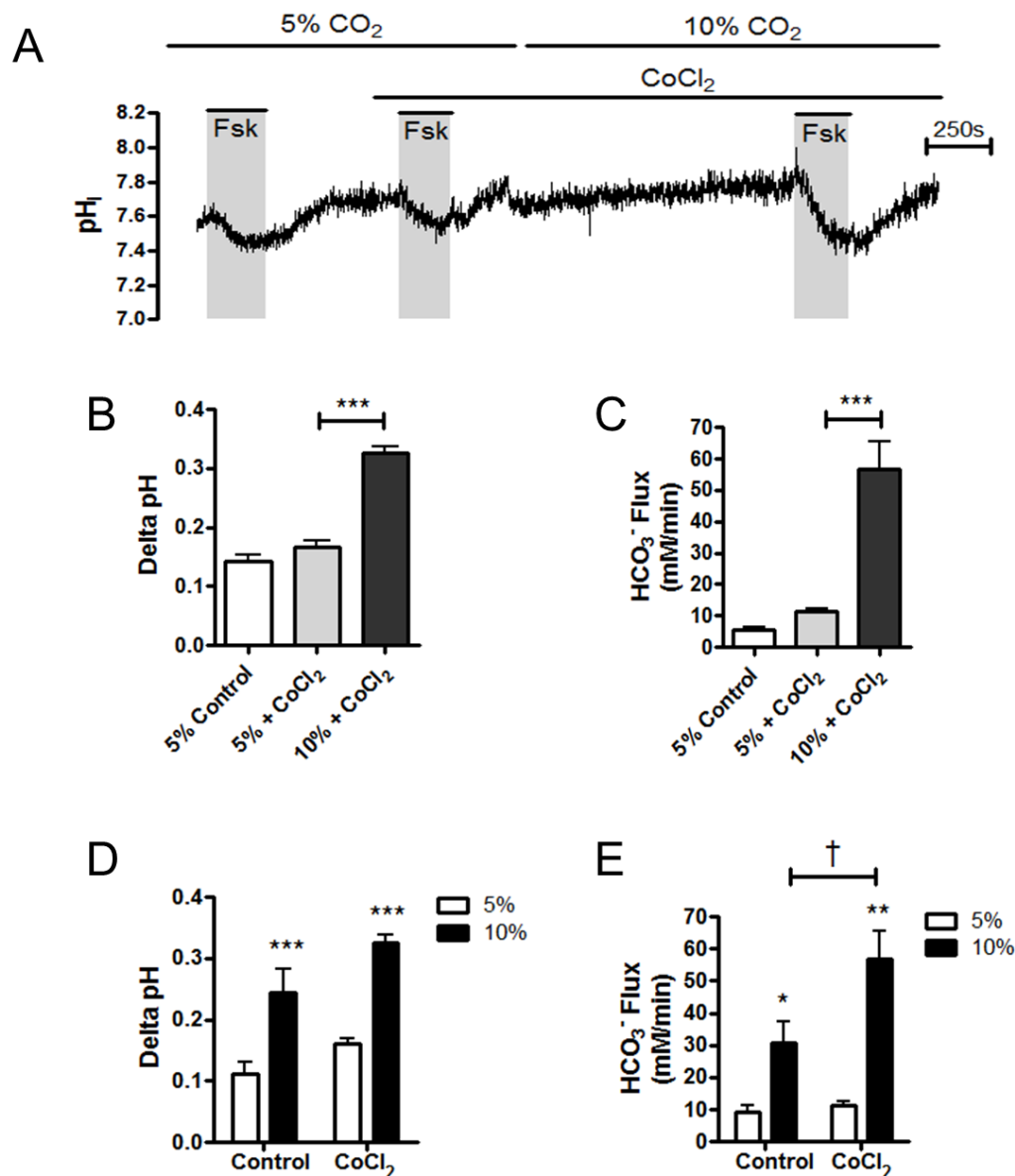


Figure 4.24: Cobalt chloride does not block the effect of hypercapnia on the forskolin-stimulated intracellular acidification. (A) shows a representative experiment in which Calu-3 cells were stimulated with 5 μM forskolin alone or 5 μM forskolin in the presence of cobalt chloride (500 μM) in normocapnia and hypercapnia. The effect of cobalt chloride on the delta pH (B) and HCO₃⁻ flux (C) resulting from forskolin stimulation is summarized. *** = significant effect of hypercapnia (p < 0.05). The effect of cobalt chloride on the delta pH and HCO₃⁻ flux resulting from forskolin stimulation was also compared to control experiments performed on the same day as shown in (D) and (E) respectively. * = significant effect of hypercapnia (p < 0.05; ** = p < 0.01; *** = p < 0.001); † = significant effect of cobalt chloride (p < 0.05). Data represents mean ± S.E.M.; n = 4 for each.

Proadifen has also been reported to be an inhibitor of connexins and has been shown to prevent gap junction mediated dye uptake in the gerbil cochlea (Spiess *et al.*, 2002; Zhao, 2005) as well as ATP release *via* connexins in rat brain tissue (Huckstepp *et al.*, 2010b). Figure 4.25A shows an example experiment of cells treated with proadifen. As with cobalt, proadifen also had no effect on the forskolin-stimulated intracellular acidification in normocapnia, as summarized in figures 4.25B and C. Furthermore, proadifen also had no effect on the pH_i recovery from CO_2 -induced acidosis with cells demonstrating a $73.7 \pm 7.6\%$ recovery of pH_i ($p > 0.05$ vs. control; $n=3$; fig. 4.26). In control experiments performed on the same day, hypercapnia increased the magnitude of the forskolin-stimulated intracellular acidification 2.3 ± 0.1 fold ($p < 0.01$; $n=3$; fig. 4.25D) and the rate of forskolin-stimulated HCO_3^- flux 6.0 ± 0.3 fold ($p < 0.001$; $n=3$; fig. 4.25E). Similar to cobalt, proadifen did not prevent the CO_2 -mediated increase of the forskolin-stimulated intracellular acidification. Here, hypercapnia increased the magnitude of the forskolin-stimulated intracellular acidification 2.0 ± 0.3 fold ($p < 0.05$; $n=3$; fig. 4.25D) and the rate of forskolin-stimulated HCO_3^- flux 3.7 ± 0.6 fold ($p < 0.01$; $n=3$; fig. 4.25E). These data support the findings from the cobalt experiments and therefore imply that there is no role for connexins in mediating the response to hypercapnia. As a result, the effects of carbenoxolone are more likely to be an effect on an offsite target of the drug.

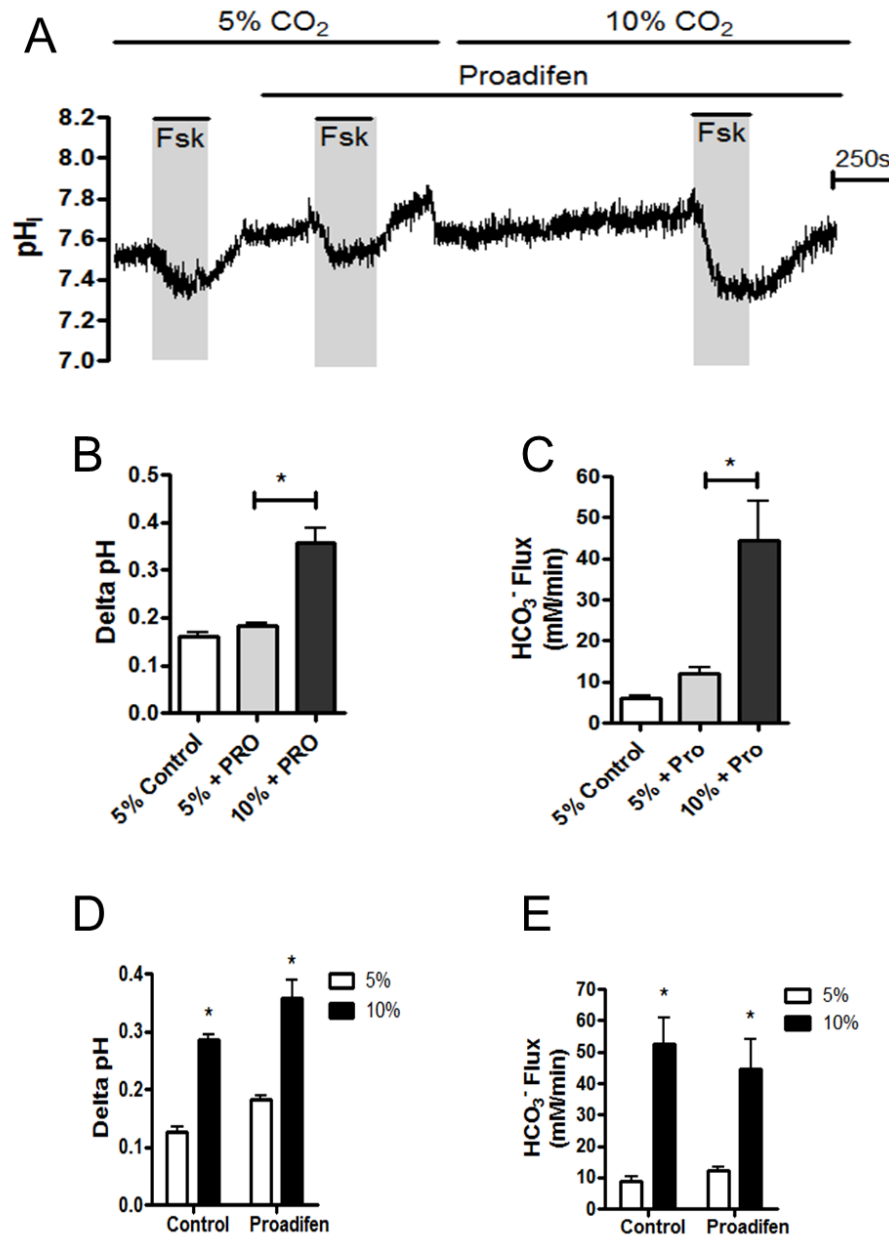


Figure 4.25: Proadifen does not block the effect of hypercapnia on the forskolin-stimulated intracellular acidification. (A) shows a representative experiment in which Calu-3 cells were stimulated with 5 μM forskolin alone or 5 μM forskolin in the presence of proadifen (200 μM) in normocapnia and hypercapnia. The effect of proadifen on the delta pH (B) and HCO_3^- flux (C) resulting from forskolin stimulation is summarized. * = significant effect of hypercapnia ($p < 0.05$). The effect of cobalt chloride on the delta pH and HCO_3^- flux resulting from forskolin stimulation was also compared to control experiments performed on the same day as shown in (D) and (E) respectively. * = significant effect of hypercapnia ($p < 0.05$). Data represents mean \pm S.E.M.; $n=3$ for each.

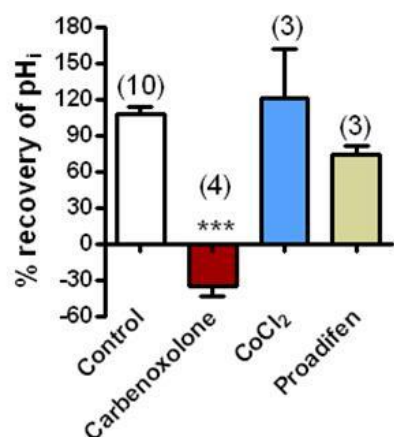


Figure 4.26: The effect of connexin inhibitors on the intracellular pH recovery in response to CO₂-induced acidosis. % recovery of pH_i calculated as described in chapter 3, section 3.3. *** = significant effect of carbenoxolone (p<0.001). Data represents mean ± S.E.M.; n numbers displayed in parenthesis.

4.4.2. Pannexins

Pannexins are proteins that are structurally very similar to connexins but pannexins function as a channel as opposed to having the ability to form gap junctions with neighbouring cells. These channels have been implicated in mediating ATP release in pannexin-1 expressing oocytes (Wang *et al.*, 2013) as well as in primary airway epithelia (Ransford *et al.*, 2009) and Calu-3 cells (Seminario-Vidal *et al.*, 2011) in which it was found that pharmacological inhibition or genetic knockdown of pannexin-1 reduced ATP release. Therefore, pannexins could mediate the proposed CO₂-induced ATP release in Calu-3 cells. Firstly, it was necessary to test whether pannexins were expressed in Calu-3 cells. End-Point PCR revealed a band of expected size (133bp) for pannexin-1 but the product size for pannexin-2 was much larger than expected and suggested the amplified product was not pannexin-2 (fig. 4.27). Thus it appeared only pannexin-1 was expressed in Calu-3 cells.

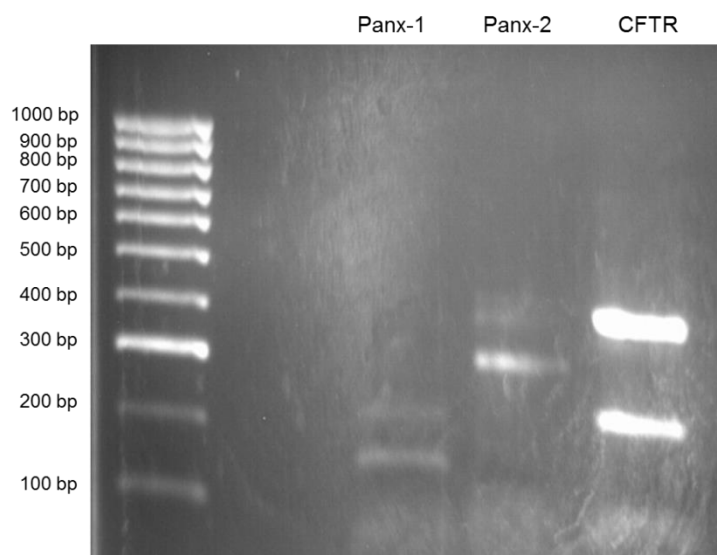


Figure 4.27: Panx-1, but not Panx-2, is expressed in Calu-3 cells. End-point PCR on RNA samples extracted from Calu-3 cells grown as a polarised monolayer were analysed for the expression of members of the pannexin family. CFTR expression was also analysed as a positive control.

To test for a role of pannexins in mediating a possible CO₂-induced ATP release, cells were treated with the pannexin inhibitor probenecid (Silverman *et al.*, 2008). An example experiment is shown in figure 4.28A. As shown in figures 4.28B and C, probenecid treatment alone did not alter the response to forskolin in normocapnic conditions. Furthermore, in the presence of probenecid, hypercapnia caused a 2.2 ± 0.2 fold increase in the magnitude of the forskolin-stimulated intracellular acidification ($p < 0.01$; $n = 4$; fig. 4.28D) and a 3.7 ± 0.5 fold increase in the rate of forskolin-stimulated HCO₃⁻ flux ($p < 0.05$; $n = 4$; fig. 4.28E). However, in control experiments performed on the same day, although hypercapnia caused a similar 2.5 ± 0.1 fold increase in the magnitude of the forskolin-stimulated intracellular acidification ($p < 0.001$; $n = 4$; fig. 4.28D), it caused a markedly higher 6.6 ± 0.8 fold increase in the rate of forskolin-stimulated HCO₃⁻ flux ($p < 0.01$ vs. normocapnia; $p < 0.05$ vs. probenecid treated cells; $n = 4$; fig. 4.28E). These data suggest that the effect of hypercapnia was significantly diminished when compared to untreated cells and indicates pannexins signalling may have a role in mediating the effects of hypercapnia on cAMP-regulated HCO₃⁻ transport in Calu-3 cells.

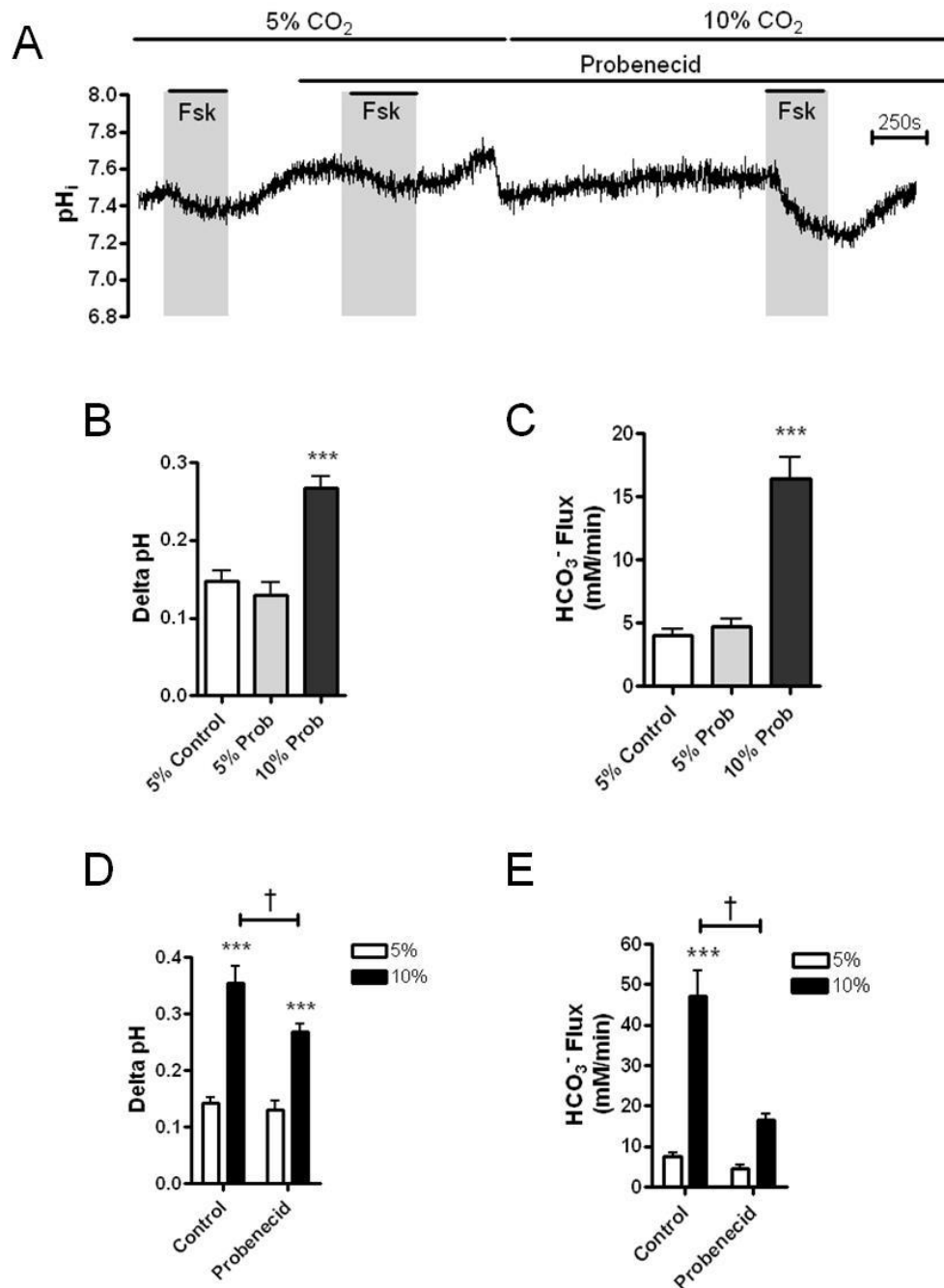


Figure 4.28: Probenecid reduces the effect of hypercapnia on the forskolin-stimulated intracellular acidification. (A) shows a representative experiment in which Calu-3 cells were stimulated with 5 μ M forskolin alone or in the presence of probenecid (500 μ M) in normocapnia and hypercapnia. The effect of probenecid on the delta pH (B) and HCO₃⁻ flux (C) resulting from forskolin stimulation is summarized. *** = significant effect of hypercapnia ($p < 0.001$). The effect of probenecid on the delta pH and HCO₃⁻ flux resulting from forskolin stimulation was also compared to control experiments performed on the same day as shown in (D) and (E) respectively. *** = significant effect of hypercapnia ($p < 0.001$); † = significant effect of probenecid ($p < 0.05$). Data represents mean \pm S.E.M.; $n = 4$ for each.

Interestingly, carbenoxolone has also been reported to inhibit pannexins and as such may explain why carbenoxolone, but not cobalt or proadifen, was able to block the effect of hypercapnia on the forskolin-stimulated intracellular acidification if CO₂ was signalling *via* pannexins as opposed to connexins. Pannexins are more sensitive to carbenoxolone than connexins, with Bruzzone *et al.* (2005) demonstrating 10μM carbenoxolone inhibited pannexin-1-mediated currents but not Cx46-mediated currents when expressed in *Xenopus* oocytes. A representative experiment showing the effects of 10μM carbenoxolone on the forskolin-stimulated intracellular acidification in normocapnia and hypercapnia is shown in figure 4.29A. Figure 4.29C shows that, like for 100μM carbenoxolone, 10μM carbenoxolone also increased the rate of forskolin-stimulated HCO₃⁻ flux in normocapnia from 4.9 ± 0.7mM HCO₃⁻ min⁻¹ to 11.4 ± 1.0mM HCO₃⁻ min⁻¹ (p<0.05; n=3) suggesting carbenoxolone modulates cAMP-regulated HCO₃⁻ transport either directly, or *via* offsite targets. In the presence of carbenoxolone, hypercapnia caused a 1.8 ± 0.2 fold increase in the magnitude of the forskolin-stimulated intracellular acidification (p<0.05; n=3; figs. 4.29B and D) and a 2.9 ± 0.2 fold increase in the rate of forskolin-stimulated HCO₃⁻ flux (p<0.05; n=3; figs. 4.29C and E). However, in control experiments performed on the same day, hypercapnia caused a significantly greater 2.5 ± 0.2 fold increase in the magnitude of the forskolin-stimulated intracellular acidification (p<0.001 *vs.* normocapnia; p<0.05 *vs.* carbenoxolone treated cells; n=3; fig. 4.29D), and a significantly greater 7.1 ± 0.7 fold increase in the rate of forskolin-stimulated HCO₃⁻ flux (p<0.001 *vs.* normocapnia; p<0.001 *vs.* carbenoxolone treated cells; n=3; fig. 4.29E). These results are very similar to those experiments which used probenecid to inhibit pannexins. Although hypercapnia was able to augment HCO₃⁻ flux in carbenoxolone treated cells, the effect of hypercapnia has been significantly diminished when compared to untreated cells. This supports the hypothesis that panx-1 expressed in Calu-3 cells may be sensitive to changes in CO₂ and therefore may induce the release of signalling molecules, such as ATP, that mediate the effects of hypercapnia on cAMP-regulated HCO₃⁻ transport in Calu-3 cells.

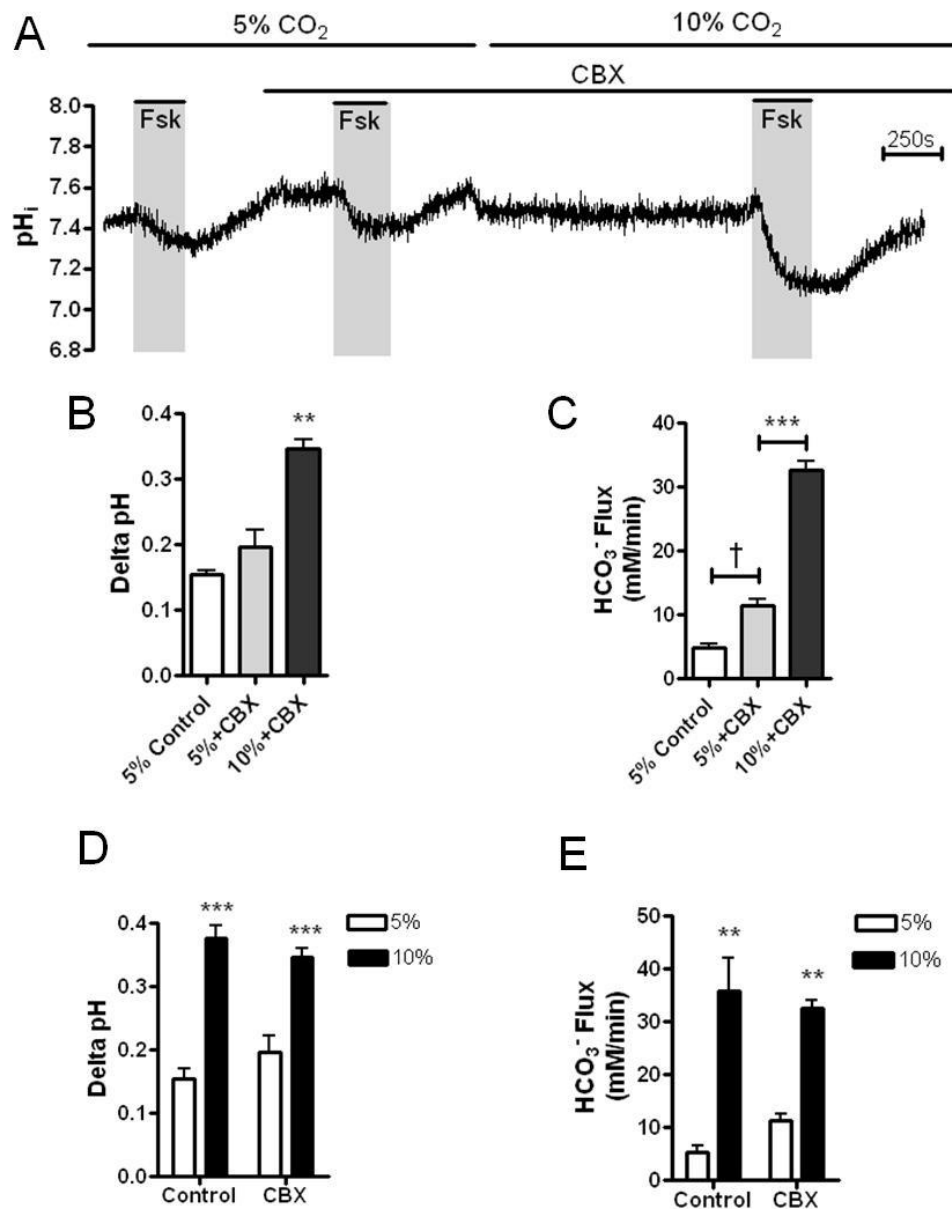


Figure 4.29: A low concentration of carbenoxolone reduces the extent by which hypercapnia enhances the forskolin-stimulated intracellular acidification. (A) shows a representative experiment in which Calu-3 cells were stimulated with 5 μM forskolin alone or 5 μM forskolin in the presence of carbenoxolone (10 μM) in normocapnia and hypercapnia. The effect of carbenoxolone on the ΔpH (B) and HCO_3^- flux (C) resulting from forskolin stimulation is summarized. ** = significant effect of hypercapnia ($p < 0.01$; *** = $p < 0.001$); † = significant effect of carbenoxolone ($p < 0.05$). The effect of carbenoxolone on the ΔpH and HCO_3^- flux resulting from forskolin stimulation was also compared to control experiments performed on the same day as shown in (D) and (E) respectively. ** = significant effect of hypercapnia ($p < 0.01$; *** = $p < 0.001$). Data represents mean \pm S.E.M.; $n=3$ for each.

Seminario-Vidal *et al.* (2011) showed that hypotonicity-induced ATP release in airway epithelia occurred *via* pannexin-1 and was dependent on activation of the mechanosensitive channel TRPV4 and activation of Rho Kinase, implying TRPV4 channels activated Rho Kinase to induce downstream activation of pannexin-1. To determine whether hypercapnia may elicit a pannexin-1-dependent ATP release *via* a similar signalling mechanism, cells were preincubated and perfused with either the TRPV4 inhibitor HC067047 or the Rho Kinase inhibitor H-1152. However, as shown in figure 4.30, neither of these inhibitors prevented the CO₂-mediated increase in either the magnitude of forskolin-stimulated intracellular acidification, or the rate of forskolin-stimulated HCO₃⁻ flux. Thus, if hypercapnia does activate pannexin-1-dependent ATP release, it is not *via* a TRPV4/Rho kinase signalling pathway.

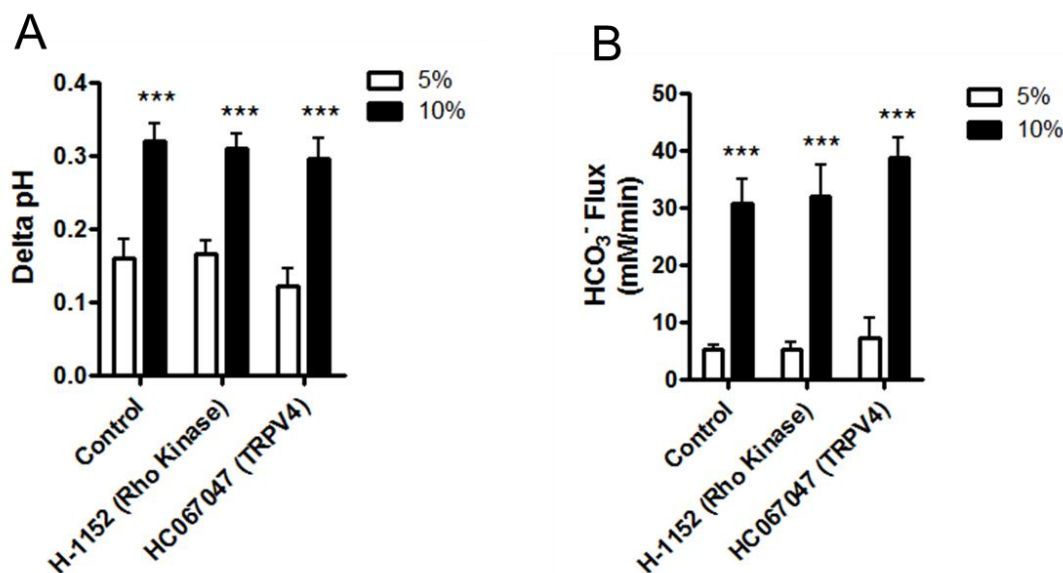


Figure 4.30: Hypercapnia does not mediate its effects on *via* activation of TRPV4 channels and Rho Kinase signalling. Calu-3 cells were stimulated with 5μM forskolin in the presence or absence of H-1152 (1μM) or HC067047 (10μM) in normocapnia and hypercapnia. The delta pH (A) and HCO₃⁻ flux (B) resulting from forskolin stimulation are summarized. *** = significant effect of hypercapnia (p<0.001); Data represents mean ± S.E.M.; n=3 for each.

4.4.3. Exocytosis of ATP-containing vesicles

Next, other reported ATP release pathways were also investigated to assess whether these had a role in the proposed CO₂-induced ATP release in Calu-3 cells. O'Grady *et al.* (2013), demonstrated that exposure of human bronchial epithelial cells to the spores of the allergen

Alternaria alternata caused an ATP release due to Ca^{2+} -dependent exocytosis of ATP-containing vesicles. This study showed brefeldin A, an agent which has been reported to disrupt the microtubule cytoskeleton network (Alvarez and Sztul, 1999) prevented vesicle trafficking and consequentially ATP release in response to *Alternaria* exposure. Therefore, the effect of hypercapnia on the forskolin-stimulated intracellular acidification was assessed in cells which had been preincubated with brefeldin A and an example experiment of brefeldin A treated cells is shown in figure 4.31A. In control experiments performed on the same day, hypercapnia increased the magnitude of the forskolin-stimulated intracellular acidification 1.9 ± 0.1 fold ($p < 0.001$; $n=3$; fig. 4.31B) and the rate of forskolin-stimulated HCO_3^- flux 5.0 ± 0.4 fold ($p < 0.001$; $n=3$; fig. 4.31C). Pretreatment with brefeldin A did not prevent the CO_2 -mediated increase of the forskolin-stimulated intracellular acidification. In these experiments, hypercapnia increased the magnitude of the forskolin-stimulated intracellular acidification 2.1 ± 0.1 fold ($p < 0.001$; $n=3$; fig. 4.31B) and the rate of forskolin-stimulated HCO_3^- flux 4.7 ± 0.2 fold ($p < 0.001$; $n=3$; fig. 4.31C). These data suggest that if CO_2 does induce an ATP release from Calu-3 cells, it is not *via* exocytosis of ATP-containing vesicles.

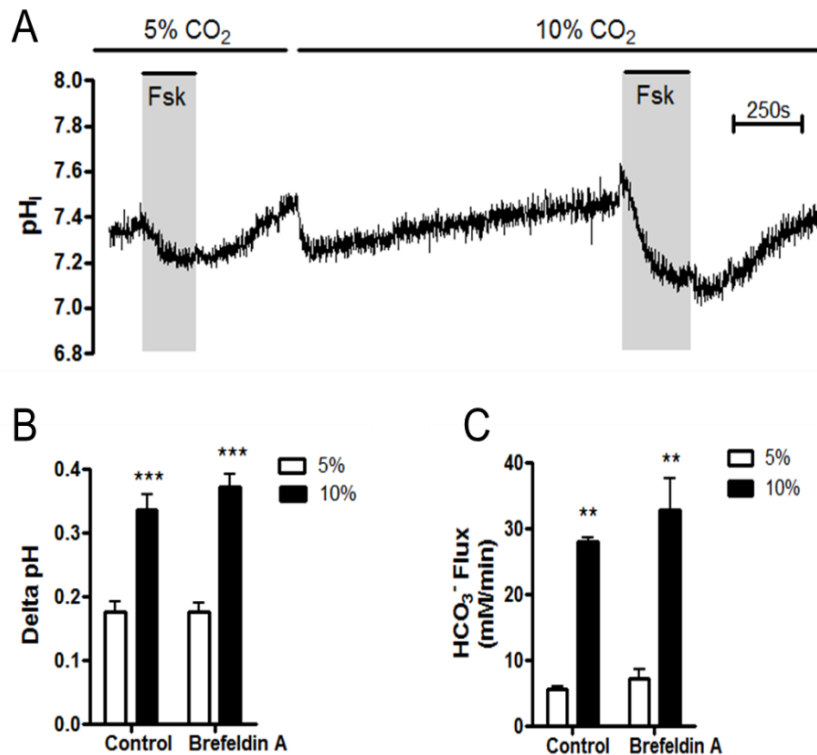


Figure 4.31: Brefeldin A does not block the effects of hypercapnia on the forskolin-stimulated intracellular acidification. (A) shows a representative experiment in which Calu-3 cells were preincubated for one hour with Brefeldin A (5 μ g/ml) and stimulated with 5 μ M forskolin in normocapnia and hypercapnia. The delta pH (B) and HCO_3^- flux (C) resulting from forskolin stimulation are summarized. ** = significant effect of hypercapnia ($p < 0.01$; *** = $p < 0.001$); Data represents mean \pm S.E.M.; $n=3$ for each.

5.4.4. P-glycoproteins

P-glycoprotein-1 - also known as multidrug resistance protein 1 (MDR1) or ABC subfamily B member 1 (ABCB1) - is an ABC transporter with a primary role of transporting xenobiotics out of cells. However, they have also been reported to have ATP transporting capacities (Abraham *et al.*, 1993; Roman *et al.*, 1997). Thus if hypercapnia does stimulate ATP release in Calu-3 cells, it is possible it is *via* activation of P-glycoproteins. Therefore, cells were treated with elacridar, a P-glycoprotein inhibitor which is unable to inhibit MRP transporters (Evers *et al.*, 2000), and the response to forskolin was assessed in normocapnia and hypercapnia as shown in figure 4.32A. Elacridar treatment had no effect on the response to forskolin in normocapnia as shown in figures 4.32B and 4.32C. In control experiments, hypercapnia caused a 2.0 ± 0.2 fold increase in the magnitude of the forskolin-stimulated intracellular acidification ($p < 0.001$; $n=3$; fig. 4.32D) and increased the rate of forskolin-

stimulated HCO_3^- flux 5.6 ± 1.0 fold ($p < 0.001$; $n = 3$; fig. 4.32E). Elacridar treatment had no effect on the CO_2 -mediated change in forskolin-stimulated intracellular acidification. In the presence of elacridar, hypercapnia caused a 1.8 ± 0.1 fold increase in the magnitude of the forskolin-stimulated intracellular acidification ($p < 0.001$; $n = 4$; fig. 4.32D) and increased the rate of forskolin-stimulated HCO_3^- flux 3.5 ± 0.4 fold ($p < 0.05$; $n = 4$; fig. 4.32E). Therefore, these data show that any putative CO_2 -induced ATP release was not mediated *via* P-glycoproteins.

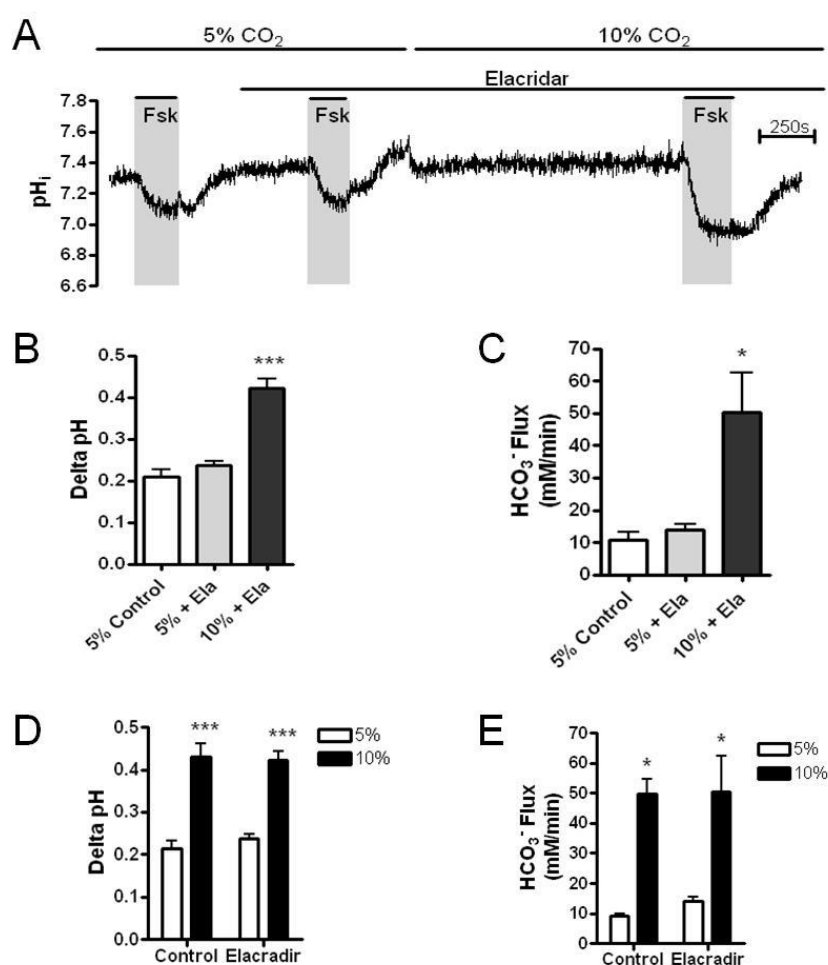


Figure 4.32: Inhibition of P-glycoproteins does not block the effects of hypercapnia on the forskolin-stimulated intracellular acidification. (A) shows a representative experiment in which Calu-3 cells were stimulated with $5\mu\text{M}$ forskolin alone or $5\mu\text{M}$ forskolin in the presence of elacridar (500nM) in normocapnia and hypercapnia. The effect of elacridar on the ΔpH (B) and HCO_3^- flux (C) resulting from forskolin stimulation is summarized. * = significant effect of hypercapnia ($p < 0.05$; *** = $p < 0.001$). The effect of elacridar on the ΔpH and HCO_3^- flux resulting from forskolin stimulation was also compared to control experiments performed on the same day as shown in (D) and (E) respectively. * = significant effect of hypercapnia ($p < 0.05$; *** = $p < 0.001$). Data represents mean \pm S.E.M.; $n = 3$ for controls and $n = 4$ for elacridar treated cells.

In an attempt to measure extracellular ATP to assess whether hypercapnia induced an ATP release in Calu-3 cells, cells were incubated in pregassed, modified high Cl^- Krebs solution in which NaCl , KCl , MgCl_2 and CaCl_2 were replaced with equimolar mannitol. The reason for this modification was because the luciferase assay used to detect ATP was highly sensitive to salt. After 20 minutes incubation, the apical and basolateral solutions were collected and ATP content in the fluid was measured. Figure 4.33 summarizes the data. In normocapnia, the amount of ATP in the apical and basolateral solutions was $23.4 \pm 11.3\text{nM}$ ($n=3$) and $73.0 \pm 45.8\text{nM}$ ($n=3$) respectively. These levels were unaffected by probenecid treatment (apical ATP = $43.6 \pm 25.1\text{nM}$ ($p>0.05$; $n=3$); basolateral ATP = $143.3 \pm 106.9\text{nM}$ ($p>0.05$; $n=3$)). In hypercapnia, the amount of apical ATP was $11.6 \pm 2.7\text{nM}$ ($p>0.05$ vs normocapnia; $n=3$) and the amount of basolateral ATP was $8.0 \pm 2.0\text{nM}$ ($p>0.05$ vs normocapnia). Again there was no effect of probenecid on the ATP measured in hypercapnic conditions. Together, these data suggest hypercapnia does not elicit an ATP release from probenecid-sensitive transporters in Calu-3 cells.

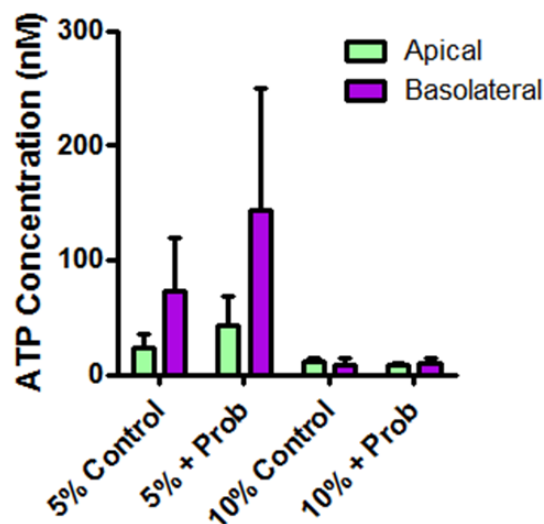


Figure 4.33: Acute hypercapnia does not increase the extracellular concentration of ATP. Calu-3 cells were incubated in modified Krebs solutions that were buffered to pH 7.4 for each CO_2 concentration and contained either 0.05% DMSO or $500\mu\text{M}$ probenecid. After 20 minutes incubation, the apical and basolateral fluid was collected and ATP concentration measured using a luciferase assay. Data represents mean \pm S.E.M., $n=3$ for each.

4.5. Other potential targets for CO₂ signalling

4.5.4. NADPH Oxidase

It has been shown that dual oxidase, a member of the NADPH Oxidase family, is activated by an acid load (i.e. hypercapnia) *via* a Ca²⁺-dependent mechanism (Seidler, 2013). Activation of dual oxidase causes an increased production of H₂O₂ (Ameziane-El-Hassani *et al.*, 2005) which may impact upon cAMP-regulated HCO₃⁻ transport. To test the role of dual oxidase in mediating the response to hypercapnia, Calu-3 cells were treated with the dual oxidase inhibitor DPI as shown in figure 4.34A. DPI treatment caused no significant changes to the forskolin-stimulated intracellular acidification in normocapnia as shown in figs 4.34B and C. In control experiments, hypercapnia caused a 1.9 ± 0.1 fold increase in the magnitude of the forskolin-induced acidification ($p < 0.01$; $n = 3$; fig. 4.34D) and increased the rate of forskolin-stimulated HCO₃⁻ flux 6.6 ± 0.5 fold ($p < 0.01$; $n = 3$; fig. 4.34E). In DPI treated cells, hypercapnia caused a 1.6 ± 0.1 fold increase in the magnitude of the forskolin-induced acidification ($p < 0.05$; $n = 3$; fig. 4.34B and D). However, although hypercapnia induced a 3.0 ± 0.5 fold increase in the rate of forskolin-stimulated HCO₃⁻ flux ($p < 0.05$; $n = 3$; fig. 4.34E), this was significantly lower than seen in control experiments ($p < 0.01$; $n = 3$) and suggests that dual oxidase inhibition may prevent the effects of hypercapnia on cAMP-regulated HCO₃⁻ transport.

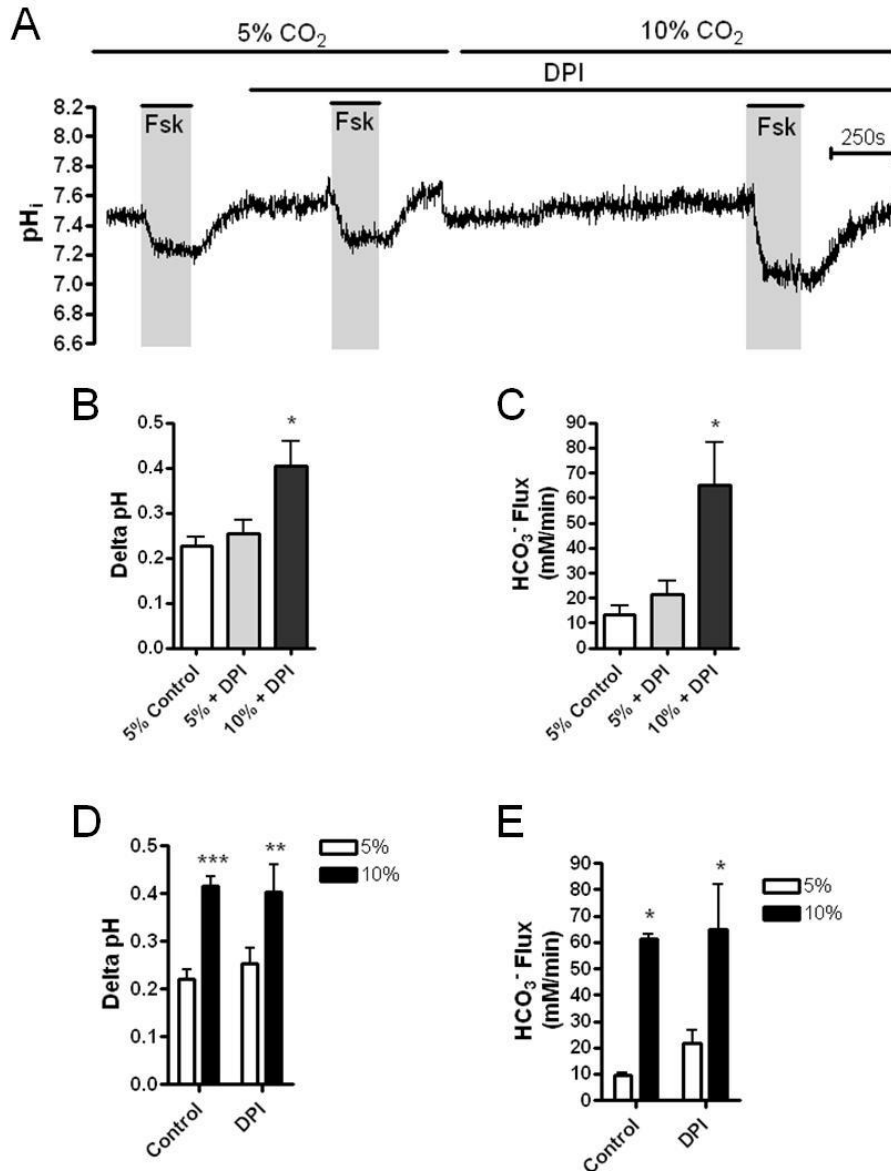


Figure 4.34: Dual oxidase inhibition reduces the effects of hypercapnia on the forskolin-stimulated intracellular acidification. (A) shows a representative experiment in which Calu-3 cells were stimulated with 5 μ M forskolin alone or 5 μ M forskolin in the presence of DPI (10 μ M) in normocapnia and hypercapnia. The effect of DPI on the delta pH (B) and HCO₃⁻ flux (C) resulting from forskolin stimulation is summarized. * = significant effect of hypercapnia (p<0.05). The effect of DPI on the delta pH and HCO₃⁻ flux resulting from forskolin stimulation was also compared to control experiments performed on the same day as shown in (D) and (E) respectively. * = significant effect of hypercapnia (p<0.05; ** = p<0.01 *** = p<0.001). Data represents mean \pm S.E.M.; n=3 for each.

4.6. Discussion

4.6.1. Indications that acute hypercapnia induced an IP₃-dependent Ca²⁺ release to modulate cAMP signalling in Calu-3 cells

As described in chapter 3, hypercapnia altered cAMP-dependent HCO₃⁻ transport in Calu-3 cells but this was not due to a change in the activity in cAMP-stimulated CFTR or NBC, but appeared to be due to CO₂-modulation of basal NBC activity and/or basolateral Na⁺/K⁺-ATPase. The present chapter aimed to investigate whether there were upstream signalling mechanisms involved in transduction of the CO₂ signal to modulate cAMP signalling. The particular emphasis was on the role of Ca²⁺ signalling, given that CO₂ has been found to alter intracellular Ca²⁺ levels to mediate effects on Na⁺/K⁺-ATPase activity in rat alveolar type II cells (Briva *et al.*, 2007; Vadasz *et al.*, 2008) and cAMP signalling in renal epithelia (Cook *et al.*, 2012). Here, I have shown that the effects of hypercapnia on cAMP-dependent HCO₃⁻ transport was dependent on PLC-mediated mobilization of intracellular Ca²⁺ as the effect of hypercapnia on cAMP-regulated HCO₃⁻ transport was eliminated in the presence of BAPTA-AM, the PLC inhibitor U73122 and the IP₃R inhibitor, 2-APB. Furthermore, BAPTA-AM and 2-APB also abolished the effect of hypercapnia on forskolin-stimulated elevations in [cAMP]_i suggesting IP₃-dependent Ca²⁺ release mediates the effect of hypercapnia on tmAC and/or MRPs to reduce [cAMP]_i. These findings support a similar mechanism to that already described by our laboratory (Cook *et al.*, 2012). The effect of BAPTA-AM and 2-APB on [cAMP]_i was interesting in that these agents did not alleviate the CO₂-induced reduction in [cAMP]_i but rather appeared to bring down [cAMP]_i in normocapnia to that of the level seen in hypercapnia. These data perhaps imply that intracellular Ca²⁺ signalling is required to generate maximal increases in forskolin-stimulated [cAMP]_i and would support findings by Tian and Laychock (2001) who demonstrated that BAPTA-AM reduced forskolin-stimulated cAMP levels in rat islet β cells. Lee and Foskett (2010) have also shown that forskolin stimulated an increase in [Ca²⁺]_i in pig serous cells which may underlie a mechanism by which tmAC are able to become fully activate by forskolin. The effects of BAPTA-AM on forskolin-stimulated HCO₃⁻ transport were similar in that BAPTA-AM did not simply bring the values measured in 10% CO₂ down to the 5% CO₂ level; rather BAPTA-AM increased the magnitude of the pH change measured in 5% to the 10% level. Furthermore, as well as reducing the rate of forskolin-stimulated HCO₃⁻ flux in 10% CO₂, BAPTA-AM also increased the rate of forskolin-stimulated HCO₃⁻ flux in normocapnia so that the two values in BAPTA-AM treated cells were effectively at an intermediate level between 5% and 10%

control values (although these values were not statistically significantly different to control values). Unfortunately, it wasn't tested whether BAPTA-AM, U73122 or 2-APB were able to eliminate the effect of hypercapnia on forskolin-stimulated I_{sc} and these would be useful experiments to perform to further establish whether CO_2 mediates its effects on cAMP signalling *via* changes in $[Ca^{2+}]_i$. Hypercapnia was still able to modulate forskolin-stimulated intracellular acidification in the absence of extracellular Ca^{2+} thus demonstrating that the CO_2 -induced changes in intracellular Ca^{2+} were due to mobilization of intracellular Ca^{2+} and not dependent on extracellular Ca^{2+} . This supports findings from Bouyer *et al.* (2003) who also showed no requirement for extracellular Ca^{2+} in CO_2 -induced changes in intracellular Ca^{2+} .

Further evidence that the effect of hypercapnia on the cAMP-stimulated intracellular acidification is dependent on changes in intracellular Ca^{2+} were from the findings that increasing intracellular Ca^{2+} in normocapnia mimicked the effect of hypercapnia. The Ca^{2+} agonists carbachol, ATP and UTP all significantly enhanced the magnitude and the rate of the forskolin-stimulated intracellular acidification in normocapnia although this was not quite as pronounced as the effect of acute hypercapnia. Inhibition of cholinergic receptors or purinergic receptors prevented the effect of carbachol and ATP respectively. These findings suggested that increases in intracellular Ca^{2+} due to activation of G_q coupled receptors and subsequent PLC-dependent IP_3 -mediated Ca^{2+} release underlied the effect of hypercapnia. The effects of carbachol and ATP were both dependent on the membrane on to which they were applied with basolateral carbachol or basolateral ATP producing a much greater effect than apical carbachol or apical ATP. These findings imply that either Calu-3 cells express cholinergic and purinergic receptors predominantly at the basolateral membrane or that only increases in Ca^{2+} at the basolateral pole is able to mimic the effect of hypercapnia, possibly due to the fact that the apparent CO_2 -sensitive transporters, the Na^+/K^+ -ATPase and NBC, are also expressed at the basolateral membrane and may be affected by a localized increase in Ca^{2+} . A common finding in experiments in which either intracellular or extracellular Ca^{2+} was reduced was the inability of Calu-3 cells to recover intracellular pH from CO_2 -induced acidosis. As discussed in chapter 3, hypercapnia caused an upregulation of NBC and a reduction in AE2 activity to favour an increase in HCO_3^- accumulation across the basolateral membrane. This appears to be the mechanism for pH_i recovery in Calu-3 cells after acidosis. Therefore, these results suggest that CO_2 -induced upregulation of NBC activity is Ca^{2+} dependent. Consistent with this hypothesis, Thornell *et al.* (2012) demonstrated that NBCe1

activity was enhanced by both PIP₂ and IP₃ injection into *Xenopus* oocytes with PIP₂-induced NBCe1 activation blocked by PLC inhibition with U73122. Furthermore, upregulation of NBCe1 activity was also sensitive to BAPTA-AM. Therefore, NBCe1 activity appears to be regulated by [Ca²⁺]_i and, as discussed in chapter 3, CO₂-induced upregulation of NBC activity under basal conditions may underlie the effect of hypercapnia on the forskolin-stimulated intracellular acidification. Therefore, should CO₂ regulate basal NBC activity due to increases in [Ca²⁺]_i, it would explain why inhibition of Ca²⁺ signalling negates the effect of hypercapnia on forskolin-stimulated intracellular acidification. Furthermore, it would also explain why, in conditions where changes in [Ca²⁺]_i were prevented, recovery of pH_i from CO₂-induced acidosis was impaired.

In a similar fashion, the Ca²⁺ mobilizing agonists endothelin, angiotensin II and 5-HT have all been shown to activate Na⁺/K⁺-ATPase in a variety of cell types whilst addition of exogenous phospholipase C also upregulated Na⁺/K⁺-ATPase activity in rat hepatic cells (Lynch *et al.*, 1986; Middleton *et al.*, 1990; Gupta *et al.*, 1991). Yuan *et al.* (2005) have also shown that Na⁺/K⁺-ATPase can physically interact with both PLC and IP₃ receptors implying any Ca²⁺-mediated modulation of Na⁺/K⁺-ATPase is highly localized in a subcellular microdomain. Thus we can speculate that hypercapnia increases IP₃-dependent Ca²⁺ release at the basolateral pole of Calu-3 cells to activate Na⁺/K⁺-ATPase which, with its reported H⁺ transporting capacities, can contribute to changes in cytosolic pH. Thus, inhibition of increases in Ca²⁺ with BAPTA-AM, U73122 and 2-APB, or Na⁺/K⁺-ATPase with ouabain, eliminates the effect of hypercapnia. It is worth noting that it has been reported that ouabain can increase intracellular Ca²⁺ in cardiac myocytes (Tian *et al.*, 2001) although this appears to be *via* a MAPK-dependent pathway, which would not be predicted to mimic the effect of hypercapnia. In summary, these findings suggest acute hypercapnia induces the release of G_q coupled receptor agonists, potentially either ATP, UTP or both, which signal to alter cAMP-regulated HCO₃⁻ transport. However, it is possible that CO₂ may not induce the release of either agents and simply the effect of ATP and UTP is due to a purinergic signalling pathway that modulates HCO₃⁻ transport *via* a different mechanism to hypercapnia. Indeed, addition of ATP alone does produce a Ca²⁺-dependent, transient acidification and therefore what simply may be being observed is an additive effect of ATP and forskolin such that the resulting acidification is augmented and therefore appears to mimic the effect of acute hypercapnia.

My work is the first work to assess the effects of hypercapnia on the expression of IRBIT, a recently discovered regulator of HCO₃⁻ transport. Acute hypercapnia appeared to reduce the

expression of p-IRBIT, therefore implying that the amount of IRBIT capable of binding to IP_3 receptors was reduced, suggesting elevations in IP_3 may have displaced some of the IP_3 R-bound IRBIT. This, therefore, supports the hypothesis that hypercapnia can induce a PLC-dependent increase in IP_3 in Calu-3 cells of which one major effect would be to increase the amount of unbound IRBIT to contribute to CO_2 -induced changes in HCO_3^- transport. However, acute hypercapnia did not increase the amount of non-phosphorylated IRBIT suggesting hypercapnia may induce degradation of p-IRBIT rather than dephosphorylation. Thus, although CO_2 may reduce p-IRBIT due to an elevation in IP_3 , this does not translate to an increased expression of IRBIT capable of binding to and regulating cAMP-regulated HCO_3^- transporters. Further investigations into the role of IRBIT in cAMP-regulated HCO_3^- secretion in Calu-3 cells is important and generation of IRBIT KO cells should provide valuable insights into the role of this protein in coordinating HCO_3^- transport in these cells as well as its sensitivity to altered CO_2 environments.

4.6.2. How do potential modulations of Ca^{2+} affect cAMP signalling?

Should hypercapnia stimulate an IP_3 -dependent Ca^{2+} release in Calu-3 cells, the link between CO_2 -induced elevations in $[\text{Ca}^{2+}]_i$ and CO_2 -induced reduction in $[\text{cAMP}]_i$ and subsequent modulation of cAMP-regulated HCO_3^- transport must be determined. The data from chapter 3 implicated CO_2 caused a reduction in forskolin-stimulated cAMP levels due to reductions in tmAC activity and/or activation of MRP-mediated cAMP efflux. Thus, one must consider that tmAC and MRPs are regulated by Ca^{2+} and thus sensitive to CO_2 -induced changes in $[\text{Ca}^{2+}]_i$. Of the 9 isoforms of tmACs, it has been shown that AC5 and AC6 are primarily inhibited by elevations in $[\text{Ca}^{2+}]_i$ (Cooper *et al.*, 1998; Hu *et al.*, 2002) and therefore a depression of the activity of these enzymes by Ca^{2+} could underlie the effect of acute hypercapnia on forskolin-stimulated elevations in $[\text{cAMP}]_i$. For comprehensive reviews of AC regulation see Hanoune and Defer (2001) and Cooper (2003). Therefore, determining which tmAC isoforms are expressed in Calu-3 cells will be important to understand further the influence of Ca^{2+} signalling on tmAC-dependent cAMP production. The regulation of tmAC by Ca^{2+} has been well described but what is less well understood is the regulation of MRPs by Ca^{2+} . Very little evidence exists on the regulation of MRPs directly by Ca^{2+} but Gekeler *et al.* (1995) describe that inhibition of PKC inhibits MRP in MRP overexpressing human leukaemia cells suggesting that PKC is able to regulate MRPs. Therefore, should CO_2

activate PLC-dependent PIP_2 hydrolysis to induce IP_3 -dependent Ca^{2+} release and activation of DAG, the resulting activation of PKC may modulate MRPs in Calu-3 cells such that cAMP efflux is enhanced.

4.6.3. Indications that acute hypercapnia does not induce an IP_3 -dependent Ca^{2+} release to modulate cAMP signalling in Calu-3 cells

Although the effects of hypercapnia on cAMP-regulated HCO_3^- transport were inhibited by BAPTA-AM, U73122 and 2-APB, and therefore suggested a CO_2 -induced IP_3 -dependent Ca^{2+} release was involved in mediating the effects of hypercapnia, several experiments provided evidence that this wasn't the case. Perhaps most importantly, depletion of the ER Ca^{2+} stores by exposing cells to thapsigargin in the absence of extracellular Ca^{2+} , did not eliminate the effect of hypercapnia, thus implying IP_3 -dependent Ca^{2+} release was not involved in mediating the CO_2 effect. Therefore, should hypercapnia induce a rise in $[\text{Ca}^{2+}]_i$, this appears to be from a thapsigargin-insensitive store and thus cannot be the ER. Interestingly, under these conditions, one must consider that socAMPs, as proposed by Lefkimmatis *et al.* (2009), may be activated should Calu-3 cells be capable of signalling in this fashion, which may contribute to changes in cAMP-regulated HCO_3^- transport and potentially mask an effect of ER depletion of Ca^{2+} . However, when attempting to measure intracellular Ca^{2+} by loading cells with the Ca^{2+} -sensitive dye Fura-2-AM, it was found that hypercapnia did not increase intracellular Ca^{2+} and thus argued against a CO_2 -induced IP_3 -dependent Ca^{2+} release. Therefore, how does one explain the findings from experiments involving BAPTA-AM, U73122 and 2-APB? As with any pharmacological inhibitors, it is always difficult to be certain of their targets. Although U73122 is widely reported as an inhibitor of PLC (Bleasdale *et al.*, 1990; Jin *et al.*, 1994), Klein *et al.* (2011) demonstrated that U73122 actually enhanced PIP_2 hydrolysis by human $\text{PLC}\beta$ and γ whilst Mogami *et al.* (1997) have shown U73122 caused a Ca^{2+} release in pancreatic acinar cells arguing against its function as an inhibitor of PLC-dependent Ca^{2+} mobilization. Similarly, 2-APB has been suggested to be an ineffective inhibitor of IP_3R with Gregory *et al.* (2001) demonstrating 2-APB was unable to prevent IP_3 -induced Ca^{2+} release in rat hepatocytes whilst offsite effects, including inhibition of Ca^{2+} release activated current (I_{CRAC}) (Prakriya and Lewis, 2001) and inhibition of Cx26 and 32 (Tao and Harris, 2007) have also been reported. Therefore, one must consider that U73122 and 2-APB may not be having the desired effect on Ca^{2+}

homeostasis and consequentially, genetic ablation of either PLC or IP₃Rs need to be performed to assess whether hypercapnia still mediates its effects in these genetically modified cells. It is worth noting that the cells used for intracellular Ca²⁺ measurements were grown non-polarised on glass as opposed to a polarised monolayer on plastic which will likely affect the cell properties, protein expression profile and thus potentially impair their CO₂ sensitivity and/or Ca²⁺ release mechanisms. I have shown that Calu-3 cells grown on coverslips exhibit identical recovery in pH_i from CO₂-induced acidosis as polarized cells suggesting that non-polarized cells do respond to acute hypercapnia in a similar fashion to polarized cells yet whether the molecular signalling mechanisms remain the same is yet to be determined. Furthermore, should CO₂ induce a highly localized increase in intracellular Ca²⁺, this assay may not be sensitive enough to detect this increase. Therefore, although the data from these experiments imply elevations in CO₂ did not cause Ca²⁺ mobilization in Calu-3 cells, more experiments are needed to ensure this is the case; primarily being able to measure changes in intracellular Ca²⁺ on polarized Calu-3 cells.

As discussed previously, addition of exogenous ATP was found to mimic the effect of hypercapnia and suggested CO₂ may induce a release of ATP to activate IP₃-dependent Ca²⁺ release *via* activation of purinergic receptors – a mechanism that has already been reported by Huckstepp *et al.* (2010b) in rat brain tissue. However, several experiments suggested this was not the case. Firstly, a non-specific purinergic receptor, suramin, was unable to block the effect of hypercapnia on the forskolin-stimulated intracellular acidification implying that the purinergic receptors were not involved in transducing the CO₂ signal. Secondly, addition of exogenous apyrase to break down ATP into ADP + P_i also was unable to block the effect of hypercapnia on the forskolin-stimulated intracellular acidification, implying that extracellular ATP is not required for transducing the CO₂ signal. One limitation of this experiment, however, was that apyrase was added over 20 minutes after cells had been exposed to hypercapnia due to limited availability of the enzyme. If an ATP release was occurring in response to hypercapnia, it would be likely that, after several minutes in hypercapnia, a high amount of ATP would have already been released into the extracellular medium and as a result addition of apyrase at this point may not be sufficient to markedly reduce total extracellular ATP levels. Thus, it would be interesting to see the effects of adding apyrase prior to exposing the cells to hypercapnia as these conditions would likely favour greater ATP metabolism. Finally, an ATP luciferase assay revealed that there was no measureable increase in extracellular ATP in cells exposed to acute hypercapnia. Again, these experiments

were limited due to the fact that the assay was highly sensitive to high salt concentrations and, as a result, the high Cl^- Krebs solution had to be modified to eliminate NaCl, KCl, CaCl_2 , and MgCl_2 to be replaced with mannitol. This non-physiological solution could have implications for the cells ability to respond to CO_2 and/or release ATP into the extracellular medium. Furthermore, extra care had to be taken when handling the plate in which the cells were located. Movement of fluid flowing over the surface of the cells does induce a mechanosensitive ATP release (Button *et al.*, 2007) and it is highly unlikely that the degree of mechanical stimulation would have been identical for all samples. Therefore the large variation in ATP levels measured, particularly in normocapnia, could be attributed to mechanostimulation of cells during handling of the plate.

Although exogenous ATP mimicked the effect of hypercapnia in normocapnia, there was little evidence to suggest that ATP release was occurring from these cells. One alternative was that CO_2 was inducing an ATP release but it was being rapidly broken down into adenosine by extracellular 5'-nucleotidases and it was adenosine signalling that was actually stimulating changes in cAMP-regulated HCO_3^- transport in hypercapnia. This would explain the lack of effect of apyrase and suramin on the effects of hypercapnia. However, inhibition of adenosine receptors using CGS-15943 was also unable to block the effect of hypercapnia on the forskolin-stimulated intracellular acidification, suggesting that adenosine signalling also does not underlie the effects of hypercapnia.

Experiments in which known release pathways of ATP were inhibited provided further insights into whether CO_2 induced an ATP release. Of the three connexin inhibitors tested, only carbenoxolone (100 μM) had an effect on cAMP-regulated HCO_3^- transport. Carbenoxolone abolished the effect of hypercapnia on the forskolin-stimulated intracellular acidification though, interestingly, similar to what was observed in BAPTA-AM treated cells, carbenoxolone increased both the forskolin-stimulated intracellular acidification in normocapnia and reduced the forskolin-stimulated intracellular acidification in hypercapnia to produce an intermediate value between the control values measured in normocapnia and hypercapnia. Also similar to BAPTA-AM was that carbenoxolone prevented pH_i recovery from CO_2 -induced acidosis. Neither CoCl_2 nor proadifen had the same effects as carbenoxolone which suggested that CO_2 was not inducing an ATP release *via* connexin hemichannels and the effect of carbenoxolone was actually an offsite target. Given the similar effects of BAPTA-AM, it suggests that carbenoxolone may be able to influence intracellular Ca^{2+} levels which would support findings from both Bramley *et al.* (2011) who reported that

100 μ M carbenoxolone blocked increases in intracellular Ca^{2+} in retinal ganglion cells and Rouach *et al.* (2003) who demonstrated that carbenoxolone prevented Ca^{2+} oscillations in neuronal cells isolated from rat hippocampus. In Calu-3 cells, it has been reported that both Cx32 and Cx43 are expressed. Interestingly, Huckstepp *et al.* (2010a) identified that Cx43 is actually insensitive to CO_2 and therefore suggest that CO_2 -induced activation of connexin-dependent ATP release may be unlikely in Calu-3 cells given the members of the connexin family expressed in these cells.

Similar to connexins, the related family of proteins, the pannexins, have also been implicated in ATP transport. End-point PCR experiments revealed Calu-3 cells expressed pannexin-1 and therefore possessed another potentially CO_2 -sensitive transporter. Although hypercapnia still significantly increased the rate of forskolin-stimulated HCO_3^- flux in the presence of the non-specific pannexin inhibitor, probenecid, or a low concentration of carbenoxolone (10 μ M), the extent of this increase was significantly smaller than in control experiments and suggested pannexins may have a minor role in mediating the CO_2 effect. However, more specific inhibitors of pannexins are needed before this can be fully concluded. I have already discussed potential offsite targets of carbenoxolone and these may still occur at the lower concentration of the drug. Probenecid has numerous offsite targets including the multidrug resistance proteins (MRPs) (Gollapudi *et al.*, 1997) and, in chapter 3, it was shown that inhibition of MRPs blocked the effect of hypercapnia and therefore probenecid may be inducing similar but less potent effects here. Experiments on cells that have had panx-1 genetically knocked out would provide further insights into whether panx-1 is CO_2 -sensitive and is involved in the effect of acute hypercapnia on cAMP-regulated HCO_3^- transport.

In summary, the transduction of the CO_2 signal to modulate cAMP-regulated HCO_3^- transport appears to be dependent on PLC-induced Ca^{2+} mobilization. Yet how CO_2 is able to do this still remains unresolved. The data suggests CO_2 may induce the release of a G_q coupled receptor agonist in order to stimulate Ca^{2+} mobilization at the basolateral pole but the evidence for the release of the prime candidate, ATP, is minimal. As a result, investigations into whether hypercapnia can stimulate the release of other endogenous cell signalling molecules need to be performed. For example, hypercapnia has been shown to trigger the release of prostaglandin E_2 (PGE_2) from human endothelial cells (Kovecs 2001) and Palmer *et al.*, (2006) have demonstrated increases in I_{sc} in Calu-3 cells in response PGE_2 treatment, as

well as expression of prostaglandin receptors at the mRNA level showing extracellular prostaglandins elicit physiological responses in Calu-3 cells. Interestingly, the PGE₂ receptor EP₃ has been shown to regulate adenylyl cyclase activity *via* activation of the PLC/Ca²⁺ signalling pathway (Yamaoka *et al.*, 2009) and indicating prostaglandins can mediate crosstalk between cAMP and Ca²⁺ signalling. Similarly, Scheckenbach *et al.* (2011) demonstrated that Calu-3 cells express the PGE₂ receptor EP₄ and that adenosine-stimulated CFTR activity was dependent on PGE₂ signalling, mediated, in part, by activation of gap junctional intercellular communication. Also of interest is that prostaglandins are transported by MRP transporters (Reid *et al.*, 2003), which may explain why inhibition of these transporters using MK-571 is able to prevent the effect of hypercapnia on the forskolin-stimulated intracellular acidification. Thus, investigations into whether hypercapnia can stimulate the release of other endogenous Ca²⁺ mobilizing agents should form the basis of future work into this area.

The major findings of this chapter are summarized below and in figure 4.35.

- The effects of acute hypercapnia on cAMP-regulated HCO₃⁻ transport were dependent on PLC-dependent mobilization of intracellular Ca²⁺.
- The effects of acute hypercapnia were mimicked by the Ca²⁺ elevating agonists carbachol, ATP and UTP but there was little evidence to suggest CO₂ is inducing an ATP release to signal to cells as suggested in other tissue (Huckstepp *et al.*, 2010b).
- Potentially, CO₂ may induce the release of an unidentified endogenous Ca²⁺ elevating agent with pannexins possibly being involved in this release process.
- Acute hypercapnia appeared to reduce expression of p-IRBIT suggesting a reduction in IRBIT binding to IP₃ receptors which could be a result of elevated levels of cytosolic IP₃.

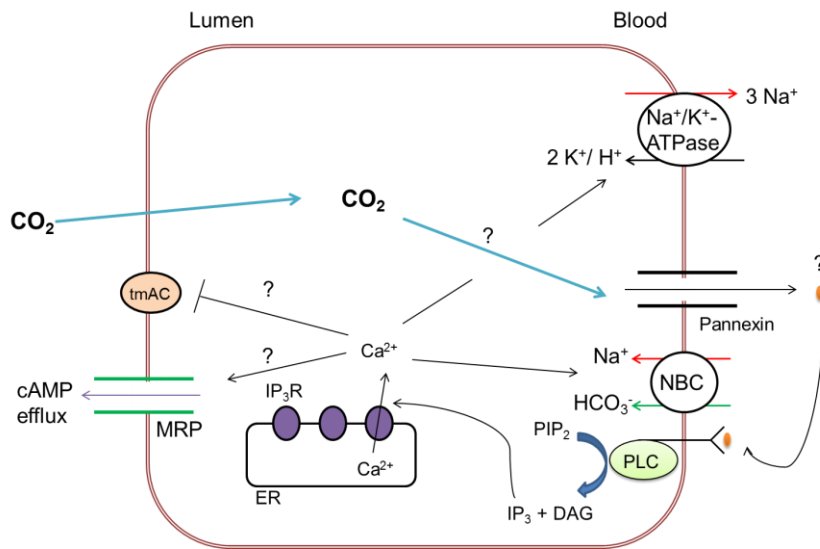


Figure 4.35: Proposed mechanism for CO₂-induced mobilization of Ca²⁺ and the potential effects this has on cAMP-regulated HCO₃⁻ transport. CO₂ potentially causes a pannexin-dependent release of an endogenous Ca²⁺ elevating agent which activates cell surface receptors to increase IP₃ formation and induce Ca²⁺ release *via* activation of IP₃Rs. Elevations in intracellular Ca²⁺ may impact upon cAMP signalling due to inhibition of tmAC and/or activation of MRP-dependent cAMP efflux as well as modulating the activity of Na⁺/K⁺-ATPase, contributing to observed effects on cAMP-regulated HCO₃⁻ transport.

Chapter 5: **The effects of chronic hypercapnia on Calu-3 cells**

5.1. Introduction

The previous chapters focussed on the effects of acute hypercapnia (20-30 minutes) on Calu-3 cell physiology, in particular cAMP-regulated HCO_3^- transport. Over this time frame, one would predict that the effects of hypercapnia were a direct effect on key cell signalling components, as opposed to more long term effects such as CO_2 -induced changes in gene expression. Given a large body of evidence focuses on the role of CO_2 impacting upon cell signalling pathways, less is understood on the effect of chronic hypercapnia on animal physiology. Older studies have revealed that chronic hypercapnia affected body electrolyte homeostasis in dogs with 11-13% CO_2 causing an increase in blood $[\text{HCO}_3^-]$, a decrease in $[\text{Cl}^-]$ and an increased $[\text{NH}_4^+]$ in urine; mechanisms to compensate for the respiratory acidosis (Polak *et al.*, 1961). Studies on guinea pigs have shown that chronic hypercapnia (15% CO_2) caused a drop in body temperature due to an increased vasodilation of peripheral blood vessels and increased body weight, blood corticosteroids and blood fatty acids concentration as well a decrease in the number of lymphocytes, demonstrating that chronic CO_2 can induce a whole host of different physiological changes in mammals (Schaefer *et al.*, 1968; Schaefer *et al.*, 1975). At the molecular level, Vohwinkel *et al.* (2011) demonstrated that exposure of A549 cells or N12 lung fibroblasts to prolonged 60mmHg CO_2 (~8% CO_2) or 120mmHg CO_2 (~16% CO_2) caused a significant reduction in cell proliferation due to a slower cell cycle, implicating chronic hypercapnia can impair an important aspect of cell physiology. In the lungs, Das *et al.* (2009) showed chronic hypercapnia increased the expression of α smooth muscle actin which the researchers suggested was involved in the formation of the higher number of alveolar buds observed in hypercapnic animals. This perhaps suggests at a mechanism by which animals increase their rate of ventilation during hypercapnia. With relevance to HCO_3^- transport, de Seigneux *et al.* (2007) found expression of NBCe1 and pendrin were upregulated and downregulated respectively in renal cells of rats exposed to chronic hypercapnia and hypoxia. Therefore, whether this is an effect of elevated CO_2 or a reduction in oxygen is difficult to determine but it does highlight the role of gases in regulation of acid/base transporters. Insights into the effect of chronic hypercapnia on ion transport have been provided by Gu *et al.* (2004) who measured neurone excitability in rat neuronal cells isolated from the hippocampus. Here, they showed that in rats exposed to 8% CO_2 for 14 days had higher neurone excitability due to an increased Na^+ conductance

mediated, in part, by an increased expression of surface Na^+ channels. Therefore, these studies provide insights into the effects of chronic hypercapnia on the expression and/or activity of ion transporters in animal cells. It has been postulated that hypercapnia can downregulate NF- κ B activity to reduce airway inflammation – a process which may underlie the benefits of permissive hypercapnia arising in ARDS/ALI treatment (Laffey *et al.*, 2000). However, this reduction in NF- κ B activity has been attributed to the hypercapnia causing a reduction in wound healing in both A549 cells and HBE cells. These findings suggest that elevated CO_2 could be detrimental in airway disease in which efficient tissue repair was needed (O'Toole *et al.*, 2009). Therefore, this chapter aims to assess the effects of chronic hypercapnia (24 hours) on cAMP-regulated ion transport as well as wound repair in Calu-3 cells.

5.2. Calu-3 transepithelial electrical resistance is unaffected by chronic hypercapnia

A useful indicator of whether epithelial cells are affected by changed environmental conditions is to assess their bioelectrical properties. Measurement of transepithelial electrical resistance (TEER) gave indications as to whether chronic hypercapnia affected the integrity of the epithelial monolayer. Thus, TEER measurements were performed on Calu-3 cells which had been incubated in 10% CO_2 (v/v) in air for 24 hours prior to being studied. TEER was not significantly different between normocapnic controls ($682 \pm 28 \Omega \text{ cm}^{-2}$; $n=6$) and cells exposed to chronic hypercapnia ($681 \pm 6 \Omega \text{ cm}^{-2}$; $p>0.05$; $n=6$). This indicates that chronic hypercapnia does not affect processes involved in tight junction formation and suggests that any changes in ion and fluid transport that may occur in chronic hypercapnia are unlikely due to a change in paracellular transport.

5.3. Chronic hypercapnia reduces the volume of forskolin-stimulated fluid secretion but has no effect on the composition on secreted fluid

The findings from chapters 3 and 4 suggest that acute hypercapnia can modulate cAMP-regulated HCO_3^- transport in a Ca^{2+} -dependent manner with a possible involvement of the Na^+/K^+ -ATPase. To study Calu-3 cell physiology over a longer time course, cAMP-regulated fluid and HCO_3^- secretion can be assessed using fluid secretion assays. Garnett *et al.* (2011) demonstrated that treatment of Calu-3 cells for 24 hours with forskolin induced a ~20%

increase in the amount of fluid secreted compared to unstimulated control cells. This increase in secretion was both Cl^- and HCO_3^- dependent and was blocked by GlyH-101 and reduced in CFTR KD cells. This implies forskolin activated CFTR-dependent Cl^- and HCO_3^- secretion to achieve an increase in fluid secretion. Furthermore, forskolin treatment also increased the pH of secreted fluid relative to unstimulated control cells. Interestingly, the change in pH was unaffected by GlyH-101 or CFTR KD. These data imply cAMP stimulates HCO_3^- secretion which is seemingly not directly *via* CFTR but likely to be through pendrin. To study how chronic hypercapnia impacted upon cAMP-regulated fluid and HCO_3^- secretion, cells were stimulated with 5 μM forskolin and incubated in either 5% CO_2 (v/v) in air or 10% CO_2 (v/v) in air for 24 hours before the amount of secreted fluid was measured and its composition analysed. In normocapnic conditions, unstimulated cells secreted $12 \pm 4 \mu\text{l}$ (n=3) fluid over 24 hours which was significantly enhanced to $49 \pm 3 \mu\text{l}$ by forskolin stimulation ($p < 0.01$; n=3; fig. 5.01A). This was calculated as a $17.1 \pm 2.6\%$ increase in the volume of fluid secreted in cells stimulated with forskolin relative to unstimulated control cells ($p < 0.01$; n=3; fig 5.01B). In hypercapnic conditions, unstimulated cells secreted $12 \pm 1 \mu\text{l}$ fluid over 24 hours which was almost identical to that seen in normocapnia ($p > 0.05$; n=3). However, although forskolin increased fluid secretion to $32 \pm 1 \mu\text{l}$ over 24 hours ($p < 0.01$; n=3; fig. 5.01A), this $9.5 \pm 0.9\%$ increase in the volume of forskolin-stimulated fluid secretion was significantly lower than that observed in normocapnia ($p < 0.05$; n=3; figs 5.01A and B). This suggests chronic hypercapnia acts to impair cAMP-regulated CFTR-dependent Cl^- secretion in airway epithelia. The pH of the secreted fluid was also measured. In normocapnia, the pH of secreted fluid increased from 7.52 ± 0.01 to 7.82 ± 0.06 ($p < 0.01$; n=3) indicative of a greater $[\text{HCO}_3^-]$ in the forskolin-stimulated secreted fluid. This pH increase of 0.31 ± 0.01 was not different to the pH increase of 0.30 ± 0.01 observed in hypercapnia (7.21 ± 0.04 to 7.51 ± 0.02 ; $p < 0.01$ *vs.* unstimulated controls; $p > 0.05$ *vs.* normocapnia; n=3; fig. 5.01C) with the lower pH values observed due to acidosis induced by elevated CO_2 . Using the Henderson-Hasselbalch equation to calculate $[\text{HCO}_3^-]$ in the secreted fluid revealed that, in normocapnia, the forskolin-stimulated fluid contained $61.6 \pm 9.5 \text{ mM}$ HCO_3^- which was not significantly different to the $58.2 \pm 2.4 \text{ mM}$ HCO_3^- in the forskolin-stimulated fluid in hypercapnia ($p > 0.05$; n=3). The glycoprotein content of the secreted fluid was also analysed by the PAS assay in order to give indications as to whether mucin secretion had been altered by treatment. In normocapnia, forskolin did not increase the amount of glycoproteins detected relative to unstimulated cells ($18.5 \mu\text{g/ml} \pm 0.5$ *vs.* $18.2 \mu\text{g/ml} \pm 1.0$ respectively; $p > 0.05$; n=3; fig. 5.01D) but may have stimulated an increase in mucus secretion due to the larger

volume of secreted fluid in forskolin-treated cells. Furthermore, hypercapnia had no effect on glycoprotein secretion from Calu-3 cells. Unstimulated cells secreted $19.2\mu\text{g/ml} \pm 0.1$ glycoprotein ($p>0.05$ vs. unstimulated cells in normocapnia; $n=3$) which was not affected by forskolin stimulation ($24.0\mu\text{g/ml} \pm 4.0$; $p>0.05$ vs. unstimulated cells; $n=3$; fig 5.01D).

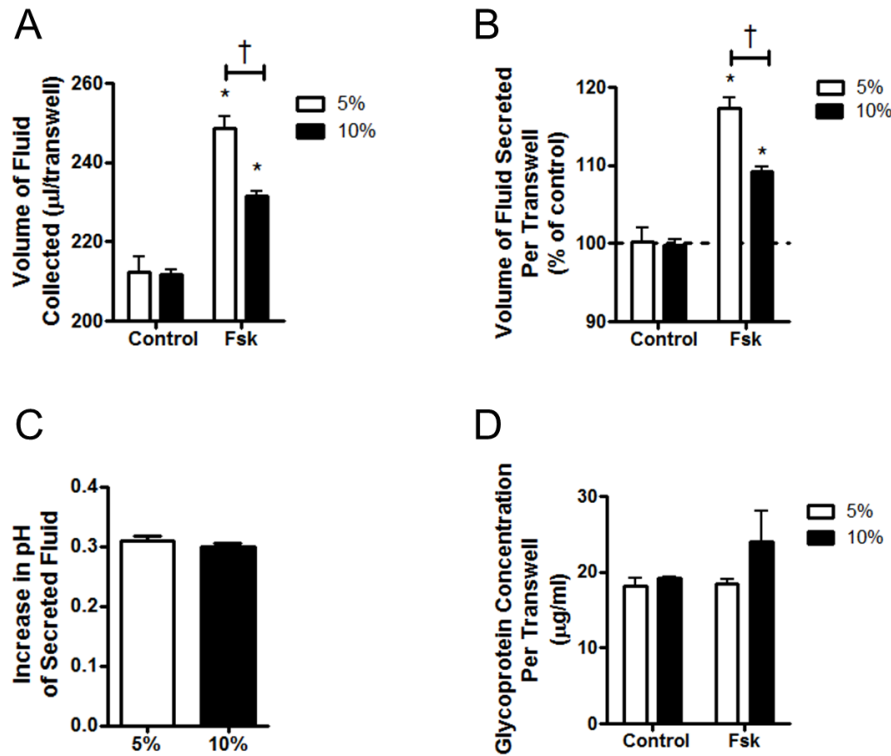


Figure 5.01: Chronic hypercapnia reduces forskolin-stimulated fluid secretion in Calu-3 cells. Cells were stimulated with $5\mu\text{M}$ forskolin and incubated for 24 hours in either 5% CO_2 (v/v) in air or 10% CO_2 (v/v) in air in high Cl^- Krebs solution at 37°C . (A) shows the effect of chronic hypercapnia on the volume of fluid secreted over 24 hours. (B) displays the relative increase in the volume of fluid secreted by forskolin when normalized to non-stimulated controls. * = significant effect of forskolin stimulation compared to unstimulated control cells ($p<0.01$); † = significant effect of 10% CO_2 ($p<0.05$). Data represents mean \pm S.E.M.; $n = 3$ for each. (C) displays the increase in pH of forskolin-stimulated secreted fluid relative to unstimulated control cells. Data represents mean \pm S.E.M.; $n = 3$ for each. (D) displays the effects of forskolin and hypercapnia on the amount of glycoprotein present in the secreted fluid, quantified by the PAS assay. Data represents mean \pm S.E.M.; $n = 3$ for each.

As shown in section in chapter 3, the effects of acute hypercapnia on cAMP-regulated HCO_3^- transport were dependent on the cAMP-elevating agonist used. Hypercapnia modulated both forskolin and adenosine-stimulated HCO_3^- transport but it did not affect IBMX-stimulated HCO_3^- transport, implying that CO_2 had specific effects on cAMP signalling, depending on how intracellular cAMP levels were elevated. Whether the same phenomenon existed in

chronic hypercapnia was determined by treating cells with 1mM IBMX for 24 hours and measuring the volume and composition of the secreted fluid. The data is displayed in figure 5.02. In normocapnia, IBMX significantly increased the volume of fluid secreted by $16.8 \pm 3.1\%$ ($p < 0.01$; $n = 3$) compared to non-stimulated control cells. The increase in fluid secretion in IBMX-stimulated cells compared to non-stimulated cells in hypercapnia was $11.8 \pm 2.9\%$ ($p < 0.01$; $n = 3$; fig. 5.02A) which was not significantly different to normocapnic conditions ($p > 0.05$). These findings suggest that, like acute hypercapnia, CO_2 was only able to modulate cAMP signalling *via* an effect upon cAMP synthesis *via* tmAC, as opposed to cAMP breakdown *via* phosphodiesterases. The increase in the pH of the secreted fluid was, like forskolin-stimulated cells, unaffected by chronic hypercapnia. pH increased by 0.25 ± 0.03 in normocapnia ($p < 0.05$ *vs.* non-stimulated cells; $n = 3$) and 0.18 ± 0.01 in hypercapnia ($p < 0.05$ *vs.* non-stimulated cells; $p > 0.05$ *vs.* normocapnia; $n = 3$; fig. 5.02B) and shows hypercapnia does not affect cAMP-regulated HCO_3^- secretion over 24 hours.

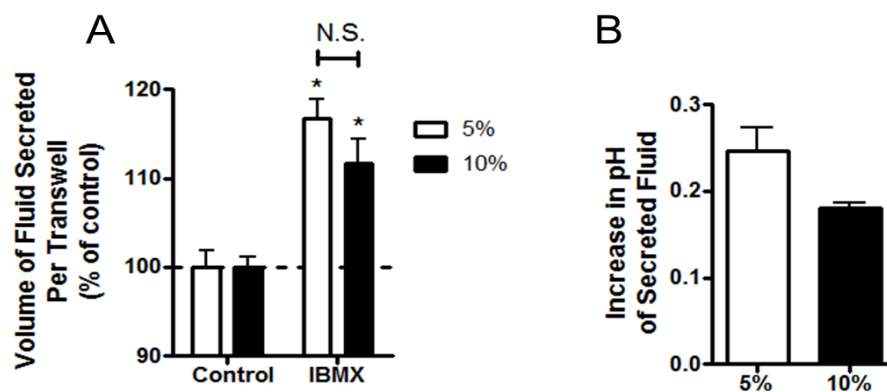


Figure 5.02: Chronic hypercapnia has no effect on IBMX-stimulated fluid secretion in Calu-3 cells. Cells were stimulated with 1mM IBMX and incubated for 24 hours in either 5% CO_2 (v/v) in air or 10% CO_2 (v/v) in air in high Cl^- Krebs solution at 37°C . (A) shows the effect of chronic hypercapnia on the volume of fluid secreted over 24 hours; * = significant effect of IBMX stimulation compared to unstimulated control cells ($p < 0.01$). Data represents mean \pm S.E.M.; $n = 3$ for each. (B) displays the increase in pH of IBMX-stimulated secreted fluid relative to unstimulated control cells. Data represents mean \pm S.E.M.; $n = 3$ for each.

Having shown that acute hypercapnia reduced the volume of forskolin-stimulated fluid secretion but had no effect on the volume of IBMX-stimulated fluid secretion, it was interesting to observe the effects of acute hypercapnia when both agonists were added at the

same time. Figure 5.03 shows that, in normocapnia, forskolin + IBMX stimulated a $24.3 \pm 2.7\%$ increase in the volume of fluid secreted compared to non-stimulated controls ($p < 0.001$; $n = 3$). This was significantly higher than the $17.0 \pm 1.2\%$ increase in forskolin + IBMX-stimulated fluid secretion observed in hypercapnia ($p < 0.001$ vs. unstimulated controls; $p < 0.01$ vs. normocapnia; $n = 3$; fig. 5.03A). However, there was no significant difference in the increase in pH of the secreted fluid with pH increasing by 0.41 ± 0.03 units in normocapnia ($p < 0.001$; $n = 3$) and by 0.32 ± 0.07 in hypercapnia ($p < 0.05$ vs. non-stimulated controls; $p > 0.05$ vs. normocapnia; $n = 3$; fig. 5.03B).

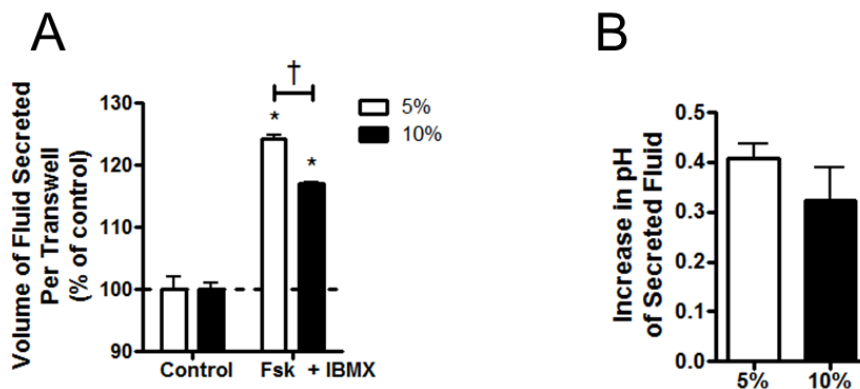


Figure 5.03: Chronic hypercapnia reduces forskolin + IBMX-stimulated fluid secretion in Calu-3 cells. Cells were stimulated with 5 μ M forskolin and 1 mM IBMX and incubated for 24 hours in either 5% CO₂ (v/v) in air or 10% CO₂ (v/v) in air in high Cl⁻ Krebs solution at 37°C. (A) shows the effect of chronic hypercapnia on the volume of fluid secreted over 24 hours; * = significant effect of forskolin + IBMX stimulation compared to unstimulated control cells ($p < 0.001$). Data represents mean \pm S.E.M.; $n = 3$ for each. (B) displays the increase in pH of IBMX-stimulated secreted fluid relative to unstimulated control cells. Data represents mean \pm S.E.M.; $n = 3$ for each.

In order to understand the role of intracellular Ca²⁺ signalling in cAMP-stimulated fluid secretion, Calu-3 cells were treated with 50 μ M BAPTA-AM and incubated for 24 hours in 5% CO₂ (v/v) in air for 24 hours. In non-stimulated conditions, BAPTA-AM reduced fluid secretion by $3.5 \pm 0.6\%$ ($p < 0.05$; $n = 3$; fig. 5.04A) implying that there is a small Ca²⁺ component to the basal level of secretion that occurs over 24 hours. Forskolin increased the volume of fluid secreted by $8.9 \pm 0.7\%$ ($n = 3$; $p < 0.05$) compared to unstimulated cells whilst in BAPTA-AM treated cells, forskolin stimulated a $6.5 \pm 1.2\%$ ($n = 3$; $p < 0.05$; fig. 5.04A) increase in fluid secretion. Although BAPTA-AM caused a significant reduction in the volume of forskolin-stimulated fluid secretion ($p < 0.01$; $n = 3$) the % increase in the volume of

forskolin-stimulated fluid secretion was not statistically significantly different between control and BAPTA-AM loaded cells ($p>0.05$; $n=3$) and indicates that there is no role for Ca^{2+} in cAMP-stimulated fluid transport. The pH of secreted fluid in basal conditions was 7.42 ± 0.07 ($n=3$) and this was unaffected by BAPTA-AM treatment in which it was 7.35 ± 0.04 ($p>0.05$; $n=3$; fig. 5.04B). Forskolin increased the pH of secreted fluid by 0.25 ± 0.09 ($n=3$) in control cells and by 0.28 ± 0.07 in BAPTA-AM-loaded cells ($p>0.05$; $n=3$ fig. 5.04B) demonstrating that chelation of intracellular Ca^{2+} did not affect cAMP-stimulated HCO_3^- secretion in Calu-3 cells.

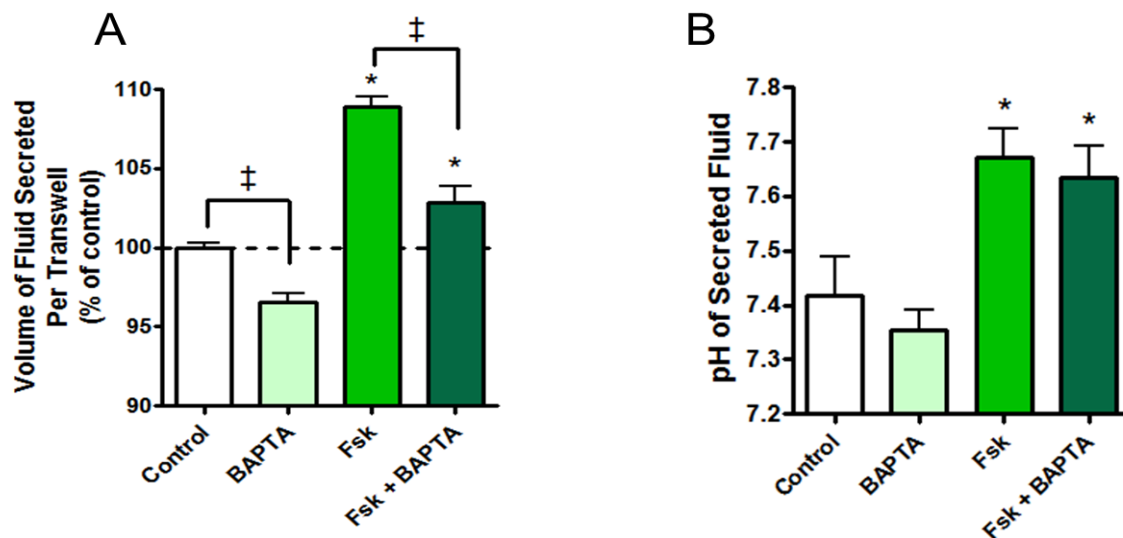


Figure 5.04: BAPTA-AM reduces basal fluid secretion in Calu-3 cells but does not prevent the increase in fluid secretion stimulated by forskolin. Cells were treated with 50 μM BAPTA-in the presence of 5 μM forskolin and incubated for 24 hours in high Cl^- Krebs solution in 5% CO_2 (v/v) in air at 37°C. (A) shows the volume of fluid secreted over 24 hours; * = significant effect of forskolin relative to non-stimulated cells ($p<0.05$); ‡ = significant effect of BAPTA-AM compared to non-BAPTA-AM treated cells ($p<0.05$). Data represents mean \pm S.E.M.; $n = 3$ for each. (B) displays the pH of the secreted fluid; * = significant effect of forskolin relative to non-stimulated cells ($p<0.05$). Data represents mean \pm S.E.M.; $n = 3$ for each.

The findings from chapter 4 showed that there appears to be a Ca^{2+} component to the effects of acute hypercapnia on cAMP-regulated HCO_3^- transport. Having shown there is a role for Ca^{2+} in maintaining a basal level of fluid secretion in Calu-3 cells (fig. 5.04A), it was important to investigate whether the effect of hypercapnia on cAMP-regulated fluid secretion required changes in intracellular Ca^{2+} . Calu-3 cells were treated with 50 μM BAPTA-AM and

incubated in either 5% CO₂ (v/v) in air or 10% CO₂ (v/v) in air for 24 hours before the volume of secreted fluid was measured. Forskolin significantly increased the volume of fluid secreted in both normocapnic (12.5 ± 1.1%; p<0.05 vs. unstimulated cells; n=3) and hypercapnic conditions (19.9 ± 7.9%; p<0.05 vs. unstimulated cells; n=3; fig. 5.05). Unlike in non-BAPTA-AM loaded cells (fig 5.01), this stimulation of the volume of fluid secreted by forskolin was not significantly different between normocapnia and hypercapnia (p>0.05; n=3) and therefore shows that BAPTA-AM abolished the effect of hypercapnia on cAMP-regulated fluid secretion. These data implied that in order for CO₂ to mediate its effects on cAMP-regulated fluid secretion, it utilized a Ca²⁺ signalling pathway, similar to what is observed in acute hypercapnia.

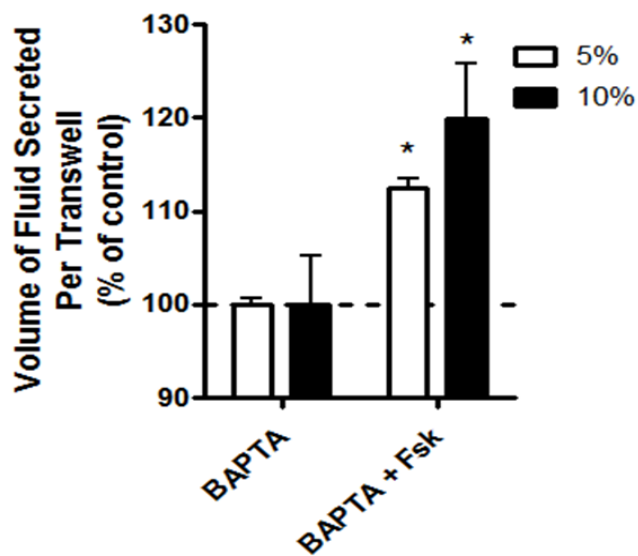


Figure 5.05: BAPTA-AM prevents the effect of hypercapnia on forskolin-stimulated fluid secretion in Calu-3 cells. Cells were treated with 50μM BAPTA-AM in the presence of 5μM forskolin and incubated for 24 hours in high Cl⁻ Krebs solution in either 5% CO₂ (v/v) in air or 10% CO₂ (v/v) in air at 37°C. * = significant effect of forskolin vs. non-stimulated cells (p<0.05). Data represents mean ± S.E.M.; n=3 for each.

5.4. Chronic hypercapnia has no effect on I_{sc} in Calu-3 cells

The results from the fluid secretion assays imply that chronic hypercapnia reduces CFTR-dependent fluid secretion likely due to a reduction in CFTR-mediated Cl⁻ secretion. Therefore, the effects of chronic hypercapnia on electrogenic Cl⁻ transport was assessed by measuring I_{sc} using an Ussing chamber. Calu-3 cells were incubated for 24 hours in 10% CO₂ (v/v) at 37°C prior to being studied. To measure electrogenic Cl⁻ secretion, cells were

stimulated with 5 μ M forskolin in the presence of a basolateral to apical Cl⁻ gradient, achieved by reducing apical Cl⁻ to 40mM (by removal of 84mM NaCl and adding equimolar Na Gluconate) whilst maintaining basolateral Cl⁻ at 124mM. The effects of both apical CFTR_{inh} 172 (20 μ M) and basolateral bumetanide (25 μ M) on forskolin-stimulated changes in I_{sc} were also assessed. Representative I_{sc} measurements recorded from cells grown in normocapnia and cells exposed to hypercapnia for 24 hours are shown in figures 5.06A and 5.06B respectively. The basal I_{sc} in normocapnia was $4.6 \pm 0.8 \mu\text{A cm}^{-2}$ (n=4) whilst in cells exposed to chronic hypercapnia, basal I_{sc} was $5.3 \pm 0.7 \mu\text{A cm}^{-2}$ (n=4; p>0.05; fig. 5.06C). These findings suggest chronic hypercapnia does not affect the basal electrogenic ion transport in non-stimulated conditions. Forskolin produced a maximal increase of $24.8 \pm 1.8 \mu\text{A cm}^{-2}$ in normocapnia (n=4) and $26.4 \pm 2.8 \mu\text{A cm}^{-2}$ in chronic hypercapnia (n=4; p>0.05; fig. 5.06D). Furthermore, the rate of this forskolin-induced increase in I_{sc} was $12.5 \pm 1.3 \mu\text{A cm}^{-2} \text{ min}^{-1}$ in normocapnia (n=4) and $9.2 \pm 1.7 \mu\text{A cm}^{-2} \text{ min}^{-1}$ in hypercapnia (n=4; p>0.05; fig. 5.06E). These data suggest that chronic hypercapnia does not affect cAMP-regulated CFTR-dependent Cl⁻ secretion which is in stark contrast to the results from the fluid secretion assays. Furthermore, given that acute hypercapnia modulated forskolin-induced increases in I_{sc}, shows a distinct difference between cAMP regulated signalling in the acute and chronic setting.

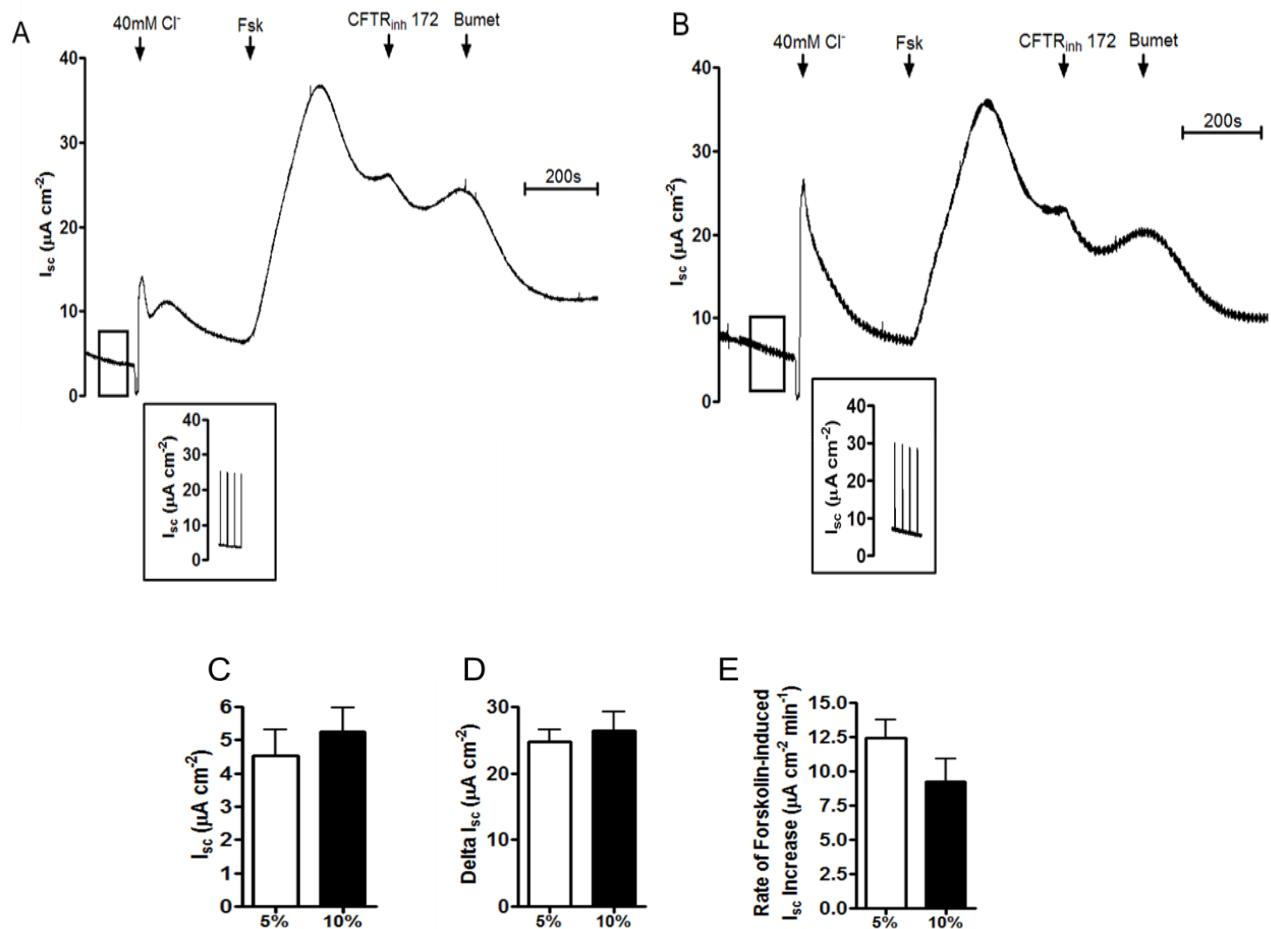


Figure 5.06. Chronic hypercapnia has no effect on forskolin-stimulated changes in I_{sc} in Calu-3 cells. Calu-3 cells were grown on permeable snapwell supports and forskolin-stimulated electrogenic Cl^- secretion was measured using an Ussing Chamber. Representative traces of control experiments (A) or experiments in which cells had been exposed to hypercapnia for 24 hours prior to study (B) are shown. The inset shows that a 2 second 10mV pulse was applied across the cells every 30 seconds to monitor transepithelial electrical resistance (TEER) but these pulses were removed from the trace in order to display the effects of treatment more clearly. The basal I_{sc} (C), the maximal forskolin-stimulated increase in I_{sc} (D) and the rate of increase in forskolin-stimulated I_{sc} (E) are displayed. Data represents mean \pm S.E.M.; $n = 4$.

It was puzzling as to why such different effects on Cl^- secretion were observed in the fluid secretion assays relative to the I_{sc} measurements. One explanation could be that in the I_{sc} measurements, a basolateral to apical Cl^- gradient exists which is not present in the fluid secretion assays. This Cl^- gradient will increase the driving force for Cl^- secretion and may mask any subtle effects of hypercapnia that exist when apical and basolateral $[Cl^-]$ was equal. Therefore, the effects of chronic hypercapnia on fluid secretion were tested on cells in which apical Cl^- was reduced to 40mM (by removal of 84mM NaCl and replacement with equimolar

Na Gluconate) and basolateral Cl^- was maintained at 124mM. The presence of a basolateral to apical Cl^- gradient caused an expected overall increase in the amount of fluid secreted over 24 hours. For example, in normocapnia, under basal conditions, $49 \pm 2\mu\text{l}$ of fluid was secreted over 24 hours which was significantly higher than the $12 \pm 4\mu\text{l}$ secreted when apical Cl^- and basolateral Cl^- were equal ($p < 0.001$; $n=3$). In normocapnia, forskolin stimulated $80 \pm 2\mu\text{l}$ fluid to be secreted over 24 hours which was calculated as a $12.6 \pm 2.0\%$ increase in the volume of fluid secreted compared to unstimulated controls ($p < 0.001$; $n=3$; fig. 5.07B). However, in hypercapnia, forskolin elicited a $7.1 \pm 2.2\%$ increase in fluid secretion ($p < 0.05$; $n=3$) which was significantly lower than that observed in normocapnia ($p < 0.05$; fig. 5.07B). Therefore, even in the presence of a basolateral to apical Cl^- gradient, chronic hypercapnia significantly reduces the volume of forskolin-stimulated fluid secretion in Calu-3 cells. Such disparity with the I_{sc} measurements, in which chronic hypercapnia appears to not effect electrogenic Cl^- secretion, are, at this stage, confusing and highlights that different experimental approaches may yield different results due to the nature of the measurements being made.

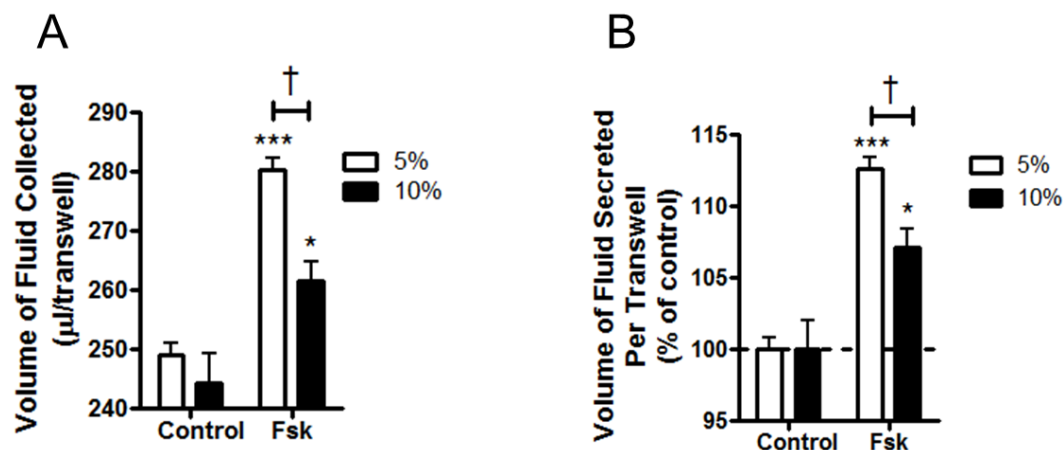


Figure 5.07: Chronic hypercapnia reduces forskolin-stimulated fluid secretion in Calu-3 cells in the presence of a basolateral to apical Cl^- gradient. Cells were stimulated with $5\mu\text{M}$ forskolin and incubated for 24 hours in either 5% CO_2 (v/v) in air or 10% CO_2 (v/v) in air. Apical Cl^- was reduced to 40mM and basolateral Cl^- was maintained at 124mM Cl^- . (A) shows the effect of chronic hypercapnia on the volume of fluid secreted over 24 hours. (B) displays the relative increase in the volume of fluid secreted by forskolin when normalized to non-stimulated controls. * = significant effect of forskolin stimulation compared to unstimulated control cells ($p < 0.01$; *** = $p < 0.001$); † = significant effect of 10% CO_2 ($p < 0.05$). Data represents mean \pm S.E.M.; $n = 3$ for each.

5.5. Chronic hypercapnia reduces the expression of CFTR in Calu-3 cells

Figure 3.04 in chapter 3 showed that acute hypercapnia caused an apparent reduction in the expression of CFTR protein in Calu-3 cells although whether this correlated with a decreased expression of CFTR at the apical membrane still remains to be determined. Here, the effect of chronic hypercapnia on total CFTR expression was assessed. Cells were incubated for 24 hours in high Cl^- Krebs solution containing either DMSO (control) or forskolin in either 5% CO_2 (v/v) in air or 10% CO_2 (v/v) in air. After 24 hours, cells were lysed and the expression of CFTR was measured and normalized to the expression of β -actin. As shown in fig. 5.08, forskolin has no effect on the expression of CFTR in either normocapnia or hypercapnia. However, it appears that chronic hypercapnia reduces total CFTR expression which is the opposite of what is observed in acute hypercapnia and this may suggest at a mechanism by which chronic hypercapnia can reduce the volume of forskolin-stimulated fluid secretion.

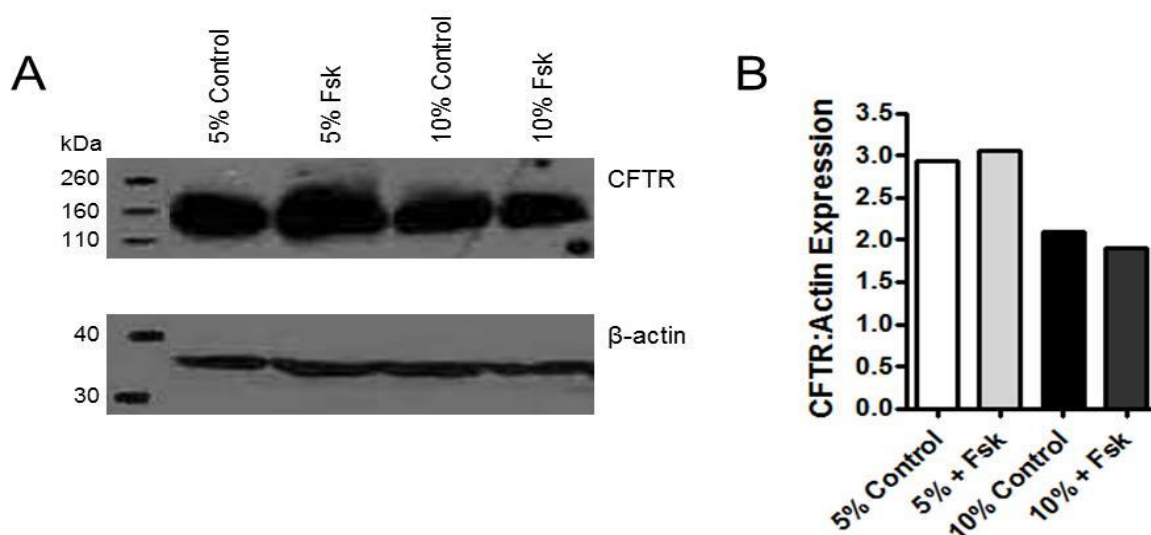


Figure 5.08: Chronic hypercapnia reduces CFTR expression in Calu-3 cells. (A) shows the results from a Western Blot in which the effect of forskolin and chronic hypercapnia on CFTR protein expression was assessed and normalized to β -actin expression. The data is summarized in (B). For each experimental condition, 3 lysates were generated from 3 separate transwell. These lysates were combined to produce one lysate for each experimental condition; thus data represents mean of $n=1$.

5.6. CFTR-dependent anion exchange activity is unaffected by chronic hypercapnia

To further investigate the effects of chronic hypercapnia on cAMP-regulated CFTR-dependent HCO_3^- transport, intracellular pH measurements were made on Calu-3 cells. These experiments allow for the measurement of CFTR-dependent anion exchange activity as

described by Garnett et al., (2009). Cells were incubated in either 5% CO₂ (v/v) in air (control) or in 10% CO₂ (v/v) in air for 24 hours prior to being studied (chronic hypercapnia). As previously described in chapter 3, section 3.14.1, to measure CFTR-dependent anion exchange activity, cells were perfused with an apical Cl⁻ free Krebs solution to reverse the anion exchanger and stimulate Cl⁻ efflux and consequentially HCO₃⁻ influx. Reintroduction of Cl⁻ to the apical perfusate causes the anion exchanger to function in its normal direction and the subsequent intracellular acidification that occurs provides a measure for CFTR-dependent HCO₃⁻ secretion. Representative experiments for normocapnia (fig. 5.09A) and chronic hypercapnia (fig 5.09B) are shown. The initial intracellular pH of cells in normocapnia was 7.41 ± 0.04 (n=4) which was unchanged in cells exposed to chronic hypercapnia (7.48 ± 0.03 ; n=3; $p > 0.05$ vs. normocapnia; fig 5.09C). This shows that Calu-3 cells are able to maintain a normal intracellular pH even after prolonged exposure to hypercapnia and is unsurprising given it has been shown these cells can recover intracellular pH from CO₂-induced acidosis within 20 minutes. As discussed at length in chapter 4, addition of forskolin induces an intracellular acidification which is significantly augmented by acute hypercapnia. In cells exposed to chronic hypercapnia, forskolin causes pH_i to decrease by 0.16 ± 0.02 (n=3) at a rate of $10.7 \pm 2.0 \text{ mM HCO}_3^- \text{ min}^{-1}$ (n=3). These findings are comparable to the forskolin-induced acidification observed in normocapnic cells. Here, pH_i decreased by 0.15 ± 0.01 (n=4; $p > 0.05$ vs. hypercapnia; fig 5.09D) at a rate of $5.9 \pm 0.7 \text{ mM HCO}_3^- \text{ min}^{-1}$ ($p > 0.05$ vs. hypercapnia; n=4; fig 5.09E). These data show that, unlike acute hypercapnia, chronic hypercapnia does not affect forskolin-stimulated HCO₃⁻ transport. In the presence of forskolin, removal of apical Cl⁻ causes an alkalization of pH_i of 0.78 ± 0.04 (n=4) in normocapnia and 0.90 ± 0.04 in hypercapnia ($p < 0.05$; n=3). Reintroduction of apical Cl⁻ causes a HCO₃⁻ influx of $232.7 \pm 83.8 \text{ mM HCO}_3^- \text{ min}^{-1}$ (n=4) in normocapnia and $371.3 \text{ mM/min} \pm 38.0 \text{ mM HCO}_3^- \text{ min}^{-1}$ in hypercapnia ($p > 0.05$; n=3). Thus, chronic hypercapnia does not affect CFTR-dependent anion exchange activity in Calu-3 cells which implies that cells are able to adapt to chronic hypercapnia and thus only acute hypercapnia can affect the pathways and components involved in HCO₃⁻ transport in airway epithelia.

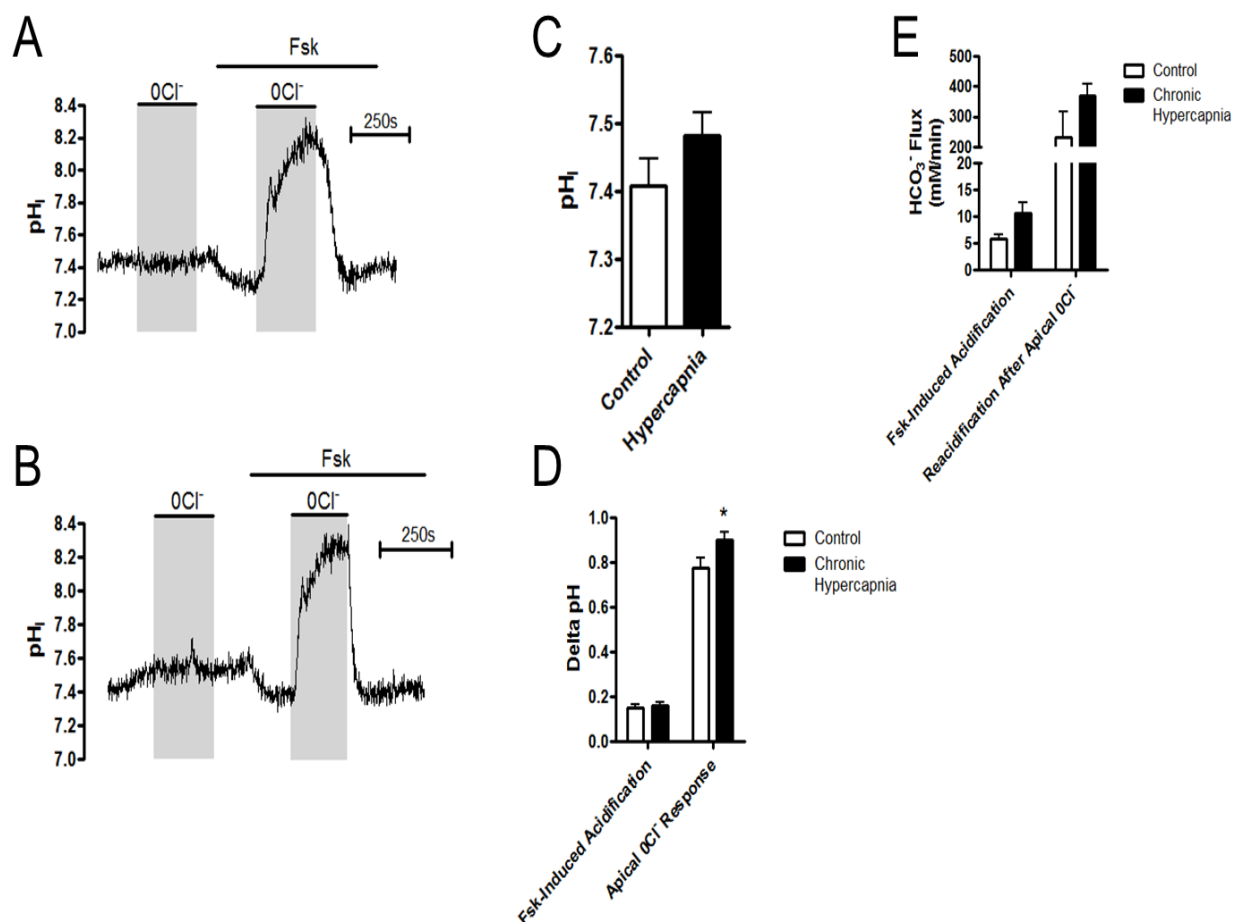


Figure 5.09: Chronic hypercapnia does not alter CFTR-dependent HCO₃⁻ transport in Calu-3 cells. (A) shows a representative experiment in normocapnia in which cAMP-regulated CFTR-dependent HCO₃⁻ transport was assessed by exposing cells to an apical 0Cl⁻ solution in the presence of 5μM forskolin. (B) shows the same experiment but after cells had been incubated in 10% CO₂ (v/v) in air for 24 hours prior to being studied. (C) shows the initial pH_i of cells whilst (D) displays the delta pH_i that occurs after forskolin-stimulation and after removal of apical Cl⁻. (E) displays the HCO₃⁻ flux that occurs after forskolin stimulation and after reintroduction of apical Cl⁻. * = significant effect of chronic hypercapnia (p<0.05). Data represents mean ± S.E.M.; n = 4 for each.

5.7. Chronic hypercapnia elicits highly variable effects on wound healing of Calu-3 cells

As already discussed, hypercapnia has been shown to reduce wound healing airway epithelial cells lines due to a downregulation of NF-κB-dependent repair mechanisms (O'Toole *et al.*, 2009). Given that airway disease can cause fibrosis of lung tissue and thus the requirement for efficient wound healing, it was of interest to investigate whether the hypercapnia resulting from airway disease would modulate wound healing of a Calu-3 cell monolayer. Calu-3 cells

were wounded by administering a single scratch using a P200 pipette tip before cells were and imaged every 4 hours using a Nikon BioStation in which ambient CO₂ could be altered. Three separate experiments were performed on three different Calu-3 cell cultures and the results for each separate experiment are shown in figures 5.11, 5.12 and 5.13. Figure 5.10 shows example screen shots of the wound size of Calu-3 cells incubated in normocapnia, taken at 0, 12, 24 and 36 hours after the cells were scratched. The size of the wound at t=0 hours was $2.22 \pm 0.06\text{mm}^2$ (n=40). Figure 5.11 shows that in one experiment, when cells were incubated in high Cl⁻ Krebs solution, hypercapnia significantly accelerated the ability of Calu-3 cells to reheel after wounding. This was also observed in another, separate experiment which also investigated whether cells incubated in growth medium as opposed to Krebs solution displayed any differences in their wound healing ability (fig 5.12). Interestingly, growth media significantly slowed wound healing in both normocapnia and hypercapnia compared to Krebs solution. This finding is surprising as it would be expected that in serum-containing conditions, cells would be able to proliferate as well as migrate, and thus increase the rate of wound healing. The final experiment aimed to assess whether the increased wound healing rate seen in hypercapnia was due to CO₂ *per se* or was due to differences in pH_e. Therefore, Calu-3 cells were incubated in either high Cl⁻ Krebs solution (control), high Cl⁻ Krebs + 10mM HEPES, 0.6mM NaOH and 15mM Mannitol (pH 7.4 when gassed with 5% CO₂ (v/v) / 95% O₂ (v/v)) or high Cl⁻ Krebs + 10mM HEPES and 10mM NaOH (pH 7.4 when gassed with 10% CO₂ (v/v) / 90% O₂ (v/v)). The data is displayed in figure 5.13. Here, there is no effect of hypercapnia on wound healing, even in control conditions. These findings do not replicate the previous experiments and therefore highlights a large variability in wound healing between different cell cultures. Furthermore, from these findings, it is impossible to ascertain whether the effects of hypercapnia observed previously are due to CO₂ *per se* or CO₂-induced acidosis of extracellular pH.

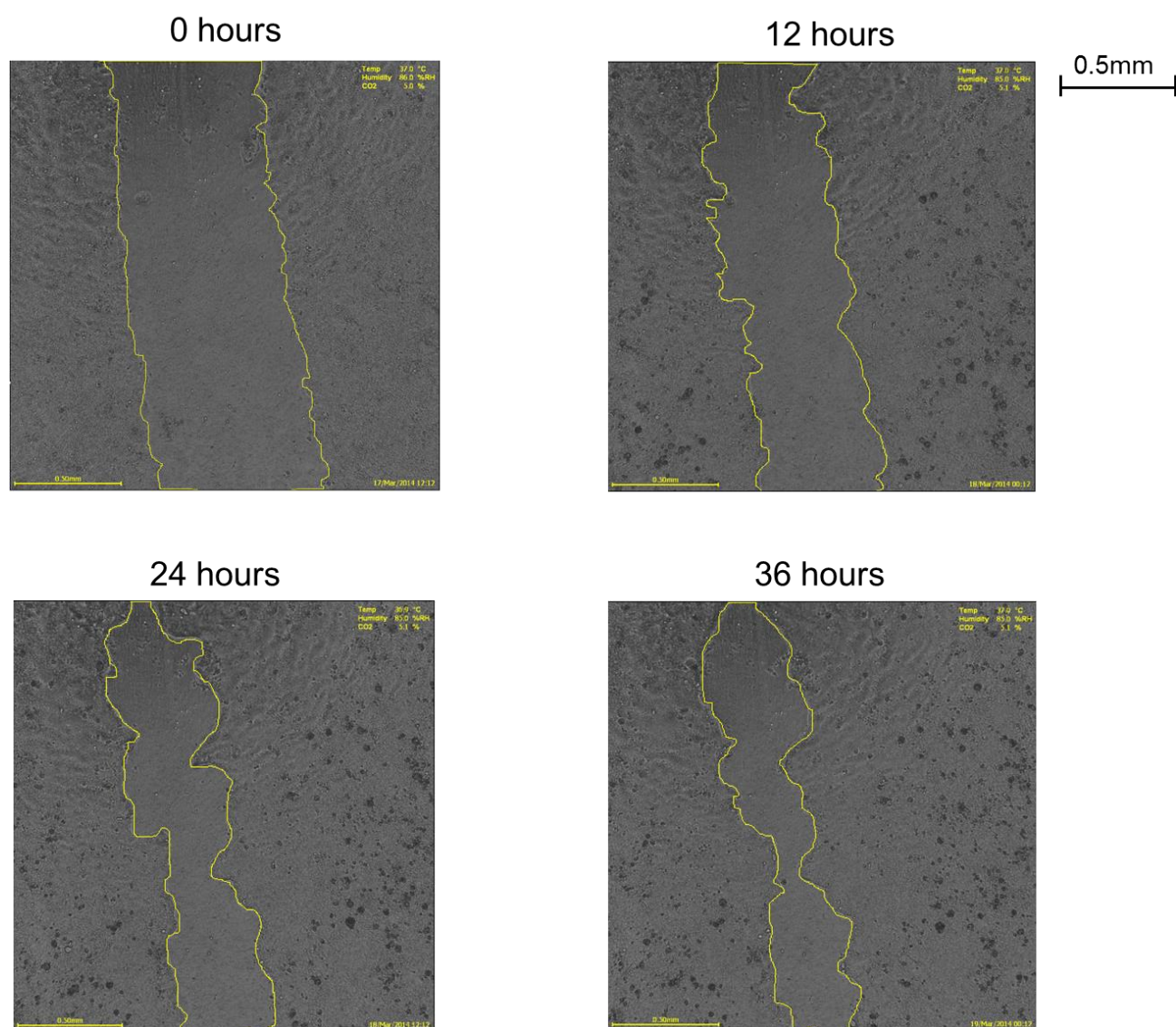


Figure 5.10: Representative images showing the wound administered to Calu-3 cells at 0, 12, 24 and 36 hours post-scratch. Images were generated at x4 magnification using a Nikon BioStation and analysed using ImageJ.

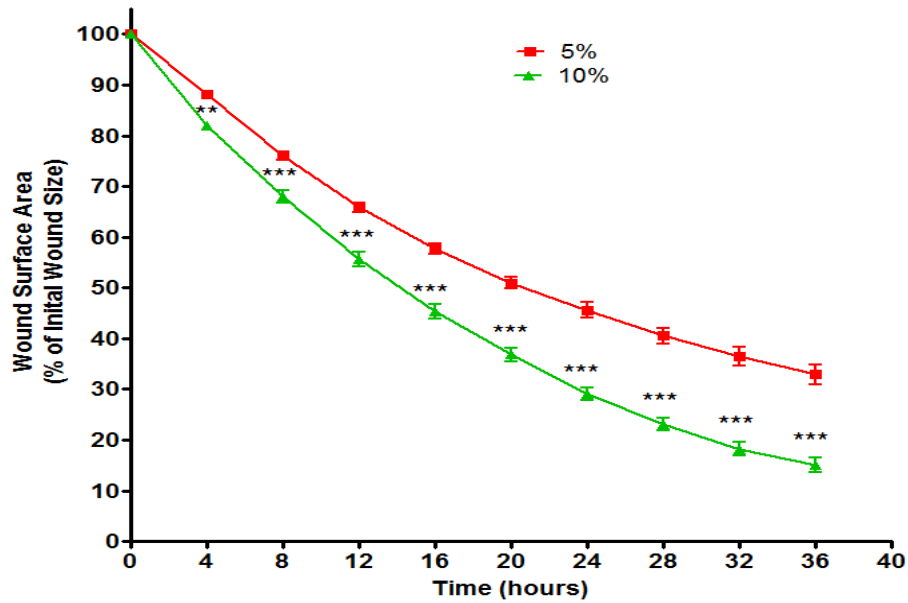


Figure 5.11: Hypercapnia increases the rate of wound healing in Calu-3 cells incubated in high Cl⁻ Krebs solution. Cells were scratched with a P200 pipette tip and imaged every 4 hours at 3 different fields of view per transwell at x4 magnification using a Nikon BoStation. The mean wound surface area for each field of view was calculated and each data point is representative of mean \pm S.E.M. of n = 6 transwells. ** = significant effect of hypercapnia (p<0.01; *** = p<0.001).

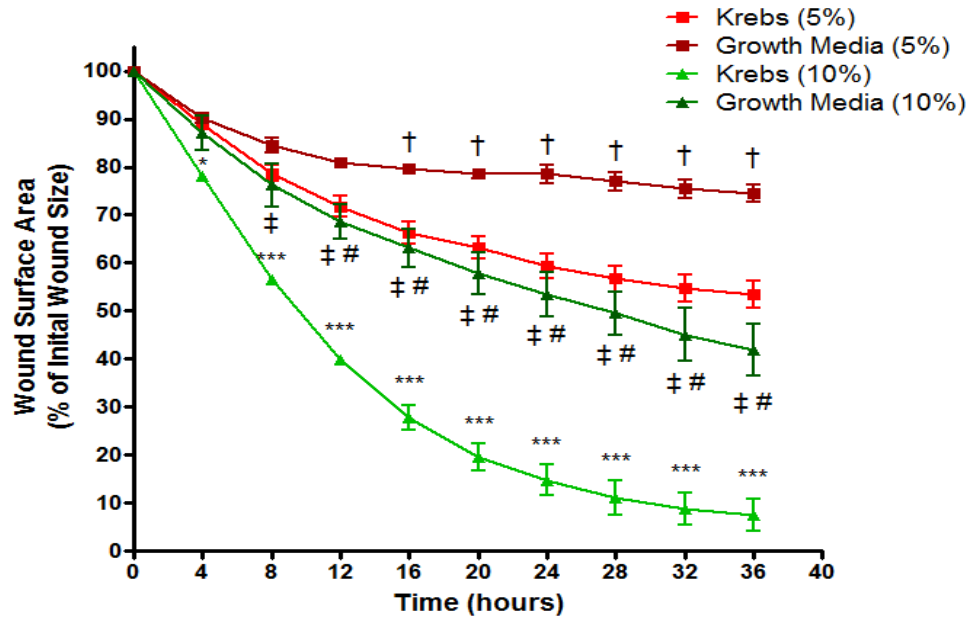


Figure 5.12: Growth medium reduces the rate of wound healing in Calu-3 cells in both normocapnia and hypercapnia. Cells were scratched with a P200 pipette tip, incubated in either high Cl^- Krebs solution or growth medium and imaged every 4 hours at 3 different fields of view per transwell at x4 magnification using a Nikon BioStation. The mean wound surface area for each field of view was calculated and each data point is representative of mean \pm S.E.M. of $n = 4$ transwells. *** = significant effect of hypercapnia in cells incubated in Krebs solution ($p < 0.001$); # = significant effect of hypercapnia in cells incubated in growth medium ($p < 0.01$); † = significant difference between high Cl^- Krebs and growth medium in normocapnia ($p < 0.01$); ‡ = significant difference between high Cl^- Krebs and growth medium in hypercapnia ($p < 0.01$).

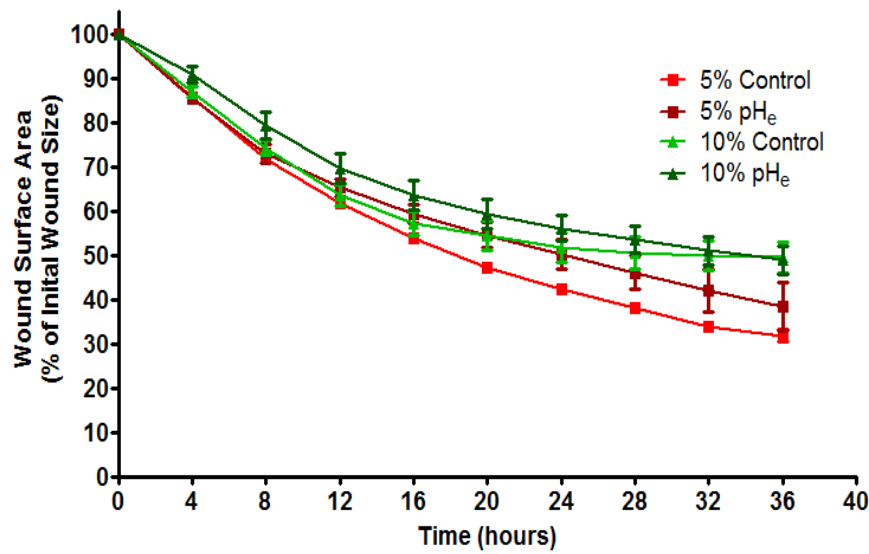


Figure 5.13: Hypercapnia has no effect on the rate of wound healing in Calu-3 cells. Cells were scratched with a P200 pipette tip, incubated in high Cl⁻ Krebs solution (control) or modified Krebs solution (pH_e) and imaged every 4 hours at 3 different fields of view per transwell at x4 magnification using a Nikon BioStation. The mean wound surface area for each field of view was calculated and each data point is representative of mean \pm S.E.M. of n = 4 transwells. No significant differences were found.

Due to the apparent differences in variability that exist between different cell cultures, the data from all three experiments in which cells had been incubated in high Cl⁻ Krebs solution was combined (fig 5.14). Combining the data shows that hypercapnia does significantly accelerate wound healing in monolayers of Calu-3 cells.

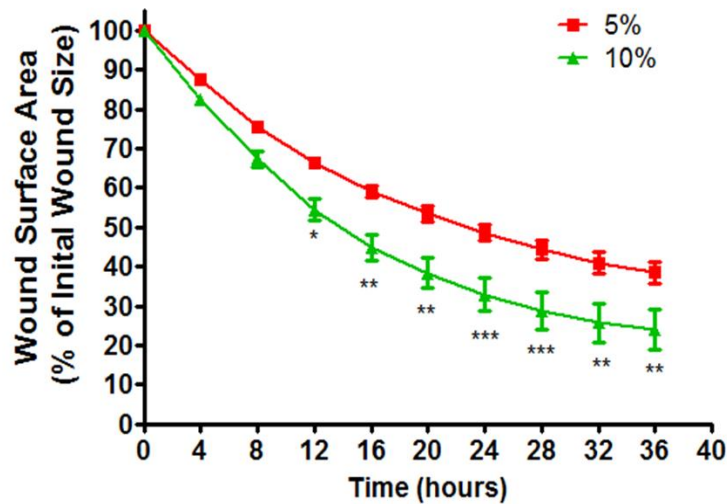


Figure 5.14: Grouping the data from three separate experiments shows that hypercapnia increases the rate of wound healing in Calu-3 cells. Cells were scratched with a P200 pipette tip and imaged every 4 hours at 3 different fields of view per transwell at x4 magnification using a Nikon BioStation and the mean wound surface area for each field of view was calculated. Each data point is representative of mean \pm S.E.M. of $n = 14$ transwells combined from 3 independent experiments. * = significant effect of hypercapnia ($p < 0.05$; ** = $p < 0.01$; *** = $p < 0.001$).

5.6. Discussion

5.6.1. The effect of chronic hypercapnia on cAMP-regulated ion and fluid transport – similar mechanisms to acute hypercapnia?

The data presented in this chapter investigated the effect of chronic hypercapnia on cAMP-regulated ion and fluid transport in Calu-3 cells as well as the effect of chronic hypercapnia on Calu-3 cell wound healing. Incubating cells for 24 hours in hypercapnia did not affect the amount of fluid secreted under basal conditions but did cause a significant reduction in the amount of fluid secreted when cells were stimulated with forskolin. Interestingly, the composition of forskolin-stimulated fluid secretion was unaffected by chronic hypercapnia. Although forskolin caused an increase in the pH of the secreted fluid, indicative of a greater $[\text{HCO}_3^-]$ in the fluid, the extent of the pH increase and the calculated $[\text{HCO}_3^-]$ was equivalent in normocapnia and hypercapnia. Garnett *et al.* (2011) demonstrated that the volume of secreted fluid from Calu-3 cells was directly regulated by CFTR given that GlyH-101 significantly reduced the volume of forskolin-stimulated fluid secreted over 24 hours. However, it was somewhat surprisingly found that GlyH-101 did not block the forskolin-stimulated increase in pH of secreted fluid, suggesting that a GlyH-101-insensitive apical

HCO_3^- transporter was responsible for the increased HCO_3^- secretion, which the researchers concluded to be pendrin. Thus, it appears that chronic hypercapnia reduced CFTR-dependent Cl^- secretion to reduce the driving force for fluid transport, but did not affect pendrin-mediated HCO_3^- secretion. Although measured over a different time course, these findings are very similar to what was observed when measuring CFTR-dependent anion transport and pendrin activity in acute hypercapnia. Here, I showed that forskolin-stimulated, CFTR-dependent increases in I_{sc} were reduced by acute hypercapnia, yet pendrin-mediated $\text{Cl}^-/\text{HCO}_3^-$ exchange was insensitive to acute hypercapnia. It is also interesting that the $36 \pm 9\%$ inhibition of forskolin-stimulated increase in $[\text{cAMP}]_i$ by acute hypercapnia, closely resembles the $35 \pm 5\%$ inhibition of forskolin-stimulated fluid secretion by chronic hypercapnia. These findings suggest that chronic hypercapnia may induce similar reductions in $[\text{cAMP}]_i$ to reduce CFTR-dependent Cl^- secretion and consequentially reduce the volume of fluid secreted. However, the reduction in CFTR activity may not be sufficient to reduce pendrin activity, hence efficient HCO_3^- secretion is maintained. Furthermore, the lack of effect of chronic hypercapnia under basal conditions is also similar to what is observed when measuring $[\text{cAMP}]_i$ in acute hypercapnia. I discussed that CO_2 may modulate the activity of tmAC to reduce $[\text{cAMP}]_i$ but, in order to do this, tmAC needed to be in a “forskolin-bound” conformation – hence the lack of effect of hypercapnia on basal levels of $[\text{cAMP}]_i$. As such, a similar mechanism may be evident here whereby chronic CO_2 reduced forskolin-stimulated $[\text{cAMP}]_i$ by reducing the activity of tmAC held in a “forskolin-bound” conformation. To further verify this, it will be important to measure $[\text{cAMP}]_i$ in cells exposed to hypercapnia for 24 hours to see whether the effect of CO_2 on $[\text{cAMP}]_i$ is also present over a longer time course.

An alternative explanation for the reduced volume of forskolin-stimulated fluid secretion is from the finding that chronic hypercapnia appeared to reduce CFTR expression. These findings are in stark contrast to the effects of acute hypercapnia, in which it was found CFTR expression appeared to increase over this time frame. However, given that chronic hypercapnia reduced CFTR expression in both basal and forskolin-stimulated conditions would suggest that, if this did underlie the effects of chronic hypercapnia on fluid secretion, the basal level of fluid secretion would be reduced also.

There were also other similarities between the effects of acute and chronic hypercapnia on cAMP-regulated ion transport. The volume of IBMX-stimulated fluid secretion was unaffected by chronic hypercapnia, similar to the finding that IBMX-stimulated intracellular

acidification was insensitive to acute hypercapnia. However, when fluid secretion was stimulated by both forskolin and IBMX, hypercapnia reduced fluid secretion. The absence of an effect of CO₂ when [cAMP]_i levels are raised independently of tmAC activity suggested that, if chronic CO₂ is having effects on [cAMP]_i, this is due to modulation of tmAC-dependent cAMP production as opposed to phosphodiesterase-dependent cAMP breakdown. BAPTA-AM also abolished the effect of chronic hypercapnia on forskolin-stimulated fluid secretion, similar to the finding that BAPTA-AM blocked the effect of acute hypercapnia on the forskolin-stimulated intracellular acidification. These findings suggest that chronic hypercapnia also elicits Ca²⁺-dependent effects on cAMP-regulated ion transport. As discussed at great length in chapter 4, there was some evidence that CO₂ mediated its effects *via* an IP₃-dependent Ca²⁺ release which may impact upon Ca²⁺-sensitive tmAC or cAMP-regulated transporters.

5.6.2. The effect of chronic hypercapnia on cAMP-regulated ion and fluid transport – differences to acute hypercapnia?

There were also notable differences between the effects of acute and chronic hypercapnia on cAMP-regulated ion transport in Calu-3 cells. I_{sc} measurements revealed that chronic hypercapnia had no effect on two parameters that were reduced by acute hypercapnia: basal I_{sc} and the rate of forskolin-stimulated increases in I_{sc}. Therefore, this suggests that, unlike the findings from fluid secretion assays, CFTR-dependent ion transport was not affected by chronic hypercapnia. This disparity was not due to the fact that I_{sc} measurements were made in the presence of a basolateral to apical Cl⁻ gradient, as hypercapnia still reduced forskolin-stimulated fluid secretion in these conditions. Notably, in the presence of a basolateral to apical Cl⁻ gradient, the amount of fluid secreted under basal and forskolin-stimulated conditions were significantly enhanced compared to fluid secretion assays in which basolateral and apical Cl⁻ were equal, which was expected given that the driving force for Cl⁻ efflux, and consequentially fluid secretion, were enhanced. The most likely explanation for the disparity between fluid secretion measurements and I_{sc} measurements is that the I_{sc} measurements were performed when the cells were in short-circuit conditions as opposed to, essentially, open-circuit conditions for fluid secretion assays. This could underlie the differences in the responses to hypercapnia and therefore repeating I_{sc} measurements in open circuit conditions is important. An odd finding of the I_{sc} measurements was in the profile of

the response, particularly after the addition of CFTR_{inh} 172. In both normocapnia and hypercapnia, CFTR_{inh} 172 caused an initial reduction in the forskolin-stimulated increase in I_{sc} , but there appeared to be a “rebound” in which I_{sc} increased again before the addition of bumetanide. This was not observed in previous experiments that aimed to investigate the effect of acute hypercapnia on I_{sc} and indicated there was some kind of reversal/wash-off of CFTR_{inh} 172. Why this should only arise in one set of experiments and not others is a mystery but the fact that it was observed in both normocapnia and hypercapnia suggested that it was not a CO₂-dependent effect.

5.6.3. Applying the effects of hypercapnia to a more clinical setting by investigating Calu-3 cell wound repair

A slightly different angle to investigate the effects of hypercapnia on Calu-3 cells was to establish the role of hypercapnia in wound repair. By monitoring the rate of wound closure following the administration of a single scratch, it was found that in two of three independent experiments, hypercapnia increased the rate of wound healing in Calu-3 cells. However, in one experiment, no effect of hypercapnia was found, thus highlighting the large amount of variability that exists between different batches of cells. However, when grouping the data from all three experiments, it was found that hypercapnia did significantly increase the rate of wound healing, although whether this was an effect of acidosis or CO₂ *per se* was unable to be deduced. Such findings would suggest that permissive hypercapnia resulting from the treatment of ARDS/ALI patients may have additional protective effects aside from the reported anti-inflammatory effects of CO₂ (Laffey *et al.*, 2000; Li *et al.*, 2006; Contreras *et al.*, 2012). In one experiment, it was surprisingly found that, in both normocapnia and hypercapnia, serum-containing media actually slowed wound healing compared to serum-free media. These findings suggest that serum-containing media, in which increased cell proliferation would be favoured, actually impaired wound healing and may imply that Calu-3 cells only repair *via* increased cell migration. Therefore, in serum-free media, cells can utilize all of their energy stores into migration and repair faster than if some energy was used during cell division. Interestingly, these findings are in contrast to Schiller *et al.* (2010) who observed no effect of serum on wound repair of Calu-3 cells with possible differences being due to the way in which a wound was induced into the monolayer, with Schiller *et al.* (2010) inducing a circular wound using an electroporation approach as opposed to a scratch-induced

linear wound used in the present study. The effect of chronic hypercapnia on CFTR expression also suggest major differences between my findings and those reported by Schiller *et al.* (2010) who showed that repair of Calu-3 cells was slowed in the presence of CFTR_{inh} 172 or genetic knockdown of CFTR, suggesting CFTR activity was required for efficient wound repair. However, given hypercapnia reduced CFTR expression yet accelerated wound healing implies that a loss of CFTR in Calu-3 cells is not a major factor in wound repair and again differences may lie in the technique for administration of the wound.

How CO₂ is able to modulate wound repair is an area of some debate within the field. There exists conflicting reports into the effect of hypercapnia on wound healing in human cells and, indeed whether these effects were dependent on CO₂-induced acidosis. In agreement with the current findings, Tsuji *et al.* (2013) demonstrated that hypoxia significantly slowed wound healing in human umbilical venous endothelial cells (HUVECs), but this was rescued in the presence of hypercapnia. This effect of CO₂ was independent of acidosis and was a result of increased proliferation of the cells, showing CO₂ *per se* accelerated human cell repair. However, this study failed to assess the role of hypercapnia on wound healing in normoxia and therefore the effect of CO₂ may only be seen because the cells are hypoxic and may not happen in a more physiological environment. Contrasting this, it was found that in HBE and A549 cells, CO₂ *per se* induced a decrease in wound healing due to a CO₂-mediated reduction in NF-κB activity and inhibition of cell migration (O'Toole *et al.*, 2009). Given that, in the current study, the effect of hypercapnia was present in both serum-free and serum-containing media suggested that hypercapnia caused an increase in cell migration as opposed to proliferation and therefore suggests Calu-3 cells display a marked difference in sensitivity to CO₂ compared to HBE and A549 cells. It would be of interest to assess whether the effects of CO₂ on wound healing in Calu-3 cells were also dependent on NF-κB signalling to further establish the mechanism behind the difference in the effects of hypercapnia on wound healing in different airway epithelia. Finally, Caples *et al.* (2009) has shown that hypercapnia slowed wound healing in A549 cells. However, increasing the pH of the media from 7.12 ± 0.18 to 7.40 ± 0.06 by the addition of HCO₃⁻ reversed the inhibitory effect of hypercapnia, suggesting that the effects were due to hypercapnic acidosis as opposed to CO₂ *per se*. Thus, it is clear there are conflicting ideas as to the role of CO₂ in human cell repair from injury and further investigations into this area are of high interest, particularly for hypercapnic lung disease patients.

The major findings of this chapter are summarized below and in figure 5.15.

- Chronic hypercapnia reduced forskolin-stimulated fluid secretion in Calu-3 cells but did not affect the composition of secreted fluid suggesting CFTR activity was reduced but was sufficient to maintain pendrin activity.
- The effect of CO₂ on forskolin-stimulated fluid secretion was abolished by BAPTA-AM but maintained in the presence of IBMX, suggesting hypercapnia affected Ca²⁺-dependent production of cAMP.
- Chronic hypercapnia accelerated wound healing in Calu-3 cells due to increased cell migration. How it does this still remains to be determined but it could involve a CO₂-dependent regulation of NF-κB.

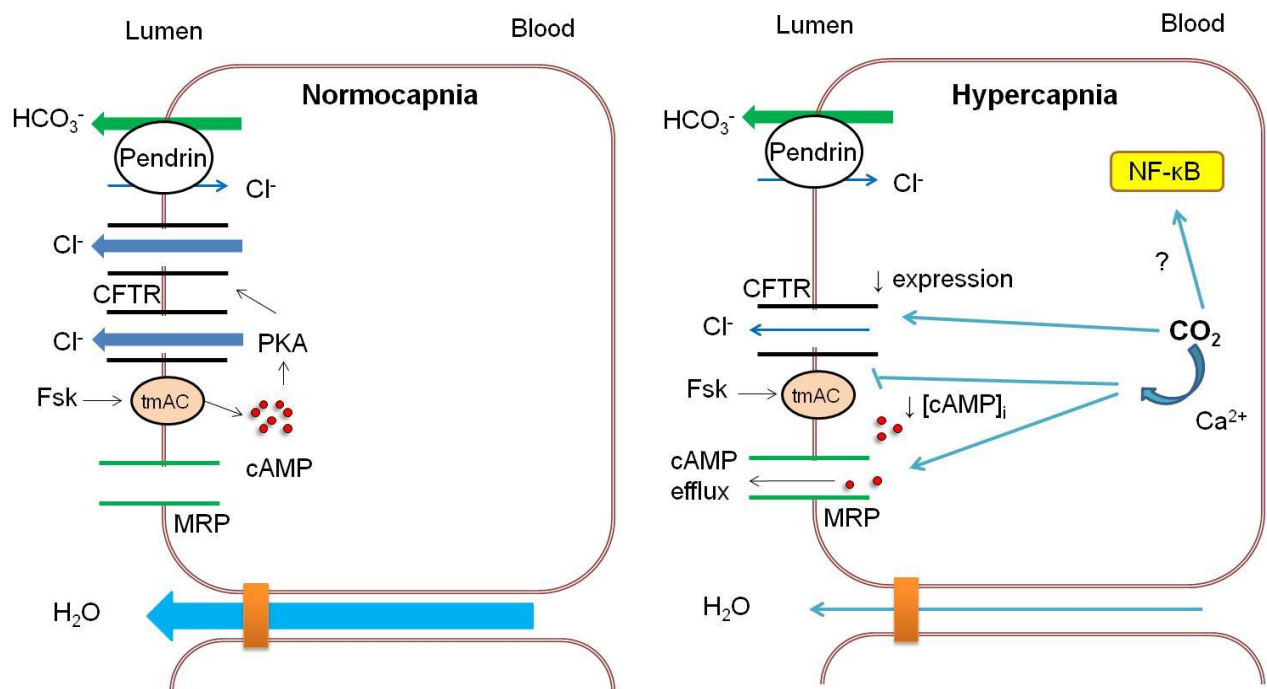


Figure 5.15: Summary of the key effects of chronic hypercapnia on cAMP-regulated ion and fluid transport in Calu-3 cells. In normocapnia, elevations in [cAMP]_i activate CFTR-dependent Cl⁻ secretion creating an osmotic driving force for fluid secretion. CFTR-dependent activation of pendrin causes the secreted fluid to contain ~60mM HCO₃⁻. In hypercapnia, potential Ca²⁺-dependent decreases in [cAMP]_i and reduced CFTR expression reduces the volume of forskolin-stimulated fluid secretion but pendrin activity is maintained, such that secreted HCO₃⁻ is not impaired. CO₂ may also modulate NF-κB to elicit changes in the ability of cell to repair following injury.

Chapter 6: Discussion

6.1. Summary of main findings

This work has been the first to investigate the effects of hypercapnia on cAMP signalling in airway epithelia. Using a model of human serous cells, which secrete a HCO_3^- rich fluid in response to elevations in $[\text{cAMP}]_i$, the effects of both acute and chronic hypercapnia on cAMP-regulated ion and fluid transport were investigated. The majority of experiments performed in this work allowed for the study of vectorial ion and fluid transport in a polarized monolayer of airway epithelia in a dynamic, non-invasive way. Thus, the experimental set up is representative of physiological conditions and thus makes the findings easily transferable to an *in vivo* setting. It was found that acute hypercapnia blunted forskolin-stimulated increases in $[\text{cAMP}]_i$ which was abolished in the presence of BAPTA-AM and 2-APB, suggesting CO_2 modulated $[\text{cAMP}]_i$ in a Ca^{2+} -dependent manner. This adds to the body of growing evidence that CO_2 acts as a cell signalling molecule in human cells by modulating the levels of important cell second messengers (Bouyer *et al.*, 2003; Briva *et al.*, 2007; Vadasz *et al.*, 2008; Townsend *et al.*, 2009; Cook *et al.*, 2012). Acute hypercapnia also caused reductions in CFTR-dependent basal I_{sc} as well as forskolin-stimulated increase in I_{sc} , suggesting that the CO_2 -induced reduction in forskolin-stimulated $[\text{cAMP}]_i$ was sufficient to reduce CFTR-dependent ion transport.

Interestingly, acute hypercapnia caused a significant increase in forskolin/adenosine-stimulated intracellular acidification, suggesting that CO_2 could augment the net difference in HCO_3^- efflux relative to HCO_3^- influx. However, there was no effect of hypercapnia on CFTR-regulated, pendrin-dependent HCO_3^- transport across the apical membrane, and although acute hypercapnia did not significantly affect the activity of cAMP-stimulated NBC activity *per se*, it was found that hypercapnia increased basal NBC activity, such that a subsequent elevation in cAMP was unable to further upregulate NBC activity. This dysregulation of HCO_3^- uptake across the basolateral membrane, under cAMP-stimulated conditions, could underlie the effects of hypercapnia in that, after addition of forskolin, apical HCO_3^- efflux would be stimulated to a much greater extent than basolateral HCO_3^- influx and contribute to the enhanced forskolin-stimulated intracellular acidification observed in hypercapnic conditions. It was also found that the effect of hypercapnia was blocked by ouabain suggesting that the Na^+/K^+ -ATPase was a target of CO_2 , possibly contributing to the

enhanced intracellular acidification *via* increased H^+ influx the transporter has been reported to be capable of (Vedovato and Gadsby, 2014).

The effects of acute hypercapnia on cAMP-stimulated HCO_3^- transport were blocked by BAPTA-AM, 2-APB and U73122 and mimicked by the Ca^{2+} elevating agonist ATP and, to a lesser extent, by carbachol and UTP. These results suggest that hypercapnia mediated its effects *via* an IP_3 -dependent Ca^{2+} release, stimulated by a CO_2 -induced release of ATP from airway cells to signal *via* an autocrine signalling mechanism. However, the effect of hypercapnia remained even when the ER stores were depleted of Ca^{2+} and there was little evidence to suggest that CO_2 induced an ATP release from the cells. Further experiments are therefore required to fully deduce the role of Ca^{2+} signalling in underlying the effects of hypercapnia on cAMP-regulated HCO_3^- transport. Inhibition of pannexins, by two reported pannexin inhibitors, caused a significant reduction in the extent by which acute hypercapnia could modulate cAMP-regulated HCO_3^- transport. This suggests that CO_2 may activate the efflux of an endogenous Ca^{2+} -elevating agonist *via* pannexin channels which activates G_q coupled receptors to trigger increases in $[Ca^{2+}]_i$. This change in $[Ca^{2+}]_i$ could then influence $[cAMP]_i$ due to modulation of the activity of Ca^{2+} -dependent tmACs or MRPs, or alter the activity of transporters seemingly involved in underlying the effect of acute hypercapnia on HCO_3^-/H^+ transport i.e. NBC and Na^+/K^+ -ATPase.

The effects of chronic hypercapnia were also investigated. Here, it was found that chronic hypercapnia reduced the volume of forskolin-stimulated, but not IBMX-stimulated, fluid secretion over 24 hours in a mechanism that required changes in $[Ca^{2+}]_i$. However, chronic hypercapnia had no effect on the change in the HCO_3^- concentration or mucus content of secreted fluid, suggesting that transporters involved in transepithelial fluid secretion and transporters involved in regulating the composition of the secreted fluid have different sensitivities to CO_2 . Interestingly, chronic hypercapnia had no effect on forskolin-stimulated ion transport measured using an Ussing chamber. This may be due to the fact that I_{sc} measurements are performed in closed-circuit conditions and therefore highlights that different experimental approaches used to measure cAMP-stimulated ion transport can lead to contrasting results. Chronic hypercapnia also appeared to accelerate the rate of wound healing of Calu-3 cell monolayers, although the data was highly variable with the effect of hypercapnia only being observed in two out of three independent experiments.

6.2. Clinical relevance of findings to hypercapnic lung disease patients

Several lung diseases lead to hypercapnia in humans with hypercapnia arising from the pathology of the disease (e.g. COPD) or as a result of treatment of the diseases (ARDS/ALI) (Lourenco and Miranda, 1968; Prin *et al.*, 2002). My findings may provide an explanation into how CO₂ can act as a cell signalling molecule to modulate cAMP-regulated ion and fluid transport in Calu-3 cells and therefore, should the same effects of CO₂ occur *in vivo*, CO₂ would be predicted to impair ion and fluid transport in serous cells of the submucosal glands. Efficient secretion of Cl⁻ and HCO₃⁻ from serous cells is crucial to maintain the properties and pH of the airway surface liquid and studies have found that a reduction in ASL pH reduces the killing of the airway pathogen *Pseudomonas aeruginosa* (Pezzulo *et al.*, 2012) which contributes to the increased airway colonization of bacteria in the airways of CF patients. I found that hypercapnia altered cAMP-regulated ion and fluid transport in Calu-3 cells suggesting that hypercapnia may impact upon the secretion of ASL from submucosal glands and thus compromise the innate defence mechanisms of the lung. Although the majority of experiments in the present study have focussed on the effects of acute hypercapnia, in terms of a clinical relevance, the most applicable findings come from those done on chronic hypercapnia, given that it would be highly unlikely for respiratory disease patients to only be hypercapnic for 20-30 minutes. Therefore, given that chronic hypercapnia caused a reduction in cAMP-stimulated fluid secretion from Calu-3 cells, it suggests that hypercapnic patients may be at risk from dehydration of the ASL. ASL dehydration would reduce the volume of the periciliary layer of the ASL and could lead to the cilia becoming clogged in the overlying mucus layer which would impair mucociliary clearance of inhaled pathogens – a phenotype similar to that observed in CF patients (Randell *et al.*, 2006; Boucher, 2007). Therefore, aside from the underlying lung disease that causes hypercapnia, patients may then become more susceptible to airway infection and therefore further complications would ensue. However, in ARDS patients, who suffer from pulmonary edema due to increased permeability of the alveolar epithelium (Grommes and Soehnlein, 2011), a decrease in cAMP-stimulated fluid secretion would actually be of benefit to the patient as it would help minimize the extent of the edema. Therefore, this may underlie an additional protective effect of the permissive hypercapnia resulting from treatment of the disease. Another potential benefit of the permissive hypercapnia in ARDS/ALI patients, could be from the accelerated wound healing hypercapnia appears to induce in airway epithelia. It has been reported that the high degree of inflammation in ARDS patients damages surrounding

tissue (Tomashefski *et al.*, 1983; Meduri *et al.*, 2007; Ito *et al.*, 2014)) and therefore permissive hypercapnia may act to help repair tissue damage. Ito *et al.* (2014) reported that ARDS/ALI patients suffer from alveolar epithelial cell injury and demonstrated that alveolar epithelial cell repair was enhanced by secretion of human growth factor from lung fibroblasts. Thus, a possible explanation for the increase in the rate of wound healing of Calu-3 cells exposed to chronic hypercapnia may be due to enhanced secretion of growth factors which would contribute to the protective effects of permissive hypercapnia in the treatment of ARDS/ALI.

6.3. Future experiments

Inevitably, there are a wide range of future experiments that should be performed in order to strengthen the conclusions made from the current study and to provide further insights into the effect of hypercapnia on cAMP signalling in airway epithelia. Interpreting data from an immortalised cell line can be problematic given that human cell lines are only models of native cells and thus findings from experiments may not reflect what happens physiologically *in vivo*. Calu-3 cells are reported to have abnormalities in chromosomes 1, 13, 15 and 17 (Ballard and Inglis, 2004) which would likely alter the genome of these cells relative to native human serous cells. These changes in gene expression could induce changes in the amino acid sequence or overall protein structure of translated proteins that may alter their CO₂ sensitivity relative to proteins expressed in native tissue. Repeating studies on primary airway epithelia is important in order to establish whether native serous cells respond to acute hypercapnia in a similar way. It is worth noting that Professor Steve Ballard (University of South Alabama, USA) performed experiments in which the amount of fluid secreted from isolated porcine bronchi was measured in normocapnia and hypercapnia. These results showed that there was no effect of hypercapnia on the amount of forskolin-stimulated fluid secreted and therefore contradicted the findings from Calu-3 cells (Ballard, 2013 – personal communication). Ballard *et al.* (2006) have shown that removal of surface epithelium from porcine trachea has no effect on the fluid secreted suggesting that the submucosal glands secrete ASL in porcine airways thus suggesting porcine serous cells are insensitive to CO₂. The pig is widely accepted as a good model for investigations into CFTR-dependent ion and fluid transport in the airways given that CF pigs exhibit similar defects to CF humans, including impaired Cl⁻ transport across airway epithelia (Rogers *et al.*, 2008). CFTR-deficient

pigs have also been shown to have a reduced rate of fluid secretion from submucosal glands in response to forskolin and carbachol – similar to what is found in humans (Choi *et al.*, 2007; Joo *et al.*, 2010) whilst comparisons between pig serous cells and human nasal cells show that the molecular mechanisms underlying VIP-stimulated Cl^- and fluid secretion in each species was highly similar (Lee and Foskett, 2010). Therefore, the literature suggests the pig is an appropriate model for studying CFTR-dependent ion and fluid transport in humans and thus further studies into the effects of hypercapnia on this process in pigs are important.

The results obtained in the present work mostly involved the use of pharmacological agents. These can be problematic due to potential off target effects that many drugs possess. For instance, the PKA inhibitor H-89 affects a host of other kinases including protein kinase B, ribosomal protein s6 kinase and mitogen and stress-activated kinase (Murray, 2008) and therefore deducing whether the effects of H-89 were due to PKA inhibition or due to inhibition of another kinase is difficult. Similarly, it was difficult to interpret the data from experiments in which carbenoxolone was used given the many offsite targets this drug possesses. Therefore, it would be important to repeat some experiments in genetically modified Calu-3 cells in which the target protein had been knocked out. Specifically, knockdown of IP_3 receptors would provide further insights into the role of IP_3 -dependent Ca^{2+} release in response to hypercapnia. DT40-K/O cells, in which $\text{IP}_3\text{R1}$, R2 and R3 have all been genetically disrupted display no IP_3 -dependent Ca^{2+} release (Sugawara *et al.*, 1997) and were used by Cook *et al.* (2012) to demonstrate that hypercapnia-induced reductions in $[\text{cAMP}]_i$ required IP_3 -dependent Ca^{2+} release. It would be of interest to attempt to knockdown IP_3R expression in Calu-3 cells given that DT40 cells are actually chicken lymphocyte cells and therefore may respond differently to CO_2 than human airway epithelia. I provided some evidence that pannexins were involved in transducing the CO_2 signal in Calu-3 cells given that non-specific pharmacological inhibition of pannexin-1 using probenecid or carbenoxolone significantly reduced the effect of hypercapnia on forskolin-stimulated HCO_3^- transport. Thus, pannexin-1 knockdown Calu-3 cells could be used to determine the role of pannexins in the effects of hypercapnia. Seminario-Vidal *et al.* (2011) used a short hairpin RNA lentiviral approach to knockdown pannexin-1 expression by 66% in Calu-3 cells and demonstrated this caused a marked reduction in the amount of ATP released from these cells. Therefore, it would be interesting to adopt the same approach to assess whether hypercapnia modulates cAMP-regulated HCO_3^- transport in pannexin-1 knockdown Calu-3 cells. It is worth noting that RNA interference approaches to silence gene expression have variable

success rates in Calu-3 cells and future strategies for efficient knockout studies could involve the recently described CRISPR-Cas9 technology, in which clustered regulatory interspaced short palindromic repeats (CRISPR) and CRISPR-associated proteins (Cas proteins), endogenous to prokaryotes, are transfected into eukaryotic cells (Mali *et al.*, 2013; Qi *et al.*, 2013). Under the direction of guide RNA, targeted to a specific DNA sequence, Cas proteins unwind and cleave the targeted DNA sequences, thus inhibiting gene expression. This powerful tool appears to be the future for manipulation of gene expression in human cells (Zhou *et al.*, 2014) and has already been used to good effect to knockout expression of the vWF gene in pigs (Hai *et al.*, 2014).

CO₂ has been shown to reduce forskolin-stimulated [cAMP]_i in Calu-3 cells with effects seemingly mediated *via* inhibition of tmAC and/or activation of cAMP efflux *via* MRPs. With this in mind, it would be interesting to identify the isoforms of tmAC expressed in Calu-3 cells using PCR and to determine whether only a subset of these (for instance, only the Ca²⁺-sensitive isoforms) are CO₂-sensitive. Once the CO₂-sensitive tmAC isoforms had been identified, they could be expressed in a heterologous expression system and mutations within the amino acid sequence could be introduced to help identify CO₂-sensitive residues or potential carbamylation (post-translational modification of amino acids by CO₂) sites within the protein. Regulation of connexin 26 by CO₂ has been suggested to be a result of carbamylation of a specific motif in the protein that caused an interaction between a lysine residue and a nearby arginine residue to facilitate channel opening (Meigh *et al.*, 2013) and investigations into protein carbamylation will form a significant part of future work into CO₂ signalling in human cells. It would also be of interest to repeat the [cAMP]_i assay in the presence of MK-571 to establish whether the CO₂-induced reduction in forskolin-stimulated cAMP is dependent on MRP activity. Similarly, expression of MRPs into cells that do not endogenously express these proteins would establish whether these proteins are CO₂ sensitive and whether they are involved in mediating CO₂-induced reductions in forskolin-stimulated [cAMP]_i.

This study has focussed predominantly on the effect of two different CO₂ concentrations: 5% CO₂, used as a representative normocapnic level and 10% CO₂ used to induce hypercapnia. It would be worth investigating whether increasing CO₂ to an even higher level caused further modulations to cAMP-regulated ion and fluid transport and a dose-response curve to CO₂ would be illuminating to establish which concentration of CO₂ induces the most pronounced effects on cAMP-regulated ion and fluid transport.

It is important to note that two important experiments were performed when cells were grown as a non-polarized monolayer. The radiolabelled [cAMP]_i assay were performed on cells grown on 12 well plates whilst measurements on [Ca²⁺]_i were performed on cells grown on glass coverslips. Therefore, the non-polarized nature of these cells are not representative of an *in vivo* setting and therefore responses to hypercapnia in these conditions may not be representative of what occurs physiologically. Therefore, it will be important to repeat these experiments on polarized Calu-3 cells. Furthermore, my data showed there existed high levels of variability between batches and passages of Calu-3 cells. Indeed, this variability was so pronounced that when observing the effect of wound healing in Calu-3 cells, it was found that hypercapnia significantly accelerated wound healing in one batch of cells but there was no effect of hypercapnia when the experiment was repeated two weeks later on a different batch of cells. In addition, when measuring the hypercapnia-induced fold increase in the rate of forskolin-stimulated HCO₃⁻ flux, this ranged from ~2 fold to ~8 fold between different passages of cells. Therefore, when testing the effects of pharmacological agents, it was important to perform control experiments at the same time to get a measure of the extent of the effect of hypercapnia on that particular batch of cells. The fact that control experiments were always run in parallel enabled me to conclude that any effects of pharmacological agents were real and not due to variability between batches of cells, but it would still be important to repeat important experiments on more than one batch of Calu-3 cells. Such variability between batches and passages of Calu-3 cells could stem from the fact that Calu-3 cells are a mixed population of both CFTR-expressing, non-mucus cells and mucus-secreting goblet-like cells (Shen *et al.*, 1994; Kreda *et al.*, 2007) and the relative population of each cell type in each separate culture was unknown. It is possible that only the CFTR-expressing cells were CO₂-sensitive and therefore the more pronounced effects of hypercapnia were observed when there was a higher proportion of these cells in the culture relative to the number of mucus-secreting cells.

To gain further insights into the effects of hypercapnia on Calu-3 cells on a more global scale, high throughput investigations into gene expression and post-translational protein modifications in response to CO₂ should be performed. Microarray analysis would identify genes in which expression had been altered by hypercapnia which could lead to further research into the potential roles these genes may have in mediating effects of hypercapnia on cAMP-signalling, amongst other effects. Microarray studies were used by Ross *et al.* (2007) and Pezzulo *et al.* (2011) to investigate the mechanisms behind the differentiation of human

bronchial epithelia when grown at an air-liquid interface (ALI) and to compare gene expression between *in vivo* and *in vitro* primary airway epithelial cells grown at ALI as well as Calu-3 cells grown at ALI. These studies provided important information about gene expression changes during airway epithelial cell differentiation and the differences that exist between primary airway epithelia when obtained from healthy individuals *in vivo* or cultured *in vitro*. These experiments uncovered a whole host of genes that were upregulated during differentiation which will pave the way for future studies into the roles of these genes in airway epithelia differentiation.

My data suggested that hypercapnia modulates both cAMP and PLC signalling pathways which would be predicted to have effects on both PKA and PKC activity. With this in mind, it would be interesting to assess the effect of hypercapnia on the phosphorylation profiles of proteins using a phosphoproteomics approach. This method has been used by Gunaratne *et al.* (2010) to investigate the proteins that became phosphorylated in response to elevations in $[cAMP]_i$ in renal cells and provided further insights into the role of vasopressin signalling in the kidney. A reduction in the phosphorylation states of PKA-regulated proteins in hypercapnia would provide further evidence of a CO_2 -induced reduction in $[cAMP]_i$ and may uncover other potential CO_2 -sensitive proteins in which further studies into CO_2 signalling can be built upon.

6.4. Final conclusions

The present work has shown that both acute and chronic hypercapnia have significant effects of cAMP-regulated ion and fluid transport in Calu-3 cells. These findings provide further evidence and insights into how CO_2 behaves as a cell signalling molecule in human cells and suggests that in hypercapnic lung disease patients, potential dysregulation of the ASL may provide important information into the underlying pathology of the elevated P_aCO_2 . Further research into this area should focus on a better understanding of the molecular mechanisms underlying the effect of CO_2 on cAMP signalling, particularly the role of Ca^{2+} signalling. Repeating these experiments in primary human or other mammalian tissue is important to observe whether the reported effects of hypercapnia occur in a more physiological setting.

References

- Abolhassani, M., Guais, A., Chaumet-Riffaud, P., Sasco, A.J. and Schwartz, L. (2009) 'Carbon dioxide inhalation causes pulmonary inflammation', *Am J Physiol Lung Cell Mol Physiol*, 296(4), pp. L657-65.
- Abraham, E.H., Prat, A.G., Gerweck, L., Seneveratne, T., Arceci, R.J., Kramer, R., Guidotti, G. and Cantiello, H.F. (1993) 'The multidrug resistance (mdr1) gene product functions as an ATP channel', *Proc Natl Acad Sci U S A*, 90(1), pp. 312-6.
- Adijanto, J., Banzon, T., Jalickee, S., Wang, N.S. and Miller, S.S. (2009) 'CO₂-induced ion and fluid transport in human retinal pigment epithelium', *J Gen Physiol*, 133(6), pp. 603-22.
- Allen, A. and Flemstrom, G. (2005) 'Gastroduodenal mucus bicarbonate barrier: protection against acid and pepsin', *Am J Physiol Cell Physiol*, 288(1), pp. C1-19.
- Alvarez, C. and Sztul, E.S. (1999) 'Brefeldin A (BFA) disrupts the organization of the microtubule and the actin cytoskeletons', *Eur J Cell Biol*, 78(1), pp. 1-14.
- Amato, M.B., Barbas, C.S., Medeiros, D.M., Magaldi, R.B., Schettino, G.P., Lorenzi-Filho, G., Kairalla, R.A., Deheinzelin, D., Munoz, C., Oliveira, R., Takagaki, T.Y. and Carvalho, C.R. (1998) 'Effect of a protective-ventilation strategy on mortality in the acute respiratory distress syndrome', *N Engl J Med*, 338(6), pp. 347-54.
- Ameziane-El-Hassani, R., Morand, S., Boucher, J.L., Frapart, Y.M., Apostolou, D., Agnandji, D., Gnidehou, S., Ohayon, R., Noel-Hudson, M.S., Francon, J., Lalaoui, K., Virion, A. and Dupuy, C. (2005) 'Dual oxidase-2 has an intrinsic Ca²⁺-dependent H₂O₂-generating activity', *J Biol Chem*, 280(34), pp. 30046-54.
- Anagnostopoulou, P., Riederer, B., Duerr, J., Michel, S., Binia, A., Agrawal, R., Liu, X., Kalitzki, K., Xiao, F., Chen, M., Schatterny, J., Hartmann, D., Thum, T., Kabesch, M., Soleimani, M., Seidler, U. and Mall, M.A. (2012) 'SLC26A9-mediated chloride secretion prevents mucus obstruction in airway inflammation', *J Clin Invest*, 122(10), pp. 3629-34.
- Anderson, M.P., Berger, H.A., Rich, D.P., Gregory, R.J., Smith, A.E. and Welsh, M.J. (1991) 'Nucleoside triphosphates are required to open the CFTR chloride channel', *Cell*, 67(4), pp. 775-84.
- Ando, H., Mizutani, A., Matsu-ura, T. and Mikoshiba, K. (2003) 'IRBIT, a novel inositol 1,4,5-trisphosphate (IP₃) receptor-binding protein, is released from the IP₃ receptor upon IP₃ binding to the receptor', *J Biol Chem*, 278(12), pp. 10602-12.
- Arch, J.R. and Newsholme, E.A. (1978) 'Activities and some properties of 5'-nucleotidase, adenosine kinase and adenosine deaminase in tissues from vertebrates and invertebrates in relation to the control of the concentration and the physiological role of adenosine', *Biochem J*, 174(3), pp. 965-77.
- Avella, M., Loriol, C., Boulukos, K., Borgese, F. and Ehrenfeld, J. (2011) 'SLC26A9 stimulates CFTR expression and function in human bronchial cell lines', *J Cell Physiol*, 226(1), pp. 212-23.

Bachmann, O., Franke, K., Yu, H., Riederer, B., Li, H.C., Soleimani, M., Manns, M.P. and Seidler, U. (2008) 'cAMP-dependent and cholinergic regulation of the electrogenic intestinal/pancreatic $\text{Na}^+/\text{HCO}_3^-$ cotransporter pNBC1 in human embryonic kidney (HEK293) cells', *BMC Cell Biol*, 9, p. 70.

Bachmann, O., Rossmann, H., Berger, U.V., Colledge, W.H., Ratcliff, R., Evans, M.J., Gregor, M. and Seidler, U. (2003) 'cAMP-mediated regulation of murine intestinal/pancreatic $\text{Na}^+/\text{HCO}_3^-$ cotransporter subtype pNBC1', *Am J Physiol Gastrointest Liver Physiol*, 284(1), pp. G37-45.

Ballard, S.T. and Inglis, S.K. (2004) 'Liquid secretion properties of airway submucosal glands', *J Physiol*, 556(Pt 1), pp. 1-10.

Ballard, S.T., Parker, J.C. and Hamm, C.R. (2006) 'Restoration of mucociliary transport in the fluid-depleted trachea by surface-active instillates', *Am J Respir Cell Mol Biol*, 34(4), pp. 500-4.

Ballard, S.T., Trout, L., Bebök, Z., Sorscher, E.J. and Crews, A. (1999) 'CFTR involvement in chloride, bicarbonate, and liquid secretion by airway submucosal glands', *American Journal of Physiology*, 277(4 Part 1), pp. L694-L699.

Banwell, J.G., Northam, B.E. and Cooke, W.T. (1967) 'Secretory response of the human pancreas to continuous intravenous infusion of secretin', *Gut*, 8(1), pp. 50-7.

Barnes, A.P., Livera, G., Huang, P., Sun, C., O'Neal, W.K., Conti, M., Stutts, M.J. and Milgram, S.L. (2005) 'Phosphodiesterase 4D forms a cAMP diffusion barrier at the apical membrane of the airway epithelium', *J Biol Chem*, 280(9), pp. 7997-8003.

Bernardo, A.A., Espiritu, D.J., Ruiz, O.S., Robey, R.B. and Arruda, J.A. (2003) 'The role of phosphatidylinositol 3-kinase (PI3K) in CO_2 stimulation of the $\text{Na}^+/\text{HCO}_3^-$ cotransporter (NBC)', *J Membr Biol*, 191(2), pp. 141-8.

Berthet, J., Rall, T.W. and Sutherland, E.W. (1957) 'The relationship of epinephrine and glucagon to liver phosphorylase. IV. Effect of epinephrine and glucagon on the reactivation of phosphorylase in liver homogenates', *J Biol Chem*, 224(1), pp. 463-75.

Bertorello, A.M., Ridge, K.M., Chibalin, A.V., Katz, A.I. and Sznajder, J.I. (1999) 'Isoproterenol increases Na^+/K^+ -ATPase activity by membrane insertion of alpha-subunits in lung alveolar cells', *Am J Physiol*, 276(1 Pt 1), pp. L20-7.

Bertrand, C.A., Zhang, R., Pilewski, J.M. and Frizzell, R.A. (2009) 'SLC26A9 is a constitutively active, CFTR-regulated anion conductance in human bronchial epithelia', *J Gen Physiol*, 133(4), pp. 421-38.

Bhaskar, K.R., Gong, D.H., Bansil, R., Pajevic, S., Hamilton, J.A., Turner, B.S. and LaMont, J.T. (1991) 'Profound increase in viscosity and aggregation of pig gastric mucin at low pH', *Am J Physiol*, 261(5 Pt 1), pp. G827-32.

Bleasdale, J.E., Thakur, N.R., Gremban, R.S., Bundy, G.L., Fitzpatrick, F.A., Smith, R.J. and Bunting, S. (1990) 'Selective inhibition of receptor-coupled phospholipase C-dependent processes in human platelets and polymorphonuclear neutrophils', *J Pharmacol Exp Ther*, 255(2), pp. 756-68.

- Bogman, K., Erne-Brand, F., Alsenz, J. and Drewe, J. (2003) 'The role of surfactants in the reversal of active transport mediated by multidrug resistance proteins', *J Pharm Sci*, 92(6), pp. 1250-61.
- Boron, W.F., Waisbren, S.J., Modlin, I.M. and Geibel, J.P. (1994) 'Unique permeability barrier of the apical surface of parietal and chief cells in isolated perfused gastric glands', *J Exp Biol*, 196, pp. 347-60.
- Boucher, R.C. (2007) 'Evidence for airway surface dehydration as the initiating event in CF airway disease', *J Intern Med*, 261(1), pp. 5-16.
- Bouyer, P., Zhou, Y. and Boron, W.F. (2003) 'An increase in intracellular calcium concentration that is induced by basolateral CO₂ in rabbit renal proximal tubule', *Am J Physiol Renal Physiol*, 285(4), pp. F674-87.
- Bove, P.F., Grubb, B.R., Okada, S.F., Ribeiro, C.M., Rogers, T.D., Randell, S.H., O'Neal, W.K. and Boucher, R.C. (2010) 'Human alveolar type II cells secrete and absorb liquid in response to local nucleotide signaling', *J Biol Chem*, 285(45), pp. 34939-49.
- Bramley, J.R., Wiles, E.M., Sollars, P.J. and Pickard, G.E. (2011) 'Carbenoxolone blocks the light-evoked rise in intracellular calcium in isolated melanopsin ganglion cell photoreceptors', *PLoS One*, 6(7), p. e22721.
- Briva, A., Santos, C., Malacrida, L., Rocchiccioli, F., Soto, J., Angulo, M., Batthyany, C., Cairoli, E. and Piriz, H. (2011) 'Adenosine triphosphate-dependent calcium signaling during ventilator-induced lung injury is amplified by hypercapnia', *Exp Lung Res*, 37(8), pp. 471-81.
- Briva, A., Vadasz, I., Lecuona, E., Welch, L.C., Chen, J., Dada, L.A., Trejo, H.E., Dumasius, V., Azzam, Z.S., Myrianthefs, P.M., Battle, D., Gruenbaum, Y. and Sznajder, J.I. (2007) 'High CO₂ levels impair alveolar epithelial function independently of pH', *PLoS One*, 2(11), p. e1238.
- Bruzzzone, R., Barbe, M.T., Jakob, N.J. and Monyer, H. (2005) 'Pharmacological properties of homomeric and heteromeric pannexin hemichannels expressed in *Xenopus* oocytes', *J Neurochem*, 92(5), pp. 1033-43.
- Button, B., Cai, L.H., Ehre, C., Kesimer, M., Hill, D.B., Sheehan, J.K., Boucher, R.C. and Rubinstein, M. (2012) 'A periciliary brush promotes the lung health by separating the mucus layer from airway epithelia', *Science*, 337(6097), pp. 937-41.
- Button, B., Picher, M. and Boucher, R.C. (2007) 'Differential effects of cyclic and constant stress on ATP release and mucociliary transport by human airway epithelia', *J Physiol*, 580(Pt. 2), pp. 577-92.
- Caples, S.M., Rasmussen, D.L., Lee, W.Y., Wolfert, M.Z. and Hubmayr, R.D. (2009) 'Impact of buffering hypercapnic acidosis on cell wounding in ventilator-injured rat lungs', *Am J Physiol Lung Cell Mol Physiol*, 296(1), pp. L140-4.
- Carranza, M.L., Feraille, E., Kiroytcheva, M., Rousselot, M. and Favre, H. (1996) 'Stimulation of ouabain-sensitive 86Rb⁺ uptake and Na⁺,K⁺-ATPase alpha-subunit phosphorylation by a cAMP-dependent signalling pathway in intact cells from rat kidney cortex', *FEBS Lett*, 396(2-3), pp. 309-14.

- Chen, E.Y., Yang, N., Quinton, P.M. and Chin, W.C. (2010) 'A new role for bicarbonate in mucus formation', *Am J Physiol Lung Cell Mol Physiol*, 299(4), pp. L542-9.
- Chen, L., Patel, R.P., Teng, X., Bosworth, C.A., Lancaster, J.R., Jr. and Matalon, S. (2006) 'Mechanisms of cystic fibrosis transmembrane conductance regulator activation by S-nitrosoglutathione', *J Biol Chem*, 281(14), pp. 9190-9.
- Chen, M., Praetorius, J., Zheng, W., Xiao, F., Riederer, B., Singh, A.K., Stieger, N., Wang, J., Shull, G.E., Aalkjaer, C. and Seidler, U. (2012) 'The electroneutral $\text{Na}^+:\text{HCO}_3^-$ cotransporter NBCn1 is a major pHi regulator in murine duodenum', *J Physiol*, 590(Pt 14), pp. 3317-33.
- Chen, Z.S., Lee, K. and Kruh, G.D. (2001) 'Transport of cyclic nucleotides and estradiol 17-beta-D-glucuronide by multidrug resistance protein 4. Resistance to 6-mercaptopurine and 6-thioguanine', *J Biol Chem*, 276(36), pp. 33747-54.
- Cheng, S.H., Rich, D.P., Marshall, J., Gregory, R.J., Welsh, M.J. and Smith, A.E. (1991) 'Phosphorylation of the R domain by cAMP-dependent protein kinase regulates the CFTR chloride channel', *Cell*, 66(5), pp. 1027-36.
- Choi, J.Y., Joo, N.S., Krouse, M.E., Wu, J.V., Robbins, R.C., Ianowski, J.P., Hanrahan, J.W. and Wine, J.J. (2007) 'Synergistic airway gland mucus secretion in response to vasoactive intestinal peptide and carbachol is lost in cystic fibrosis', *J Clin Invest*, 117(10), pp. 3118-27.
- Choi, J.Y., Muallem, D., Kiselyov, K., Lee, M.G., Thomas, P.J. and Muallem, S. (2001) 'Aberrant CFTR-dependent HCO_3^- transport in mutations associated with cystic fibrosis', *Nature*, 410(6824), pp. 94-7.
- Coakley, R.D., Grubb, B.R., Paradiso, A.M., Gatzky, J.T., Johnson, L.G., Kreda, S.M., O'Neal, W.K. and Boucher, R.C. (2003) 'Abnormal surface liquid pH regulation by cultured cystic fibrosis bronchial epithelium', *Proc Natl Acad Sci U S A*, 100(26), pp. 16083-8.
- Cobb, B.R., Fan, L., Kovacs, T.E., Sorscher, E.J. and Clancy, J.P. (2003) 'Adenosine receptors and phosphodiesterase inhibitors stimulate Cl^- secretion in Calu-3 cells', *Am J Respir Cell Mol Biol*, 29(3 Pt 1), pp. 410-8.
- Cobb, B.R., Ruiz, F., King, C.M., Fortenberry, J., Greer, H., Kovacs, T., Sorscher, E.J. and Clancy, J.P. (2002) ' A_2 adenosine receptors regulate CFTR through PKA and PLA_2 ', *Am J Physiol Lung Cell Mol Physiol*, 282(1), pp. L12-25.
- Conti, M. and Beavo, J. (2007) 'Biochemistry and physiology of cyclic nucleotide phosphodiesterases: essential components in cyclic nucleotide signaling', *Annu Rev Biochem*, 76, pp. 481-511.
- Contreras, M., Ansari, B., Curley, G., Higgins, B.D., Hassett, P., O'Toole, D. and Laffey, J.G. (2012) 'Hypercapnic acidosis attenuates ventilation-induced lung injury by a nuclear factor-kappaB-dependent mechanism', *Crit Care Med*, 40(9), pp. 2622-30.
- Cook, Z.C., Gray, M.A. and Cann, M.J. (2012) 'Elevated Carbon Dioxide Blunts Mammalian cAMP Signaling Dependent on Inositol 1,4,5-Triphosphate Receptor-mediated Ca^{2+} Release', *J Biol Chem*, 287(31), pp. 26291-301.

- Cooper, D.M. (2003) 'Regulation and organization of adenylyl cyclases and cAMP', *Biochem J*, 375(Pt 3), pp. 517-29.
- Cooper, D.M., Karpen, J.W., Fagan, K.A. and Mons, N.E. (1998) ' Ca^{2+} -sensitive adenylyl cyclases', *Adv Second Messenger Phosphoprotein Res*, 32, pp. 23-51.
- Cooper, D.M., Mons, N. and Karpen, J.W. (1995) 'Adenylyl cyclases and the interaction between calcium and cAMP signalling', *Nature*, 374(6521), pp. 421-4.
- Coue, M., Brenner, S.L., Spector, I. and Korn, E.D. (1987) 'Inhibition of actin polymerization by latrunculin A', *FEBS Lett*, 213(2), pp. 316-8.
- Dagenais, A., Denis, C., Vives, M.F., Girouard, S., Masse, C., Nguyen, T., Yamagata, T., Grygorczyk, C., Kothary, R. and Berthiaume, Y. (2001) 'Modulation of α -ENaC and α 1- Na^+ - K^+ -ATPase by cAMP and dexamethasone in alveolar epithelial cells', *Am J Physiol Lung Cell Mol Physiol*, 281(1), pp. L217-30.
- Dahms, T., Horvath, S.M., Luzzana, M., Rossi-Bernardi, L., Roughton, F.J. and Stella, G. (1972) 'The regulation of oxygen affinity of human haemoglobin', *J Physiol*, 223(1), pp. 29P-31P.
- Damkier, H.H., Nielsen, S. and Praetorius, J. (2007) 'Molecular expression of SLC4-derived Na^+ -dependent anion transporters in selected human tissues', *Am J Physiol Regul Integr Comp Physiol*, 293(5), pp. R2136-46.
- Das, S., Du, Z., Bassly, S., Singer, L. and Vicencio, A.G. (2009) 'Effects of chronic hypercapnia in the neonatal mouse lung and brain', *Pediatr Pulmonol*, 44(2), pp. 176-82.
- de Seigneux, S., Malte, H., Dimke, H., Frokiaer, J., Nielsen, S. and Frische, S. (2007) 'Renal compensation to chronic hypoxic hypercapnia: downregulation of pendrin and adaptation of the proximal tubule', *Am J Physiol Renal Physiol*, 292(4), pp. F1256-66.
- De Smet, H.R., Bersten, A.D., Barr, H.A. and Doyle, I.R. (2007) 'Hypercapnic acidosis modulates inflammation, lung mechanics, and edema in the isolated perfused lung', *J Crit Care*, 22(4), pp. 305-13.
- Derand, R., Montoni, A., Bulteau-Pignoux, L., Janet, T., Moreau, B., Muller, J.M. and Becq, F. (2004) 'Activation of VPAC1 receptors by VIP and PACAP-27 in human bronchial epithelial cells induces CFTR-dependent chloride secretion', *Br J Pharmacol*, 141(4), pp. 698-708.
- Devor, D.C., Singh, A.K., Lambert, L.C., DeLuca, A., Frizzell, R.A. and Bridges, R.J. (1999) 'Bicarbonate and chloride secretion in Calu-3 human airway epithelial cells', *J Gen Physiol*, 113(5), pp. 743-60.
- Endeward, V., Musa-Aziz, R., Cooper, G.J., Chen, L.M., Pelletier, M.F., Virkki, L.V., Supuran, C.T., King, L.S., Boron, W.F. and Gros, G. (2006) 'Evidence that aquaporin 1 is a major pathway for CO_2 transport across the human erythrocyte membrane', *FASEB J*, 20(12), pp. 1974-81.

- Engelhardt, J.F., Zepeda, M., Cohn, J.A., Yankaskas, J.R. and Wilson, J.M. (1994) 'Expression of the cystic fibrosis gene in adult human lung', *Journal of Clinical Investigation*, 93(2), pp. 737-749.
- Espinosa, M., Noe, G., Troncoso, C., Ho, S.B. and Villalon, M. (2002) 'Acidic pH and increasing $[Ca^{2+}]$ reduce the swelling of mucins in primary cultures of human cervical cells', *Hum Reprod*, 17(8), pp. 1964-72.
- Espiritu, D.J., Bernardo, A.A., Robey, R.B. and Arruda, J.A. (2002) 'A central role for Pyk2-Src interaction in coupling diverse stimuli to increased epithelial NBC activity', *Am J Physiol Renal Physiol*, 283(4), pp. F663-70.
- Evers, R., Kool, M., Smith, A.J., van Deemter, L., de Haas, M. and Borst, P. (2000) 'Inhibitory effect of the reversal agents V-104, GF120918 and Pluronic L61 on MDR1 Pgp-, MRP1- and MRP2-mediated transport', *Br J Cancer*, 83(3), pp. 366-74.
- Fang, X., Fukuda, N., Barbry, P., Sartori, C., S.Verkmann, A. and Matthay, M.A. (2002) 'Novel role for CFTR in fluid absorption from the distal airspaces of the lung', *The Journal of General Physiology*, 119(2), pp. 199-207.
- Flemstrom, G., Bergman, A. and Briden, S. (1984) 'Stimulation of mucosal bicarbonate secretion in rat duodenum in vivo by BW755C', *Acta Physiol Scand*, 121(1), pp. 39-43.
- Flemstrom, G., Garner, A., Nylander, O., Hurst, B.C. and Heylings, J.R. (1982) 'Surface epithelial HCO_3^- transport by mammalian duodenum in vivo', *Am J Physiol*, 243(5), pp. G348-58.
- Flemstrom, G. and Isenberg, J.I. (2001) 'Gastroduodenal mucosal alkaline secretion and mucosal protection', *News Physiol Sci*, 16, pp. 23-8.
- Fowler, W.S. (1948) 'Respiratory dead space', *Fed Proc*, 7(1 Pt 1), p. 35.
- Garcia, M.A., Yang, N. and Quinton, P.M. (2009) 'Normal mouse intestinal mucus release requires cystic fibrosis transmembrane regulator-dependent bicarbonate secretion', *J Clin Invest*, 119(9), pp. 2613-22.
- Garnett, J.P., Hickman, E., Burrows, R., Hegyi, P., Tiszlavicz, L., Cuthbert, A.W., Fong, P. and Gray, M.A. (2011) 'Novel role for pendrin in orchestrating bicarbonate secretion in cystic fibrosis transmembrane conductance regulator (CFTR)-expressing airway serous cells', *J Biol Chem*, 286(47), pp. 41069-82.
- Garnett, J.P., Hickman, E., Tunkamnerdthai, O., Cuthbert, A.W. and Gray, M.A. (2013) 'Protein phosphatase 1 coordinates CFTR-dependent airway epithelial HCO_3^- secretion by reciprocal regulation of apical and basolateral membrane $Cl^-HCO_3^-$ exchangers', *Br J Pharmacol*, 168(8), pp. 1946-60.
- Gekeler, V., Boer, R., Ise, W., Sanders, K.H., Schachtele, C. and Beck, J. (1995) 'The specific bisindolylmaleimide PKC-inhibitor GF 109203X efficiently modulates MRP-associated multiple drug resistance', *Biochem Biophys Res Commun*, 206(1), pp. 119-26.

- Go, M., Kojima, T., Takano, K., Murata, M., Koizumi, J., Kurose, M., Kamekura, R., Osanai, M., Chiba, H., Spray, D.C., Himi, T. and Sawada, N. (2006) 'Connexin 26 expression prevents down-regulation of barrier and fence functions of tight junctions by Na^+/K^+ -ATPase inhibitor ouabain in human airway epithelial cell line Calu-3', *Exp Cell Res*, 312(19), pp. 3847-56.
- Gollapudi, S., Kim, C.H., Tran, B.N., Sangha, S. and Gupta, S. (1997) 'Probenecid reverses multidrug resistance in multidrug resistance-associated protein-overexpressing HL60/AR and H69/AR cells but not in P-glycoprotein-overexpressing HL60/Tax and P388/ADR cells', *Cancer Chemother Pharmacol*, 40(2), pp. 150-8.
- Gray, M.A. (2004) 'Bicarbonate secretion: it takes two to tango', *Nat Cell Biol*, 6(4), pp. 292-4.
- Gregory, R.B., Rychkov, G. and Barritt, G.J. (2001) 'Evidence that 2-aminoethyl diphenylborate is a novel inhibitor of store-operated Ca^{2+} channels in liver cells, and acts through a mechanism which does not involve inositol trisphosphate receptors', *Biochem J*, 354(Pt 2), pp. 285-90.
- Grommes, J. and Soehnlein, O. (2011) 'Contribution of neutrophils to acute lung injury', *Mol Med*, 17(3-4), pp. 293-307.
- Gryniewicz, G., Poenie, M. and Tsien, R.Y. (1985) 'A new generation of Ca^{2+} indicators with greatly improved fluorescence properties', *J Biol Chem*, 260(6), pp. 3440-50.
- Gu, X.Q., Xue, J. and Haddad, G.G. (2004) 'Effect of chronically elevated CO_2 on CA1 neuronal excitability', *Am J Physiol Cell Physiol*, 287(3), pp. C691-7.
- Guggino, W.B. and Stanton, B.A. (2006) 'New insights into cystic fibrosis: molecular switches that regulate CFTR', *Nat Rev Mol Cell Biol*, 7(6), pp. 426-36.
- Gunaratne, R., Braucht, D.W., Rinschen, M.M., Chou, C.L., Hoffert, J.D., Pisitkun, T. and Knepper, M.A. (2010) 'Quantitative phosphoproteomic analysis reveals cAMP/vasopressin-dependent signaling pathways in native renal thick ascending limb cells', *Proc Natl Acad Sci U S A*, 107(35), pp. 15653-8.
- Gupta, S., Ruderman, N.B., Cragoe, E.J., Jr. and Sussman, I. (1991) 'Endothelin stimulates Na^+/K^+ -ATPase activity by a protein kinase C-dependent pathway in rabbit aorta', *Am J Physiol*, 261(1 Pt 2), pp. H38-45.
- Gustafsson, J.K., Ermund, A., Ambort, D., Johansson, M.E., Nilsson, H.E., Thorell, K., Hebert, H., Sjoval, H. and Hansson, G.C. (2012) 'Bicarbonate and functional CFTR channel are required for proper mucin secretion and link cystic fibrosis with its mucus phenotype', *J Exp Med*, 209(7), pp. 1263-72.
- Hai, T., Teng, F., Guo, R., Li, W. and Zhou, Q. (2014) 'One-step generation of knockout pigs by zygote injection of CRISPR/Cas system', *Cell Res*, 24(3), pp. 372-5.
- Hamilton, K.O., Topp, E., Makagiansar, I., Siahaan, T., Yazdanian, M. and Audus, K.L. (2001) 'Multidrug resistance-associated protein-1 functional activity in Calu-3 cells', *J Pharmacol Exp Ther*, 298(3), pp. 1199-205.

- Hammer, A., Hodgson, D.R. and Cann, M.J. (2006) 'Regulation of prokaryotic adenylyl cyclases by CO₂', *The Biochemical Journal*, 396(2), pp. 215-218.
- Hanoune, J. and Defer, N. (2001) 'Regulation and role of adenylyl cyclase isoforms', *Annu Rev Pharmacol Toxicol*, 41, pp. 145-74.
- Harrison, S.M., Frampton, J.E., McCall, E., Boyett, M.R. and Orchard, C.H. (1992) 'Contraction and intracellular Ca²⁺, Na⁺, and H⁺ during acidosis in rat ventricular myocytes', *Am J Physiol*, 262(2 Pt 1), pp. C348-57.
- Haws, C., Finkbeiner, W.E., Widdicombe, J.H. and Wine, J.J. (1994) 'CFTR in Calu-3 human airway cells: channel properties and role in cAMP-activated Cl⁻ conductance', *Am J Physiol*, 266(5 Pt 1), pp. L502-12.
- Hegyi, P., Gray, M.A. and Argent, B.E. (2003) 'Substance P inhibits bicarbonate secretion from guinea pig pancreatic ducts by modulating an anion exchanger', *Am J Physiol Cell Physiol*, 285(2), pp. C268-76.
- Helenius, I.T., Krupinski, T., Turnbull, D.W., Gruenbaum, Y., Silverman, N., Johnson, E.A., Sporn, P.H., Sznajder, J.I. and Beitel, G.J. (2009) 'Elevated CO₂ suppresses specific Drosophila innate immune responses and resistance to bacterial infection', *Proc Natl Acad Sci U S A*, 106(44), pp. 18710-5.
- Hentchel-Franks, K., Lozano, D., Eubanks-Tarn, V., Cobb, B., Fan, L., Oster, R., Sorscher, E. and Clancy, J.P. (2004) 'Activation of airway Cl⁻ secretion in human subjects by adenosine', *Am J Respir Cell Mol Biol*, 31(2), pp. 140-6.
- Herrera, M. and Garvin, J.L. (2011) 'Aquaporins as gas channels', *Pflugers Arch*, 462(4), pp. 623-30.
- Hess, K.C., Jones, B.H., Marquez, B., Chen, Y., Ord, T.S., Kamenetsky, M., Miyamoto, C., Zippin, J.H., Kopf, G.S., Suarez, S.S., Levin, L.R., Williams, C.J., Buck, J. and Moss, S.B. (2005) 'The "soluble" adenylyl cyclase in sperm mediates multiple signaling events required for fertilization', *Dev Cell*, 9(2), pp. 249-59.
- Homolya, L., Steinberg, T.H. and Boucher, R.C. (2000) 'Cell to cell communication in response to mechanical stress via bilateral release of ATP and UTP in polarized epithelia', *J Cell Biol*, 150(6), pp. 1349-60.
- Hong, J.H., Yang, D., Shcheynikov, N., Ohana, E., Shin, D.M. and Muallem, S. (2013) 'Convergence of IRBIT, phosphatidylinositol (4,5) bisphosphate, and WNK/SPAK kinases in regulation of the Na⁺-HCO₃⁻ cotransporters family', *Proc Natl Acad Sci U S A*, 110(10), pp. 4105-10.
- Hu, B., Nakata, H., Gu, C., De Beer, T. and Cooper, D.M. (2002) 'A critical interplay between Ca²⁺ inhibition and activation by Mg²⁺ of AC5 revealed by mutants and chimeric constructs', *J Biol Chem*, 277(36), pp. 33139-47.
- Huang, J., Shan, J., Kim, D., Liao, J., Evagelidis, A., Alper, S.L. and Hanrahan, J.W. (2012) 'Basolateral chloride loading by the anion exchanger type 2: role in fluid secretion by the human airway epithelial cell line Calu-3', *J Physiol*, 590(Pt 21), pp. 5299-316.

- Huang, P., Lazarowski, E.R., Tarran, R., Milgram, S.L., Boucher, R.C. and Stutts, M.J. (2001) 'Compartmentalized autocrine signaling to cystic fibrosis transmembrane conductance regulator at the apical membrane of airway epithelial cells', *Proc Natl Acad Sci U S A*, 98(24), pp. 14120-5.
- Huckstepp, R.T. and Dale, N. (2011) 'CO₂-dependent opening of an inwardly rectifying K⁺ channel', *Pflugers Arch*, 461(3), pp. 337-44.
- Huckstepp, R.T., Eason, R., Sachdev, A. and Dale, N. (2010a) 'CO₂-dependent opening of connexin 26 and related beta connexins', *J Physiol*, 588(Pt 20), pp. 3921-31.
- Huckstepp, R.T., id Bihi, R., Eason, R., Spyer, K.M., Dicke, N., Willecke, K., Marina, N., Gourine, A.V. and Dale, N. (2010b) 'Connexin hemichannel-mediated CO₂-dependent release of ATP in the medulla oblongata contributes to central respiratory chemosensitivity', *J Physiol*, 588(Pt 20), pp. 3901-20.
- Hug, M.J., Tamada, T. and Bridges, R.J. (2003) 'CFTR and bicarbonate secretion by [correction of to] epithelial cells', *News Physiol Sci*, 18, pp. 38-42.
- Ianowski, J.P., Choi, J.Y., Wine, J.J. and Hanrahan, J.W. (2007) 'Mucus secretion by single tracheal submucosal glands from normal and cystic fibrosis transmembrane conductance regulator knockout mice', *J Physiol*, 580(Pt 1), pp. 301-14.
- Illek, B., Yankaskas, J.R. and Machen, T.E. (1997) 'cAMP and genistein stimulate HCO₃⁻ conductance through CFTR in human airway epithelia', *Am J Physiol*, 272(4 Pt 1), pp. L752-61.
- Ishiguro, H., Steward, M.C., Wilson, R.W. and Case, R.M. (1996) 'Bicarbonate secretion in interlobular ducts from guinea-pig pancreas', *J Physiol*, 495 (Pt 1), pp. 179-91.
- Itel, F., Al-Samir, S., Oberg, F., Chami, M., Kumar, M., Supuran, C.T., Deen, P.M., Meier, W., Hedfalk, K., Gros, G. and Endeward, V. (2012) 'CO₂ permeability of cell membranes is regulated by membrane cholesterol and protein gas channels', *FASEB J*.
- Ito, Y., Correll, K., Schiel, J.A., Finigan, J.H., Prekeris, R. and Mason, R.J. (2014) 'Lung fibroblasts accelerate wound closure in human alveolar epithelial cells through hepatocyte growth factor/c-Met signaling', *Am J Physiol Lung Cell Mol Physiol*, 307(1), pp. L94-105.
- Jacob, P., Christiani, S., Rossmann, H., Lamprecht, G., Vieillard-Baron, D., Muller, R., Gregor, M. and Seidler, U. (2000) 'Role of Na⁺-HCO₃⁻ cotransporter NBC1, Na⁺/H⁺ exchanger NHE1, and carbonic anhydrase in rabbit duodenal bicarbonate secretion', *Gastroenterology*, 119(2), pp. 406-19.
- Jedlitschky, G., Burchell, B. and Keppler, D. (2000) 'The multidrug resistance protein 5 functions as an ATP-dependent export pump for cyclic nucleotides', *J Biol Chem*, 275(39), pp. 30069-74.
- Jiang, Q., Bai, T., Shen, S., Li, L., Ding, H. and Wang, P. (2011) 'Increase of cytosolic calcium induced by trichosanthin suppresses cAMP/PKC levels through the inhibition of adenylyl cyclase activity in HeLa cells', *Mol Biol Rep*, 38(4), pp. 2863-8.

- Jin, W., Lo, T.M., Loh, H.H. and Thayer, S.A. (1994) 'U73122 inhibits phospholipase C-dependent calcium mobilization in neuronal cells', *Brain Res*, 642(1-2), pp. 237-43.
- Johnson, R.A., Alvarez, R. and Salomon, Y. (1994) 'Determination of adenylyl cyclase catalytic activity using single and double column procedures', *Methods Enzymol*, 238, pp. 31-56.
- Jones, W.D., Cayirlioglu, P., Kadow, I.G. and Vosshall, L.B. (2007) 'Two chemosensory receptors together mediate carbon dioxide detection in *Drosophila*', *Nature*, 445(7123), pp. 86-90.
- Joo, N.S., Cho, H.J., Khansaheb, M. and Wine, J.J. (2010) 'Hyposcretion of fluid from tracheal submucosal glands of CFTR-deficient pigs', *J Clin Invest*, 120(9), pp. 3161-6.
- Joo, N.S., Irokawa, T., Wu, J.V., Robbins, R.C., Whyte, R.I. and Wine, J.J. (2002) 'Absent secretion to vasoactive intestinal peptide in cystic fibrosis airway glands', *The Journal of Biological Chemistry*, 277(52), pp. 50710-50715.
- Karippacheril, J.G. and Joseph, T.T. (2010) 'Negative pressure pulmonary oedema and haemorrhage, after a single breath-hold: Diaphragm the culprit?', *Indian J Anaesth*, 54(4), pp. 361-3.
- Kilmartin, J.V. (1976) 'Interaction of haemoglobin with protons, CO₂ and 2,3-diphosphoglycerate', *Br Med Bull*, 32(3), pp. 209-12.
- Kim, D., Kim, J., Burghardt, B., Best, L. and Steward, M.C. (2014) 'Role of anion exchangers in Cl⁻ and HCO₃⁻ secretion by the human airway epithelial cell line Calu-3', *Am J Physiol Cell Physiol*, 307(2), pp. C208-19.
- Klein, R.R., Bourdon, D.M., Costales, C.L., Wagner, C.D., White, W.L., Williams, J.D., Hicks, S.N., Sondek, J. and Thakker, D.R. (2011) 'Direct activation of human phospholipase C by its well known inhibitor u73122', *J Biol Chem*, 286(14), pp. 12407-16.
- Knowles, M.R. and Boucher, R.C. (2002) 'Mucus clearance as a primary innate defense mechanism for mammalian airways', *J Clin Invest*, 109(5), pp. 571-7.
- Ko, S.B., Zeng, W., Dorwart, M.R., Luo, X., Kim, K.H., Millen, L., Goto, H., Naruse, S., Soyombo, A., Thomas, P.J. and Muallem, S. (2004) 'Gating of CFTR by the STAS domain of SLC26 transporters', *Nat Cell Biol*, 6(4), pp. 343-50.
- Kreda, S.M., Gynn, M.C., Fenstermacher, D.A., Boucher, R.C. and Gabriel, S.E. (2001) 'Expression and localization of epithelial aquaporins in the adult human lung', *Am J Respir Cell Mol Biol*, 24(3), pp. 224-34.
- Kreda, S.M., Okada, S.F., van Heusden, C.A., O'Neal, W., Gabriel, S., Abdullah, L., Davis, C.W., Boucher, R.C. and Lazarowski, E.R. (2007) 'Coordinated release of nucleotides and mucin from human airway epithelial Calu-3 cells', *J Physiol*, 584(Pt 1), pp. 245-59.
- Kreindler, J.L., Peters, K.W., Frizzell, R.A. and Bridges, R.J. (2006) 'Identification and membrane localization of electrogenic sodium bicarbonate cotransporters in Calu-3 cells', *Biochim Biophys Acta*, 1762(7), pp. 704-10.

- Krouse, M.E., Talbott, J.F., Lee, M.M., Joo, N.S. and Wine, J.J. (2004) 'Acid and base secretion in the Calu-3 model of human serous cells', *Am J Physiol Lung Cell Mol Physiol*, 287(6), pp. L1274-83.
- Krupinski, J., Coussen, F., Bakalyar, H.A., Tang, W.J., Feinstein, P.G., Orth, K., Slaughter, C., Reed, R.R. and Gilman, A.G. (1989) 'Adenylyl cyclase amino acid sequence: possible channel- or transporter-like structure', *Science*, 244(4912), pp. 1558-64.
- Kubiet, M. and Ramphal, R. (1995) 'Adhesion of nontypeable *Haemophilus influenzae* from blood and sputum to human tracheobronchial mucins and lactoferrin', *Infect Immun*, 63(3), pp. 899-902.
- Laffey, J.G., Tanaka, M., Engelberts, D., Luo, X., Yuan, S., Tanswell, A.K., Post, M., Lindsay, T. and Kavanagh, B.P. (2000) 'Therapeutic hypercapnia reduces pulmonary and systemic injury following in vivo lung reperfusion', *Am J Respir Crit Care Med*, 162(6), pp. 2287-94.
- Lavista-Llanos, S., Centanin, L., Irisarri, M., Russo, D.M., Gleadle, J.M., Bocca, S.N., Muzzopappa, M., Ratcliffe, P.J. and Wappner, P. (2002) 'Control of the hypoxic response in *Drosophila melanogaster* by the basic helix-loop-helix PAS protein similar', *Mol Cell Biol*, 22(19), pp. 6842-53.
- Lee, H.J. and Zheng, J.J. (2010) 'PDZ domains and their binding partners: structure, specificity, and modification', *Cell Commun Signal*, 8, p. 8.
- Lee, M.C., Penland, C.M., Widdicombe, J.H. and Wine, J.J. (1998) 'Evidence that Calu-3 human airway cells secrete bicarbonate', *Am J Physiol*, 274(3 Pt 1), pp. L450-3.
- Lee, R.J. and Foskett, J.K. (2010) 'cAMP-activated Ca^{2+} signaling is required for CFTR-mediated serous cell fluid secretion in porcine and human airways', *The Journal of Clinical Investigation*, 120(9), pp. 3137-3148.
- Lee, R.J. and Foskett, J.K. (2012) 'Why mouse airway submucosal gland serous cells do not secrete fluid in response to cAMP stimulation', *J Biol Chem*, 287(45), pp. 38316-26.
- Lefkimmatis, K., Srikanthan, M., Maiellaro, I., Moyer, M.P., Curci, S. and Hofer, A.M. (2009) 'Store-operated cyclic AMP signalling mediated by STIM1', *Nat Cell Biol*, 11(4), pp. 433-42.
- Li, C., Krishnamurthy, P.C., Penmatsa, H., Marrs, K.L., Wang, X.Q., Zaccolo, M., Jalink, K., Li, M., Nelson, D.J., Schuetz, J.D. and Naren, A.P. (2007) 'Spatiotemporal coupling of cAMP transporter to CFTR chloride channel function in the gut epithelia', *Cell*, 131(5), pp. 940-51.
- Li, G., Zhou, D., Vicencio, A.G., Ryu, J., Xue, J., Kanaan, A., Gavrilov, O. and Haddad, G.G. (2006) 'Effect of carbon dioxide on neonatal mouse lung: a genomic approach', *J Appl Physiol*, 101(6), pp. 1556-64.
- Liedtke, C.M., Cody, D. and Cole, T.S. (2001) 'Differential regulation of Cl^- transport proteins by PKC in Calu-3 cells', *Am J Physiol Lung Cell Mol Physiol*, 280(4), pp. L739-47.

- Lohi, H., Kujala, M., Makela, S., Lehtonen, E., Kestila, M., Saarialho-Kere, U., Markovich, D. and Kere, J. (2002) 'Functional characterization of three novel tissue-specific anion exchangers SLC26A7, -A8, and -A9', *J Biol Chem*, 277(16), pp. 14246-54.
- Lohi, H., Lamprecht, G., Markovich, D., Heil, A., Kujala, M., Seidler, U. and Kere, J. (2003) 'Isoforms of SLC26A6 mediate anion transport and have functional PDZ interaction domains', *Am J Physiol Cell Physiol*, 284(3), pp. C769-79.
- Losa, D., Kohler, T., Bellec, J., Dudez, T., Crespin, S., Bacchetta, M., Boulanger, P., Hong, S.S., Morel, S., Nguyen, T.H., van Delden, C. and Chanson, M. (2014) 'Pseudomonas aeruginosa-induced apoptosis in airway epithelial cells is mediated by gap junctional communication in a JNK-dependent manner', *J Immunol*, 192(10), pp. 4804-12.
- Lourenco, R.V. and Miranda, J.M. (1968) 'Drive and performance of the ventilatory apparatus in chronic obstructive lung disease', *N Engl J Med*, 279(2), pp. 53-9.
- Lynch, C.J., Wilson, P.B., Blackmore, P.F. and Exton, J.H. (1986) 'The hormone-sensitive hepatic Na⁺-pump. Evidence for regulation by diacylglycerol and tumor promoters', *J Biol Chem*, 261(31), pp. 14551-6.
- Mackay, A. and Al Haddad, M. (2009) 'Acute lung injury and acute respiratory distress syndrome', *Continuing Education in Anaesthesia, Critical Care & Pain*, 9(5), pp. 152-156.
- Maiellaro, I., Lefkimmatis, K., Moyer, M.P., Curci, S. and Hofer, A.M. (2012) 'Termination and activation of store-operated cyclic AMP production', *J Cell Mol Med*, 16(11), pp. 2715-25.
- Mali, P., Yang, L., Esvelt, K.M., Aach, J., Guell, M., DiCarlo, J.E., Norville, J.E. and Church, G.M. (2013) 'RNA-guided human genome engineering via Cas9', *Science*, 339(6121), pp. 823-6.
- Mall, M., Bleich, M., Kuehr, J., Brandis, M., Greger, R. and Kunzelmann, K. (1999) 'CFTR-mediated inhibition of epithelial Na⁺ conductance in human colon is defective in cystic fibrosis', *Am J Physiol*, 277(3 Pt 1), pp. G709-16.
- Marques, P.A., Magalhaes, M.C. and Correia, R.N. (2003) 'Inorganic plasma with physiological CO₂/HCO₃⁻ buffer', *Biomaterials*, 24(9), pp. 1541-8.
- Martin, T.R. (1999) 'Lung cytokines and ARDS: Roger S. Mitchell Lecture', *Chest*, 116(1 Suppl), pp. 2S-8S.
- Maruyama, T., Kanaji, T., Nakade, S., Kanno, T. and Mikoshiba, K. (1997) '2APB, 2-aminoethoxydiphenyl borate, a membrane-penetrable modulator of Ins(1,4,5)P₃-induced Ca²⁺ release', *J Biochem*, 122(3), pp. 498-505.
- Matsui, H., Randell, S.H., Peretti, S.W., Davis, C.W. and Boucher, R.C. (1998) 'Coordinated clearance of periciliary liquid and mucus from airway surfaces', *J Clin Invest*, 102(6), pp. 1125-31.
- Matsuuchi, L. and Naus, C.C. (2013) 'Gap junction proteins on the move: connexins, the cytoskeleton and migration', *Biochim Biophys Acta*, 1828(1), pp. 94-108.

Meduri, G.U., Golden, E., Freire, A.X., Taylor, E., Zaman, M., Carson, S.J., Gibson, M. and Umberger, R. (2007) 'Methylprednisolone infusion in early severe ARDS: results of a randomized controlled trial', *Chest*, 131(4), pp. 954-63.

Meigh, L., Greenhalgh, S.A., Rodgers, T.L., Cann, M.J., Roper, D.I. and Dale, N. (2013) 'CO₂ directly modulates connexin 26 by formation of carbamate bridges between subunits', *Elife*, 2, p. e01213.

Middleton, J.P., Raymond, J.R., Whorton, A.R. and Dennis, V.W. (1990) 'Short-term regulation of Na⁺/K⁺ adenosine triphosphatase by recombinant human serotonin 5-HT_{1A} receptor expressed in HeLa cells', *J Clin Invest*, 86(6), pp. 1799-805.

Mogami, H., Lloyd Mills, C. and Gallacher, D.V. (1997) 'Phospholipase C inhibitor, U73122, releases intracellular Ca²⁺, potentiates Ins(1,4,5)P₃-mediated Ca²⁺ release and directly activates ion channels in mouse pancreatic acinar cells', *Biochem J*, 324 (Pt 2), pp. 645-51.

Monterisi, S., Favia, M., Guerra, L., Cardone, R.A., Marzulli, D., Reshkin, S.J., Casavola, V. and Zaccolo, M. (2012) 'CFTR regulation in human airway epithelial cells requires integrity of the actin cytoskeleton and compartmentalized cAMP and PKA activity', *J Cell Sci*, 125(Pt 5), pp. 1106-17.

Morton, W.M., Ayscough, K.R. and McLaughlin, P.J. (2000) 'Latrunculin alters the actin-monomer subunit interface to prevent polymerization', *Nat Cell Biol*, 2(6), pp. 376-8.

Muanprasat, C., Sonawane, N.D., Salinas, D., Taddei, A., Galiotta, L.J. and Verkman, A.S. (2004) 'Discovery of glycine hydrazide pore-occluding CFTR inhibitors: mechanism, structure-activity analysis, and in vivo efficacy', *J Gen Physiol*, 124(2), pp. 125-37.

Murray, A.J. (2008) 'Pharmacological PKA inhibition: all may not be what it seems', *Sci Signal*, 1(22), p. re4.

Musa-Aziz, R., Chen, L.M., Pelletier, M.F. and Boron, W.F. (2009) 'Relative CO₂/NH₃ selectivities of AQP1, AQP4, AQP5, AmtB, and RhAG', *Proc Natl Acad Sci U S A*, 106(13), pp. 5406-11.

Nakhoul, N.L., Davis, B.A., Romero, M.F. and Boron, W.F. (1998) 'Effect of expressing the water channel aquaporin-1 on the CO₂ permeability of *Xenopus* oocytes', *Am J Physiol*, 274(2 Pt 1), pp. C543-8.

Namkung, W., Finkbeiner, W.E. and Verkman, A.S. (2010) 'CFTR-adenylyl cyclase I association responsible for UTP activation of CFTR in well-differentiated primary human bronchial cell cultures', *Mol Biol Cell*, 21(15), pp. 2639-48.

Network, T.A.R.D.S. (2000) *Ventilation with lower tidal volumes as compared with traditional tidal volumes for acute lung injury and the acute respiratory distress syndrome. The Acute Respiratory Distress Syndrome Network* (18) (0028-4793 (Print)

0028-4793 (Linking)). [Online]. Available at:
<http://www.ncbi.nlm.nih.gov/pubmed/10793162>.

Nishio, K., Suzuki, Y., Takeshita, K., Aoki, T., Kudo, H., Sato, N., Naoki, K., Miyao, N., Ishii, M. and Yamaguchi, K. (2001) 'Effects of hypercapnia and hypocapnia on $[Ca^{2+}]_i$ mobilization in human pulmonary artery endothelial cells', *J Appl Physiol* (1985), 90(6), pp. 2094-100.

O'Grady, S.M., Patil, N., Melkamu, T., Maniak, P.J., Lancto, C. and Kita, H. (2013) 'ATP release and Ca^{2+} signalling by human bronchial epithelial cells following *Alternaria* aeroallergen exposure', *J Physiol*, 591(Pt 18), pp. 4595-609.

O'Toole, D., Hassett, P., Contreras, M., Higgins, B.D., McKeown, S.T., McAuley, D.F., O'Brien, T. and Laffey, J.G. (2009) 'Hypercapnic acidosis attenuates pulmonary epithelial wound repair by an NF-kappaB dependent mechanism', *Thorax*, 64(11), pp. 976-82.

Oliver, K.M., Lenihan, C.R., Bruning, U., Cheong, A., Laffey, J.G., McLoughlin, P., Taylor, C.T. and Cummins, E.P. (2012) 'Hypercapnia induces cleavage and nuclear localization of RelB protein, giving insight into CO_2 sensing and signaling', *J Biol Chem*, 287(17), pp. 14004-11.

Osycka-Salut, C., Diez, F., Burdet, J., Gervasi, M.G., Franchi, A., Bianciotti, L.G., Davio, C. and Perez-Martinez, S. (2014) 'Cyclic AMP efflux, via MRPs and A_1 adenosine receptors, is critical for bovine sperm capacitation', *Mol Hum Reprod*, 20(1), pp. 89-99.

Paradiso, A.M., Coakley, R.D. and Boucher, R.C. (2003) 'Polarized distribution of HCO_3^- transport in human normal and cystic fibrosis nasal epithelia', *J Physiol*, 548(Pt 1), pp. 203-18.

Parfenova, H. and Leffler, C.W. (1996) 'Effects of hypercapnia on prostanoid and cAMP production by cerebral microvascular cell cultures', *Am J Physiol*, 270(5 Pt 1), pp. C1503-10.

Penmatsa, H., Zhang, W., Yarlagadda, S., Li, C., Conoley, V.G., Yue, J., Bahouth, S.W., Buddington, R.K., Zhang, G., Nelson, D.J., Sonecha, M.D., Manganiello, V., Wine, J.J. and Naren, A.P. (2010) 'Compartmentalized cyclic adenosine 3',5'-monophosphate at the plasma membrane clusters PDE3A and cystic fibrosis transmembrane conductance regulator into microdomains', *Mol Biol Cell*, 21(6), pp. 1097-110.

Peppiatt, C.M., Collins, T.J., Mackenzie, L., Conway, S.J., Holmes, A.B., Bootman, M.D., Berridge, M.J., Seo, J.T. and Roderick, H.L. (2003) '2-Aminoethoxydiphenyl borate (2-APB) antagonises inositol 1,4,5-trisphosphate-induced calcium release, inhibits calcium pumps and has a use-dependent and slowly reversible action on store-operated calcium entry channels', *Cell Calcium*, 34(1), pp. 97-108.

Pezzulo, A.A., Starner, T.D., Scheetz, T.E., Traver, G.L., Tilley, A.E., Harvey, B.G., Crystal, R.G., McCray, P.B., Jr. and Zabner, J. (2011) 'The air-liquid interface and use of primary cell cultures are important to recapitulate the transcriptional profile of in vivo airway epithelia', *Am J Physiol Lung Cell Mol Physiol*, 300(1), pp. L25-31.

Pezzulo, A.A., Tang, X.X., Hoegger, M.J., Alaiwa, M.H., Ramachandran, S., Moninger, T.O., Karp, P.H., Wohlford-Lenane, C.L., Haagsman, H.P., van Eijk, M., Banfi, B., Horswill, A.R., Stoltz, D.A., McCray, P.B., Jr., Welsh, M.J. and Zabner, J. (2012) 'Reduced airway surface pH impairs bacterial killing in the porcine cystic fibrosis lung', *Nature*, 487(7405), pp. 109-13.

- Pfeuffer, E., Mollner, S. and Pfeuffer, T. (1985) 'Adenylate cyclase from bovine brain cortex: purification and characterization of the catalytic unit', *EMBO J*, 4(13B), pp. 3675-9.
- Picciotto, M.R., Cohn, J.A., Bertuzzi, G., Greengard, P. and Nairn, A.C. (1992) 'Phosphorylation of the cystic fibrosis transmembrane conductance regulator', *J Biol Chem*, 267(18), pp. 12742-52.
- Pierrakos, C., Karanikolas, M., Scolletta, S., Karamouzos, V. and Velissaris, D. (2012) 'Acute respiratory distress syndrome: pathophysiology and therapeutic options', *J Clin Med Res*, 4(1), pp. 7-16.
- Polak, A., Haynie, G.D., Hays, R.M. and Schwartz, W.B. (1961) 'Effects of chronic hypercapnia on electrolyte and acid-base equilibrium. I. Adaptation', *J Clin Invest*, 40, pp. 1223-37.
- Prakriya, M. and Lewis, R.S. (2001) 'Potentiation and inhibition of Ca^{2+} release-activated Ca^{2+} channels by 2-aminoethyldiphenyl borate (2-APB) occurs independently of IP_3 receptors', *J Physiol*, 536(Pt 1), pp. 3-19.
- Prin, S., Chergui, K., Augarde, R., Page, B., Jardin, F. and Vieillard-Baron, A. (2002) 'Ability and safety of a heated humidifier to control hypercapnic acidosis in severe ARDS', *Intensive Care Med*, 28(12), pp. 1756-60.
- Pushkin, A., Abuladze, N., Lee, I., Newman, D., Hwang, J. and Kurtz, I. (1999) 'Cloning, tissue distribution, genomic organization, and functional characterization of NBC3, a new member of the sodium bicarbonate cotransporter family', *J Biol Chem*, 274(23), pp. 16569-75.
- Qi, L.S., Larson, M.H., Gilbert, L.A., Doudna, J.A., Weissman, J.S., Arkin, A.P. and Lim, W.A. (2013) 'Repurposing CRISPR as an RNA-guided platform for sequence-specific control of gene expression', *Cell*, 152(5), pp. 1173-83.
- Rahman, N., Buck, J. and Levin, L.R. (2013) 'pH sensing via bicarbonate-regulated "soluble" adenylyl cyclase (sAC)', *Front Physiol*, 4, p. 343.
- Randell, S.H., Boucher, R.C. and University of North Carolina Virtual Lung, G. (2006) 'Effective mucus clearance is essential for respiratory health', *Am J Respir Cell Mol Biol*, 35(1), pp. 20-8.
- Ransford, G.A., Fregien, N., Qiu, F., Dahl, G., Conner, G.E. and Salathe, M. (2009) 'Pannexin 1 contributes to ATP release in airway epithelia', *Am J Respir Cell Mol Biol*, 41(5), pp. 525-34.
- Rasgado-Flores, H., Krishna Mandava, V., Siman, H., Van Driessche, W., Pilewski, J.M., Randell, S.H. and Bridges, R.J. (2013) 'Effect of apical hyperosmotic sodium challenge and amiloride on sodium transport in human bronchial epithelial cells from cystic fibrosis donors', *Am J Physiol Cell Physiol*, 305(11), pp. C1114-22.
- Reid, G., Wielinga, P., Zelcer, N., van der Heijden, I., Kuil, A., de Haas, M., Wijnholds, J. and Borst, P. (2003) 'The human multidrug resistance protein MRP4 functions as a prostaglandin efflux transporter and is inhibited by nonsteroidal antiinflammatory drugs', *Proc Natl Acad Sci U S A*, 100(16), pp. 9244-9.

- Ridley, C., Kouvatso, N., Raynal, B.D., Howard, M., Collins, R.F., Desseyn, J.L., Jowitt, T.A., Baldock, C., Davis, C.W., Hardingham, T.E. and Thornton, D.J. (2014) 'Assembly of the Respiratory Mucin MUC5B: A NEW MODEL FOR A GEL-FORMING MUCIN', *J Biol Chem*, 289(23), pp. 16409-20.
- Riordan, J.R., Rommens, J.M., Kerem, B., Alon, N., Rozmahel, R., Grzelczak, Z., Zielenski, J., Lok, S., Plavsic, N., Chou, J.L. and et al. (1989) 'Identification of the cystic fibrosis gene: cloning and characterization of complementary DNA', *Science*, 245(4922), pp. 1066-73.
- Rogers, C.S., Abraham, W.M., Brogden, K.A., Engelhardt, J.F., Fisher, J.T., McCray, P.B., Jr., McLennan, G., Meyerholz, D.K., Namati, E., Ostedgaard, L.S., Prather, R.S., Sabater, J.R., Stoltz, D.A., Zabner, J. and Welsh, M.J. (2008) 'The porcine lung as a potential model for cystic fibrosis', *Am J Physiol Lung Cell Mol Physiol*, 295(2), pp. L240-63.
- Rollins, B.M., Burn, M., Coakley, R.D., Chambers, L.A., Hirsh, A.J., Clunes, M.T., Lethem, M.I., Donaldson, S.H. and Tarran, R. (2008) 'A_{2B} adenosine receptors regulate the mucus clearance component of the lung's innate defense system', *Am J Respir Cell Mol Biol*, 39(2), pp. 190-7.
- Roman, R.M., Wang, Y., Lidofsky, S.D., Feranchak, A.P., Lomri, N., Scharschmidt, B.F. and Fitz, J.G. (1997) 'Hepatocellular ATP-binding cassette protein expression enhances ATP release and autocrine regulation of cell volume', *J Biol Chem*, 272(35), pp. 21970-6.
- Romero, M.F., Hediger, M.A., Boulpaep, E.L. and Boron, W.F. (1997) 'Expression cloning and characterization of a renal electrogenic Na⁺/HCO₃⁻ cotransporter', *Nature*, 387(6631), pp. 409-13.
- Roos, A. and Boron, W.F. (1981) 'Intracellular pH', *Physiol Rev*, 61(2), pp. 296-434.
- Ross, A.J., Dailey, L.A., Brighton, L.E. and Devlin, R.B. (2007) 'Transcriptional profiling of mucociliary differentiation in human airway epithelial cells', *Am J Respir Cell Mol Biol*, 37(2), pp. 169-85.
- Rossmann, H., Jacob, P., Baisch, S., Hassoun, R., Meier, J., Natour, D., Yahya, K., Yun, C., Biber, J., Lackner, K.J., Fiehn, W., Gregor, M., Seidler, U. and Lamprecht, G. (2005) 'The CFTR associated protein CAP70 interacts with the apical Cl⁻/HCO₃⁻ exchanger DRA in rabbit small intestinal mucosa', *Biochemistry*, 44(11), pp. 4477-87.
- Rouach, N., Segal, M., Koulakoff, A., Giaume, C. and Avignone, E. (2003) 'Carbenoxolone blockade of neuronal network activity in culture is not mediated by an action on gap junctions', *J Physiol*, 553(Pt 3), pp. 729-45.
- Ruiz, O.S. and Arruda, J.A. (1992) 'Regulation of the renal Na-HCO₃ cotransporter by cAMP and Ca-dependent protein kinases', *Am J Physiol*, 262(4 Pt 2), pp. F560-5.
- Ruiz, O.S., Robey, R.B., Qiu, Y.Y., Wang, L.J., Li, C.J., Ma, J. and Arruda, J.A. (1999) 'Regulation of the renal Na-HCO₃ cotransporter. XI. Signal transduction underlying CO₂ stimulation', *Am J Physiol*, 277(4 Pt 2), pp. F580-6.
- Sagar, G.D. and Larson, D.M. (2006) 'Carbenoxolone inhibits junctional transfer and upregulates Connexin43 expression by a protein kinase A-dependent pathway', *J Cell Biochem*, 98(6), pp. 1543-51.

- Salinas, D., Haggie, P.M., Thiagarajah, J.R., Song, Y., Rosbe, K., Finkbeiner, W.E., Nielson, D.W. and Verkman, A.S. (2005) 'Submucosal gland dysfunction as a primary defect in cystic fibrosis', *FASEB J*, 19(3), pp. 431-3.
- Sampath, P. and Pollard, T.D. (1991) 'Effects of cytochalasin, phalloidin, and pH on the elongation of actin filaments', *Biochemistry*, 30(7), pp. 1973-80.
- Schaefer, K.E., McCabe, N. and Withers, J. (1968) 'Stress response in chronic hypercapnia', *Am J Physiol*, 214(3), pp. 543-8.
- Schaefer, K.E., Messier, A.A., Morgan, C. and Baker, G.T., 3rd (1975) 'Effect of chronic hypercapnia on body temperature regulation', *J Appl Physiol*, 38(5), pp. 900-6.
- Scheckenbach, K.E., Losa, D., Dudez, T., Bacchetta, M., O'Grady, S., Crespin, S. and Chanson, M. (2011) 'Prostaglandin E₂ regulation of cystic fibrosis transmembrane conductance regulator activity and airway surface liquid volume requires gap junctional communication', *Am J Respir Cell Mol Biol*, 44(1), pp. 74-82.
- Schiller, K.R., Maniak, P.J. and O'Grady, S.M. (2010) 'Cystic fibrosis transmembrane conductance regulator is involved in airway epithelial wound repair', *Am J Physiol Cell Physiol*, 299(5), pp. C912-21.
- Schmid, A., Sutto, Z., Schmid, N., Novak, L., Ivonnet, P., Horvath, G., Conner, G., Fregien, N. and Salathe, M. (2010) 'Decreased soluble adenylyl cyclase activity in cystic fibrosis is related to defective apical bicarbonate exchange and affects ciliary beat frequency regulation', *The Journal of Biological Chemistry*, 285(29), pp. 29998-30007.
- Schwarzer, C., Wong, S., Shi, J., Matthes, E., Illek, B., Ianowski, J.P., Arant, R.J., Isacoff, E., Vais, H., Foscett, J.K., Maiellaro, I., Hofer, A.M. and Machen, T.E. (2010) 'Pseudomonas aeruginosa Homoserine lactone activates store-operated cAMP and cystic fibrosis transmembrane regulator-dependent Cl⁻ secretion by human airway epithelia', *J Biol Chem*, 285(45), pp. 34850-63.
- Scratcherd, T. and Case, R.M. (1973) 'The secretion of electrolytes by the pancreas', *Am J Clin Nutr*, 26(3), pp. 326-39.
- Seidler, U., Blumenstein, I., Kretz, A., Viellard-Baron, D., Rossmann, H., Colledge, W.H., Evans, M., Ratcliff, R. and Gregor, M. (1997) 'A functional CFTR protein is required for mouse intestinal cAMP-, cGMP- and Ca²⁺-dependent HCO₃⁻ secretion', *J Physiol*, 505 (Pt 2), pp. 411-23.
- Seidler, U.E. (2013) 'Gastrointestinal HCO₃⁻ transport and epithelial protection in the gut: new techniques, transport pathways and regulatory pathways', *Curr Opin Pharmacol*, 13(6), pp. 900-8.
- Seminario-Vidal, L., Okada, S.F., Sesma, J.I., Kreda, S.M., van Heusden, C.A., Zhu, Y., Jones, L.C., O'Neal, W.K., Penuela, S., Laird, D.W., Boucher, R.C. and Lazarowski, E.R. (2011) 'Rho signaling regulates pannexin 1-mediated ATP release from airway epithelia', *J Biol Chem*, 286(30), pp. 26277-86.

- Serohijos, A.W., Hegedus, T., Aleksandrov, A.A., He, L., Cui, L., Dokholyan, N.V. and Riordan, J.R. (2008) 'Phenylalanine-508 mediates a cytoplasmic-membrane domain contact in the CFTR 3D structure crucial to assembly and channel function', *Proc Natl Acad Sci U S A*, 105(9), pp. 3256-61.
- Shan, J., Liao, J., Huang, J., Robert, R., Palmer, M.L., Fahrenkrug, S.C., O'Grady, S.M. and Hanrahan, J.W. (2012) 'Bicarbonate-dependent chloride transport drives fluid secretion by the human airway epithelial cell line Calu-3', *J Physiol*.
- Sharabi, K., Hurwitz, A., Simon, A.J., Beitel, G.J., Morimoto, R.I., Rechavi, G., Sznajder, J.I. and Gruenbaum, Y. (2009) 'Elevated CO₂ levels affect development, motility, and fertility and extend life span in *Caenorhabditis elegans*', *Proc Natl Acad Sci U S A*, 106(10), pp. 4024-9.
- Shen, B.Q., Finkbeiner, W.E., Wine, J.J., Mrsny, R.J. and Widdicombe, J.H. (1994) 'Calu-3: a human airway epithelial cell line that shows cAMP-dependent Cl⁻ secretion', *Am J Physiol*, 266(5 Pt 1), pp. L493-501.
- Sheppard, D.N. and Welsh, M.J. (1999) 'Structure and function of the CFTR chloride channel', *Physiol Rev*, 79(1 Suppl), pp. S23-45.
- Silverman, W., Locovei, S. and Dahl, G. (2008) 'Probenecid, a gout remedy, inhibits pannexin 1 channels', *Am J Physiol Cell Physiol*, 295(3), pp. C761-7.
- Sinclair, S.E., Kregenow, D.A., Lamm, W.J., Starr, I.R., Chi, E.Y. and Hlastala, M.P. (2002) 'Hypercapnic acidosis is protective in an in vivo model of ventilator-induced lung injury', *Am J Respir Crit Care Med*, 166(3), pp. 403-8.
- Smith, E.S., Martinez-Velazquez, L. and Ringstad, N. (2013) 'A chemoreceptor that detects molecular carbon dioxide', *J Biol Chem*, 288(52), pp. 37071-81.
- Smith, J.J. and Welsh, M.J. (1992) 'cAMP stimulates bicarbonate secretion across normal, but not cystic fibrosis airway epithelia', *J Clin Invest*, 89(4), pp. 1148-53.
- Soleimani, M., Greeley, T., Petrovic, S., Wang, Z., Amlal, H., Kopp, P. and Burnham, C.E. (2001) 'Pendrin: an apical Cl⁻/OH⁻/HCO₃⁻ exchanger in the kidney cortex', *Am J Physiol Renal Physiol*, 280(2), pp. F356-64.
- Son, M., Ito, Y., Sato, S., Ishikawa, T., Kondo, M., Nakayama, S., Shimokata, K. and Kume, H. (2004) 'Apical and basolateral ATP-induced anion secretion in polarized human airway epithelia', *Am J Respir Cell Mol Biol*, 30(3), pp. 411-9.
- Spiess, A.C., Lang, H., Schulte, B.A., Spicer, S.S. and Schmiedt, R.A. (2002) 'Effects of gap junction uncoupling in the gerbil cochlea', *Laryngoscope*, 112(9), pp. 1635-41.
- Stewart, A.K., Shmukler, B.E., Vantorpe, D.H., Reimold, F., Heneghan, J.F., Nakakuki, M., Akhavein, A., Ko, S., Ishiguro, H. and Alper, S.L. (2011) 'SLC26 anion exchangers of guinea pig pancreatic duct: molecular cloning and functional characterization', *Am J Physiol Cell Physiol*, 301(2), pp. C289-303.
- Suda, J., Zhu, L. and Karvar, S. (2011) 'Phosphorylation of radixin regulates cell polarity and Mrp-2 distribution in hepatocytes', *Am J Physiol Cell Physiol*, 300(3), pp. C416-24.

- Sugawara, H., Kurosaki, M., Takata, M. and Kurosaki, T. (1997) 'Genetic evidence for involvement of type 1, type 2 and type 3 inositol 1,4,5-trisphosphate receptors in signal transduction through the B-cell antigen receptor', *EMBO J*, 16(11), pp. 3078-88.
- Sun, F., Hug, M.J., Bradbury, N.A. and Frizzell, R.A. (2000a) 'Protein kinase A associates with cystic fibrosis transmembrane conductance regulator via an interaction with ezrin', *J Biol Chem*, 275(19), pp. 14360-6.
- Sun, F., Hug, M.J., Lewarchik, C.M., Yun, C.H., Bradbury, N.A. and Frizzell, R.A. (2000b) 'E3KARP mediates the association of ezrin and protein kinase A with the cystic fibrosis transmembrane conductance regulator in airway cells', *J Biol Chem*, 275(38), pp. 29539-46.
- Suzuki, S., Zuege, D. and Berthiaume, Y. (1995) 'Sodium-independent modulation of Na^+ - K^+ -ATPase activity by beta-adrenergic agonist in alveolar type II cells', *Am J Physiol*, 268(6 Pt 1), pp. L983-90.
- Tao, L. and Harris, A.L. (2007) '2-aminoethoxydiphenyl borate directly inhibits channels composed of connexin26 and/or connexin32', *Mol Pharmacol*, 71(2), pp. 570-9.
- Tarran, R., Trout, L., Donaldson, S.H. and Boucher, R.C. (2006) 'Soluble mediators, not cilia, determine airway surface liquid volume in normal and cystic fibrosis superficial airway epithelia', *J Gen Physiol*, 127(5), pp. 591-604.
- Tesmer, J.J., Sunahara, R.K., Gilman, A.G. and Sprang, S.R. (1997) 'Crystal structure of the catalytic domains of adenylyl cyclase in a complex with G α .GTP γ S', *Science*, 278(5345), pp. 1907-16.
- Thornell, I.M., Wu, J., Liu, X. and Bevensee, M.O. (2012) 'PIP₂ hydrolysis stimulates electrogenic Na/bicarbonate cotransporter NBCe1-B and -C variants expressed in *Xenopus laevis* oocytes', *J Physiol*.
- Tian, J., Gong, X. and Xie, Z. (2001) 'Signal-transducing function of Na^+ - K^+ -ATPase is essential for ouabain's effect on $[\text{Ca}^{2+}]_i$ in rat cardiac myocytes', *Am J Physiol Heart Circ Physiol*, 281(5), pp. H1899-907.
- Tian, Y. and Laychock, S.G. (2001) 'Protein kinase C and calcium regulation of adenylyl cyclase in isolated rat pancreatic islets', *Diabetes*, 50(11), pp. 2505-13.
- Tomashefski, J.F., Jr., Davies, P., Boggis, C., Greene, R., Zapol, W.M. and Reid, L.M. (1983) 'The pulmonary vascular lesions of the adult respiratory distress syndrome', *Am J Pathol*, 112(1), pp. 112-26.
- Tovey, S.C., Dedos, S.G., Rahman, T., Taylor, E.J., Pantazaka, E. and Taylor, C.W. (2010) 'Regulation of inositol 1,4,5-trisphosphate receptors by cAMP independent of cAMP-dependent protein kinase', *J Biol Chem*, 285(17), pp. 12979-89.
- Townsend, P.D., Holliday, P.M., Fenyk, S., Hess, K.C., Gray, M.A., Hodgson, D.R. and Cann, M.J. (2009) 'Stimulation of mammalian G-protein-responsive adenylyl cyclases by carbon dioxide', *J Biol Chem*, 284(2), pp. 784-91.

Tsuji, T., Aoshiba, K., Itoh, M., Nakamura, H. and Yamaguchi, K. (2013) 'Hypercapnia accelerates wound healing in endothelial cell monolayers exposed to hypoxia', *Open Respir Med J*, 7, pp. 6-12.

Ussing, H.H. and Zerahn, K. (1951) 'Active transport of sodium as the source of electric current in the short-circuited isolated frog skin', *Acta Physiol Scand*, 23(2-3), pp. 110-27.

Vadasz, I., Dada, L.A., Briva, A., Trejo, H.E., Welch, L.C., Chen, J., Toth, P.T., Lecuona, E., Witters, L.A., Schumacker, P.T., Chandel, N.S., Seeger, W. and Sznajder, J.I. (2008) 'AMP-activated protein kinase regulates CO₂-induced alveolar epithelial dysfunction in rats and human cells by promoting Na,K-ATPase endocytosis', *J Clin Invest*, 118(2), pp. 752-62.

van Aubel, R.A., Smeets, P.H., Peters, J.G., Bindels, R.J. and Russel, F.G. (2002) 'The MRP4/ABCC4 gene encodes a novel apical organic anion transporter in human kidney proximal tubules: putative efflux pump for urinary cAMP and cGMP', *J Am Soc Nephrol*, 13(3), pp. 595-603.

Vedovato, N. and Gadsby, D.C. (2014) 'Route, mechanism, and implications of proton import during Na⁺/K⁺ exchange by native Na⁺/K⁺-ATPase pumps', *J Gen Physiol*, 143(4), pp. 449-64.

Verkman, A.S. (2002) 'Physiological importance of aquaporin water channels', *Ann Med*, 34(3), pp. 192-200.

Vishwanath, S. and Ramphal, R. (1984) 'Adherence of *Pseudomonas aeruginosa* to human tracheobronchial mucin', *Infect Immun*, 45(1), pp. 197-202.

Vohwinkel, C.U., Lecuona, E., Sun, H., Sommer, N., Vadasz, I., Chandel, N.S. and Sznajder, J.I. (2011) 'Elevated CO₂ Levels Cause Mitochondrial Dysfunction and Impair Cell Proliferation', *J Biol Chem*, 286(43), pp. 37067-76.

von Bethmann, A.N., Brasch, F., Nusing, R., Vogt, K., Volk, H.D., Muller, K.M., Wendel, A. and Uhlig, S. (1998) 'Hyperventilation induces release of cytokines from perfused mouse lung', *Am J Respir Crit Care Med*, 157(1), pp. 263-72.

Walley, K.R., Lewis, T.H. and Wood, L.D. (1990) 'Acute respiratory acidosis decreases left ventricular contractility but increases cardiac output in dogs', *Circ Res*, 67(3), pp. 628-35.

Wang, D., Sun, Y., Zhang, W. and Huang, P. (2008) 'Apical adenosine regulates basolateral Ca²⁺-activated potassium channels in human airway Calu-3 epithelial cells', *Am J Physiol Cell Physiol*, 294(6), pp. C1443-53.

Wang, J., Jackson, D.G. and Dahl, G. (2013) 'The food dye FD&C Blue No. 1 is a selective inhibitor of the ATP release channel Panx1', *J Gen Physiol*, 141(5), pp. 649-56.

Wenker, I.C., Sobrinho, C.R., Takakura, A.C., Moreira, T.S. and Mulkey, D.K. (2012) 'Regulation of ventral surface CO₂/H⁺-sensitive neurons by purinergic signalling', *J Physiol*, 590(Pt 9), pp. 2137-50.

- Xiao, F., Li, J., Singh, A.K., Riederer, B., Wang, J., Sultan, A., Park, H., Lee, M.G., Lamprecht, G., Scholte, B.J., De Jonge, H.R. and Seidler, U. (2012) 'Rescue of epithelial HCO_3^- secretion in murine intestine by apical membrane expression of the cystic fibrosis transmembrane conductance regulator mutant F508del', *J Physiol*, 590(Pt 21), pp. 5317-34.
- Xie, M., Rich, T.C., Scheitrum, C., Conti, M. and Richter, W. (2011) 'Inactivation of multidrug resistance proteins disrupts both cellular extrusion and intracellular degradation of cAMP', *Mol Pharmacol*, 80(2), pp. 281-93.
- Yamaoka, K., Yano, A., Kuroiwa, K., Morimoto, K., Inazumi, T., Hatae, N., Tabata, H., Segi-Nishida, E., Tanaka, S., Ichikawa, A. and Sugimoto, Y. (2009) 'Prostaglandin EP3 receptor superactivates adenylyl cyclase via the Gq/PLC/ Ca^{2+} pathway in a lipid raft-dependent manner', *Biochem Biophys Res Commun*, 389(4), pp. 678-82.
- Yang, D., Li, Q., So, I., Huang, C.L., Ando, H., Mizutani, A., Seki, G., Mikoshiba, K., Thomas, P.J. and Muallem, S. (2011a) 'IRBIT governs epithelial secretion in mice by antagonizing the WNK/SPAK kinase pathway', *J Clin Invest*, 121(3), pp. 956-65.
- Yang, D., Shcheynikov, N. and Muallem, S. (2011b) 'IRBIT: it is everywhere', *Neurochem Res*, 36(7), pp. 1166-74.
- Yang, D., Shcheynikov, N., Zeng, W., Ohana, E., So, I., Ando, H., Mizutani, A., Mikoshiba, K. and Muallem, S. (2009) 'IRBIT coordinates epithelial fluid and HCO_3^- secretion by stimulating the transporters pNBC1 and CFTR in the murine pancreatic duct', *J Clin Invest*, 119(1), pp. 193-202.
- Yanos, J., Wood, L.D., Davis, K. and Keamy, M., 3rd (1993) 'The effect of respiratory and lactic acidosis on diaphragm function', *Am Rev Respir Dis*, 147(3), pp. 616-9.
- Yuan, Z., Cai, T., Tian, J., Ivanov, A.V., Giovannucci, D.R. and Xie, Z. (2005) 'Na/K-ATPase tethers phospholipase C and IP_3 receptor into a calcium-regulatory complex', *Mol Biol Cell*, 16(9), pp. 4034-45.
- Zeng, Y., Clark, E.N. and Florman, H.M. (1995) 'Sperm membrane potential: hyperpolarization during capacitation regulates zona pellucida-dependent acrosomal secretion', *Dev Biol*, 171(2), pp. 554-63.
- Zhang, G., Liu, Y., Ruoho, A.E. and Hurley, J.H. (1997) 'Structure of the adenylyl cyclase catalytic core', *Nature*, 386(6622), pp. 247-53.
- Zhao, H.B. (2005) 'Connexin26 is responsible for anionic molecule permeability in the cochlea for intercellular signalling and metabolic communications', *Eur J Neurosci*, 21(7), pp. 1859-68.
- Zhou, Y., Zhu, S., Cai, C., Yuan, P., Li, C., Huang, Y. and Wei, W. (2014) 'High-throughput screening of a CRISPR/Cas9 library for functional genomics in human cells', *Nature*, 509(7501), pp. 487-91.
- Zuo, W.L., Li, S., Huang, J.H., Yang, D.L., Zhang, G., Chen, S.L., Ruan, Y.C., Ye, K.N., Cheng, C.H. and Zhou, W.L. (2011) 'Sodium coupled bicarbonate influx regulates intracellular and apical pH in cultured rat caput epididymal epithelium', *PLoS One*, 6(8), p. e22283.